The Role of MicroRNA-29 in Osteoarthritis

Perry J. Smith

A thesis submitted for the degree of Doctor of Philosophy (Ph.D.) in Biomolecular Science

University of East Anglia
School of Biological Sciences

March 2022

Abstract

Osteoarthritis (OA) is the most common type of joint disease, characterised by destruction of the articular cartilage and progressive joint failure, ultimately resulting in restricted mobility and chronic pain. Current treatments for OA are mainly limited to lifestyle changes, short-term pain relief and eventual joint replacement surgery. MicroRNAs are short non-coding RNAs which primarily downregulate expression of target genes by binding to complimentary sequences in the 3'-UTR of mRNAs. Previous research in our group highlighted a potential role for miR-29 in OA. MiR-29 family members were upregulated in OA cartilage and directly regulated the expression of several genes involved in OA. In this study, the role of miR-29 in cartilage and OA was further explored using *in vitro* and *in vivo* models.

Members of the ADAMTS family of metalloproteinases were targeted by miR-29b-3p in 3'-UTR luciferase reporter assays. In SW1353 cells and HACs overexpression of miR-29b-3p downregulated expression of *ADAMTS12*. TGF-β1 treatment of HACs downregulated expression of *ADAMTS1*, *ADAMTS3*, *ADAMTS5*, *ADAMTS9*, *ADAMTS12*, *ADAMTS13*, *ADAMTS15, ADAMTS19* and *ADAMTS20*, whereas expression of *ADAMTS2*, *ADAMTS4*, *ADAMTS6*, *ADAMTS10* and *ADAMTS14* was upregulated. The miR-29 family are recognised as key epi-miRNAs and overexpression of miR-29b-3p in SW1353 cells and HACs downregulated expression of *DNMT3A*, *TET2* and *TDG*. In SW1353 cells miR-29b-3p reduced global 5-methylcytosine levels but methylation array and bisulfite PCR pyrosequencing analyses failed corroborate this.

To investigate the role of miR-29 *in vivo*, mice with cartilage-specific knockout of *miR-29ab1* and *miR-29b2c*, independently (AB1-KO and B2C-KO) and simultaneously (DKO), were generated. AB1-KO and DKO mice were born at lower frequencies and weighed less than littermate controls at 12 weeks. MiR-29 knockout mice also had shorter femurs by 12 weeks with no differences in femur width or bone density. For DKO mice, preliminary analyses ($n \leq 3$) of 12-week aged legs found reduced growth plate area and cell count, and increased OA following surgical induction. Analysis of a larger sample size will be needed confirm this. In 3-week aged DKO hip cartilage, mRNA-sequencing identified 1324 differentially expressed genes (683 upregulated and 641 downregulated) with upregulated genes enriched for extracellular matrix, TGF-β signalling and endochondral ontologies.

In conclusion, these data suggest an important role for miR-29 in cartilage development and the pathogenesis of osteoarthritis through antifibrotic effects, mediated by regulation of ADAMTSs and TGF-β signalling.

Contents

List of figures

List of tables

List of appendices

Abbreviations

5-Aza	5-azacytidine
5-mC	5-methylcytosine
AbF	Antibiotic-free
Acan	Aggrecan
ACLT	Anterior cruciate ligament tear
ADAM	A disintegrin and metalloproteinase
ADAMTS	A disintegrin and metalloproteinase with thrombospondin motifs
AGO	Argonaute
BMI	Body mass index
BMP	Bone morphogenetic protein
BMSC	Bone marrow mesenchymal stem cell
CACNB1	Calcium voltage-gated channel auxiliary subunit beta 1
cDNA	Complimentary DNA
CI	Collagenase-induced
COMP	Cartilage oligomeric matrix protein
CS	Chondroitin sulfate
CTGF	Connective tissue growth factor
DE	Differential expression
DGCR8	DiGeorge syndrome critical region in gene 8
DMM	Destabilisation of the medial meniscus
DMR	Differentially methylated regions
DMSO	Dimethyl sulfoxide
DNMT	DNA methyltransferase
DPBS	Dulbecco's phosphate-buffered saline
DTT	Dithiothreitol

ECM	Extracellular matrix
EDTA	Ethylenediaminetetraacetic acid
FAM	Fluorescein amidite
FBS	Foetal bovine serum
FGF	Fibroblast growth factor
Floxed	Flanked by loxP sites
FZD	Frizzled
GAG	Glycosaminoglycan
GDF	Growth and differentiation factor
gDNA	Genomic DNA
GO	Gene ontology
HAC	Human articular chondrocytes
HBSS	Hanks' balanced salt solution
HIF-1α	Hypoxia-inducible factor 1α
IGD	Interglobular domain
IGFP	Inguinal fat pad
IL1	Interleukin-1
IL-1R1	IL-1 receptor type 1
IL-1Ra	IL-1 receptor agonist
IκB	Inhibitor of NF-κB
JNK	c-Jun N-terminal kinase
KLF4	Kruppel-like factor 4
KS	Keratan sulfate
LAP	Latency associated peptide
LB	Lysogeny broth
LEF	Lymphoid enhancer factor
LFC	Lateral femoral condyle

lncRNA	Long non-coding RNA
LRP-1	Lipoprotein receptor-related protein 1
LTP	Lateral tibial plateau
MAPK	Mitogen-activated protein kinase
MFC	Medial femoral condyle
miRNA	MicroRNA
MMP	Matrix metalloproteinase
MMTL	Meniscotibial ligament
mRISC	MiRNA-induced silencing complex
mRNA	Messenger RNA
mRNA-seq	mRNA-sequencing
MSC	Mesenchymal stem cell
MTP	Medial tibial plateau
NBF	Neutral buffered formalin
ncRNA	Non-coding RNA
NF-κB	Nuclear factor-κB
NGF	Nerve growth factor
NOF	Neck of femur
NSAID	Non-steroidal anti-inflammatory drugs
nt	Nucleotide
OA	Osteoarthritis
PAI-1	Plasminogen activator inhibitor-1
PC	Pixel classifier
PCA	Principle component analysis
Pre-miRNA	Precursor miRNA
Pri-miRNA	Primary miRNA
PVDF	Polyvinylidene fluoride

qRT-PCR	Quantitative real time PCR
RA	Rheumatoid arthritis
RAN-GTP	Ras-related nuclear protein guanine triphosphate
RIN	RNA integrity
ROI	Region of interest
rRNA	Ribosomal RNA
R-SMAD	Receptor-regulated SMAD
RUNX2	Runt-related transcription factor 2
SDS	Sodium dodecyl sulfate
SE	Standard error
siRNA	Short interfering RNA
SMAD	Suppressor of mothers against decapentaplegic
SNP	Single nucleotide polymorphism
snRNA	Small nucleolar RNA
SOX9	SRY-related HMG box-containing 9
SP1	Specificity protein 1
TAE	Tris-acetate EDTA
TAK1	TGF-β-activated kinase 1
TBS-T	Tris-buffered saline
TCF	T-cell factor
TDG	Thymine DNA glycosylase
TE	Trypsin/EDTA
TET	Ten-eleven translocation
TGF-β	Transforming growth factor-β
TGFβrI	TGF- β receptor type I
TGFβrII	TGF- β receptor type II
TGP	Tibial growth plate

TIMP	Tissue inhibitors of metalloproteinase
TMA	TaqMan microRNA assays
TNF-R1	TNF-receptor type I
TNF-α	Tumour necrosis factor- α
TRAP	Tartrate-resistant acid phosphatase
TRIM58	Tripartite motif containing 58
UTR	Untranslated region
VWF	Von-Willebrand factor
WIF1	Wnt inhibitory factor 1
WISP1	Wnt-induced signalling protein 1
WMS	Weill-Marchesani syndrome

Acknowledgements

Right, here we go. Although this is the shortest section of my thesis, it has been the most difficult to find the words for. Yet it is the most important to me, as it is my opportunity to thank all the amazing people, without whom, this thesis would not have been possible. So, I'll give it my best shot.

First and foremost, I would like to thank Prof. Ian Clark. You have been an amazing supervisor, your support and advice during the past four and a half years has been invaluable. You have been patient, compassionate and most of all, you have become a friend and a role model.

I would particularly like Dr. Tracey Swingler for all her help and mentoring throughout this project. You have been an extremely patient teacher, even when greeted in the early hours of the morning with a disassembled PCR machine or a lab bench that resembles a nuclear disaster. You are a truly exceptional scientist and it has been a pleasure to work with you.

Thank you to members of the Clark lab, past and present, for their friendship, help and for putting up with me. Dr. Rose Davidson's qPCR masterclasses were second to none. Liz, you're an absolute machine and a brilliant scientist. Paige, I can't believe we both made it to the end. Molly-Kay and Daniel, if we can do it, you guys can too! Dr. Linh Le, thank you for laying the foundations for this project.

Sharing a pint (or three) after work with Anni, Jess, Sonia, Michelle, Chay, Rob and Stefan (sorry if I missed anyone) has kept me sane over these last few years. Kayleigh, don't feel safe now I've left, I will be back when you least expect it. Thank you also to Dr. David Monk for all of his help with the DNA methylation experiments in this project, despite my apparent determination to sabotage them.

I would like to say a special thank you to all the technical staff who made my project possible. Andy is always happy to help anyone who asks and without him the BMRC would fall apart (even more). To the staff in the DMU, your technical knowledge and compassion for the animals above all else has been inspirational.

To my family, thank you for all your support, patience and long journeys to Norwich which have kept me going through the difficult times. Last, but certainly not least, thank you Sophie for being by my side through this journey - I could not have done this without you. You have been my rock during the hardest times, and you have shared some of my happiest times.

Chapter 1

Introduction

1 Introduction

Osteoarthritis (OA) is a degenerative joint disease characterised by progressive destruction of articular cartilage as a result of an imbalance in extracellular matrix (ECM) turnover and ultimately, remodelling of the joint (Umlauf *et al.*, 2010). Consequently, OA leads to significant pain and impairment of joint movement that can be severely debilitating to the sufferer (Loeser *et al.*, 2012). OA is estimated to affect around 8.5 million people in the UK (Versus Arthritis, 2021) with 9.6% and 18% of men and women over 60 respectively predicted to have OA worldwide (WHO, 2016). The cost of direct and indirect care for rheumatoid arthritis (RA) and OA was estimated to be £21.6 billion in the UK for 2010 with £5.2 billion being spent on direct care for OA alone (Economics, 2010). Moreover, as life expectancy increases, it is predicted that degenerative joint disorders will affect more than 130 million people by 2050 (Maiese, 2016). Therefore, it is clear that there is much to be gained from an increased understanding of the aetiology of OA and the development of therapies for its treatment.

1.1 Physiology of the synovial joint

Synovial joints such as those found in the knee, elbow, hip and fingers function to allow the movement of skeletal elements about one or more axes relative to each other – they are freely movable or diarthrodial (Figure 1.1) (Tortora *et al.*, 2017). Typically, these skeletal elements are separated by a narrow articular cavity in which the interfacing bone surfaces are covered with a layer of hyaline cartilage acting to protect the ends of the bones by distributing loads, absorbing pressure and reducing friction. The articular cavity is surrounded by the joint capsule, consisting of the inner synovial and outer fibrous membranes.

The synovial membrane is made up of highly vascular areolar tissue, sometimes interspersed with cushioning adipose tissue, and secretes lubricating synovial fluid into the joint cavity in order to reduce friction thus allowing for wear-resistant articular movement (Drake *et al.*, 2009). Synovial fluid is an ultrafiltrate of blood plasma and contains the lubricating molecules hyaluronan and lubricin (Hui *et al.* 2012). In addition to functioning as a lubricant, synovial fluid also plays an important role in joint metabolism allowing for the transport of nutrients, waste and signalling molecules within the joint cavity (Hui *et al.* 2012). Phagocytic cells may also be found in the synovial fluid functioning to eliminate potential pathogens and tissue debris from joint wear and tear (Tortora *et al.*, 2017).

In contrast, the outer fibrous membrane plays a more structural role in synovial joints. Composed mostly of collagen fibrils, the dense connective tissue in the fibrous membrane confers the necessary flexibility required for joint movement along with a high tensile strength which prevents joint dislocation (Drake *et al.*, 2009; Tortora *et al.*, 2017). Whilst the synovial membrane is attached to the bone at the point at which it interfaces with the cartilage, the fibrous membrane can be seen as a continuation of the periosteum, a tough layer of connective tissue surrounding the bone (Drake *et al.*, 2009; Tortora *et al.*, 2017).

Finally, synovial joints may contain several other structures. Bursae are small sacs of synovial fluid found close to tendons, bone or skin and function to reduce friction in these areas. Extracapsular and intracapsular tendons are sometimes found outside or inside the articular capsule respectively and provide additional tensile strength to these joints (Tortora *et al.*, 2017). Articular pads or menisci are pads of fibrocartilage found in the knee joint. As well as providing additional shock resistance, these structures are also thought to be involved in the distribution of weight and synovial fluid across the articular surfaces (Drake *et al.*, 2009; Tortora *et al.*, 2017).

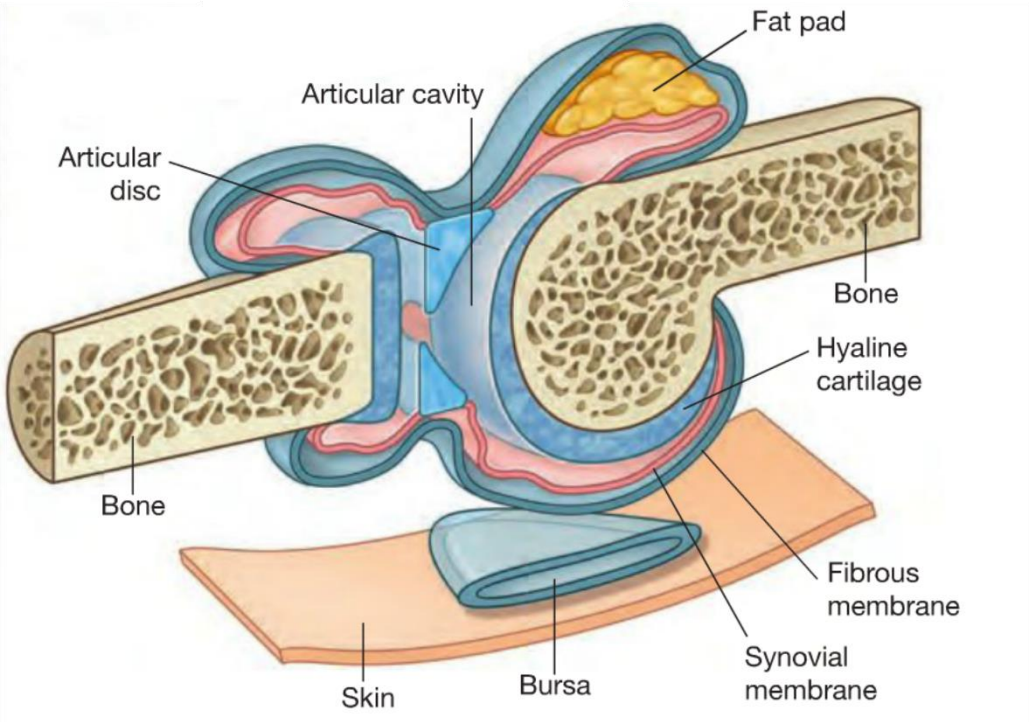

Figure 1.1. Structure of the synovial joint. *Synovial joints allow for uni or multiaxial movement of skeletal bones relative to each other. Hyaline cartilage protects the articular bone surfaces and in conjunction with lubricating molecules secreted by the synovial membrane, provides a low friction surface for movement. Taken from Drake et al., 2009.*

1.1.1 Articular Cartilage

The opposing bone surfaces in the articular joint are covered with a layer of hyaline cartilage (the articular cartilage). Articular cartilage consists of a highly specialised ECM maintained by specialised cells called chondrocytes and functions in reducing friction and protecting articular bone surfaces during joint movement. Therefore, correct formation of articular cartilage is important for the functioning of the articular joint.

1.1.1.1 Chondrocytes

Chondrocytes are the sole cellular occupants of articular cartilage making up only 1-5% of the cartilage volume (Stockwell, 1967; Bhosale *et al.*, 2008). They are highly specialised cells responsible for maintaining cartilage homeostasis by regulating the production and turnover of the ECM. Maintenance of the ECM is achieved through the synthesis of structural matrix components such as collagens (type II, IX, and XI), glycoproteins, proteoglycans and hyaluronan (Archer *et al.*, 2003; Akkiraju *et al.*, 2015). Conversely, along with cells in the synovium, chondrocytes produce catabolic proteases such as members of the matrix metalloproteinase (MMP), a disintegrin and metalloproteinase (ADAM) proteinase, and a disintegrin and metalloproteinase with thrombospondin motifs (ADAMTS) families in response to a variety of cytokines and growth factors (Rowan, 2001).

Chondrocytes originate from mesenchymal stem cells (MSCs) in the developing embryo which subsequently undergo a programme of chondrogenesis (Archer *et al.*, 2003) (Figure 1.2). Chondrogenesis begins with migration towards, and condensation at future skeletal elements of MSCs. Condensation of MSCs leads to the formation of dense cell aggregates which are separated from surrounding tissues by the perichondrium - a thin layer of elongated cells (Prein *et al.*, 2019). Inside the cartilage anlagen expression of transcription factors such as SRY-related HMG box-containing 9 (SOX9), a so-called ‘master regulator’ of chondrogenesis, causes the rapid differentiation of MSCs into chondrocytes (Bi *et al.*, 1999; Akiyama *et al.*, 2002). SOX9 expression also triggers the expression of molecules such as collagen II and aggrecan leading to the deposition of ECM (Lefebvre *et al.*, 1998; Sekiya *et al.*, 2000)

Moving forwards, chondrocytes have multiple fates. Those destined for the articular cartilage will continue to proliferate in the developing anlagen and contribute to the formation of the ECM, a process which is tightly coordinated by a complex network of regulators including many members of the bone morphogenetic protein (BMP) and fibroblast growth factor (FGF) families (Goldring *et al.*, 2017). Whereas cells destined to contribute to growth plate and bone formation will further differentiate into hypertrophic cells,

undergo cartilage matrix calcification and ultimately facilitate endochondral ossification (Archer *et al.*, 2003; Goldring *et al.*, 2006).

In articular cartilage, chondrocytes are isolated within a dense ECM. The articular cartilage is avascular, therefore chondrocytes rely on diffusion for the receipt of nutrients and metabolites (Sophia Fox *et al.*, 2009). In addition, given that the microenvironment of the chondrocyte is hypoxic (as low as 1% v/v in the deep zone), chondrocyte metabolism is dependent on anaerobic respiration. Chondrocytes are therefore heavily reliant on glycolysis (occurring in the cytoplasm) and are found to possess very few mitochondria (Archer *et al.*, 2003). In light of this, it has been shown that genes involved in the hypoxic response such as hypoxia-inducible factor-1α (HIF-1α) are essential for chondrocyte survival in differentiated cartilage (Schipani *et al.*, 2001) and that HIF-1α can promote chondrogenesis by upregulating SOX9 and inhibiting BMP2-induced osteogenesis (Zhou *et al.*, 2015).

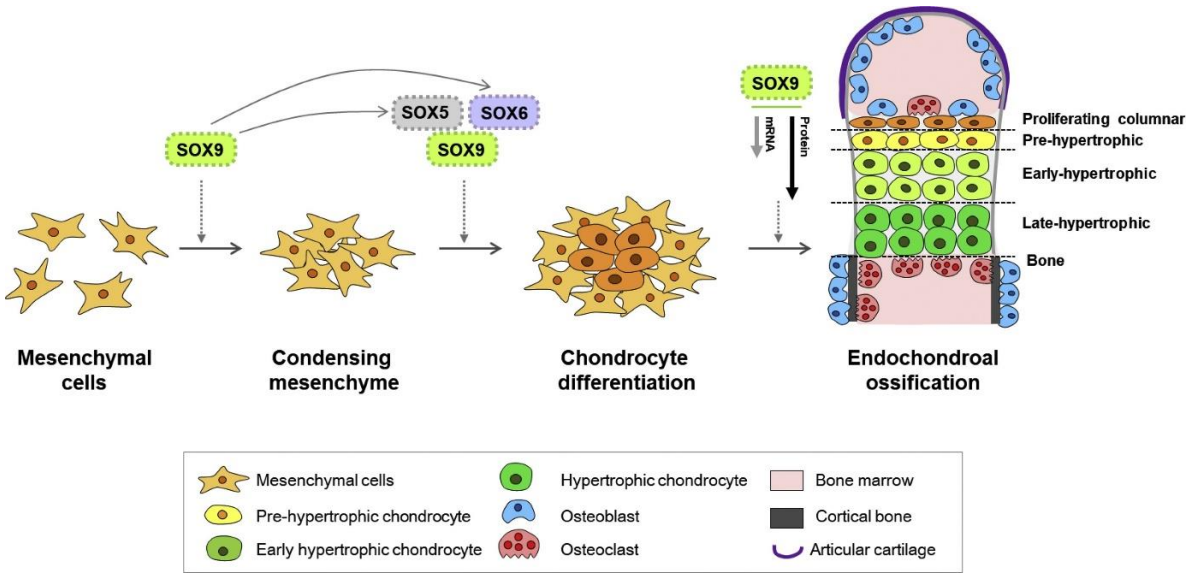

Figure 1.2. Overview of chondrogenesis. *Chondrogenesis begins with the condensation of MSCs. Within the condensing cell aggregate expression of SOX9 in conjunction with its cofactors, SOX5 and SOX6, promotes the differentiation of MSCs into chondrocytes. Depending on the fate of differentiating chondrocytes, they may continue to proliferate and form cartilage, or undergo further hypertrophic differentiation culminating in endochondral ossification and bone formation. Taken from Song and Park, 2020.*

1.1.1.2 Extracellular matrix

Articular cartilage consists of a dense ECM made up primarily of water, collagen and proteoglycans with various other non-collagenous proteins and glycoproteins being present to lesser extents (Buckwalter et al. 2005). The ECM of articular cartilage is sparsely populated with and maintained by a small number of chondrocytes. It is also aneural, avascular and alymphatic meaning that chondrocytes therefore rely on diffusion from the synovial fluid and subchondral bone vasculature for the receipt of nutrients and signalling molecules (Bhosale and Richardson 2008).

The complex network of collagen and proteoglycans (primarily aggrecan), interspersed with glycoproteins and water gives the ECM of articular cartilage the characteristic resistance to compression required to protect the articulating joint. Moreover, the secretion of lubricants such as lubricin and hyaluronan at the surface of the articular cartilage allow for the friction-free movement of joint surfaces during articulation.

Zones

It is important to consider that the ECM of articular cartilage is not homogeneous in its structure, function or morphology. Therefore, four zones have been identified: superficial, transitional, middle (or deep), and calcified cartilage (Figure 1.3) (Buckwalter *et al.*, 2005; Pearle *et al.*, 2005; Bhosale *et al.*, 2008; Sophia Fox *et al.*, 2009).

The superficial zone is the outermost and thinnest zone of the articular cartilage making up between 10% and 20% of the cartilage thickness (Pearle *et al.*, 2005; Sophia Fox *et al.*, 2009; Shetty *et al.*, 2014). Consisting of a dense layer of collagen fibrils laying parallel to the articular surface and covering a similarly parallel layer of ellipsoid chondrocytes, the superficial zone provides the smooth surface required for articular movement whilst also resisting shear (Pearle *et al.*, 2005). In addition, the superficial zone may also function as a kind of ‘skin’ for the articular cartilage, preventing the exchange of large molecules with the synovial fluid and isolating it from the immune system (Buckwalter *et al.*, 2005). Given the superficial zone is the outermost layer of the articular cartilage and is responsible for allowing smooth articulation, it is not surprising that structural damage to superficial zone is one of the first changes observed in induced models of OA (Guilak *et al.*, 1994; Bo *et al.*, 2012; Boyce *et al.*, 2013). Interestingly, recent evidence suggests that cells in the superficial zone are actually self-renewing progenitors of middle and deep chondrocytes (Li *et al.*, 2017). Therefore, the superficial zone may represent a stem cell niche capable of producing new chondrocytes that could participate in and/or augment cartilage repair.

Beneath the superficial zone, making up 40-60% of the cartilage volume, is the transitional zone (Pearle *et al.*, 2005; Sophia Fox *et al.*, 2009). As the name implies the transitional zone is morphologically intermediate between the superficial and deep zones (Buckwalter *et al.*, 2005). Collagen fibrils within this zone are thicker than those in the superficial zone and are arranged obliquely (Pearle *et al.*, 2005). Whilst increased amounts of proteoglycans are present in the transitional zone compared to the superficial zone, less water is found in this zone (Buckwalter *et al.*, 2005). Chondrocytes of the transitional zone are typically spheroidal and less densely populated (Sophia Fox *et al.*, 2009) while possessing an increased amount of synthetic organelles (Buckwalter *et al.*, 2005). Collectively, these characteristics confer increased resistance to compression when compared to the superficial zone (Pearle *et al.*, 2005) and as such, the transitional zone is recognised as the first with resistance to articular cartilage compression (Sophia Fox *et al.*, 2009).

Continuing down into the articular cartilage, we find the deep zone, representing 30% of the articular cartilage (Pearle *et al.*, 2005). Compared to the transitional zone, the deep zone contains yet thicker collagen fibrils arranged perpendicular to the articular surface, the highest concentration of proteoglycans and the lowest concentration of water (Buckwalter *et al.*, 2005). Consequently, the deep zone is responsible for the majority of resistance to compression (Pearle *et al.*, 2005). Chondrocytes in the deep zone are again spheroidal, however they are arranged in columns parallel to the collagen fibrils and perpendicular to the articular surface (Sophia Fox *et al.*, 2009). Finally, a thin calcified cartilage zone separates the deep zone from the subchondral bone which is marked by a so-called ‘tide mark’ (Pearle *et al.*, 2005). The ECM in this zone is highly calcified and sparsely populated with hypertrophic chondrocytes (Sophia Fox *et al.*, 2009). As well as providing shock absorption, the calcified cartilage zone also functions to anchor the collagen fibrils of the deep zone to the underlying subchondral bone (Sophia Fox *et al.*, 2009).

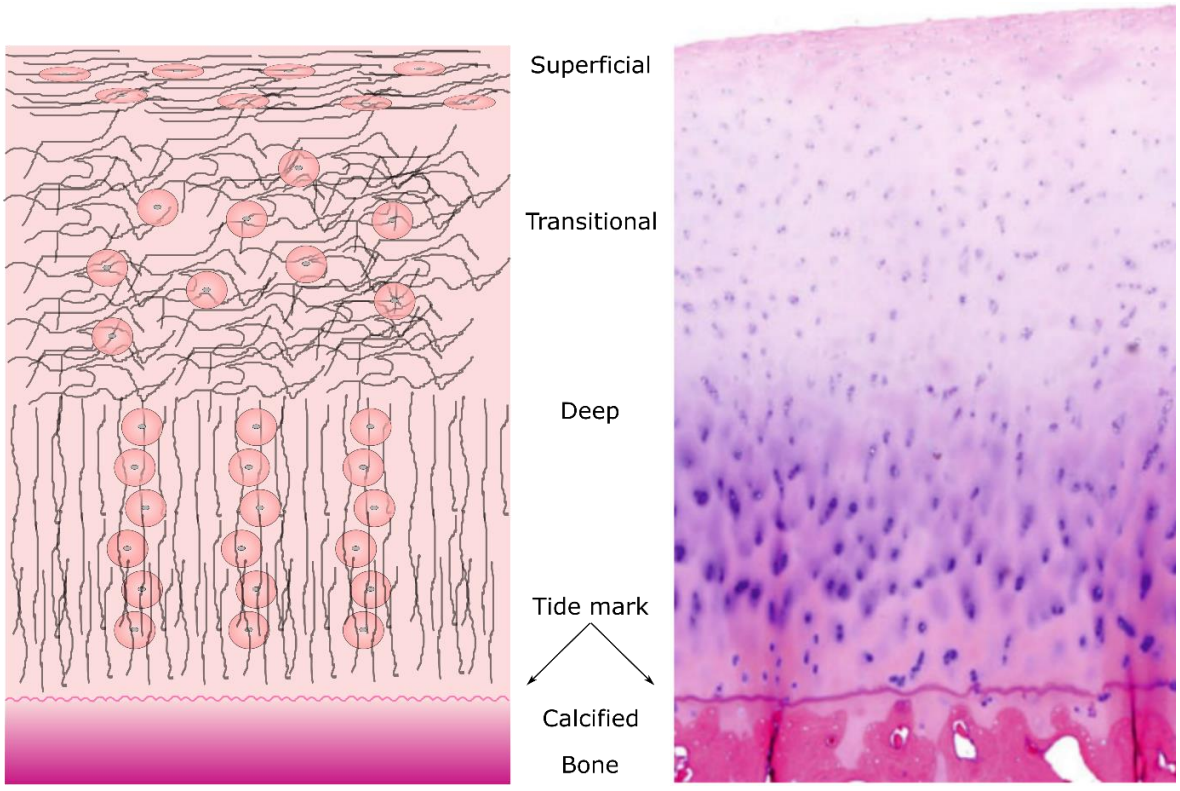

Figure 1.3. Articular cartilage zones. *Four zones are often identified in articular cartilage: Superficial, transitional, deep and calcified. In the superficial zone chondrocytes are ellipsoid and collagen fibrils are parallel to the articular surface. In the transitional zone, chondrocytes are spheroid and collagen fibrils randomly orientated. Chondrocytes in the deep zone are arranged in columns and collagen fibrils are perpendicular to the articular surface. The tide mark separates the deep zone from the calcified cartilage which interfaces with the subchondral bone. Histological section of a normal articular surface (right) adapted from Shetty et al. 2014.*

Regions

In addition to the previously discussed zones in articular cartilage, three regions or compartments are also distinguished in the ECM based on their proximity to the chondrocyte: pericellular, territorial and interterritorial (Buckwalter *et al.*, 2005; Sophia Fox *et al.*, 2009; Heinegård *et al.*, 2011).

The pericellular region is rich in proteoglycans and non-fibrillar collagens but contains few collagen fibrils (Buckwalter *et al.*, 2005). Directly surrounding the chondrocyte, the pericellular region attaches to the cell membrane and communicates mechanical stress and changes in the ECM to the chondrocyte via cell surface receptors, for example: the interaction between hyaluronan and CD44 receptor (Andhare *et al.*, 2009; Heinegård *et al.*, 2011; Houard *et al.*, 2013). Adjacent to the pericellular region, the territorial region forms a basket-like structure of collagen around one or clusters of chondrocytes and is thought to provide structural protection during mechanical loading of the tissue (Buckwalter *et al.*, 2005). Finally, making up the majority of the ECM in articular cartilage is the interterritorial region. Collagen fibril orientation and proteoglycan abundance in this region vary according to cartilage zone and thus, the interterritorial zone confers most of the biomechanical properties of articular cartilage (Sophia Fox *et al.*, 2009).

1.1.1.2.1 Collagen

Collagens are the most abundant proteins in animals and account for one third of total protein in humans (Shoulders *et al.*, 2009) and two thirds of the dry weight of articular cartilage (Eyre, 2002). The majority of the biomechanical properties of articular cartilage arise from the network of cross-linked collagen fibrils in collaboration with proteoglycans such as aggrecan. As previously discussed, the differential arrangement of collagen fibrils within different zones of the articular cartilage confers the specialised function of this tissue.

Collagens are initially secreted as pro-peptides (procollagens) by chondrocytes. Individual collagen pro-α chains are translated by endoplasmic bound-ribosomes and subsequently combine in parallel with two other α-chains to form the triple stranded helical procollagen molecule which is then secreted into ECM. Cleavage of procollagen by specific N (e.g. ADAMTS-2, 3 and 14) and C-terminal proteases (e.g. BMP-1 and mTLD) produces mature collagen fibrils which are less soluble (Bekhouche *et al.*, 2015; Vadon-Le Goff *et al.*, 2015), and self-assemble into the macroscopic fibrils and networks which form the majority of the ECM in articular cartilage (Shoulders *et al.*, 2009). This self-assembly process is regulated by extrinsic factors which facilitate the complex 3D organisation and tissue-specific arrangement of collagen (Holmes *et al.*, 2018).

1.1.1.2.1.1 Type II collagen

Articular collagen fibrils consist predominantly (≥90%) of type II collagen with the minor collagens (VI, IX, X, XI, XII, XIV and XXVII) being present to lesser extents (Eyre, 2002; Luo *et al.*, 2017). Type II collagen is transcribed from the *COL2A1* gene and is expressed mainly in articular cartilage, intervertebral discs and with limited expression in the vitreous of the eye (Cheah *et al.*, 1991; Khetarpal *et al.*, 1994). Post-secretion, three α1 collagen II fibrils assemble into a three dimensional triple helical polymer in which the molecules are heavily cross linked in a head-to-tail (N-to-C) orientation (Bruckner *et al.*, 1994). Typically, type II collagen is coassembled with type XI collagen and accompanied by covalent crosslinking to type IX collagen and interactions with small proteoglycans (Mendler *et al.*, 1989) (Figure 1.4). Due to the low turnover of collagen (predicted turnover rate of 400 years), the tissue regeneration needed to repair ECM damage typical of OA pathogenesis is slow and difficult (Maroudas *et al.*, 1992).

Given the major role of collagen II in cartilage structure and function, it is unsurprising that mutations associated with the *COL2A1* locus can have significant consequences. Homozygous knockout of type II collagen in mice results in early lethality, either just before or shortly after birth with disorganised and atypical organisation of both cartilage and long bone structures (Li *et al.*, 1995). In humans over 30 mutations in the collagen II locus have been identified with the general clinical phenotype being mild to severe spondyloepiphyseal dysplasia (Horton, 1996).

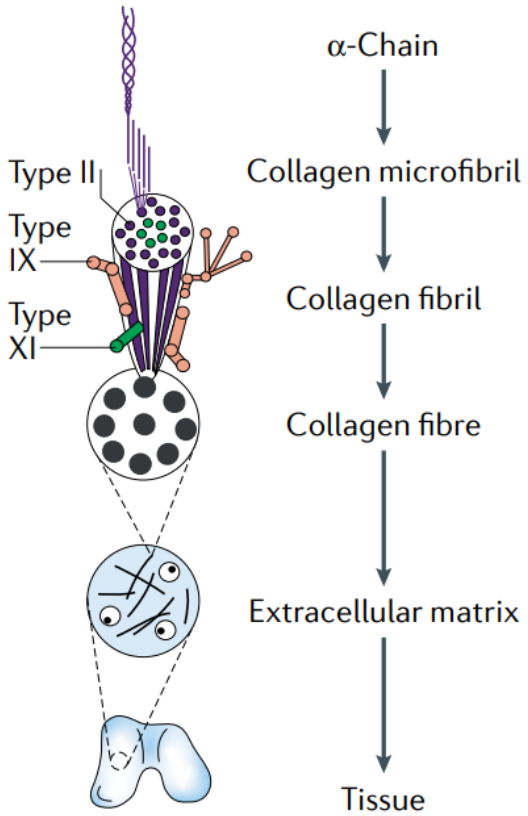

Figure 1.4. Collagen assembly. *Assembly of collagen fibril proceeds by trimerization of α1 collagen II units followed by the addition of minor collagens including type IX and XI. Fibrils are further assembled in collagen fibres, ultimately forming part of the extracellular matrix and articular cartilage. Modified from Bielajew et al, 2020.*

1.1.1.2.1.2 Minor collagens

Minor collagens identified in articular cartilage include types IX, X, XI, VI, XII, XIV, and XXVII, and although present to a lesser extent than type II, they are still important. Minor collagens extensively cross link with collagen II and other minor collagens contributing significantly to the physical properties of articular cartilage (van der Rest *et al.*, 1988; Luo *et al.*, 2017). Type VI collagen is a microfibrillar collagen involved in the anchoring of chondrocytes to the pericellular matrix by binding ECM proteins such as collagen II (Bidanset *et al.*, 1992) and facilitating cell-matrix interactions (Pfaff *et al.*, 1993). Type IX, XII, XIV, XVI, and XXII collagen do not form fibrils alone, but associate with the surface of other fibrils such as type II and VI (Luo *et al.*, 2017)

Evidence of the importance of the minor collagens can be seen in the fact that mutations, either in engineered mice or humans with genetic diseases, result in overt and often severe phenotypes. Knockout of collagen IX in mice results early onset degenerative joint disease (Fässler *et al.*, 1994) and concurrently, linkage and gene associated studies have highlighted an association between type IX collagen and hip OA (Mustafa *et al.*, 2000; Näkki *et al.*, 2010). Similarly, knockout of collagen VI accelerated development of OA in mice

(Alexopoulos *et al.*, 2009) with altered distribution and upregulation of collagen VI being observed in human osteoarthritic cartilage samples (Nugent *et al.*, 2009).

1.1.1.2.2 Aggrecan

Proteoglycans, consisting of glycosaminoglycans (GAGs) covalently attached to a core protein, are another major structural component of articular cartilage (Watanabe *et al.*, 1998). In contrast to the tensile strength conferred by collagen, the turgor generated by proteoglycan water retention contributes to the compression resistance of articular cartilage (Venn *et al.*, 1977).

The major proteoglycan in articular cartilage is aggrecan. In articular cartilage, aggrecan molecules associate with hyaluronan and link proteins in aggregates that are immobilised in a collagen network (Dudhia, 2005). Aggrecan consists of two N-terminal globular domains (G1 and G2) separated by an interglobular domain (IGD) followed by a long GAG-attachment domain between G2 and the C-terminal globular domain (G3) (Hardingham *et al.*, 1992). The G1 region is responsible for interacting with hyaluronan whereas the function of the G2 region remains unclear (Hascall *et al.*, 1974). In contrast to the G1 domain, the IGD region has been shown to be susceptible to degradation by many matrix degrading enzymes (Fosang *et al.*, 1992). The GAG-attachment region is long and has numerous keratan sulfate (KS) and chondroitin sulfate (CS) chains attached. It is these negatively charged CS and KS GAG chains which are responsible for the osmotic properties of aggrecan (Venn *et al.*, 1977). Finally, the G3 is essential for proper intracellular trafficking and secretion of aggrecan (Zheng *et al.*, 1998) however it is often proteolytically cleaved in the ECM (Dudhia *et al.*, 1996).

Up to 100 CS and 60 KS chains may be attached to the GAG-attachment region of an aggrecan molecule (Kiani *et al.*, 2002). Therefore, aggrecan molecules are polyanionic and attract counter mobile ions such as Na^+ which, in turn, draws water into the cartilage causing the ECM to expand (Venn *et al.*, 1977; Kiani *et al.*, 2002). It is the swelling of these dense aggrecan aggregates immobilised within the collagen network that confers the characteristic resistance to compression of articular cartilage. In addition, while the movement of large molecules is inhibited, the negative charge of the proteoglycans does allow for the diffusion of smaller molecules which is essential for chondrocyte nutrition and exchange of metabolites with the synovial fluid (Dudhia, 2005).

1.1.2 Subchondral bone

Along with the articular cartilage, the subchondral bone is said to form a functional osteochondral unit responsible for shock absorption and load distribution in the synovial joint (Hügle *et al.*, 2017). In contrast to articular cartilage, subchondral bone is highly vascularised and dynamic. Subchondral bone is constantly being remodelled due to reciprocal resorption and formation (Imhof *et al.*, 2000) and, as opposed to growing via internal expansion, bone growth occurs through the apposition of matrix and osteoblasts on existing surfaces (Rauch, 2005).

In the synovial joint, the bone layer directly beneath the cartilage is called the subchondral bone plate or the cortical end plate. The cartilage protrudes irregularly into the underlying bone - somewhat resembling a jigsaw puzzle - allowing for the transformation of shear forces into tensile and compressive forces (Imhof *et al.*, 2000). The subchondral bone plate vasculature is in close proximity to the articular cartilage, breaching into the calcified cartilage zone in places and thus, these vessels contribute at least 50% of the glucose, water and oxygen supplied to the cartilage whilst also playing a role in the absorption of metabolic waste (Imhof *et al.*, 2000).

Bone formation and development in the appendicular skeleton is achieved through the replacement of cartilage with mineralised bone, or endochondral ossification. Briefly, subsequent to the differentiation of chondrocytes into non-proliferating hypertrophic cells, osteoblast progenitors, osteoclasts (bone resorbing cells), blood vessel endothelial cells and hematopoietic cells invade the now vacant lacuna (Berendsen *et al.*, 2015). Hypertrophic cartilage is then resorbed and the osteoblast progenitors give rise to trabecular bone forming osteoblasts, osteocytes and stromal cells while hematopoietic and endothelial cells form the bone marrow (Maes *et al.*, 2010).

Similar to articular cartilage, bone consists predominantly of cross-linked collagen fibrils. However, whereas collagen II is the major collagen in articular cartilage, collagen I accounts for approximately 80% of the total protein in bone with collagens III and V being present to lesser extents (Viguet-Carrin *et al.*, 2006). Following secretion of the osteoid bone matrix by osteoblasts, deposition of calcium phosphate crystals on and within the collagen I matrix results in calcification of the bone matrix around osteocytes conferring the stiffness of the bone (Viguet-Carrin *et al.*, 2006). Although osteoblasts may appear isolated from other cells due to immobilisation in the bone matrix, communication with other osteoblasts and osteoclasts and thus, bone homeostasis, is facilitated by direct cell-cell contact (Furuya *et al.*, 2018), gap junctions and the diffusion of paracrine factors (Jeansonne *et al.*, 1979; Matsuo *et al.*, 2008).

1.1.1 Synovium

The non-cartilaginous surfaces of the synovial joint are lined with the synovial membrane or synovium. Two layers are distinguished in the synovium: the relatively thin (1-2 cells) inner-facing intima and the mostly acellular outer subintima layer (Smith, 2011). The synovium provides a deformable packing allowing for movement of the joint and is responsible for the production and maintenance of the synovial fluid responsible for joint lubrication. Moreover, the synovium facilitates nutrient exchange and acts as a barrier controlling what can and cannot enter the joint capsule (Monemdjou *et al.*, 2010; Smith, 2011).

Cells of the synovium are referred to as synoviocytes and are broadly divided into type A and B synoviocytes (Barland *et al.*, 1962). Type A synoviocytes are macrophage-like cells responsible for the clearance of debris and pathogens from the joint space along with the secretion of pro-inflammatory cytokines and cartilage degrading enzymes. In contrast, type B synoviocytes are fibroblasts which secrete hyaluronan and lubricin – major components of the synovial fluid (Monemdjou *et al.*, 2010). Hyaluronan and lubricin are glycoproteins responsible for allowing near-frictionless movement of articular surfaces (Radin *et al.*, 1971; Swann *et al.*, 1985).

1.2 Osteoarthritis

Osteoarthritis is the most common type of joint disease and is characterised by degradation of the articular cartilage, thickening of the subchondral bone, osteophyte formation and inflammation of multiple joint components. Not only does OA contribute a significant economic burden in terms of the cost of care and losses in productivity, patients with OA suffer from chronic pain and disability. Significantly, current treatments are largely palliative with paracetamol and non-steroidal anti-inflammatory drugs (NSAID) frequently recommended for short-term pain relief and joint replacement being offered at the end point of the disease. There are no disease modifying drugs capable of slowing, stopping or reversing disease progression which are in routine use (Hunter *et al.*, 2019; Vincent *et al.*, 2022). Clearly then, there is much to be gained from an increased understanding of the pathophysiology of OA and the development of treatments for this disease.

OA is traditionally classified as either primary or secondary, primary being idiopathic and secondary being the result of injury or predisposing factors such as obesity (Vincent *et al.*, 2022). However, given that pain mostly precedes cartilage destruction, patients often present with advanced joint degeneration and thus, distinction between primary and secondary OA can be complicated. Regardless, a universal aetiological feature of OA is an altered mechanical load with other factors such as age, obesity and genetics likely

contributing to the heterogenous and unpredictable nature of disease progression (Vincent *et al.*, 2022)

Functionally, OA progression is driven by an imbalance in cartilage anabolism and catabolism whereby tissue homeostasis is shifted towards matrix degradation. Through injury, age, or predisposing factors the mechanical load experienced by the articular cartilage, or indeed the ability of the articular cartilage to resist otherwise normal load is altered, leading to tissue damage. Following this, disease progression is characterised by loss of articular cartilage, inflammation of the synovium and formation of osteophytes and subchondral bone lesions (damage) (Figure 1.5) (Vincent *et al.*, 2022).

In OA, chondrocytes undergo an injury-like response, recapitulating early developmental programs (Goldring *et al.*, 2009). Chondrocytes secrete increased levels of matrix remodelling enzymes as well as inflammatory mediators, such as interleukin-1β (IL-1β) and tumour necrosis factor-α (TNF-α) (Melchiorri *et al.*, 1998). Although normally involved in cartilage formation, repair, and remodelling, in OA, these enzymes drive cartilage degradation. In addition, chondrocytes begin to undergo hypertrophy, proliferation and calcification in a process comparable to endochondral ossification (Goldring *et al.*, 2009). Changes in the mineral content and thickness of calcified cartilage are associated with an advancement of the tide mark which may compromise the mechanical properties of the articular cartilage (Oettmeier *et al.*, 1989; Bonde *et al.*, 2005).

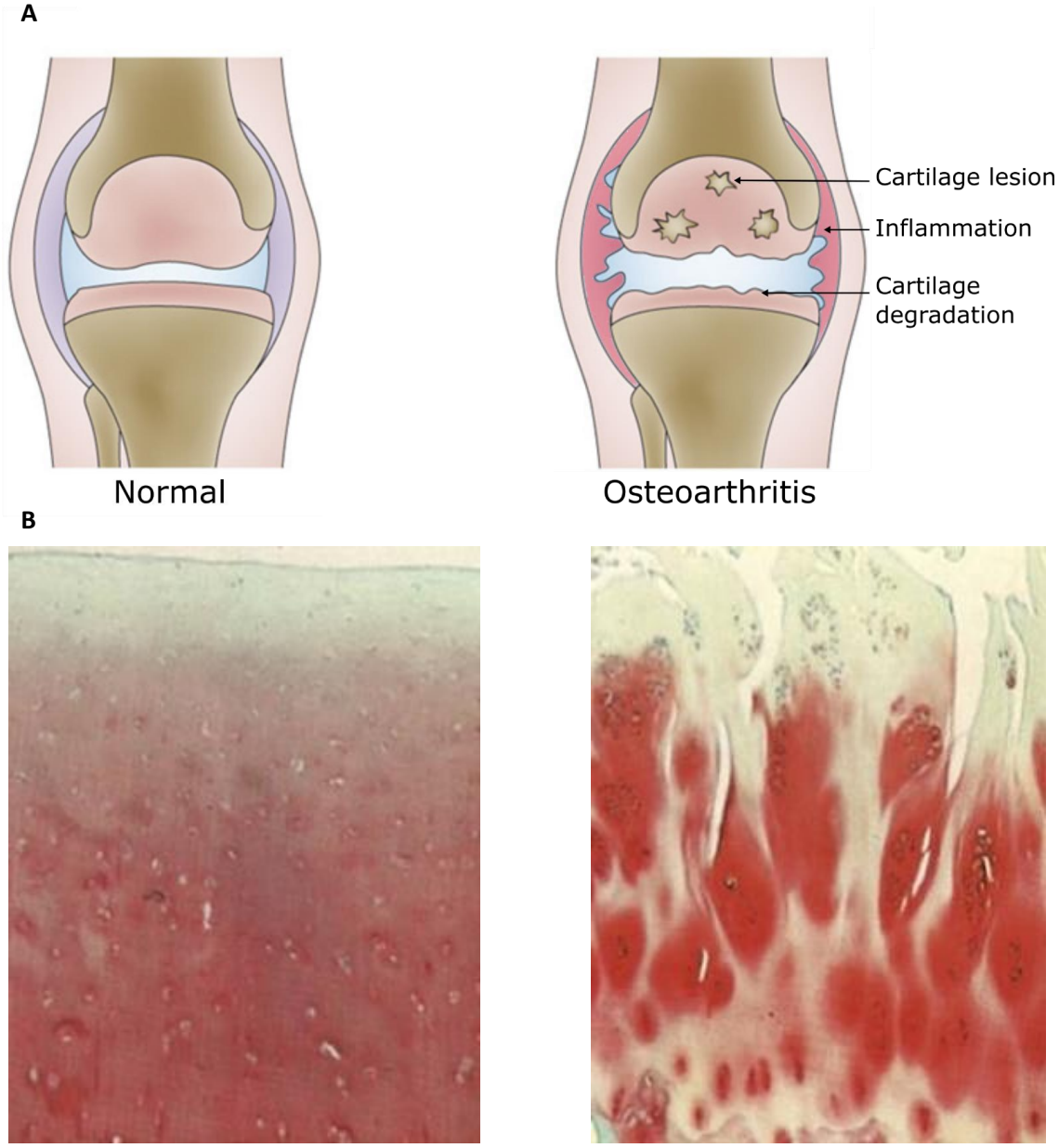

Figure 1.5. Pathologic changes associated with osteoarthritis. *(A) Osteoarthritis is characterised by progressive cartilage degradation, thickening of the subchondral bone, the formation of cartilage lesions and inflammation of the joint (red). Modified from Cicuttini and Wluka (2014). (B) Safranin-O staining of normal (left) and osteoarthritic (right) articular cartilage shows damage to the superficial zone, loss of GAGs (red) and a reduction and clustering of chondrocytes. Taken from Vincent and Watt (2022).*

1.2.1 Risk factors

The aetiology of OA is complex with biological factors such as genetics, age and gender, as well as environmental factors such as weight, injury and smoking all influencing disease progression (Loeser *et al.*, 2016; M. B. Johnsen *et al.*, 2017; Marianne Bakke Johnsen *et al.*, 2017; Vincent *et al.*, 2022). Importantly, although many risk factors such as obesity and physical activity are modifiable and thus amenable to preventative interventions, others such as age, sex and genetics are not. Whilst uncovering the mechanisms behind non-modifiable risk factors can aid our understanding of OA pathogenesis and the development of novel therapies, studies highlighting modifiable risk factors may be more informative if we want to prevent OA progression in the first place. Much work has been done using statistical analysis to identify OA risk factors in large cohorts, but it is important that such work is supported by experimental studies *in vitro* and *in vivo* to elucidate causal links between risk factors and OA.

1.2.1.1 Age

Increased age is the greatest risk factor for OA with a recent study showing older age to explain up to 56% of the variation in lumbar spine OA severity (Calce *et al.*, 2018). In line with this, in the Johnston County Osteoarthritis Project, incidence of radiographic knee OA rose from 15% in participants aged 45-54 to 50% in those aged 75 and over (Jordan *et al.*, 2009). However, it is important to make a distinction. It is not age itself that is the causal mechanism in OA, but age-related changes affecting the joint which predispose older people to OA. As well as intrinsic changes like abnormal wear and tear over time, extrinsic changes such as sarcopenia, altered bone remodelling and reduced proprioception are thought to contribute to OA development (Loeser, 2010). Moreover, although the association between increased age and risk of OA is well established, the mechanisms through which ageing predisposes OA are still poorly understood (Loeser, 2010; Calce *et al.*, 2018). With age the structure of articular cartilage becomes compromised with changes in ECM composition causing the cartilage to become stiff and brittle, and chondrocyte senescence preventing damage repair and even promoting catabolism through altered signalling (O'Brien *et al.*, 2019).

1.2.1.2 Obesity

Obesity has long been known as a risk factor for OA. Intuitively, increased body weight results in an increased load on weight-bearing joints and consequently, increased wear and tear of articular cartilage. In line with this, many epidemiological studies have identified a positive association between body mass index (BMI) (and weight) and risk of OA (Holmberg *et al.*, 2005; Järvholm *et al.*, 2005; Blagojevic *et al.*, 2010; Toivanen *et al.*, 2010; Apold *et al.*, 2014; Marianne Bakke Johnsen *et al.*, 2017). A meta-analysis of 85 studies found that overweight or obese subjects had 3 times higher risk of OA compared to those of normal weight (Blagojevic *et al.*, 2010). Similarly, in a cohort of over 300 000 people, men and women in the highest BMI quartile were 6 and 11 times more likely, respectively, to undergo knee replacement as a result of OA than those in the lowest BMI quartile (Apold *et al.*, 2014). More recently Raud *et al.* (2020) found a positive association between level of obesity and clinical outcomes in knee OA with higher BMI being associated with increased pain and disability. Increased BMI was also associated with lower levels of physical activity highlighting the interaction between risk factors. Unsurprisingly, weight loss has been shown to reduce OA progression and therefore is often recommended as an early intervention by clinicians (Salis *et al.*, 2022; Vincent *et al.*, 2022)

While it seems plausible that the association between OA and being overweight is due to increased mechanical load, obesity has also been found to be a significantly associated with hand OA and thus, this cannot be the whole story (Grotle *et al.*, 2008). Moreover, it is becoming increasingly evident that other metabolic syndromes including type 2 diabetes (Schett *et al.*, 2013; Louati *et al.*, 2015), dyslipidaemia (Baudart *et al.*, 2017) and hypertension (Yasuda *et al.*, 2018) are associated with OA. It is thought that chronic low-grade inflammation that accompanies metabolic syndromes may favour the development of OA (Gao *et al.*, 2020).

It has been suggested that leptin, an inflammatory adipokine (adipose derived cytokine), may play a role in OA. Leptin levels are increased in OA cartilage and synovial fluid and also correlate with fat mass and BMI in plasma and synovial fluid (Zhang *et al.*, 1994; Dumond *et al.*, 2003; Ku *et al.*, 2009; Sandell, 2009; Martel-Pelletier *et al.*, 2016). Serum levels of leptin are also negatively associated with knee cartilage volume, thickness and total knee replacement in OA (Ding *et al.*, 2007; Stannus *et al.*, 2013; Martel-Pelletier *et al.*, 2016). Abolition of leptin signalling in mice lead to severe obesity but protection against OA (Griffin *et al.*, 2009) whilst treatment of chondrocytes with leptin induced expression of MMP-1 and 13 and ADAMTS-4, 5 and 9 (Hui *et al.*, 2012; Yaykasli *et al.*, 2015). Therefore, it has been proposed that leptin may link chronic low-grade inflammation in obesity with an increased risk of developing OA.

1.2.1.3 Injury

A universal factor in the development of OA is altered mechanical loading of the joint. Therefore, injuries that lead to destabilisation of the joint, such as anterior cruciate ligament tears (ACLT) can alter mechanical loading and predispose patients to OA (Vincent *et al.*, 2022). Indeed, a meta-analysis including 53 studies found the risk of developing OA increased by 4.2 times following ACLT (Poulsen *et al.*, 2019). Similarly, a meta-analysis of 24 observational studies including over 20 000 subjects along with a cohort study of over 300 000 subjects both found that a history of knee injury increased the risk of developing knee by more than fourfold (Toivanen *et al.*, 2010; Muthuri *et al.*, 2011). As a result patients with prior knee trauma are diagnosed with knee OA over 10 years earlier than normal patients (Brown *et al.*, 2006). Therefore, interventions which reduce the likelihood of joint injury should decrease the risk of developing OA later in life. Where joint injury does occur, interventions such as high tibial osteotomy or joint distraction may be implemented to reduce future OA progression (Vincent *et al.*, 2022).

1.2.1.4 Smoking

Cigarette smoking is well known to have a multitude of negative health effects ranging from increased risk of developing cancer to heart disease and impaired healing. Curiously however, smoking may have a protective role in OA. Two recent studies in Japan and South Korea found an inverse correlation between smoking and OA, particularly in males (Takiguchi *et al.*, 2019; Kwon *et al.*, 2020). Similarly, a cohort study by Johnsen *et al.* (2017) found a significant negative correlation between smoking and total joint replacement due to OA. Multiple other studies have also found similar results with smoking being negatively associated with risk of developing hand, knee, hip and back OA (Wilder *et al.*, 2003; Mnatzaganian *et al.*, 2013; Leung *et al.*, 2014). It is important to highlight that not all studies have been able to replicate this association (Dubé *et al.*, 2016; Kong *et al.*, 2017; Johnsen *et al.*, 2019).

Several explanations for the apparent protection conferred by smoking have been put forward. Smokers tend to have lower BMIs (Åsvold *et al.*, 2014). Given that BMI also negatively correlates with OA risk, it has been hypothesised that smoking may be acting as proxy for BMI (Johnsen *et al.* 2017). However, a follow-up study found that BMI could only account for a small amount of the effect of smoking on OA risk (Marianne Bakke Johnsen *et al.*, 2017). Consistent with this, smoking has also been found to protect against OA, even in subjects that are overweight (Sandmark *et al.*, 1999).

A second proposed explanation is that nicotine may have an anabolic effect on cartilage. In support of this idea, nicotine has been shown to promote collagen II synthesis and proliferation in human chondrocytes (Gullahorn *et al.*, 2005; Ying *et al.*, 2012). In rat and mouse models of OA nicotine treatment prevented cartilage degradation and reduced inflammation by inhibiting expression of *Mmp9* and *Tnf-α* (Gu *et al.*, 2015; Teng *et al.*, 2019). However, some studies have found a negative effect of nicotine on OA. Prenatal exposure to nicotine in rats predisposed OA progression and increased expression of *IL-1*, *IL-6*, *Mmp3* and *Mmp13* (Chen *et al.*, 2019). Similarly, in MSCs undergoing chondrogenesis, nicotine impaired chondrogenesis by reducing expression of *SOX9*, *COL2A1* and a*ggrecan* (*ACAN*), likely via the α7 nicotinic acetylcholine receptor (X. Yang *et al.*, 2017).

Although smoking may protect against the development of OA, it is unlikely that this outweighs the plethora of other negative health consequences associated with smoking. If the mechanism by which smoking protects against OA can be elucidated, this may be exploited in the development of future therapies. It has been proposed that binding to nicotinic acetylcholine receptors may mediate the positive effects of nicotine in OA (Felson *et al.*, 2015) and indeed, this is believed to be the mechanism by which smoking also appears to protect against the development of Parkinson's disease (Noyce *et al.*, 2012)..

1.2.2 Cartilage degradation

Cartilage degradation is a key feature of OA and driver of disease progression. In healthy articular cartilage, ECM turnover and production are finely balanced in order to ensure maintenance of the tissue. A major hallmark of OA is a shift in this balance towards cartilage degradation.

1.2.2.1 Matrix degrading proteases

Two major families of matrix-degrading proteases are implicated in the degradation of cartilage associated with OA: MMPs and ADAMTSs. MMPs are zinc-dependent endopeptidases capable of degrading many components of the ECM although, specifically in the context of OA, MMP-13 hydrolysis of collagen II is recognised as contributing significantly to cartilage degradation (Mitchell *et al.*, 1996). Notably, whilst collagen II degradation is mostly irreversible, aggrecan can be replenished (Karsdal *et al.*, 2008) and is able to protect collagen II from degradation (Pratta *et al.* 2003). MMPs were initially thought to be responsible for aggrecan degradation in OA due to their ability to cleave aggrecan (Fosang *et al.*, 1992, 1996). However, it was subsequently found that cleavage at the aggrecanase (later renamed ADAMTS-4) sensitive Glu^{373}-Ala^{374} site, as opposed the MMP-sensitive Asn^{341}-Phe^{342} site, was responsible for the majority of cleaved aggrecan

fragments in both human OA synovial fluid and cytokine stimulated bovine cartilage explants (Sandy *et al.*, 1991, 1992; Westling *et al.*, 2002).

1.2.2.1.1 MMPs

As previously discussed, type II collagen makes up the majority of the fibrous ECM in articular cartilage. Therefore, it is not surprising that collagenases such as members of the MMP family are implicated in OA. In humans, 23 MMPs have been identified although not all are expressed in cartilage (Yamamoto *et al.*, 2021). Expression profiling in human articular cartilage identified moderate expression of *MMP1*, *MMP9*, *MMP13*, *MMP16*, *MMP21*, *MMP23*, *MMP24* and *MMP26* and high expression of *MMP2*, *MMP12*, *MMP14*, *MMP19* and *MMP27* (Kevorkian *et al.*, 2004). While many of the MMPs are implicated in cartilage degradation, MMP-13 is considered the primary collagenase in OA (Bau *et al.*, 2002; Kevorkian *et al.*, 2004). Many studies have found upregulation of *MMP13* both in human OA cartilage (Reboul *et al.*, 1996; Billinghurst *et al.*, 1997; Kevorkian *et al.*, 2004; Troeberg *et al.*, 2012) and in surgical animal models (Kamekura *et al.*, 2005; Chia *et al.*, 2009; Xu *et al.*, 2009; Pickarski *et al.*, 2011; Bo *et al.*, 2012). Moreover, *Mmp13*-null mice are protected from cartilage degradation in the destabilisation of the medial meniscus (DMM) model (Little *et al.*, 2009) and concurrently, constitutive postnatal expression of *Mmp-13* leads to cartilage degradation (Neuhold *et al.*, 2001). For an up to date review of the role of MMPs in OA see Yamamoto, Wilkinson and Bou-Gharios (2021).

1.2.2.1.2 ADAMTS

The ADAMTSs are a family of 19 secreted multi-domain zinc metalloproteinases known to play a variety of roles in tissue development and homeostasis. Broadly, ADAMTSs can be separated in to 5 groups based on their known substrates: proteoglycanases (ADAMTS-1, 4, 5, 8, 9, 15, and 20), the procollagen N-proteinases (ADAMTS-2, 3 and 14), the cartilage oligomeric matrix protein (COMP) cleaving enzymes (ADAMTS-7 and 12), the von-Willebrand Factor (VWF) proteinase (ADAMTS-13) and a group of orphan enzymes (ADAMTS-6, 10, 16, 17, 18 and 19) whose substrates are as yet unknown (Kelwick, Desanlis, *et al.*, 2015). Significantly, members of the ADAMTS family are often found to be dysregulated in OA (Figure 1.6).

Proteoglycanases

To date, ADAMTS-4 and 5 are the most well-known contributors to OA, causing cartilage degradation through the cleavage of proteoglycans, primarily aggrecan (Tortorella *et al.*, 1999; Gendron *et al.*, 2007). *ADAMTS4* expression is increased in human OA cartilage (Naito *et al.*, 2007) and *Adamts5*-null mice are protected from cartilage damage in a surgical model (Glasson *et al.*, 2005). Interestingly, whilst short interfering RNA (siRNA) knockdown

of *ADAMTS4* and *5* attenuates aggrecan degradation in human cartilage (Song *et al.*, 2007), *Adamts4-Adamts5* double knockout mice show comparable resistance to aggrecan degradation to *Adamts5* knockouts suggesting that *Adamts4* may be less important in mice (Majumdar *et al.*, 2007).

The role of other proteoglycanases in OA is less well characterised but equally important to understand. ADAMTS-8 and 20 have been shown to be upregulated in OA whereas ADAMTS9 is downregulated. ADAMTS-1 and 15 are known to cleave both aggrecan and versican (Carlos Rodríguez-Manzaneque *et al.*, 2002; Dancevic *et al.*, 2013; Kelwick, Wagstaff, *et al.*, 2015) and while some studies have shown upregulation of ADAMTS-1 and 15 in OA, others have shown the opposite (Kevorkian *et al.*, 2004; Davidson *et al.*, 2006; Gardiner *et al.*, 2015). ADAMTS-8 and 9 have been shown to cleave aggrecan whereas ADAMTS-9 and 20 cleave versican during development (Collins-racie *et al.*, 2004; Nandadasa *et al.*, 2019; Rogerson *et al.*, 2019).

Procollagen N-proteinases

ADAMTS-2, 3 and 14, the procollagen N-proteinases, are essential for the N-terminal cleavage of procollagens I, II, III and V which facilitates mature fibril assembly (Colige *et al.*, 2002; Bekhouche *et al.*, 2015). As previously discussed, collagen plays an important role in articular cartilage. Intuitively all three procollagen N-proteinases are upregulated in OA, potentially in an attempt to undergo anabolic repair of the damaged tissue (Davidson *et al.*, 2006; Gardiner *et al.*, 2015; Dunn *et al.*, 2016; C. Y.-Y. Yang *et al.*, 2017). On the other hand, mutations in *ADAMTS2* cause Ehlers-Danlos Syndrome in humans (Colige *et al.*, 1999) with *Adamts2*-null mice demonstrating a similar fragile skin phenotype, however no joint phenotype is described (Li *et al.*, 2001). Knockout of *Adamts3* is embryonic lethal in mice (Janssen *et al.*, 2016) however mice lacking *Adamts14* are phenotypically normal (Dupont *et al.*, 2018) suggesting that there may be a degree of redundancy with in the procollagen N-proteinases.

COMP-cleaving enzymes

COMP is a non-collagenous thrombospondin that binds to collagens I, II, IX, fibronectin and aggrecan. Therefore, it is thought to play a role in the assembly and stabilisation of the ECM and is also considered to be a biological marker of cartilage breakdown (Tseng *et al.*, 2009). ADAMTS-7 and 12 are both upregulated in OA cartilage consistent with their ability to degrade COMP (Davidson *et al.*, 2006; Swingler *et al.*, 2009). Cartilage-specific overexpression of *Adamts7* in mice increased surgically induced OA progression and COMP degradation whereas the opposite was seen when *Adamts7* was knocked out (Lai *et al.*, 2014). While knockdown of ADAMTS-12 *in vitro* has been shown to reduce COMP

degradation (Luan *et al.*, 2008) no joint phenotype has been described in knockout mice (El Hour *et al.*, 2010; Paulissen *et al.*, 2012).

VWF proteinase

ADAMTS-13 is the only ADAMTS known to cleave VWF, a circulating glycoprotein required for the adhesion of platelets to the subendothelium during primary haemostasis (Fujikawa *et al.*, 2001). Inefficient cleavage of VWF causes thrombotic thrombocytopenic purpura, a disease characterised by the formation of blood clots within the microcirculation, low blood platelet and red blood cell count. Severe ADAMTS-13 deficiency (<10%), brought about either by inheritance of *ADAMTS13* mutations or the production of anti-ADAMTS-13 autoantibodies has been identified as the cause of this disease (Kremer Hovinga *et al.*, 2017). Although ADAMTS-13 has been found to be upregulated in OA synovium (Davidson *et al.*, 2006) little is known about its role in OA.

Orphan enzymes

The role of orphan enzymes in OA is poorly studied and potential roles are difficult to infer given that substrates of these enzymes are yet to be identified. Some studies have found upregulation of ADAMTS-6, 10, 16 and 18 in OA cartilage and upregulation of ADAMTS-10, 16 and 17 in OA synovium (Davidson *et al.*, 2006; Swingler *et al.*, 2009) however a functional link for these changes is yet to be described. ADAMTS-6 and 10 have been implicated in the regulation of cell-cell junctions with mutations in *ADAMTS10* being associated with Weill-Marchesani syndrome (WMS) (Cain *et al.*, 2016). Mutation of *Adamts10* in model a of WMS led to mice with shorter long bones along with shorter resting and expanded hypertrophic growth plate zones, indicative of altered bone development (Mularczyk *et al.*, 2018). Similarly, mutations in *ADAMTS17* are also associated with WMS with knockout mice having shorter long bones, brachydactyly, and thick skin (Oichi *et al.*, 2019). A truncated form of ADAMTS-16 was found to show some aggrecanase activity (Zeng *et al.*, 2006) and *Adamts16* mutation has been shown to reduce blood pressure in a rat model of hypertension, suggestive of a role in the vascular system (Gopalakrishnan *et al.*, 2012). *Adamts18* was recently found to be required for eye, lung, female reproductive tract and kidney development in mice (Rutledge *et al.*, 2019). Finally, a mutation in *Adamts19* has been linked to valvular heart disease however in *Adamts19*-null mice, there is no observation of joint abnormalities (Wünnemann *et al.*, 2020) or report of altered expression in OA.

	Murine									Human								
	Early OA						Late OA			Late OA								
	1 -Bateman*	2 weeks - Bateman*	2 weeks - Gardiner*	2 weeks - Loeser*	4 weeks - Gardiner*	4 weeks - Loeser*	8 weeks - Gardiner*	8 weeks - Loeser*	16 weeks - Loeser*	Sato*	Geyer*	Dunn**	Ramos*	Snelling*	Karlsson*	Swingler***	Kevorkian****	Davidson****
ADAMTS1			1.6		1.4		1.1				1.7	1.8	1.2		7.6	0.4		
ADAMTS2			2	1.4	1.5	1.6	1.4	1.1	1.3			1.5			7.3	8.1		
ADAMTS3			1.3	1.7		1.9	1.2	1.2	1.5			0.3				1.9		
ADAMTS4			2.9		8.9		1.1									0.4		
ADAMTS5		2.3									1.7	2.3			6.4	0.6		
ADAMTS6			0.8		0.7								1.3	2.2		2		
ADAMTS7												1.5				15		
ADAMTS8			1.2		1.7		1.2											syn
ADAMTS9			1.5		1.4							0.4				0.1		
ADAMTS10		2.4					1.4					1.1				1.6		
ADAMTS12			2	1.5	1.4	2.1	1.1		1.3			1.8				20.3		
ADAMTS13												0.3						syn
ADAMTS14	2.3											3.7				11.1		
ADAMTS15			2		3.3							0.4				23.7		
ADAMTS16			1.7		0.7		1.3					1.5				19.6		
ADAMTS17			0.6		0.4		0.9					1.5				0.7		syn
ADAMTS18	6.1		0.9		1.2		1.7									17.9		
ADAMTS19																		
ADAMTS20																		

Figure 1.6. ADAMTSs expression in osteoarthritis. *Fold change expression of ADAMTSs in OA versus normal cartilage. Upregulated genes highlighted red (p < 0.05) or pink (p > 0.05). Down-regulated genes highlighted dark blue (p < 0.05) or light blue (p > 0.05). For Bateman et al. (2013), Gardiner et al. (2015) and Loeser et al. (2013) expression was measured in knee cartilage from DMM operated mice. For Sato et al. (2006), Geyer et al. (2009), Dunn et al. (2016), Ramos et al. (2014) and Snelling et al. (2014) expression was measured in joint matched intact and OA lesion human cartilage. For Karlsson et al. (2010) expression was measured in healthy and OA knee cartilage. For Swingler et al. (2009), Kevorkian (2004) and Davidson (2006) expression was measured in femoral head cartilage from OA and fracture patients. * Microarray, ** RNA-sequencing, *** TaqMan low density array, **** qRT-PCR. Syn, synovium. Adapted from C.-Y. Yang et al. (2017).*

1.2.2.2 Altered cytokine production and cell signalling

Inflammation of the joint is another key feature of OA. During the progression of OA, the fine balance between cartilage anabolism and catabolism is perturbed and this is, to a large extent, due to altered mechanical load, production of inflammatory cytokines and subsequent cell signalling. Cytokines such as IL-1, transforming growth factor-β (TGF-β) and TNF-α are known to have significant impacts on cartilage turnover by regulating ECM production and degradation (Shen *et al.*, 2014; Wojdasiewicz *et al.*, 2014). Furthermore, these effects are mediated through cell signalling pathways such as Wnt and nuclear factor-κB (NF-κB) which themselves are altered in OA (Saito *et al.*, 2017; Y. Zhou *et al.*, 2017).

1.2.2.2.1 Interleukin-1

IL-1 represents a functionally diverse family of 11 cytokines. Specifically, IL-1α, IL-1β and IL-1 receptor antagonist (IL-1Ra) were, up until recently, identified as being the most clinically relevant in chronic inflammatory diseases and thus, received a lot of attention with regards to OA (Schett *et al.*, 2016). Briefly, binding of IL-1β or IL-1α to IL-1 receptor type 1 (IL-1R1) causes the recruitment of an the IL-1R1 accessory protein, subsequent intracellular signalling and ultimately, alteration of gene expression via activation of transcriptional regulators such as NF-κB, p38 and c-Jun N-terminal kinase (JNK) (Schett *et al.*, 2016).

IL-1 is increased in the joints of OA patients (Farahat *et al.*, 1993; Melchiorri *et al.*, 1998) and has been shown to promote cartilage catabolism. IL-1β and IL-1α have been shown to increase expression of MMPs including MMP-13 in several relevant cell types (Borden *et al.*, 1996; Kusano *et al.*, 1998; Mengshol *et al.*, 2000) and concurrently, IL-1β induces ADAMTS-4 activity in bovine articular cartilage and chondrocytes (Pratta *et al.* 2003). Increased ADAMTS-5 activity, but not expression, is induced by IL-1 through inhibition of endocytic re-uptake brought about by shedding of low-density lipoprotein receptor-related protein 1 (LRP-1) (Yamamoto *et al.*, 2013, 2017; Ismail *et al.*, 2015). Given that ADAMTS-4 and MMP-13 are also endocytosed by LRP-1, it is possible their activity is regulated via a similar mechanism (Yamamoto *et al.*, 2014, 2016). IL-1β has also been shown to prevent ECM formation by reducing production of both collagen II and aggrecan in chondrocytes (Tyler, 1985; Goldring *et al.*, 1994). Finally, stimulation of SW1353 cells with IL-1β was shown to increase the translation of several inflammatory genes including *CCL2*, *IL-6*, *NFKB1* and *TNFAIP2* as well as SOD2 to counteract a concomitant increase in reactive oxygen production (McDermott *et al.*, 2019).

Despite evidence suggesting IL-1 might be potential therapeutic target, such therapies have largely failed to demonstrate efficacy to date. Overexpression of IL-1Ra in rabbits with surgically induced OA resulted in reduced cartilage damage (Fernandes *et al.*, 1999). However, clinical trials have shown limited efficacy. Targeting of IL-1R1 with a monoclonal antibody in knee OA patients resulted in a slight (but non-significant) reduction in pain (Cohen *et al.*, 2011). Similarly, intra-articular injection of Anakinra (an IL-1R1 antagonist) to treat knee OA showed no significant benefit over placebo (Chevalier *et al.*, 2009), although later studies have found reduced pain and improved joint function in patients with cruciate ligament tears and post-operative knee inflammation (Brown *et al.*, 2011; Kraus *et al.*, 2012). Finally, more recent trials looking at the efficacy of Lutikizumab, an antibody capable of simultaneously binding and inhibiting IL-1α and IL-1β found little to no improvement in both hand and knee osteoarthritis (Fleischmann *et al.*, 2019; Kloppenburg *et al.*, 2019).

Therefore, although *in vitro* evidence posits IL-1 as an attractive therapeutic target, the lack of efficacy coming from trials of IL-1-targeting therapies calls this into question. Whilst IL-1 is stimulation may be useful for promoting an OA-like response from chondrocytes *in vitro*, the relevance of this *in vivo* remains uncompelling.

1.2.2.2.2 Tumour necrosis factor-α

Much like IL-1, TNF-α is an inflammatory cytokine implicated in OA. Initially cleaved from a homotrimeric transmembrane protein type II (mTNF-α) by ADAM17, TNF-α binds TNF-receptor type I (TNF-R1) and TNF-R2 and ultimately activates intracellular signalling through NF-κB, P38 and JNK (Wojdasiewicz *et al.*, 2014). TNF-α is also increased in joints of OA patients where it promotes cartilage degradation (Farahat *et al.*, 1993; Melchiorri *et al.*, 1998) and as such, TNF-α may be an important therapeutic target.

TNF-α has been proposed to act synergistically with IL-1 in the orchestration of cartilage degradation (Henderson *et al.*, 1989). Therefore, it is not surprising that TNF-α has been found to upregulate MMP-1 and MMP-13 in human chondrosarcoma cell lines (Mengshol *et al.*, 2000; Yoon *et al.*, 2008) and ADAMTS-4 in human osteoarthritic chondrocytes and synoviocytes (Yamanishi *et al.*, 2002; Xue *et al.*, 2013). Similarly to IL-1, TNF-α may also increase MMP-13 and ADAMTS-4 activity via inhibition of LRP-1 mediated endocytosis (Yamamoto *et al.*, 2017). Moreover, in combination with IL-1, TNF-α supresses proteoglycan and collagen II synthesis via NF-κB (Saklatvala, 1986; Séguin *et al.*, 2003) whilst also contributing to cartilage mineralisation by upregulating collagen I (Kunisch *et al.*, 2016).

So far, therapies targeting TNF-α have shown little promise (Ghouri *et al.*, 2021). Adalimumab is a monoclonal antibody that binds to TNF-α and prevents TNF-α receptor activation. Several studies found that subcutaneous injection of Adalimumab did not significantly improve progression or pain in patients with hand OA (Verbruggen *et al.*, 2012; Chevalier *et al.*, 2014; Aitken *et al.*, 2018). Another TNF-α inhibitor, etanercept, was also shown to have limited efficacy in pain reduction in hand OA although a small subgroup of patients did demonstrate a reduction in bone marrow legions after 12 months (Kloppenburg *et al.*, 2018).

1.2.2.2.3 Transforming growth factor-β

TGF-β1, 2 and 3 are a group of small secreted signalling proteins important in a range of processes in vertebrates such as development, cell proliferation, differentiation, apoptosis and cell migration (Hinck, 2012; Shen *et al.*, 2014). They belong to the TGF-β superfamily containing over 30 members which also includes activin, nodal, BMP, growth and differentiation factor (GDF) and Mullerian inhibiting substance (Zhai *et al.*, 2015). Upon secretion, TGF-β binds to a latency associated peptide (LAP) requiring proteolytic cleavage for activation (Robertson *et al.*, 2015).

Canonical TGF-β signalling begins with dimerisation of TGF-β ligands and binding to two type I (TGF-βrI) and two type II cell surface receptors (TGF-βrII). Following this, TGF-βrII transphosphorylates TGF-βrI which subsequently phosphorylates suppressor of mothers against decapentaplegic 2 (SMAD2), SMAD3 and the receptor-regulated SMAD (R-SMAD). The R-SMADs along with the common mediator SMAD4 form a trimeric complex which translocates to the nucleus where they interact with transcription factors to regulate TGF-β responsive genes (Tzavlaki *et al.*, 2020) (Figure 1.7).

Whereas IL-1 and TNF-α can be said to promote catabolism, the role of TGF-β in OA is not so straightforward. Congruent with a role in cartilage catabolism, TGF-β1 has been found to induce expression of MMP-13 in human articular chondrocytes (Shlopov *et al.*, 1999) and MMP-1 and ADAMTS-4 in fibroblast-like synoviocytes (Cheon *et al.*, 2002; Yamanishi *et al.*, 2002). Overexpression of TGF-β1 in mouse knees by intra-articular injection of recombinant human TGF-β1 or adenoviral vector induced OA-like changes including the formation of osteophytes, synovial inflammation and hyperplasia (van Beuningen *et al.*, 2000; Bakker *et al.*, 2001). In line with this, inhibition of TGF-β signalling has been shown to reduce cartilage degradation and calcification in surgically induced OA models (Zhen *et al.*, 2013).

Based on this one might conclude that TGF-β plays a catabolic role in OA, however it does not appear to that clear-cut. *In vitro*, treatment of rat chondrocytes with TGF-β1 upregulated expression of type II collagen and aggrecan (Zhu *et al.*, 2015). Clearly this would be

beneficial in the context of OA. *In vivo*, tissue specific inhibition of TGF-β signalling, via conditional knockout or expression of a dominant-negative mutant of TGF-βrII, was found to promote terminal differentiation of articular chondrocytes and an OA-like phenotype in mice with a concomitant upregulation of *Mmp13*, *Adamts4* and *Adamts5* found in TGF-βrII knockout animals (Serra *et al.*, 1997; Shen *et al.*, 2013). TGF-β1 is decreased in heavily degraded human OA cartilage (Verdier *et al.*, 2005) and mutation of *Smad3* results in an OA-like phenotype (Yang *et al.*, 2001). Finally, a recent large genome-wide association study found single nucleotide polymorphism (SNPs) in TGF-β1 and Smad3 amongst other TGF-β signalling components to be significantly associated with OA (Tachmazidou *et al.*, 2019).

Therefore, whilst TGF-β may favour the progression of OA by stimulating the expression of cartilage-degrading enzymes, inhibition of TGF-β signalling causes terminal differentiation of articular chondrocytes, another feature of OA. In light of this, Baugé *et al.* (2014) propose a model in which short term stimulation (30-60 minutes) with TGF-βI activates SMAD2/3 and TGF-βrII expression but longer term stimulation (24 hours) results in a reduction in SMAD3 and TGF-βrII expression due to a negative feedback loop (Baugé *et al.*, 2011). In this scenario TGF-β signalling would require tight regulation in order to maintain homeostasis within the joint with both positive and negative perturbations contributing to pathogenesis.

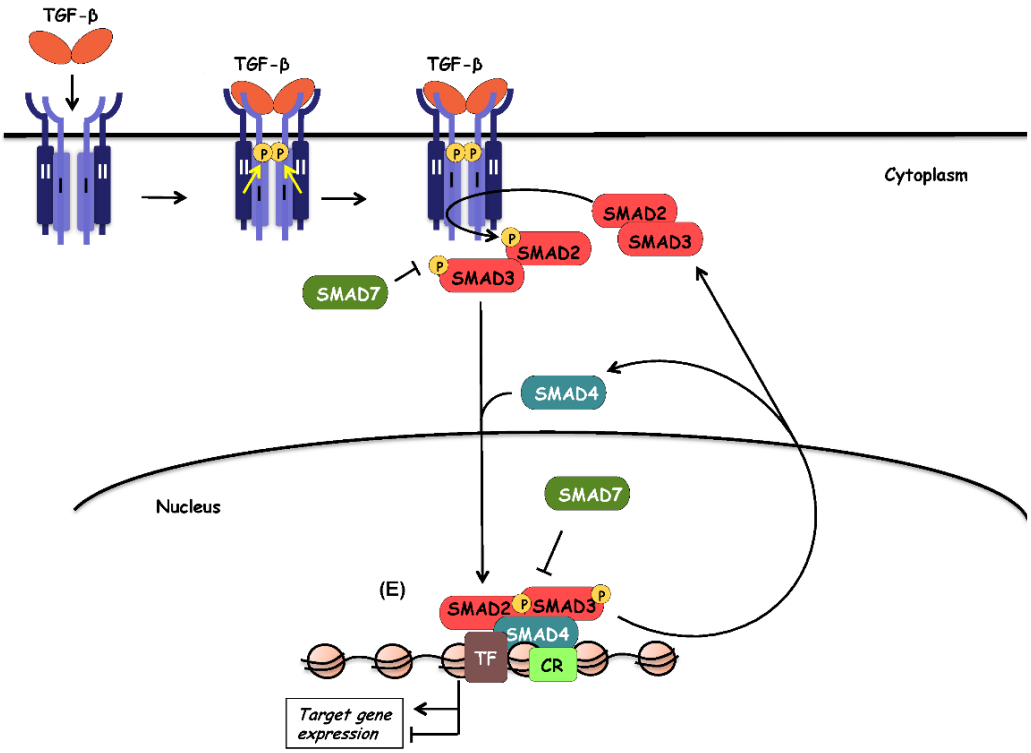

Figure 1.7. Overview of TGF-β signalling. *In canonical TGF-β signalling a TGF-β dimer binds to a heteromer of type I and type II receptors. Signalling proceeds with transphosphorylation of type I receptors by type II, phosphorylation of SMAD2 and SMAD3, and translocation along with SMAD4 to the nucleus to mediate TGF-β responsive gene expression. Taken from Tzavlaki and Moustakas, 2020.*

1.2.2.2.4 Wnt signalling

Wnt ligands consist of 19 secreted glycoproteins with roles in development, growth, homeostasis and disease (Majidinia *et al.*, 2018). Activation of Wnt receptors can trigger several different intracellular signalling pathways, broadly categorised as either canonical or non-canonical, however the canonical Wnt/β-catenin pathway is best studied and apparently the most relevant in bone and cartilage. In canonical Wnt signalling, association of a Wnt glycoprotein with a frizzled (FZD) receptor and LRP-5 or 6 leads to phosphorylation and inhibition of GSK-3β, part of the β-catenin destruction complex (Lodewyckx *et al.*, 2009). Following this, cytoplasmic β-catenin is able to accumulate and translocate to the nucleus where it regulates Wnt target gene expression through interactions with members of the T-cell factor (TCF) and lymphoid enhancer factor (LEF) families (Corr, 2008; Y. Wang *et al.*, 2019).

Wnt signalling plays an important role in cartilage and bone development and thus, dysregulation contributes to OA pathogenesis (Zhu *et al.*, 2009; Y. Wang *et al.*, 2019). Protein levels of Wnt-3a and β-catenin were increased in a rat model of OA (Liu *et al.*, 2016) and cartilage specific overexpression of β-catenin in adult mice produced an OA-like phenotype (Zhu *et al.*, 2009). This can be explained by the fact that acute activation of Wnt/β-catenin signalling in rabbit articular chondrocytes induced the expression of MMP-3 and 13 as well as ADAMTS-4 and 5 (Yuasa *et al.*, 2008). Similarly, recombinant Wnt-induced signalling protein 1 (WISP1) increased expression of ADAMTS-4, MMP-3, 9 and 13 in murine macrophages and MMP-3 and 9 in human chondrocytes with both WISP1 and β-catenin being upregulated in murine and human OA joints (Blom *et al.*, 2009).

On the other hand, reduced Wnt signalling may also contribute to OA development. Cartilage-specific inhibition of β-catenin signalling caused severe cartilage degradation and chondrocyte apoptosis (Zhu *et al.*, 2008). Therefore, similarly to TGF-β, it appears that tight regulation of Wnt signalling may be required for joint articular cartilage homeostasis with dysregulation either way contributing to OA pathogenesis.

1.2.2.2.5 Nuclear factor-κB

As previously discussed, inflammatory cytokines such as IL-1 and TNF-α are known to play a role in OA. This being said, whether OA is an inflammatory disease remains controversial (Nishimura *et al.*, 2020). Members of the NF-κB inducible transcription factor family regulate a plethora of genes involved in both immune and inflammatory responses (T. Liu *et al.*, 2017) and thus, it is not surprising that NF-κB is widely involved in OA (Marcu *et al.*, 2010). In response to intracellular signalling triggered by IL-1 or TNF-α for example, sequestration of NF-κB by its cognate inhibitory protein, inhibitor of NF-κB (IκB), is relieved due to IκB

degradation (canonical) or processing (non-canonical) which permits nuclear translocation and regulation of target genes (T. Liu *et al.*, 2017).

NF-κB is a major downstream effector of IL-1 and TNF-α signalling. IL-1β induction of MMP-1 and MMP-13 expression has been shown to be dependent on NF-κB (Mengshol *et al.*, 2000) as has TNF-α induced attenuation of collagen type II synthesis (Séguin *et al.*, 2003). Consistent with this, overexpression of IκB has been shown to block IL-1β induced gene expression (Grall *et al.*, 2003). In contrast to typical IκB proteins which solely inhibit NF-κB, IκBζ appears to modulate NF-κB signalling by acting as a transcriptional cofactor. IκBζ was upregulated in OA cartilage with cartilage-specific overexpression promoting an OA-like phenotype and knockout protecting against OA in the DMM mouse model (Choi *et al.*, 2018).

Cartilage specific homozygous knockout of *RelA* (a NF-κB subunit) accelerated OA progression in mice through chondrocyte apoptosis however, heterozygous knockout protected against OA by inhibiting catabolism whilst preventing chondrocyte apoptosis (Kobayashi *et al.*, 2016). *RelA* expression has also been reported to be increased in the synovium of OA patients (Ahmed *et al.*, 2018). Therefore, NF-κB regulation in OA may be viewed as biphasic with perturbation of homeostasis, as opposed to specifically increased or decreased NF-κB signalling being responsible for OA progression (Kobayashi *et al.*, 2016).

1.2.2.2.6 Mechanoflammation

Inflammation is clearly a part of OA however it has become clear that the inflammation seen in OA is distinct from that seen in RA (Vincent, 2020). As opposed to RA where inflammation is driven by an inappropriate immune response, inflammation in OA is thought to be a response to mechanical injury – “mechanoflammation” (Smolen et al., 2018; Vincent, 2019). As previously discussed, mechanical load is an important factor in OA with abnormal wear of a normal joint or normal wear of a structurally compromised joint contributing to the disease process. While evidence has pointed towards an important role for inflammatory cytokines such as IL-1 and TNF-α, treatments targeting these have shown little promise. More recent evidence has demonstrated the mechanosensory ability of articular cartilage, injury induced stimulation of inflammatory pathways and subsequent catabolic protease release (Vincent and Wann, 2019).

Disuse of joints through paralysis, lower limb amputation or joint immobilisation has been shown to reduce articular cartilage thickness (Pool, 1974; Anderson and Breidahl, 1981; Benichou and Wirotius, 1982; Hudelmaier et al., 2006; Liphardt et al., 2009) whereas research using in vivo models points to an increase in cartilage thickness in response to

exercise training (Kiviranta et al., 1988; Ni et al., 2013). Importantly, although moderate exercise may increase cartilage thickness, excessive mechanical load through strenuous exercise or cartilage injury may have an adverse effect (Ni et al., 2013). In line with this, prevention of joint flexion (but not complete abolition of load bearing) by simultaneous sciatic neurectomy and DMM surgery protected against OA development in mice (Burleigh et al., 2012). Initially, changes in cartilage thickness in response to mechanical load were speculated to be mediated though increased nutrient diffusion (Pool, 1974), however more recently molecular responses to mechanical load by chondrocytes have emerged as the primary driver.

Several molecular responses to mechanical load by chondrocytes have been identified. Rapid induction of Wnt signalling has been observed in response to cartilage injury (Dell'Accio et al., 2006, 2008) with transient bursts of Wnt signalling being associated with increased cartilage thickness in mice (Yuasa et al., 2009). Mechanical loading and injury have been shown to stimulate the release of heparan sulfate-bound growth factors from the pericellular matrix including FGF2 and TGF-β (Vincent et al., 2002, 2004; Chia et al., 2009; Tang et al., 2018). Growth factor release upon mechanical stress was mediated by a sodium flux and consequent reduction in affinity for heparan sulfate (Keppie et al., 2021). In porcine cartilage, simple mechanical injury has been shown to activate mitogen-activated protein kinase (MAPK), NF-κB and TGF-β-activated kinase 1 (TAK1) signalling pathways along with inducing expression of IL-1α and IL-1β (Gruber et al., 2004; Ismail et al., 2017). TAK1 is upstream of the MAPKs and its activation, either by cytokines such as IL-1, TGF-β and TNF or by mechanical injury, induces aggrecan degradation, largely by ADAMTS-5 (Ismail et al., 2015, 2016).

In light of the above, it is clear that the inflammation seen in OA is distinct from that seen in RA, and unsurprising that RA therapies are showing little promise in the treatment of OA (Vincent, 2020). For example, whilst IL-1β is upregulated in OA patients (Farahat et al., 1993; Melchiorri et al., 1998) and stimulates protease activity in vitro (Pratta et al., 2003), therapies targeting IL-1β are yet to demonstrate efficacy (Vincent, 2020). Therapeutic strategies targeting mechanical load may be more effective. A study using joint distraction (two months) to reduce joint compression and prevent joint flexion has shown promising results with improved pain scores, decreased joint space narrowing and increased cartilage thickness reported after one and two years (Intema et al., 2011; Wiegant et al., 2013). Improved pain scores and decreased joint space narrowing persisted even after 5 years (van der Woude et al., 2016). While current evidence is remains limited, a recent meta-analysis of 11 studies found promising clinical outcomes from knee joint distraction (Jansen et al., 2021).

1.2.2.3 DNA methylation

DNA methylation is one of several epigenetic mechanisms - heritable changes in gene expression occurring without the mutation of DNA sequence (Bird, 2007). Briefly, DNA methylation involves the addition of a methyl group to the fifth carbon of a cytosine nucleotide. Broadly, DNA methylation is associated with the repression of gene expression, often inhibiting the binding of methylation sensitive transcription factors to gene promoters (Greenberg *et al.*, 2019), however methylation within genes has been associated with increased gene expression, regulation of splicing and transcription from alternative promoters (Maunakea *et al.*, 2010; Lev Maor *et al.*, 2015).

The major mediators of DNA methylation are the DNA methyltransferases (DNMTs) which catalyse the addition of a methyl group to cytosine generating 5-methylcytosine (5-mC). Establishment of DNA methylation is carried out by the *de novo* DNMTs, DNMT3A and DNMT3B (Okano *et al.*, 1999) whereas DNMT1 is responsible for the maintenance of DNA methylation through cell division and consequent DNA replication (Bestor, 2000). DNMT3L is catalytically inactive however has been found to promote the activity of the *de novo* DNMTs (Bourc'his *et al.*, 2001; Ooi *et al.*, 2007). Removal of DNA methylation can occur passively as a result of DNA replication. Alternatively, active demethylation is initiated by ten-eleven translocation (TET) driven oxidation of 5-mC, followed by replication driven demethylation or thymine DNA glycosylase (TDG) base removal and base excision repair (Greenberg *et al.*, 2019).

Dysregulation of DNA methylation is a documented feature of many diseases, most notably in cancer, however the role of DNA methylation in OA is less understood. When comparing global DNA methylation and expression of *DNMT1* and *DNMT3A*, Sesselmann *et al.* (2009) found no significant differences in chondrocytes from femoral head cartilage and OA knee cartilage. However, more recent research demonstrated a decrease in *DNMT3B* expression in human OA chondrocytes, as well as in a surgically induced OA mouse model, associated with augmented metabolism (Shen *et al.*, 2017). No difference in the expression of *TET2* and *TET3* was found in OA chondrocytes however expression of *TET1* was significantly downregulated (Taylor *et al.*, 2014). Moreover, *Tet1* knockout mice were protected from OA development after DMM surgery (Smeriglio *et al.*, 2020).

Hypomethylation in the promoters of *ACAN, COL2A1*, *SOX9* and runt-related transcription factor 2 (*RUNX2*) was found to be unrelated to expression patterns in chondrocytes (Fernández *et al.*, 1985; Pöschl *et al.*, 2005; Dickhut *et al.*, 2008; Ezura *et al.*, 2009; Imagawa *et al.*, 2014). The role of DNA methylation in OA may be more nuanced than broad changes in promoter regions. For *ADAMTS4*, *MMP3*, *MMP9* and *MMP13*, OA-related changes in expression were associated with the methylation of specific CpG sites (Roach

et al., 2005). On the other hand, hypermethylation of CpG sites in the promoters of *SOX9*, *SOD2* and *COL9A1* has been associated with downregulation of these genes in OA (Scott *et al.*, 2010; Kim *et al.*, 2013; Imagawa *et al.*, 2014).

More recently, genome-wide analyses have provided further insights with global methylation patterns being able to reliably distinguish between healthy and OA chondrocytes (Fernández-Tajes *et al.*, 2014; Jeffries *et al.*, 2014; Rushton *et al.*, 2014). Differentially methylated loci in OA have also been found to be enriched for relevant pathways including TGF-β signalling, cartilage development, ECM and inflammatory response (Rushton *et al.*, 2014; Li *et al.*, 2018) Finally, genome-wide analyses have identified distinct epigenetic signatures in knee and hip cartilage suggesting that changes in methylation in relation to OA may heterogenous across affected tissues (den Hollander *et al.*, 2014; Wu *et al.*, 2020).

1.3 MicroRNAs

MicroRNAs (miRNA) are small non-coding double stranded RNAs (ncRNA) approximately 22 nucleotides (nt) in length that regulate gene expression at the posttranscriptional level. Initially identified as small antisense RNAs involved in *Caenorhabditis elegans* development (Lee *et al.*, 1993; Reinhart *et al.*, 2000), miRNAs have since been found to be a common feature of eukaryotic genomes. To date more than 2500 miRNAs have been identified in humans (miRbase v22.1; mirbase.org; Kozomara, Birgaoanu and Griffiths-Jones, 2019) with miRNAs predicted to target more than 60% of human genes (Friedman *et al.*, 2009). With that in mind, it is not surprising that miRNA biogenesis and function are tightly regulated, and their dysregulation is associated with a wide range of human diseases (Paul *et al.*, 2017).

1.3.1 Biogenesis

Although microRNAs are found ubiquitously amongst both plants and animals, stark differences in the biogenesis of microRNAs in plants and animals exist. Therefore, only microRNA biogenesis in animals will be discussed (Figure 1.8).

In humans, the majority of miRNAs are found in the introns of coding and non-coding genes and thus, primary miRNAs (pri-miRNA) are liberated during the splicing of RNA pol II transcribed messenger RNA (mRNA) and expression is often regulated by the host gene promoter (Ha *et al.*, 2014). However some miRNAs are found in exons, intron-exon junctions and antisense strands and many have been found to possess their own promoters and regulatory elements (Monteys *et al.*, 2010; Liu *et al.*, 2018). MiRNAs can also be found in polycistronic units - often functionally related - which are subsequently processed into individual mature miRNAs (Lee *et al.*, 2002).

In canonical miRNA biogenesis, following transcription of the pri-miRNA, the stem loop structure is cleaved by the microprocessor complex, containing Drosha, a nuclear RNase III and its cofactor DiGeorge syndrome critical region in gene 8 (DGCR8), releasing the approximately 70 nt pre-miRNA for nuclear export (Lee *et al.*, 2003; Denli *et al.*, 2004). In association with exportin-5 and Ras-related nuclear protein guanine triphosphate (RAN-GTP), precursor miRNA (pre-miRNA) is exported into the cytoplasm through a nuclear pore complex (Bohnsack *et al.*, 2004; Lund *et al.*, 2004) and once in the cytoplasm, pre-miRNA is cleaved near the stem loop by Dicer forming a miRNA duplex composed of a 5 prime (-5p) and 3 prime (-3p) strand (Bernstein *et al.*, 2001; Hutvágner *et al.*, 2001; Knight *et al.*, 2001). This short RNA duplex is loaded onto an Argonaute protein (AGO) forming the effector complex: miRNA-induced silencing complex (mRISC) (Tabara *et al.*, 1999; Hammond *et al.*, 2001). Specifically, formation of RISC can be seen as occurring via a two-step process. Firstly, the RNA duplex is inserted into AGO and secondly, the duplex is unwound with the passenger strand being discarded and the guide strand remaining to form the mature mRISC (Kawamata *et al.*, 2010). However this is not always the case as some passenger strands have been shown to be active miRNAs themselves (L. Guo *et al.*, 2010). It is thought that decreased stability in the 5' end of the guide strand compared to the passenger strand in addition to a preference for strands beginning with a U nucleotide is what drives asymmetric strand selection (Khvorova *et al.*, 2003; Schwarz *et al.*, 2003; Ha *et al.*, 2014). RISC is then able to regulate gene expression by exploiting base complementarity between the miRNA and its target.

Although the canonical miRNA biogenesis pathway is the dominant pathway, multiple non-canonical pathways have been identified, broadly categorised as Drosha/DGCR8-independent and Dicer-independent (O'Brien *et al.*, 2018). In Drosha/DGCR8-independent biogenesis, pre-miRNAs suitable for Dicer processing are produced without the need for Drosha/DGCR8 processing, for example mirtrons bypass Drosha cleavage instead being directly spliced from introns (Ruby *et al.*, 2007). Alternatively, in Dicer-independent biogenesis short hairpin RNAs are processed by Drosha, exported to the cytoplasm and directly loaded into AGO. Yang *et al.* (2010) found that mature miR-451 was still produced in Dicer-knockout cells whereas depletion of Drosha, DGCR8 or AGO2 significantly reduced its production.

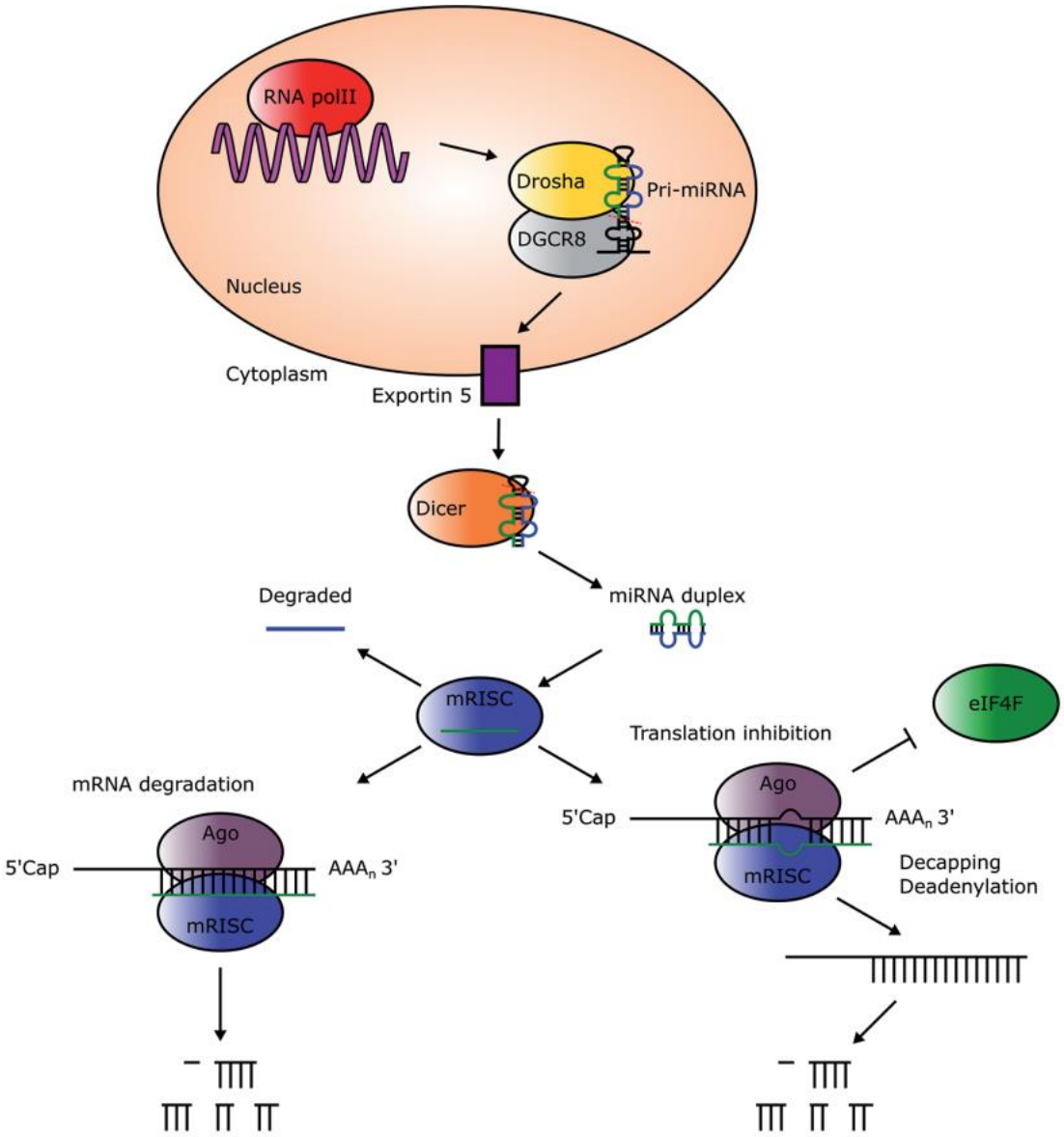

Figure 1.8. Canonical microRNA biogenesis. *MiRNAs are transcribed by RNA polymerase II (pol II) into a pri-miRNA prior to cropping by the microprocessor and nuclear export associated with exportin 5. Once in the cytoplasm, Dicer processes the pre-miRNA forming a small RNA duplex of which, one strand is used to form mRISC. Using this ~22nt RNA strand as a guide, mRISC targets translational repression or degradation of mRNAs. Taken from Swingler et al. 2019.*

1.3.2 Mechanism of action

Predominantly, miRNAs regulate gene expression through binding to complimentary sequences in target mRNA 3'-untranslated region (UTR) and subsequent repression of translation (Ha *et al.*, 2014). In plants, miRNAs are nearly or completely complementary to their targets whereas in animals complementarity is usually partial (Voinnet, 2009). Because of this, initially, plant miRNA repression was thought to be exclusively through mRNA cleavage and animal miRNA repression through translation inhibition. However it has now been found that mRNA cleavage and translation inhibition take place in both to varying extents (Huntzinger *et al.*, 2011)

In animals, miRNAs primarily recognise their targets through Watson-Crick base pairing to a 6-8 bp seed sequence in the 3'-UTR of target genes (Lewis *et al.*, 2003). Initially, it was thought that miRNAs negatively regulated targets through blocking of elongation and termination during protein synthesis given that mRISC and target mRNAs were found to be associated with polyribosomes in both *C. elegans* and rats (Olsen *et al.*, 1999; Seggerson *et al.*, 2002; Kim *et al.*, 2004). However, whilst miRNAs are associated with ribosomes, more recent evidence suggests that mRISC downregulates targets via inhibition of translational initiation (Ingolia *et al.*, 2009; Bazzini *et al.*, 2012). Moreover, translation repression and mRNA degradation may be part of a sequential process in which inhibition of translation precedes mRNA degradation (Djuranovic *et al.*, 2012; Meijer *et al.*, 2013). Whilst it was traditionally thought that miRNAs negatively regulated expression via inhibition of translation, mRNA degradation has been shown to account for at least 84% of miRNA repression of protein production (H. Guo *et al.*, 2010; Eichhorn *et al.*, 2014). Degradation of mRNAs proceeds by deadenylation and/or decapping of mRNAs leaving them vulnerable to exonucleolytic degradation (Figure 1.8) (Valinezhad Orang *et al.*, 2014).

Interestingly, miRNA binding sites are not limited to 3'-UTRs, neither are their actions limited to repression. Functional miRNA binding sites have been found in the 5'-UTRs as well as in the coding sequence of target genes (Lytle *et al.*, 2007; Lee *et al.*, 2009; Forman *et al.*, 2010; Xu *et al.*, 2014). Whilst miRNA binding in 5'-UTRs and coding regions represses gene expression (Forman *et al.*, 2008; Zhang *et al.*, 2018), binding of miR-324 to the RelA promoter increases gene expression (Dharap *et al.*, 2013). Similarly, miR-145 and miR-206 have been shown to upregulate myocardin and Kruppel-like factor 4 (KLF4) respectively however the mechanism for this upregulation remains unclear (Cordes *et al.*, 2009; Lin *et al.*, 2011).

1.3.3 Role of microRNAs in osteoarthritis

MiRNAs play a critical role in animal development. Inhibition of miRNA biogenesis via Dicer knockout caused mice to die early in embryonic development (E7.5) with embryos being depleted of stem cells (Bernstein *et al.*, 2003). Knockout of Dicer in murine limb mesenchyme resulted in the formation of smaller limbs (Harfe *et al.*, 2005) whereas conditional knockout of *Dicer*, *Dgcr8* or *Drosha* in chondrocytes reduced cell proliferation, accelerated hypertrophic differentiation in the growth plates and caused premature death (Kobayashi *et al.*, 2008, 2015). Therefore, miRNAs are clearly important in skeletogenesis and embryonic development more broadly.

Multiple studies have identified miRNAs that are differentially expressed in cartilage from OA patients compared to normal cartilage (Table 1.1) (Iliopoulos *et al.*, 2008; Jones *et al.*, 2009; Díaz-Prado *et al.*, 2012; Balaskas *et al.*, 2017). Likely due to differences in samples as well as methodolgies there is poor overlap in differentially expressed miRNAs in both microarray and RNA-seq experiments (Swingler *et al.*, 2019). That being said, bioinformatics analyses integrating data from multiple miRNA expression studies have identified common miRNA signatures which may represent groups of miRNAs that are functionally involved in OA pathogenesis (Cong *et al.*, 2017; Wang *et al.*, 2018).

Table 1.1. Differentially regulated microRNAs in OA and functional effects

MicroRNA	Functional effect	Tissue / platform			References
miR-16 ↑	Inhibition of FGFR by targeting SMAD3, altered proliferation and increased apoptosis, TGF-β signalling pathway affected	Plasma / TLDA* and qRT-PCR^{ns}			(Borgonio Cuadra *et al.*, 2014)
miR-21 ↑	Inhibition of GDF-5 expression	Knee cartilage / qRT-PCR*			(Zhang *et al.*, 2014)
miR-23a ↑	Inhibition of COL2A1 and ACAN by targeting SMAD3, targeting of RC3H1 and QKI	Knee cartilage / qRT-PCR*	Synovial fluid (early vs late OA) / Exiqon PCR array* and qRT-PCR*		(Kang *et al.*, 2016; Y. H. Li *et al.*, 2016)
miR-25 ↑	WFA-induced upregulation of COX-2 expression, mediation of inflammatory responses in chondrocytes	Knee cartilage / qRT-PCR*			(Jones *et al.*, 2009)
miR-27b ↑	Suppression of RC3H1 and QKI in OA synovium, inhibition of MMP-13 and osteogenic differentiation	Synovial fluid (early vs late OA) / Exiqon PCR array* and qRT-PCR*	Knee bone / qRT-PCR*	Synovial fluid / qRT-PCR*	(Jones *et al.*, 2009; Y. H. Li *et al.*, 2016; Lv *et al.*, 2020; Zhang *et al.*, 2020)
miR-29b ↑	Induction of chondrocyte apoptosis by targeting progranulin, inhibition of TGF-β signalling	Hip cartilage / qRT-PCR*	Hip cartilage / qRT-PCR^{ns}		(Le *et al.*, 2016; L. Chen *et al.*, 2017)
miR-29c ↑	Inhibition of TGF-β signaling	Plasma / TLDA* and qRT-PCR^{ns}	Hip cartilage / qRT-PCR*	Synovial fluid (early vs late OA) / Exiqon PCR array* and qRT-PCR*	(Borgonio Cuadra *et al.*, 2014; Le *et al.*, 2016; Y. H. Li *et al.*, 2016)
miR-30b ↑	Cartilage matrix degradation by targeting SOX9, ADAMTS-5 and ERG	Plasma / TLDA*			(Borgonio Cuadra *et al.*, 2014)
miR-30c ↑	Cartilage matrix degradation by targeting SOX9, ADAMTS-5 and ERG	Plasma / TLDA^{ns}			(Borgonio Cuadra *et al.*, 2014)
miR-33a ↑	Upregulation of MMP-13 and ECM degradation, regulation of cholesterol synthesis in TGF-β1/Akt/SREBP-2 pathway and cholesterol efflux-related ApoA1 and ABCA1	Knee cartilage / qRT-PCR*			(Kostopoulou *et al.*, 2015)

miR-34b ↑	Modulation of OA chondrocyte proliferation by targeting CYR61, which inhibits ADAMTS-4 induced aggrecan degradation in cartilage	Knee bone / qRT-PCR*			(Jones *et al.*, 2009)
miR-104 ↑	Unknown	Knee bone / qRT-PCR*			(Jones *et al.*, 2009)
miR-122a ↑	Unknown	Knee bone / qRT-PCR*			(Jones *et al.*, 2009)
miR-126 ↑	Unknown	Plasma / TLDA* and qRT-PCR^{ns}			(Borgonio Cuadra *et al.*, 2014)
miR-128a ↑	Repression of chondrocyte autophagy by targeting Atg12	Knee cartilage / qRT-PCR*			(Lian *et al.*, 2018)
miR-135a ↑	Unknown	Knee bone / qRT-PCR*			(Jones *et al.*, 2009)
miR-135b ↑	Unknown	Knee bone / qRT-PCR*			(Jones *et al.*, 2009)
miR-139 ↑	Inhibition of MCPIP1, activation of IL-6 and apoptosis	Knee bone / qRT-PCR*			(Jones *et al.*, 2009)
miR-144 ↑	Unknown	Knee bone / qRT-PCR*			(Jones *et al.*, 2009)
miR-146a ↑	Targeting SMAD4 disturbing TGF-β pathway, increased apoptosis, upregulation of VEGF	Plasma / TLDA^{ns} and qRT-PCR^{ns}	Hip cartilage / qRT-PCR*	Synovial tissue / qRT-PCR^{ns}	(Li *et al.*, 2012; Wang *et al.*, 2013; Borgonio Cuadra *et al.*, 2014; Cheleschi *et al.*, 2019)
miR-147 ↑	Unknown	Knee bone / qRT-PCR*			(Jones *et al.*, 2009)
miR-181a ↑	Inhibition of chondrocytes proliferation and induction of apoptosis by targeting PTEN	Facet cartilage / Exiqon miRNA array (n = 2) and qRT-PCR*			(Nakamura *et al.*, 2016)
miR-181b ↑	Articular cartilage degeneration, destruction of lumbar facet joint cartilage	Knee cartilage / qRT-PCR*			(Song, Lee, *et al.*, 2013)
miR-184 ↑	Unknown	Plasma / TLDA* and qRT-PCR*			(Borgonio Cuadra *et al.*, 2014)
miR-186 ↑	Unknown	Plasma / TLDA* and qRT-PCR*	Synovial fluid (early vs late OA) / Exiqon PCR array* and qRT-PCR*		(Borgonio Cuadra *et al.*, 2014; Y. H. Li *et al.*, 2016)

miR-200a ↑	Unknown	Knee cartilage / qRT-PCR*		(Jones *et al.*, 2009)
miR-210 ↑	Inhibition of NF-κB signaling pathway by targeting DR6 increasing inflammation	Knee bone / qRT-PCR^{ns}	Synovial fluid / qRT-PCR*	(Jones *et al.*, 2009; D. Zhang *et al.*, 2015; Xie *et al.*, 2019)
miR-215 ↑	Inhibition of synovium pain-related genes, especially DST and TBXAS1	Synovial tissue / RNA-seq*		(Zhou *et al.*, 2020)
miR-218 ↑	Inhibition the PI3K/Akt/mTOR signalling pathway, cartilage destruction	Knee cartilage / qRT-PCR*		(Lu *et al.*, 2017)
miR-224 ↓	Regulation of synovium pain-related genes, especially DST and TBXAS1, targeting CCL2	Knee cartilage / qRT-PCR*		(Haiming Wang *et al.*, 2019; Zhang *et al.*, 2021)
miR-299 ↑	Unknown	Knee cartilage / qRT-PCR*		(Jones *et al.*, 2009)
miR-335 ↑	Inhibition of synovium pain-related genes, especially DST and TBXAS1, inhibition of MSC differentiation	Hip cartilage / qRT-PCR*		(Kopańska *et al.*, 2017; Haiming Wang *et al.*, 2019)
miR-345 ↑	Unknown	Plasma / TLDA* and qRT-PCR*		(Borgonio Cuadra *et al.*, 2014)
miR-365 ↑	Upregulated expression of catabolic COL10A1 and MMP-13 by targeting HDAC4, activation of IL-6 and apoptosis	Knee cartilage / qRT-PCR*		(Yang *et al.*, 2016)
miR-381 ↑	Upregulation of MMP13 and RUNX2 expression via targeting of HDAC4 cartilage degeneration, targeting of IkBα	Synovial tissue / qRT-PCR*		(Chen *et al.*, 2016; Xia *et al.*, 2016)
miR-455 ↑	Regulating TGF-β signalling by suppression of the Smad2/3 pathway, targeting ACVR2B, SMAD2, CHRDL1	Hip cartilage / qRT-PCR*		(Swingler *et al.*, 2012)
miR-486 ↑	Inhibition of chondrocyte proliferation and migration by suppressing SMAD2 gene	Knee cartilage / qRT-PCR*		(Shi *et al.*, 2018)
miR-885 ↑	Unknown	Plasma / TLDA^{ns} and qRT-PCR*		(Borgonio Cuadra *et al.*, 2014)

miR-9 ↓/↑	Increased chondrocytes proliferation and inhibition of cell apoptosis by targeting NF-κB	Knee cartilage / qRT-PCR*		Knee cartilage and bone / qRT-PCR*	(Jones *et al.*, 2009; Gu *et al.*, 2016)
miR-26 ↓	Induction of NF-κB signaling pathway	Knee cartilage / qRT-PCR*			(Yin *et al.*, 2017; Z. Zhao *et al.*, 2019)
miR-29a ↓/↑	Inhibition of SMAD3, NFκB and WNT signaling pathway, downregulated expression of collagen III, TGF-β1, MMP-9, MMP-13, and ADAMTS-5, targeted VEGF	Plasma / TLDA^{ns}	Synovial tissue / qRT-PCR*	Hip cartilage / qRT-PCR*	(Borgonio Cuadra *et al.*, 2014; Le *et al.*, 2016; Ko *et al.*, 2017)
miR-107 ↓	Unknown	Knee cartilage / qRT-PCR*			(Jones *et al.*, 2009)
miR-125b ↓	ADAMTS-4 - induced aggrecan degradation in cartilage	Hip cartilage / qRT-PCR*			(Rasheed *et al.*, 2019)
miR-127 ↓	decreased ECM synthesis by targeting IL-1β induced MMP-13	Knee cartilage (hip control) / qRT-PCR*			(Su Jin Park *et al.*, 2013)
miR-130a ↓	Reciprocal sponging of HOTAIR lncRNA, increased apoptosis suppression of autophagy in chondrocytes	Knee cartilage / qRT-PCR*			(He *et al.*, 2020)
miR-140 ↓	Targeting IGFR, ADAMTS5, MMP-13, IGFBP5 and RALA, cartilage development and homeostasis, development of age-related OA-like changes	Knee cartilage / qRT-PCR*		Knee cartilage and synovial fluid / qRT-PCR*	(Miyaki *et al.*, 2009, 2010; Liang *et al.*, 2012; Karlsen *et al.*, 2014; Si *et al.*, 2017)
miR-145 ↓	Promotion of TNF-α-driven cartilage matrix degradation via MMP-3, MMP-13, and ADAMTS-5	Knee cartilage / qRT-PCR*			(B. Yang *et al.*, 2011)
miR-148a ↓	Targeting COL10A1, MMP13 and ADAMTS5, inhibition of hypertrophic differentiation, production and deposition of type II collagen and proteoglycan retention	Knee cartilage / qRT-PCR*			(Vonk *et al.*, 2014)
miR-149 ↓/↑	Upregulation of TNFα, IL1β and IL6, activation of inflammation by targeting TNFα	Knee cartilage / qRT-PCR*	Knee cartilage / qRT-PCR*	Knee bone / qRT-PCR*	(Jones *et al.*, 2009; Santini *et al.*, 2014)

miR-221 ↓	Activation of expression of catabolic genes, degeneration of cartilage tissues by upregulated expression of SDF1	Knee cartilage / RNA-seq* and qRT-PCR*	(Zheng *et al.*, 2017)
miR-483 ↓	Upregulation of catabolic genes expression, inhibition of TGF-β signaling pathway	Plasma / TLDA^{ns}	(Borgonio Cuadra *et al.*, 2014)
miR-488 ↓	Upregulation of catabolic genes expression by targeting ZIP8	Knee cartilage / qRT-PCR*	(Song, Kim, *et al.*, 2013)
miR-558 ↓	Inhibition of COX-2 expression, inhibition of IL-1β-stimulated catabolic effect, altered inhibition of inflammatory factors	Knee cartilage (hip control) / qRT-PCR*	(S J Park *et al.*, 2013)

*Modified from Zacharjasz et al., 2021, * $p < 0.05$, ns = not significant .*

1.3.3.1 Role of microRNAs in cartilage

Many miRNAs have been shown to play roles in chondrogenesis and thus, cartilage development and homeostasis. Moreover, increasing evidence from *in vivo* mouse models and *in vitro* studies utilising human cartilage explants points to dysregulation of miRNAs as an important feature of OA with miRNAs targeting components of key signalling pathways and being regulated by these pathways themselves.

In a bioinformatic analysis of 57 studies Cong *et al.* (2017) identified 46 miRNAs which were differentially expressed in OA cartilage and targeted genes involved in autophagy, inflammation, chondrocyte apoptosis, chondrocyte differentiation & homeostasis, chondrocyte metabolism and degradation of the ECM. Similarly, in a meta-analysis of 8 miRNA expression studies Wang *et al.* (2018) identified 87 differentially expressed miRNAs along with a "miRNA meta-signature" of 6 significantly dysregulated miRNAs. This miRNA meta-signature included upregulation of miR-23b-3p, miR-27b-3p, miR-211-5p and miR-16-5p, and downregulation of miR-25-3p and miR-149-5p. Using healthy and OA cartilage from the same patient, RNA sequencing revealed differential expression (DE) of 142 miRNAs and 2387 mRNAs with miR-206 and miR-504-5p being the most upregulated and downregulated respectively (Coutinho de Almeida *et al.*, 2019). Using these data, an OA miRNA interactome was generated consisting of 62 miRNAs targeting 238 mRNAs highlighting the fact that in a complex tissue such as cartilage, miRNAs will have multiple target genes. Whilst studies identifying differentially expressed miRNAs in OA cartilage are useful in highlighting potentially important interactions, more in-depth studies of these interactions utilising *in vivo* and *in vitro* models are required to fully understand their relevance in disease and how they may be targeted for therapies.

To date, miR-140 is the best studied miRNA in OA. MiR-140 was found to be specifically expressed in cartilage tissues during murine embryonic development (Tuddenham *et al.*, 2006) and although deletion of miR-140 did not appear to affect embryonic skeletal development, postnatally it resulted in smaller, lower weight mice which exhibited craniofacial deformities (Miyaki *et al.*, 2010). Moreover, miR-140-null mice had accelerated age-related OA and more severe OA in a surgically induced model whereas cartilage specific overexpression of miR-140 protected against OA (Miyaki *et al.*, 2010). Functionally, miR-140 has been shown to regulate the expression of *ADAMTS5*, *MMP13*, tissue inhibitors of metalloproteinase 1 (*TIMP1*), *DNPEP*, specificity protein 1 (*SP1*), *RALA* and *FZD6* (Miyaki *et al.*, 2010; J. Yang *et al.*, 2011; Nakamura *et al.*, 2011; Liang *et al.*, 2012; Karlsen *et al.*, 2014; Barter *et al.*, 2015), whereas miR-140 was positively regulated by SOX9 (J. Yang *et al.*, 2011; Nakamura *et al.*, 2012). Therefore miR-140 is a key player in cartilage development and may be an attractive therapeutic target.

Given the significant role of miR-140 in OA, it is not surprising that subsequent studies have shed light on other miRNAs which may also be important. In total knee joint tissue from DMM and sham operated mice, miR-146a-5p, miR-3474, miR-615–3p and miR-151–5p were differentially expressed (Castanheira *et al.*, 2021). Simultaneous knockout of miR-204 and miR-211 (homologues sharing identical seed sequences) in mesenchymal progenitor cells predisposed mice to OA (Huang *et al.*, 2019). Knockout of miR-204 and miR-211 in mice led to an accumulation of RUNX2 and thus upregulation of RUNX2-induced gene expression including the matrix-degrading enzymes *Mmp13*, *Adamts4* and *Adamts5*. Conversely, cartilage-specific knockout of miR-21-5p protected against spontaneous and DMM-induced OA (X. B. Wang *et al.*, 2019). *Fgf18*, *Col2a1* and *Acan* expression was significantly increased in articular cartilage from miR-21 knockout mice whereas expression of *Mmp13* and *Adamts5* was significantly decreased.

Aside from studies utilising knockout out animals, *in vitro* models of chondrogenesis have also been used to highlight the role of specific miRNAs cartilage. MiR-455 has been shown to be coregulated with miR-140 in models of chondrogenesis, upregulated in OA cartilage and has been shown to regulate components of TGF-β signalling such as SMAD2 (Swingler *et al.*, 2012). Moreover, miR-455 was found to directly target RUNX2 and its expression was induced by SOX9 (Swingler *et al.*, 2012; Z. Zhang *et al.*, 2015). MiR-145 has been shown to directly target *SOX9* with overexpression resulting in a concomitant decrease in chondrogenic markers including *COL2A1*, *COL9A2*, *COL11A1* and *ACAN* and increase in hypertrophic markers such as *RUNX2* and *MMP13* (B. Yang *et al.*, 2011; Martinez-Sanchez *et al.*, 2012).

Many miRNAs appear to be significantly dysregulated in OA cartilage and it seems likely that that identification of miRNA signatures, as opposed to changes in individual miRNAs may be more useful in understanding their role in pathogenesis. Moreover, studies utilising OA models continue to implicate miRNAs in the regulation of cartilage metabolism and aspects of OA signalling including NF-κB, TGF-β and SOX9 (Xu *et al.*, 2016). Therefore, there may be much to be gained from an increased understanding of the roles of miRNAs in cartilage homeostasis and OA progression and furthermore, how this may be exploited in the development of therapies against OA.

1.3.3.2 MicroRNAs as biomarkers

Currently, OA diagnosis relies heavily on physical examination and radiographic imaging of affected joints. OA severity is commonly graded using the Kellgren-Lawrence scale and is based on gross joint features such as degree of joint space narrowing and bone end shape as visualised in radiographic images (Kellgren *et al.*, 1957). Given that radiography suffers from poor sensitivity and precision, OA diagnoses are reactive and thus significant disease progression is likely to already have taken place (Munjal *et al.*, 2019).

In contrast to physical and radiographic examinations, biomarkers may enable earlier and, as such, predictive diagnosis of OA. Biomarkers can be found in many biological fluids including blood, urine and synovial fluid, all of which are relatively easy to access. Interleukins have received a lot of attention as potential biomarkers as they are strongly implicated in OA pathogenesis and easily detected in blood serum. IL-21, IL-17A, IL-4R are all significantly increased in the serum of patients with OA (Silvestri *et al.*, 2006; Shan *et al.*, 2017) whereas IL-17, IL-6 are significantly increased synovial fluid (Doß *et al.*, 2007; Liu *et al.*, 2015). Articular cartilage undergoes a multitude of changes in OA and these changes, such as degradation or altered composition of the ECM may be mirrored in biological fluids. In light of this, levels of collagen X and COMP have been shown to be increased in the serum of OA patients (Verma *et al.*, 2013; He *et al.*, 2014) whilst levels of lubricin were decreased in OA synovial fluid (Musumeci *et al.*, 2014).

Recently, circulating miRNAs have been proposed as biomarkers for OA. Circulating miRNAs are highly stable and are protected from degradation in biological fluids via association with proteins such as AGO2 and incorporation into vesicles such as exosomes, microvesicles and apoptotic bodies (Turchinovich *et al.*, 2011; Gallo *et al.*, 2012). Many circulating miRNAs are by-products of cellular death (Turchinovich *et al.*, 2011) however active secretion and intercellular functioning of exosomal miRNAs has also been reported (Kosaka *et al.*, 2010). Therefore, changes in circulating miRNAs may reflect processes in early OA progression, making them attractive and potentially predictive biomarkers for OA.

Multiple miRNAs have shown promise as biomarkers for OA. In blood plasma of patients with OA, levels of miR-136 negatively correlated with disease severity and levels of its target gene IL-17 (Wan *et al.*, 2018) whereas levels of miR-98 were increased in OA patients (Zheng *et al.*, 2018). MiRNA array and microarray studies have found many other miRNAs that are differentially regulated in serum of OA patients. Ntoumou *et al.* (2017) identified 279 differentially expressed miRNAs in the serum of OA patients and used quantitative real time PCR (qRT-PCR) to validate miR-33b-3p, miR-671-3p, and miR-140-3p as being significantly downregulated. On the other hand, Borgonio Cuadra *et al.* (2014) showed that miR-16, miR-146a, miR-29c, miR-93, miR-126, miR-184, miR-186, miR-195, miR-345, and

miR-885-5p were significantly upregulated in OA blood serum. More recently, miR-146a-5p was found to be increased in the blood serum of women with OA whereas, miR-186-5p was increased in women who developed radiographic knee OA in the following 4 years suggesting its utility as a preclinical marker (Rousseau *et al.*, 2020).

Due to its proximity to the articular cartilage and integral role in the joint, synovial fluid is the first biological fluid to be altered during OA pathogenesis making it potentially the most ideal for the assessment of biomarkers. However, the benefits of using synovial fluid compared to blood must be weighed against the increased invasiveness of extraction. Congruent with its role in animal models of OA, miR-140 has been found to be significantly reduced in the synovial fluid of patients with OA compared to healthy controls (Si *et al.*, 2016). When comparing synovial fluid from patients with late-stage and early-stage OA expression of miR-23a-3p, miR-24-3p, miR-27a-3p, miR-27b-3p, miR-29c-3p, miR-34a-5p and miR-186-5p was significantly higher suggesting that these could be used as markers of disease progression (Y. H. Li *et al.*, 2016). Interestingly, sex-specific differentially expressed miRNAs have been identified in OA synovial fluid. Whilst miR-504-3p was significantly upregulated in synovial extracellular vesicles, miR-16-2-3p was increased (non-significant) and miR26a-5p, miR-146a-5p and miR-6821-5p decreased specifically in females with miR-6878-3p and miR-210-5p being downregulated (non-significant) and upregulated (non-significant) respectively in males (Kolhe *et al.*, 2017). This highlights the importance of accounting for potential sex differences in the analysis of potential OA biomarkers.

Currently, diagnosis of OA generally occurs after significant disease progression has already taken place. Much work has been invested in the identification of biomarkers which may be used for earlier diagnosis of OA, however very few are currently used in the clinic (Nguyen *et al.*, 2017). Circulating miRNAs are easily detectable in blood serum and synovial fluid with many showing promise as predictive biomarkers for OA. Identification of consistent and reliable differentially expressed miRNAs in biological fluid may lead to earlier diagnosis of OA and thus allow for treatments that proactively prevent disease progression.

1.3.3.3 miRNAs as therapies

There are currently no disease-modifying treatments for OA. Management of OA focuses on pain relief with paracetamol, NSAIDS and opioids in the short-term and joint replacement when these become insufficient. Although clinical trials are underway for a number of potential disease modifying treatments - for example trials of the anti-nerve growth factor (NGF) antibody tanezumab show symptomatic improvement (J. Chen *et al.*, 2017) – none have been approved as yet. Given that miRNA dysregulation contributes to OA pathogenesis, it stands to reason that correction of this could be a viable option for therapy;

inhibition of an upregulated miRNA or replacement of a downregulated miRNA may limit disease progression.

As previously discussed, miR-140 is one of the better studied miRNAs with a role in OA. It is downregulated in OA cartilage and miR-140 knockout mice are predisposed to OA development (Miyaki *et al.*, 2010). Using chondrocytes derived from OA and healthy human cartilage in conjunction with a surgically induced rat model of OA, Si *et al.* (2017) investigated whether intra-articular injection of miR-140-5p agomir (a modified mimic) could be an effective therapy. Transfection of OA and healthy chondrocytes with miR-140 mimic upregulated expression of collagen II and downregulated expression of ADAMTS-5 and MMP-13 whereas miR-140 inhibitor had the opposite effect. Intra-articular injection of miR-140 agomir in a surgical rat model of OA significantly attenuated chondrocyte and cartilage loss, increased collagen II positive chondrocytes and decreased ADAMTS-5 and MMP-13 positive chondrocytes. Therefore, intra-articular injection of miR-140 may be a viable therapeutic option for human OA. Similarly, intra-articular injection of miR-210 and anti-miR-449a have been shown to reduce cartilage degradation in rat surgical injury models (Kawanishi *et al.*, 2014; Baek *et al.*, 2018).

Although multiple miRNAs show promise for use as disease modifying agents, a major hurdle in their clinical application is delivery. Naked RNAs are unstable *in vivo* and must be effectively targeted and taken up by target cells. Currently, lipid-vesicles which encapsulate miRNAs in vesicles and are endocytosed by target cells are the most promising delivery vehicles (Oliviero *et al.*, 2019). More research and development of miRNA delivery systems will be needed if miRNA-based OA therapies are to find routine use in the clinic.

1.3.4 MicroRNA-29

The miR-29 family consists of three closely related miRNAs: miR-29a, miR-29b and miR-29c which differ by only two or three bases in the mature miRNA and share the same 6 bp seed sequence at positions 2-7 (Figure 1.9). Therefore, they are predicted to target many of the same genes. Although the mature sequences of miR-29a, miR-29b and miR-29c are largely similar, it has been suggested that small sequence differences may be functionally relevant. The hexanucleotide sequence at positions 18-23 in miR-29b was found to act as a nuclear localisation signal (Hwang *et al.*, 2007) whereas interruption of the tri-uracil sequence at positions 9-11 with a cytosine at position 10 reduced the turnover rate of miR-29a compared to miR-29b and miR-29c leading to greater stability (Zhang *et al.*, 2011). For all three miR-29 family members, the overwhelmingly abundant and apparently most functional arm is the 3p strand therefore, unless otherwise stated the 3p strand will be discussed (Jiang *et al.*, 2014; Kwon *et al.*, 2018).

MiR-29 is transcribed from two separate intergenic genomic loci with *miR-29a* and *miR-29b-1* located on human chromosome 7q32.3 and *miR-29b-2* and *miR-29c* located on chromosome 1q32.2; *miR-29b-1* and *miR-29b-2* produce an identical mature miR-29b sequence. Both loci are transcribed as polycistronic units with the pri-miRNAs subsequently being spliced out however, whereas miR-29a and miR-29b-1 are encoded by the last intron and introns of primary transcripts (GenBank) EU154353 and GU321462 respectively, miR-29b-2 and miR-29c are encoded by the last exon of the primary transcripts EU154351 and EU154352 (Chang *et al.*, 2008; Mott *et al.*, 2010). In mice, the broad genomic organisation of miR-29 is comparable to humans with *miR-29a* and *miR-29b1* located on chromosome 6A3.3 and *miR-29b-2* and *miR-29c* located on chromosome 1H6.

It is well established that miR-29 plays an important role in development, general physiology and a number of diseases. Global knockout of both miR-29 loci in mice results in premature death (within 42 days), growth retardation, kyphosis and severe ataxia amongst other phenotypes (Cushing *et al.*, 2015; Caravia *et al.*, 2018). The miR-29ab1 locus is generally recognised as being the major source of miR-29 and so although knockout of this locus alone resulted in a similar - albeit less severe - phenotype to the double knockout, deletion of the miR-29b2c locus alone resulted in a comparatively mild phenotype with a modest decrease in weight and lifespan (Smith *et al.*, 2012; Papadopoulou *et al.*, 2015; Sassi *et al.*, 2017; Caravia *et al.*, 2018).

One of the better studied roles for miR-29 in disease is in cancer where miR-29 predominantly functions as a tumour suppressor (Kwon *et al.*, 2018). In line with this, miR-29 is downregulated in the majority of cancers (Jiang *et al.*, 2014; Alizadeh *et al.*, 2019) and known to target genes involved in proliferation, apoptosis, metabolism and DNA methylation, all of which are strongly implicated in cancer (Kwon *et al.*, 2018). In acute myeloid leukaemia miR-29b was found to negatively regulate *DNMT3A* and *DNMT3B*, and indirectly downregulate *DNMT1* via SP1, leading to global hypomethylation and thus reexpression of hypermethylated and silenced tumour suppressor genes including $p15^{INK4b}$ and *ESR1* (Garzon *et al.*, 2009). Downregulation of miR-29a in pancreatic cancer cells relieved repression of the autophagy-related genes *TFEB* and *ATG9A* thus promoting autophagy, resistance to gemcitabine treatment and cell survival (Kwon *et al.*, 2016). In non-small cell lung cancer patients and cell lines, increased expression of miR-29c promoted responsiveness to cisplatin chemotherapy by negatively regulating the PI3k/Akt pathway (Sun *et al.*, 2018), whereas reduced expression of miR-29a lead to hypermethylation of the Wnt inhibitory factor 1 (WIF1) promoter, aberrant Wnt activation and increased cell proliferation and survival (Tan *et al.*, 2013).

Another well-known role for miR-29 is in fibrotic disease, characterised by an excessive accumulation of fibrous connective tissue and eventual loss of organ function (Deng *et al.*, 2017). In cardiac, liver, lung and kidney fibrosis miR-29 expression is downregulated and this is thought to be largely mediated by an increase in TGF-β signalling (van Rooij *et al.*, 2008; He *et al.*, 2012; Wang *et al.*, 2012; Xiao *et al.*, 2012). Stimulation of a human foetal lung cell line with TGF-β1 downregulated miR-29a, miR-29b and miR-29c with a concomitant upregulation of predicted miR-29 targets including *COL1A1*, *COL3A1*, and *COL1A2*, all of which are strongly implicated in fibrosis (Cushing *et al.*, 2011). Similarly, knockout of *Smad3* in a mouse model of renal fibrosis caused significant upregulation of all three miR-29 members, whereas overexpression of miR-29b blocked TGF-β1 induction of collagen I and III suggesting a potential negative feedback loop between miR-29 and TGF-β signalling (Qin *et al.*, 2011).

The miR-29 family plays a critical role in normal development and physiology with global knockout being lethal (Cushing *et al.*, 2015). Therefore, it is unsurprising that dysregulation of miR-29 expression is implicated in a range of diseases. Along with cancer and fibrosis miR-29 is implicated in a wide range of diseases including HIV-1 infection (Ahluwalia *et al.*, 2008) and Alzheimer's disease (Pereira *et al.*, 2016) highlighting diverse roles for miR-29. Studying the role of miR-29 in diseases will further increase our understanding of their pathophysiology and may eventually lead to the development of therapies that specifically target miR-29 expression.

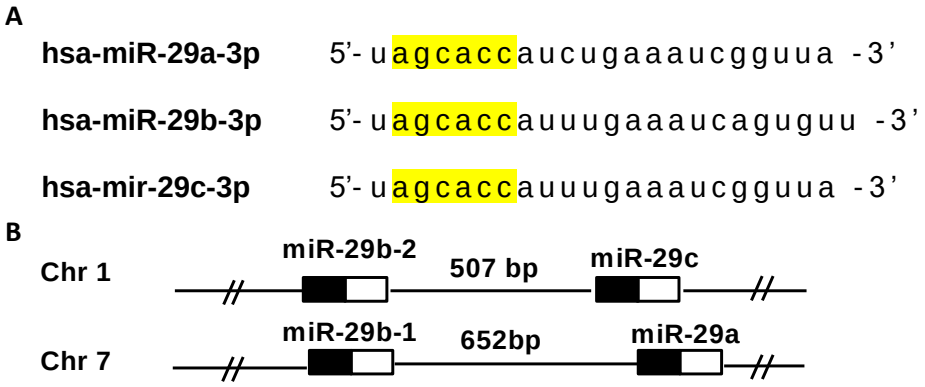

Figure 1.9. Organisation and sequence of the miRNA-29 family. *(A) All three members of the miR-29 family share almost the same mature sequences and identical 6 bp seed sequences (yellow). (B) MiR-29a and miR-29b1 are located on chromosome 7, and miR-29b2 and miR-29c are located on chromosome 1. Sequences obtained from miRbase.org* (Kozomara *et al.*, 2014)***.***

1.3.4.1 MicroRNA-29 in osteoarthritis

As opposed to other diseases such as cancer and fibrosis, the role of miR-29 in OA is less well understood. Multiple studies have shown that miR-29 is dysregulated in OA. Le *et al.* (2016) showed that miR-29a, miR-29b and miR-29c were upregulated in human osteoarthritis hip cartilage compared to healthy controls and in murine OA models with a concomitant decrease in the expression of predicted targets. When comparing OA cartilage to healthy cartilage from the same patient miR-29b and miR-29c were found to be significantly upregulated (Coutinho de Almeida *et al.*, 2019). Similarly, miR-29c was significantly upregulated in the blood plasma of patients with knee OA (Borgonio Cuadra *et al.*, 2014) and in the synovial fluid of patients with late-stage knee OA compared to early-stage (Li *et al.*, 2016) suggesting potential utility as a biomarker. Therefore, miR-29 may play an important role in OA pathogenesis.

MiR-29 is implicated in the regulation of many OA related genes including ECM components, matrix degrading enzymes and multiple signalling pathways. In murine chondrocytes miR-29a and miR-29b were found to negatively regulate *Col2a1* (Yan *et al.*, 2011). Similarly, in murine MSCs undergoing hypertrophic chondrogenesis, miR-29b negatively regulated *Col2a1* and *Sox9* expression as well as GAG synthesis while expression of *Col10a1*, *Runx2* and *Mmp13* was increased (C. Zhao *et al.*, 2019). In human chondrogenic MSCs, transfection with pre-miR29a significantly downregulated expression of *COL2A1*, *ACAN* and *SOX9* (Guérit *et al.*, 2014). On the other hand, in mice overexpressing miR-29a *Mmp9*, *Mmp13* and *Col3a1* were downregulated in synovial fibroblasts (Ko *et al.*, 2017).

In addition to regulating the expression of ECM components, miR-29 has also been shown to regulate several matrix-degrading enzymes and is predicted to target many more. In human primary chondrocytes, overexpression of miR-29b downregulated *ADAMTS5*, *ADAMTS6*, *ADAMTS14*, *ADAMTS17* and *ADAMTS19* with luciferase reporter assays confirming direct targeting by miR-29b (Le *et al.*, 2014). In rat vascular smooth muscle cells miR-29a and miR-29b were shown to directly target *Adamts7* (Du *et al.*, 2012). Whereas, in a mouse model of abdominal aortic aneurysm lentiviral transduction with miR-29b upregulated expression of *Mmp2* and *Mmp9* and downregulated expression of *Col1a1* and *Col3a1* (Maegdefessel *et al.*, 2012).

Several signalling pathways involved in OA development are also targeted by miR-29. Using luciferase reporter assays along with measuring known responsive gene expression Le *et al.* (2016) demonstrated that TGF-β, NF-κB and canonical Wnt signalling were negatively regulated by miR-29b. In a mouse model of pulmonary fibrosis miR-29b was shown to suppress TGF-β/Smad3 signalling by reducing expression of TGF-β1 and

phosphorylation of SMAD3 (Xiao *et al.*, 2012). Downregulation of Wnt signalling by miR-29 in non-small cell lung cancer was found to act through targeting of DNMT3a and DNMT3b and subsequent demethylation of the WIF1 promoter (Tan *et al.*, 2013), whereas in human chondrocytes, miR-29 negatively regulated expression of the Wnt receptors FZD3 and FZD5 (Le *et al.*, 2016). The mechanism through which miR-29 regulates NF-κB signalling is yet to be elucidated, however miR-29 is predicted to target REL (or c-Rel) (mirdb.org), an NF-κB subunit and SP1, a transcription factor known to activate REL (Hirano *et al.*, 1998) and RELA (Sif *et al.*, 1994). Interestingly, regulation of TGF-β and NF-κB by miR-29 may be reciprocal. In human primary chondrocytes TGF-β1 reduced expression of mature miR-29 (Le *et al.*, 2014), in myoblasts YY1 NF-κB was shown to negatively regulate transcription of miR-29 (Wang *et al.*, 2008), and in an acute myeloid leukaemia cell line SP1 in complex with NF-κB downregulated the miR-29 promoter (Liu *et al.*, 2010).

Some studies have suggested that miR-29 may be a negative regulator of chondrogenesis. SOX9 is expressed in all chondrocytes and chondrocyte progenitors (Zhao *et al.*, 1997; Song *et al.*, 2020) and is essential for chondrogenesis (Akiyama *et al.*, 2002). Moreover, SOX9 is recognised as a 'master regulator' of transcription during chondrogenesis binding to and activating the promoters of key genes including *COL2A1* and *ACAN* (Han *et al.*, 2008). SOX9 has also been shown to negatively regulate miR-29. Overexpression in SW1353 cells reduced expression of miR-29a, miR-29b and miR-29c and a luciferase reporter assay showed that SOX9 negatively regulated the miR-29ab1 promoter (Le *et al.*, 2016). There is some evidence of a negative feedback loop between miR-29 and SOX9 with overexpression of miR-29a and miR-29b leading to a downregulation of SOX9 in human and murine MSCs respectively (Guérit *et al.*, 2014; C. Zhao *et al.*, 2019) however not all studies have been able to replicate this (Le *et al.*, 2016). Therefore, a negative feedback loop between miR-29 and SOX9 may allow for the fine-tuning gene expression during chondrogenesis, though more evidence of this interaction would be needed to confirm this.

Given the potentially important role of miR-29 dysregulation in OA, targeting of miR-29 may be an attractive therapeutic option for disease treatment. Indeed, overexpression of miR-29a in murine chondrocytes not only protected against the antiproliferative effects of IL-1β, but reversed a concomitant increase in *Col10a1*, *Mmp1*, and *Mmp13*, and decrease in *Col2a1* and *Timp1* (X. Li *et al.*, 2016). Overexpression of miR-29a and miR-140 together had an additive effect in promoting proliferation, reducing *Mmp13* and increasing *Timp1* expression (X. Li *et al.*, 2016). In synoviocytes isolated from end-stage OA knees and a collagenase-induced (CI) mouse model of OA, overexpression of miR-29a significantly downregulated the expression of the profibrotic factors COL3A1, TGF-β1, TIMP1, PLOD2 and ADAM12 and the cartilage degrading enzymes MMP-9, MMP-13 and ADAMTS-5 (Ko

et al., 2017). Moreover, miR-29 overexpression or intra-articular injection of lentiviral-shuttled miR-29a protected against cartilage loss and altered gait in a CI model of OA (Ko *et al.*, 2017). In a mouse model of rotator cuff injury both transgenic and lentiviral overexpression of miR-29a protected against fibrosis and reduced the expression of *Col3a1* (Ko *et al.*, 2019). Similarly, in an equine CI model of tendon injury, administration of miR-29a 1 week post injury reduced levels of type III collagen while significantly improving the rate of healing when compared to placebo treated horses (Watts *et al.*, 2017). Finally, in the ATDC5 chondrogenic cell line miR-29a mimic significantly reduced apoptosis through direct targeting of the pro-apoptotic protein BAX suggesting that treatment with exogenous miR-29 could prevent chondrocyte death in OA (Miao *et al.*, 2019). Taken together, there is a strong case to be made that augmentation of miR-29 expression in OA joints may be a potential disease modifying therapy. This being said, more in-depth studies into the global effect of miR-29 on gene expression in the joint followed by animal and eventually human clinical trials would be needed before such a treatment was available in the clinic.

1.4 Hypothesis and aims

OA is one of the most prevalent degenerative joint diseases inflicting millions of people around the world with debilitating pain and reduced quality of life. Yet treatment options for patients suffering from OA are limited with disease modifying drugs remaining elusive. MiRNAs are short RNAs that typically downregulate the expression of target genes through interactions with the 3'-UTRs of mRNAs, many of which have been implicated in OA. Previous work in our group highlighted a potential role for the miR-29 family in OA. MiR-29 was upregulated in human OA cartilage and murine models of OA, in addition to interacting with OA-related genes and signalling pathways (Le, 2015; Le *et al.*, 2016). This project aims to further study the role of the miR-29 family in OA and understand whether augmentation maybe a viable therapeutic option. Therefore, the hypothesis of this project is:

The microRNA-29 family plays an important role in cartilage development and the pathogenesis of osteoarthritis.

This hypothesis will be addressed through the following aims:

- Identify members of the ADAMTS family which are regulated by miR-29 and TGF-β using *in vitro* models including cell lines and primary human chondrocytes.

- Investigate the role of miR-29 in the regulation of DNA methylation in chondrocytes and OA.

- Generate cartilage-specific miR-29 knockout models to study the role of miR-29 in cartilage development and OA pathogenesis.

Chapter 2

Materials and methods

2 Materials and methods

2.1 Cells and mouse models

2.1.1 *E. coli* strains

For cloning of constructs, *E. coli* were either Stellar™ Competent Cells (Clonetech), XL10-Gold® Ultracompetent Cells (Agilent Technologies) or DH5α chemically competent cells.

2.1.2 Mammalian cell lines

SW1353 is a chondrosarcoma cell line originally derived from a primary grade II chondrosarcoma in 1977 (ATCC®, cat# HTB-94™). DF1 is a spontaneously immortalised chicken fibroblast cell line and was a kind gift from Prof. Andrea Munsterberg, University of East Anglia (UEA), UK.

2.1.3 Human primary articular chondrocytes

Articular cartilage was obtained from patients undergoing total hip replacement surgery following fracture of the neck of femur (NOF). Tissues were collected at Norfolk and Norwich University Hospital (NNUH) under ethical approval with all patients giving informed consent.

Cartilage was incubated in digestion medium containing Dulbecco's modified Eagle Medium (DMEM), GlutaMAX™ (Life Technologies), 1 mg/ml collagenase (Sigma-Aldrich, C1639), 0.4% (w/v) Hepes (Fisher Scientific, BP310-100), 100 IU/ml penicillin, 100 µg/ml streptomycin (Sigma-Aldrich, P4333) at 37 °C, 180 rpm overnight. Cells were isolated using a 70 µm cell strainer, plated at $4x10^4$ cells/cm^2 and grown to 80% confluence. Cells were washed in Hanks' Balanced Salt Solution (HBSS) (Life Technologies), incubated in 0.25% (w/v) trypsin/ethylenediaminetetraacetic acid (EDTA) (Life Technologies) (TE) until they were removed from the plate and resuspended in fresh media. Cells were pelleted by centrifugation at 180 x *g* for 5 minutes, the supernatant removed and cells resuspended in 1 ml heat-inactivated foetal bovine serum (FBS) (Life Technologies) with 10% (v/v) dimethyl sulfoxide (DMSO) prior being stored at -180 °C. Cells were used by passage three.

2.1.4 Mouse models

Mice were maintained in a specific-pathogen-free facility in accordance with Home Office regulations. Mice were housed in individually ventilated cages and fed Rat and Mouse No.3 Breeding Expanded Diet (Special Diet Services) and water ad-lib. All mice were bred on a C57BL/6 background.

MiR-29ab1$^{fl/fl}$ mice have the *miR-29ab1* locus flanked by loxP sites (Figure 2.1A) and were a kind gift from Prof. Carlo Croce, Ohio State University, USA. Generation of *miR-29ab1*$^{fl/fl}$ mice is described in Smith *et al.* (2012) and mice were rederived upon receipt. *MiR-29b2c*$^{fl/fl}$ mice have the *miR-29b2c* locus flanked by loxP sites (Figure 2.1B) and were obtained from The Jackson Laboratory, USA (stock number: 405371).

Col2a1-cre mice express Cre recombinase under the control of the *collagen-2a1* (*col2a1*) promoter (Figure 2.1C) and were a kind gift from Dr. Attila Aszodi, Ludwig Maximilian University of Munich, Germany. Generation and characterisation of *col2a1-cre* mice is described in Sakai *et al.* (2001). *Acan-creERT2/CTGF*$^{fl/fl}$ mice have the connective tissue growth factor (CTGF) gene flanked by loxP sites (floxed), and a tamoxifen inducible Cre recombinase under control of the cartilage specific aggrecan promoter and were a kind gift from Prof. George Bou-Gharios, University of Liverpool, UK.

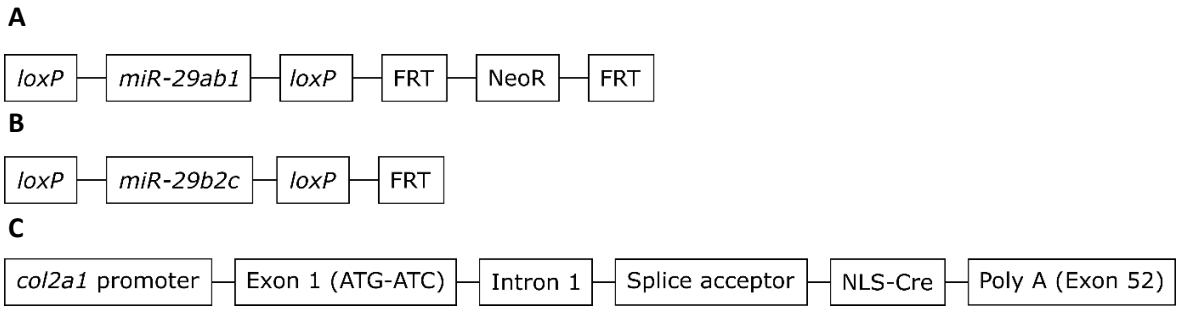

Figure 2.1. Transgenic mouse models used for miR-29 knockout breeding. *(A) miR-29ab1*$^{fl/fl}$ *contains the mir-29ab1 locus flanked by loxP sites and downstream neomycin resistance (NeoR) marker flanked by flippase recognition target (FRT) sites. (B) miR-29b2c*$^{fl/fl}$ *contains the mir-29b2c locus flanked by loxP sites. A neomycin cassette has been removed using Flp recombination leaving a single FRT site. (C) The col2a1 cassette contains the promoter, exon 1 with a mutated initiation codon and part of intron 1 from col2a1 followed by a splice acceptor site, a 1.2kb fragment from pMC1-Cre containing nuclear localisation signal (NLS) and Cre recombinase, and exon 52 of col2a1 with the polyadenylation site (Poly A).*

2.2 Cell culture

2.2.1 Mammalian cell culture conditions

SW1353 and DF1 cells were maintained in DMEM, GlutaMAX™ supplemented with 10% (v/v) FBS, 100 IU/ml penicillin and 100 µg/ml streptomycin (complete media) at 37 °C and 5% (v/v) CO_2. Both cell lines were passaged at 80-100% confluence by washing with HBSS, incubation in 0.25% TE at 37 °C for 3-5 minutes and diluting 1:10 in complete media.

Primary articular chondrocytes were thawed at 37 °C and maintained as described for SW1353 and DF1 cells with media being refreshed every 2 or 3 days.

For plating, cells were grown until 80-90% confluent, washed with HBSS, incubated in TE at 37 °C for three to five minutes and resuspended in fresh media. Cells were counted using a haemocytometer and diluted to the required concentration in complete media.

2.2.2 Bacterial cell culture conditions

E. coli were plated on lysogeny broth (LB) agar (bacto-tryptone 10 g/L, yeast extract 5 g/L, NaCl 5 g/L, agar 15 g/L) containing 100 µg/ml ampicillin (Sigma-Aldrich) and incubated at 37 °C overnight. For liquid cultures, *E. coli* was inoculated in LB (bacto-tryptone 10 g/L, yeast extract 5 g/L, NaCl 5 g/L) and incubated at 37 °C, 200 rpm overnight.

2.3 Molecular methods

2.3.1 Constructs

The pmirGLO dual-luciferase miRNA target expression vector (Promega) contains the firefly luciferase primary reporter gene (luc2) upstream of a multiple cloning site, a Renilla luciferase control reporter and an ampicillin resistance marker (Figure 2.2).

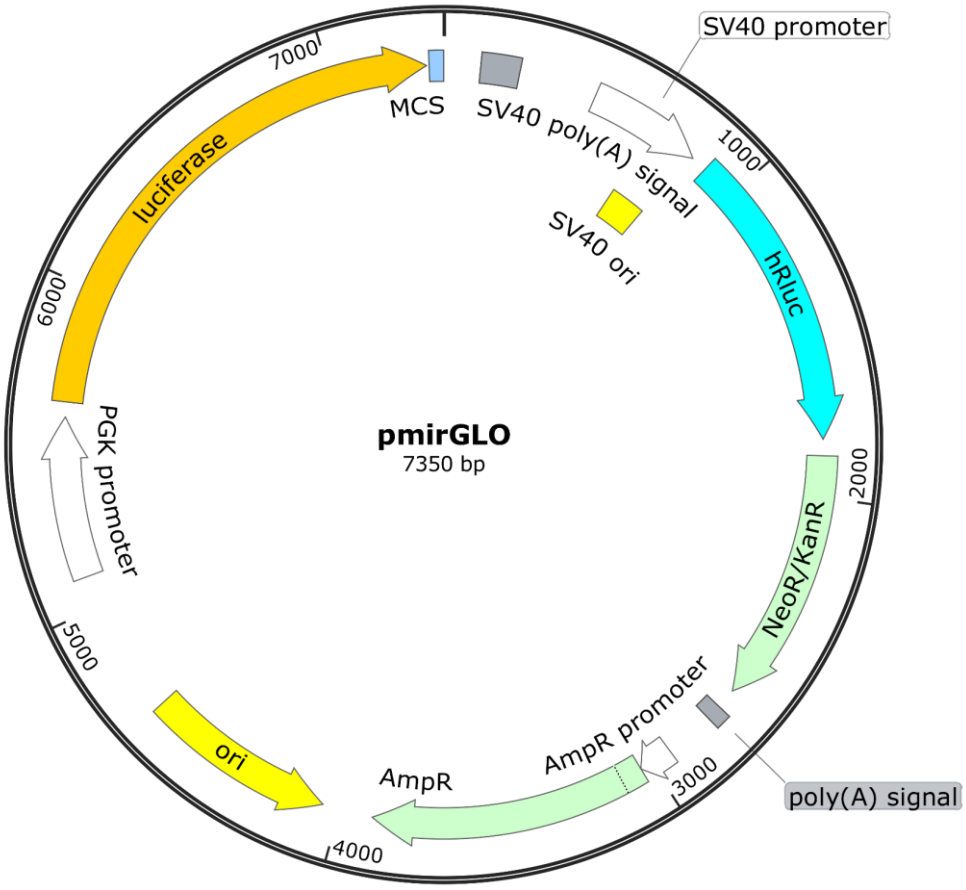

Figure 2.2. Plasmid map of pmirGLO. *Map of the pmirGLO plasmid containing the firefly luciferase primary reporter and Renilla luciferase control reporter. Figure generated using SnapGene Viewer.*

2.3.2 Gel electrophoresis

Unless otherwise stated agarose gels were prepared with 1% agarose (w/v) in 1x TAE buffer (Tris-acetate 40 mM, EDTA 1 mM) and run at 120 V prior to staining with ethidium bromide (Sigma-Aldrich) and visualisation with a Bio-Rad Gel Doc™ EZ Gel Documentation System or UVP ChemiDoc-It2™ 810 Imager.

2.3.3 Cloning of ADAMTS 3'-UTRs

2.3.3.1 Primer design

Members of the ADAMTS family predicted to be targeted by miR-29 were identified using the miRNA body map (Mestdagh *et al.*, 2011). In addition, 3'-UTR sequences were downloaded for the ADAMTS gene family from Ensemble genome browser (Howe *et al.*, 2021) and screened for the miR-29 6mer seed sequence (GGTGCT). For 3' UTRs containing at least one seed sequence site, primers were designed to amplify 500 bp - 1000 bp surrounding this sequence (Appendix table 1). Where multiple seed sequences were spread over more than 1000 bp, two primer sets were designed to amplify the 3'-UTR in two parts.

2.3.3.2 Isolation of human genomic DNA

Genomic DNA (gDNA) was isolated from SW1353 cells as follows. Cells were washed with HBSS (Fisher Scientific, UK), incubated in 0.25% TE at 37 °C for 3-5 minutes and resuspended in media. Cells were pelleted by centrifugation at 500 x *g* at 4 °C for 5 minutes, washed with cold Dulbecco's phosphate-buffered saline (DPBS) (Life Technologies), re-pelleted and suspended in 300 µl digestion buffer (100 mM NaCl, 10 mM Tris pH 8.0, 25 mM EDTA pH 8.0, 0.5%, sodium dodecyl sulfate (SDS), 0.1 mg/ml proteinase K) prior to incubation at 50 °C for 18 hours. DNA was purified using UltraPure™ phenol:chloroform:isoamyl alcohol (25:24:1, v/v) (Invitrogen) according to manufacturer's protocol.

2.3.3.3 PCR

GDNA isolated from SW1353 cells was used as a template for PCR amplification of ADAMTS 3'-UTR amplicons. 3'-UTR amplicons were amplified from 50 ng gDNA using Phire Hot Start II DNA polymerase (Fisher Scientific, UK) according to manufacturer's protocol (thermal cycle: 98 °C 30 seconds, 35 cycles of 98 °C 5 seconds, 60 °C 5 seconds and 72 °C 20 seconds followed by 1 cycle of 72 °C 60 seconds) using a Veriti™ 96-Well Thermal Cycler (Applied Biosystems). Target amplification was confirmed by gel electrophoresis of 5µl PCR product.

2.3.3.4 Isolation of ADAMTS 3'-UTR amplicons

ADAMTS 3'-UTR amplicons were separated using gel electrophoresis. The respective bands were purified using the QIAquick Gel Extraction Kit (Qiagen) or NucleoSpin® Gel and PCR Clean-up kit (Machery-Nagel) according to manufacturer's protocol and eluted in nuclease free water (Sigma-Aldrich). DNA concentration was analysed using a NanoDrop™ 1000 (Thermo Scientific).

2.3.3.5 Assembly of ADAMTS 3'-UTR pmirGLO constructs

ADAMTS 3'-UTR amplicons were cloned into the pmirGLO vector (Figure 2.2). PmirGLO was digested with Xho1 (Promega) at 37 °C for 16 hours (10x buffer D 5 µl, XhoI 2 µl, pmirGLO 5 µg, water up to 50 µl), linearised vector was purified by gel extraction and DNA concentration determined. ADAMTS 3'-UTR amplicons were ligated into pmirGLO (3:1 molar ratio of insert to vector) using the In-Fusion® HD Cloning Kit (Clontech) and transformed into Stellar™ Competent Cells according to the manufacturer's protocol. Transformed cells (100 µl) were plated on selective LB agar and grown overnight at 37 °C.

2.3.3.6 Colony PCR

E. coli colonies containing the desired ADAMTS 3'-UTR constructs were identified using colony PCR. Colony PCR was performed using OneTaq Hot Start DNA Polymerase (New England Biolabs) in 10 µl reactions according to the manufacturer's protocol. Colonies were inoculated in the PCR reactions prior to streaking on selective LB agar and incubation overnight at 37 °C. PCR was performed (thermal cycle: 94 °C 5 minutes, 35 cycles of 94 °C 30 seconds, 60 °C 30 seconds and 68 °C 30 seconds followed by 1 cycle of 68 °C 5 minutes) and reactions were analysed by gel electrophoresis. Positive colonies were grown in 5 ml LB 100 µg/ml ampicillin and plasmid DNA was isolated using the QIAprep Spin Miniprep Kit (Qiagen) prior to sequencing (Source BioScience) to confirm construct assembly. For primers see Appendix table 1.

2.3.3.7 Mutagenesis of ADAMTS 3'-UTR constructs

Seed sequences for miR-29 in ADAMTS 3'-UTR pmirGLO constructs were mutated. All miR-29 6mer seed sequences within the cloned regions of ADAMTS 3'-UTR pmirGLO constructs were mutated to one of several restriction sites (EcoRI, GAATTC; SalI site, GTCGAC; XbaI, TCTAGA) to allow for easy screening of mutants using restriction digestion. Mutagenesis was achieved using the QuikChange Lightning Multi Site-Directed Mutagenesis Kit (Agilent Technologies) according to manufacturer's protocol. For primers see Appendix table 1. Restriction digestion with the respective restriction enzyme followed by sequencing (Source BioScience) was used to confirm mutagenesis.

2.3.4 Total RNA isolation

2.3.4.1 Total RNA isolation from cultured cells

Media was removed from cultured cells prior to washing twice with 1 ml cold DPBS. Total RNA was isolated by adding 500 µl TRIzol™ Reagent (15596026, Invitrogen) and 200 µl chloroform to each well according to manufacturer's protocol. RNA concentration was determined using a NanoDrop 2000 (Thermo Scientific) and DNase treatment was performed using the TURBO DNA-free™ Kit (AM1907, Invitrogen) according to manufacturer's protocol.

2.3.4.2 Total RNA isolation murine tissues

Liver tissue and cartilage isolated from murine femoral heads were ground in liquid nitrogen using a disposable pestle and 500 µl TRIzol™ Reagent was added. Samples were vortexed and incubated for 15 minutes at room temperature before transferring to a Phasemaker™ tube (A33248, Invitrogen), 200 µl chloroform was added, incubated for 2-15 minutes, and centrifuged at 12000 x *g* at 4 °C for 5 minutes. The aqueous phase was transferred to a new tube and total RNA isolation performed using the total RNA isolation procedure for the mirVana™ miRNA Isolation Kit (AM1561, Life Technologies). DNase treatment was performed using the TURBO DNA-free™ Kit according to manufacturer's protocol. RNA was further purified using ethanol precipitation as follows. On ice, 0.1 volume 3 M sodium acetate and 2.5 volumes 100% ethanol were added prior to vortexing and precipitation overnight at -80 °C. RNA was pelleted by centrifugation at 14000 x *g* at 4 °C for 30 minutes, washed in 500 µl ice-cold 70% ethanol, centrifuged 14000 x *g* for 15 minutes and resuspended in 20 µl nuclease-free water. RNA was stored at -80 °C.

2.3.5 Quantitative real time PCR (qRT-PCR)

2.3.5.1 cDNA synthesis

Total RNA from cultured cells, murine hip cartilage or liver tissue was reverse transcribed using SuperScript™ II Reverse Transcriptase (RT) (18064-071, Invitrogen). RNA was diluted in 10 µl nuclease-free water, 2 µl random primers (Invitrogen) or TaqMan® microRNA reverse transcription primer pool (see section 2.3.4.3.2) added and incubated at 70 °C for 10 minutes. On ice, 4 µl First Strand Buffer, 2 µl 0.1 M dithiothreitol (DTT), 1 µl 10 mM dNTP mix (Bioline) and 1 µl SuperScript™ II RT were added followed by incubation at 42 °C for 60 minutes and 70 °C for 10 minutes. Complimentary DNA (cDNA) was stored at -20 °C.

2.3.5.2 Quantification of gene expression

Gene expression was quantified using standard probe-based qPCR or the Universal Probe Library (Roche) and normalised to 18S ribosomal RNA (rRNA) expression. Differences in 18S rRNA expression were not significant between control and experimental conditions in respective qRT-PCR experiments (Appendix table 2). This being said, in future work a panel of housekeep genes should be screened to identify the most reliable candidate for normalisation. For primers and probes see Appendix table 3. For qPCR reactions, cDNA was diluted to 0.5 ng/µl and 5 µl added to each reaction in addition to 200 nM forward and reverse primer, 100 nM probe, 8.33 µl qPCRBIO Probe Mix Lo-ROX (PCR Biosystems) and nuclease-free water to 25 µl. Relative quantification (comparative CT) was performed using

an Applied Biosystems™ 7500 Real-Time PCR System and the following PCR conditions: 50 °C 2 minutes, 95 °C 10 minutes and 40 cycles of 95 °C 15 seconds and 60 °C for 1 minute.

2.3.5.3 Quantification of mature microRNA-29 expression

Mature miR-29a-3p, miR-29b-3p and miR-29c-3p expression was quantified using TaqMan® microRNA assays and normalised to U6 small nucleolar RNA (snRNA) (assay ID: 002112, 000413, 000587, 001973, Applied Biosystems). Differences in U6 snRNA expression were not significant between control and knockout conditions (Appendix table 2) however as previously mentioned, in future experiments an appropriate housekeeping gene should be selected from a panel of candidates. CDNA synthesis was performed as in section 2.4.3.2 using a primer pool containing 0.5 µl miR-29a-3p, miR-29b-3p, miR-29c-3p and U6 snRNA reverse transcription primers. qPCR was performed as in section 2.3.4.3.1 using 1.5 µl of respective PCR primer and probe mix.

2.3.6 mRNA-sequencing

Total RNA was extracted from P21 murine femoral head cartilage as in section 2.3.4.2 and cartilage purity was assessed by measuring the expression of cartilage and bone markers using qRT-PCR as in section 2.3.5. RNA quantity and RNA integrity (RIN) mRNA-sequencing (mRNA-seq) was performed by Novogene (Cambridge, UK) using the Illumina NovaSeq 6000 platform with a paired-end 150 bp sequencing strategy and ≥ 20 million read pairs per sample.

Data were kindly analysed by Dr. Simon Moxon (University of East Anglia, UK). Reads were aligned to Mus musculus GRCm39 using HISAT2 (Kim *et al.*, 2019) using default parameters for paired-end alignment. Samtools was used to convert SAM alignments to BAM format and sort and index the files (Li *et al.*, 2009). Htseq-count (Anders *et al.*, 2015) was used to count reads aligning to gene annotations from Ensembl release 104 (Yates *et al.*, 2020). Counts from each of the samples were combined into a count matrix and imported into DESeq2 (Love *et al.*, 2014) which was used to calculate DE and fold-changes between conditions and create PCA plots. The DESeq2 model accounts for inter-replicate noise, therefore lowly expressed and highly variable genes are unlikely to be called as differentially expressed. In addition, DESeq2 performs an independent filtering step to remove weekly expressed genes and thus, reduce power loss due to multiple testing adjustment (Love *et al.*, 2014).

2.3.7 DNA methylation analysis

2.3.7.1 Dot blot

2.3.7.1.1 Isolation of genomic DNA

Cells from section 2.4.4 were washed with 1 ml DPBS and incubated in 500 µl digestion buffer (100 mM Tris-HCl pH 8, 100 mM NaCl, 50 mM EDTA pH 8, 1% SDS, 0.2 mg/ml proteinase K) for 2-3 hours. DNA was purified using UltraPure™ phenol:chloroform:isoamyl alcohol (25:24:1, v/v) according to manufacturer's protocol.

2.3.7.1.2 Quantification of methylation

DNA (100 ng) was denatured in 30 µl 0.1 M NaOH at 95 °C for 10 minutes followed by neutralisation with 1 M NH_4OAc. DNA diluted to 50 µg/µl and 25 µg/µl, and 2 µl was spotted onto a methanol-activated Immobilon®-FL PVDF membrane (Merck Millipore). The membrane was blotted at 80 °C for 30 minutes, blocked with 5% (w/v) milk in TBS-T (tris-buffered saline (20 mM Tris, 150 mM NaCl), 0.1% v/v Tween-20, pH 7.5) at room temperature for 1 hour and incubated with a 5-mC recombinant rabbit monoclonal antibody (Fisher, MA5-24694) 1:1000 at 4 °C overnight. The membrane was washed three times with TBS-T, incubated with HRP-conjugated goat anti-rabbit immunoglobulin-G secondary antibody (Invitrogen, A16096) 1:500 at room temperature for one hour and washed three times with TBS-T. Finally, the membrane was visualised using Pierce™ ECL western blotting substrate and imaged with a Bio-Rad ChemiDoc XRS+ imager. Relative dot intensity was quantified by measuring the integrated dot density with ImageJ.

2.3.7.2 Methylation array

SW1353 cells were transfected with 50 nM miR-29b-3p mimic or negative control as in section 2.4.2.1. Cells were harvested by incubation in 500 µl 0.25% TE for 2 minutes followed by scraping to detach cells from the well. Cells were resuspended in 5 ml antibiotic-free (AbF) media, pelleted by centrifugation at 500 x *g* at 4 °C for 5 minutes and flash frozen in liquid nitrogen before being stored at -80 °C.

GDNA and RNA were isolated simultaneously using the Qiagen AllPrep DNA/RNA mini kit (Qiagen). RNA was reverse transcribed as in section 2.3.4.2 and gene expression was measured using qRT-PCR as in section 2.3.4.3.1. For DNA, one miR-29b-3p treated sample and one negative control sample were quantified using a Qubit 4 (Thermo Scientific) and Qubit 1x dsDNA HS assay kit (Thermo Scientific, Q33230) prior to the methylation array (kindly performed by Dr. David Monk).

Methylation datasets were generated using the Illumina Infinium MethylationEPIC BeadChip arrays, which simultaneously quantify approximately 4% of all CpG dinucleotides. GDNA was bisulfite converted according to the manufacturer's recommendations for the Illumina Infinium Assay (EZ DNA methylation kit, ZYMO). The bisulfite-converted DNA (250 ng) was used for hybridization following the Illumina Infinium HD methylation protocol at genomic facilities of the Josep Carreras Leukemia Research Institute (Barcelona, Spain).

Data from the methylation array were kindly analysed by Dr. Claudia Buhigas (University of East Anglia, UK). Prior to data analysis, possible sources of technical bias that could influence results were excluded. Signal background subtraction was applied, and interplate variation was normalised using default control probes in BeadStudio (version 2011.1 Infinium HD). Probes with a detection p-value > 0.01 were discarded. Probes that lacked signal values in one or more of the DNA samples analysed were also excluded. Differential methylation interval between samples was identified using Bumphunter or bioinformatics pipelines developed by the Monk lab (using R-package).

2.3.7.3 Bisulfite PCR pyrosequencing

Bisulfite PCR was used to amplify 50 ng bisulfite-converted DNA with one unmodified and one biotinylated primer using Immolase Taq polymerase (Bioline) (95 °C for 10 minutes followed by 45 cycles of 95 °C for 5 seconds, 54 °C for 5 seconds and 72 °C for 15 seconds). The biotinylated PCR product (diluted to 40 µl) was mixed with 38 µl of binding buffer and 2 µl (10 mg/ml) streptavidin-coated polystyrene beads. After incubation at 65 °C, DNA was denatured with 50 µl 0.5 M NaOH. Single-stranded DNA was hybridized to 40 pmol sequencing primers dissolved in 11 µl annealing buffer at 90 °C. For sequencing, a primer was designed to the opposite strand of the biotinylated primer used in the PCR reaction. The pyrosequencing reaction was carried out on a PyroMark Q96 instrument (Qiagen). The peak heights were determined using Pyro Q-CpG1.0.9 software (Qiagen). For primers see Table 2.1.

Table 2.1. Bisulfite PCR primers

Primer	**Sequence (5'-3')**
TRIM58 OutF	ATAAAGATGGAAGGAAGGAGGGA
TRIM58 OutR BIOT1	(Biotin)-AAAACAAACGCCAACGAATAATATCC
TRIM58 OutR BIOT2	(Biotin)-AAAACAAACACCAACAAATAATATCC
CACNBI R	AGGGTGATAGGTAGTTTATT
CACNBI R BIOT	(Biotin)-CTAAATAACTAAACCRAATACTAAC
TRIM58 seqF	TAGTTTTTTGGGTGTGTGTG
CACNB1 seqF	GATTATGGAGAGGAGTTTTTTTT

2.4 Cell culture assays

2.4.1 Assessing microRNA-29b targeting of ADAMTS 3'-UTRs

2.4.1.1 Transfection of ADAMTS 3'-UTR constructs and microRNA-29b

DF1 cells were plated in 96-well plates ($1x10^4$ cells/well) in 90 µl AbF media (DMEM, GlutaMAX™, supplemented with 10% (v/v) FBS) and incubated for 16 hours. Cells were transfected with 100 ng ADAMTS 3'-UTR pmirGLO construct using Lipofectamine 3000 reagent (L3000015, Invitrogen) according to manufacturer's protocol and incubated for 6 hours, after which, media was replaced with 90 µl AbF media. Cells were transfected with either 50 nM miR-29b-3p miRCURY LNA miRNA mimic (YM00473486-ADA,Qiagen), 50 nM negative control miRCURY LNA miRNA mimic (YM00479902-AGA, Qiagen) or water (mock) using Lipofectamine 3000 reagent according to manufacturer's protocol. Cells were incubated for 48 hours before harvesting for luciferase assays.

2.4.1.2 Luciferase assay

Media was replaced with 50 µl AbF media. Luciferase activity was measured using the Dual-Glo® luciferase assay system (E2940, Promega) according to manufacturer's protocol in opaque 96 well plates and with an EnVision™ 2103 multilabel microplate reader (Perkin Elmer). Luciferase activity was normalised to the Renilla luciferase internal control.

2.4.2 Mammalian cell transfection

2.4.2.1 Transfection of SW1353 cells with microRNA-29b

SW1353 cells were plated in 6-well plates ($1x10^5$ cells/well) in 1 ml AbF media and incubated until 80-90% confluent. Cells were transfected with 50 nM miR-29b-3p miRCURY LNA miRNA mimic, 50 nM negative control miRCURY LNA miRNA mimic or mock in 1 ml fresh AbF media using 2 µl Lipofectamine 3000 reagent per well according to manufacturer's protocol. Cells were incubated for 48 hours prior to being harvested in TRIzol™ Reagent.

2.4.2.2 Transfection of human articular chondrocytes with microRNA-29b

Human articular chondrocytes (HACs) were plated in 12-well plates ($1x10^5$ cells/well) in 1 ml AbF media and incubated until 80-90% confluent. Cells were transfected with 50 nM miR-29b-3p miRCURY LNA miRNA mimic, 50 nM negative control miRCURY LNA miRNA mimic or mock (water) in 1 ml fresh AbF media using 2 µl Lipofectamine 3000 reagent per well according to manufacturer's protocol. Cells were incubated for 48 hours prior to being harvested in TRIzol™ Reagent.

2.4.3 Mammalian cell cytokine stimulation

2.4.3.1 Stimulation of human articular chondrocytes with TGF-β1

2.4.3.2 Stimulation of SW1353 cells with TGF-β1

SW1353 cells were plated in 6-well plates ($1.5x10^5$ cells/well) in 2 ml maintenance media and incubated for 24 hours. Cells were serum starved by replacing media with 2 ml serum free media (DMEM plus GlutaMAX™ supplemented with 100 IU/ml penicillin and 100 µg/ml streptomycin) and incubated for a further 24 hours. Cells were stimulated with human recombinant TGF-β1 (5 ng/ml) for 8 or 24 hours or vehicle control (4 mM HCl with 0.5% (w/v) BSA) before being harvested in TRIzol™ Reagent. RNA was suspended 20 µl nuclease-free water (Sigma-Aldrich) and stored at -80 °C.

2.4.4 Treatment of SW1353 cells for dot blot

SW1353 cells were plated in 6-well plates ($1x10^5$ cells/well) in 1 ml AbF media and incubated until 80-90% confluent. Cells were transfected with 50 nM miR-29b-3p miRCURY LNA miRNA mimic (Qiagen), 50 nM negative control miRCURY LNA miRNA mimic (Qiagen) or mock (water) as in section 2.4.2.1. In addition, cells were treated with 5 µM 5-azacytidine (5-Aza), vehicle control (0.5% (v/v) DMSO) or left untreated. DNA was isolated as in section 2.3.7.1.1.

2.5 *In vivo* models

Mice were weaned at approximately 21 days old and separated by sex. Ear notches were taken for genotyping as described in 2.5.3.1. Surplus and experimental animals were sacrificed by exposure to carbon dioxide gas in a rising concentration followed by cervical dislocation as confirmation of death in accordance with Home Office regulations and Schedule 1 of the Animals (Scientific Procedures) Act 1986.

2.5.1 Cartilage specific knockout of microRNA-29

2.5.1.1 Breeding

To achieve cartilage-specific knockout of either the *miR-29ab1* or *miR-29b2c* loci, *miR-29ab1* floxed and *miR-29b2c* floxed mice respectively were crossed with *col2a1-cre* mice to produce *miR-29ab1*$^{fl/fl}$*:col2a1-cre* and *miR-29b2c*$^{fl/fl}$*:col2a1-cre* mice respectively.

To achieve cartilage-specific knockout of both the *miR-29ab1* and *miR-b2c* loci simultaneously, *miR-29ab1* and *miR-29b2c* floxed mice were crossed to produce homozygous double floxed mice. Double floxed mice were then crossed with *miR-29b2c* knockout mice to produce *miR-29ab1*$^{fl/fl}$*:miR-29b2c*$^{fl/fl}$*:col2a1-cre* mice.

For breeding and colony maintenance, *col2a1-cre* positive breeders were always male. Firstly, this was under advice from Dr. Attila Aszodi as to the best breeding practice for this line. Secondly, this strategy ensured the generation of Cre-positive and Cre-negative offspring enabling littermate controls to be used for *in vivo* experiments and reducing overall animal usage.

2.5.1.2 Genotyping

Ear tissue biopsies were obtained using an ear punch. GDNA was extracted from tissues using either a REDExtract-N-Amp™ tissue PCR kit (R4775, Sigma-Aldrich) or a Phire Tissue Direct PCR kit (F170L, Thermo Scientific) and PCR was performed using either REDExtract-N-Amp™ PCR reaction mix or Phire Tissue Direct PCR Master Mix respectively according to manufacturer's protocol.

Primers used to genotype for the *miR-29ab1* floxed locus were mir-29ab1-forward and mir-29ab1-loxP-reverse (wildtype, 419 bp; loxP, 581 bp). Primers used to genotype for the *miR-29b2c* floxed locus were mir-29b2c-forward and mir-29b2c-reverse (wildtype, 354 bp; loxP, 447 bp). Primers used to genotype for the *col2a1-cre* locus were cre2 and col2ex52b (wild-type no band; cre, 450 bp). See Figure 2.2 for example genotyping.

For gDNA knockout genotyping, gDNA was extracted from ear biopsies and liver tissue using the Phire Tissue Direct PCR kit. Hip cartilage gDNA was extracted using TRIzol reagent according to manufacturer's protocol. PCR was performed using Phire Tissue Direct PCR Master Mix. For *miR-29ab1* knockout primers were mir-29ab1-forward and miR-29ab1KO-reverse (wildtype, ~1350 bp; knockout, ~650 bp), and for *miR-29b2c* knockout primers were miR-29b2cKO-forward and miR-29b2cKO-reverse (wildtype, ~2000 bp; knockout,~700 bp).

For primer sequences see Table 2.2. Genotyping PCRs were performed using a Veriti™ 96-Well Thermal Cycler and PCR products were analysed using gel electrophoresis. Cycling conditions for the *miR-29ab1* locus, *miR-29b2c* locus and *col2a1-cre* locus are in Tables 2.3, 2.4 and 2.5 respectively. PCR products were analysed using gel electrophoresis.

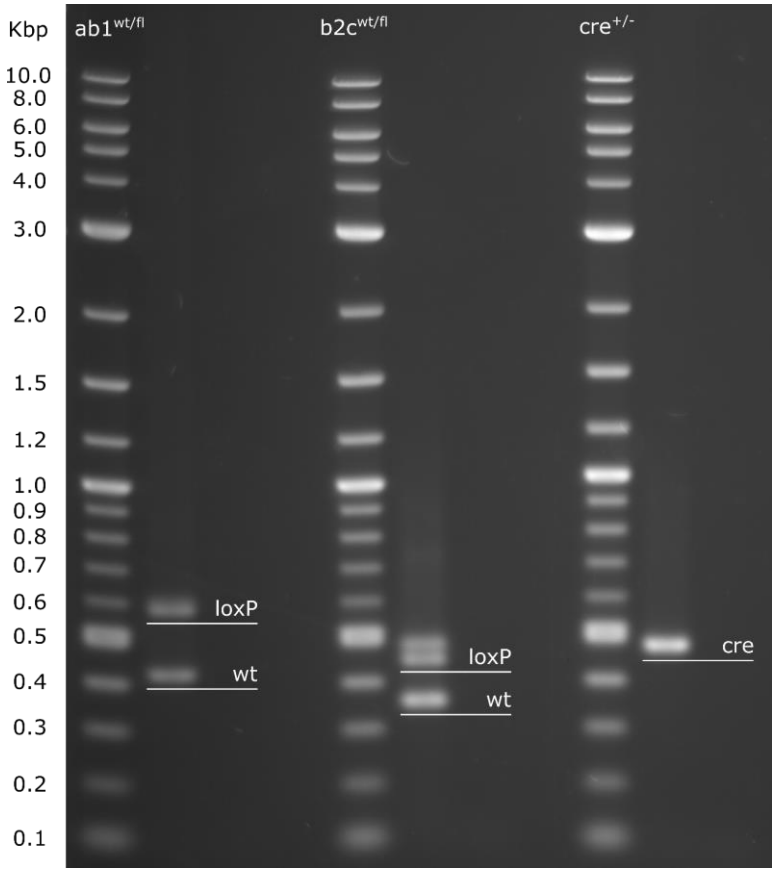

Figure 2.3. Example genotyping PCR. *Gel electrophoresis of genotyping for miR-29ab1$^{wt/fl}$, miR-29b2c$^{wt/fl}$ and cre$^{+/-}$. For miR-29ab1 wildtype (wt) band is 419 bp and loxP band is 581 bp. For miR-29b2c, wt band is 354 bp and loxP band is 447 bp. For col2a1-cre, wt band is absent and cre band is 450 bp.*

2.5.2 Destabilisation of the medial meniscus model

Table 2.2. Genotyping primers

Primer	Sequence (5'-3')
mir-29ab1-forward	TGTGTTGCTTTGCCTTTGAG
mir-29ab1-loxP-reverse	CCACCAAGAACACTGATTTCAA
miR-29ab1KO-reverse	CGAATTCGCCAATGACAAGACGCT
mir-29b2c-forward	AGTTAATTTGCTGTGCCAATCATA
mir-29b2c-reverse	ATAGAACTTTTTCACCGCCTACTG
mir-29b2cKO-forward	GGGATAGCATGTTTACAGTGAGTCT
mir-29b2cKO-reverse	TGGGATGAAGGCTTAGAAGAAGC
cre2	TCTGGTGTAGCTGATGATCCG
col2ex52b	TATGTCCACACCAAATTCCTG

Table 2.3. MiR-29ab1 genotyping cycle conditions

	REDExtract-N-Amp		Phire Tissue Direct		
Cycle step	**Temp**	**Time**	**Temp**	**Time**	**Cycles**
Initial denaturation	95 °C	5 min	98 °C	5 min	1
Denaturation	94 °C	30 s	98 °C	5 s	10
Annealing	70 °C(-1/cycle)	30 s	70 °C(-1/cycle)	5 s	
Extension	72 °C	1 min	72 °C	20 s	
Denaturation	94 °C	30 s	98 °C	5 s	25
Annealing	53 °C	30 s	53 °C	5 s	
Extension	72 °C	1 min	72 °C	20 s	
Final extension	72 °C	10 min	72 °C	1 min	1

Table 2.4. MiR-29b2c genotyping cycle conditions

	REDExtract-N-Amp		Phire Tissue Direct		
Cycle step	**Temp**	**Time**	**Temp**	**Time**	**Cycles**
Initial denaturation	94 °C	3 min	98 °C	5 min	1
Denaturation	94 °C	30 s	98 °C	5 s	10
Annealing	65 °C(-0.5/cycle)	30 s	65 °C(-0.5/cycle)	5 s	
Extension	72 °C	1 min	72 °C	20 s	
Denaturation	94 °C	30 s	98 °C	5 s	28
Annealing	60 °C	30 s	60 °C	5 s	
Extension	72 °C	1 min	72 °C	20 s	
Final extension	72 °C	2 min	72 °C	1 min	1

Table 2.5. Col2a1-cre genotyping cycle conditions

	REDExtract-N-Amp		Phire Tissue Direct		
Cycle step	**Temp**	**Time**	**Temp**	**Time**	**Cycles**
Initial denaturation	94 °C	5 min	98 °C	5 min	1
Denaturation	94 °C	30 s	98 °C	5 s	10
Annealing	63 °C	30 s	63 °C	5 s	
Extension	72 °C	30 s	72 °C	20 s	
Denaturation	94 °C	30 s	98 °C	5 s	20
Annealing	53 °C	30 s	53 °C	5 s	
Extension	72 °C	30 s	72 °C	20 s	
Final extension	72 °C	10 min	72 °C	1 min	1

DMM surgery was kindly performed by Dr. Tracey Swingler (University of East Anglia) and Mr. Richard Croft (University of East Anglia) as described in Blease *et al.* (2018). Male mice

aged 12 weeks were anaesthetised using 3% (v/v) isoflurane and maintained at 2% (v/v) prior to subcutaneous injection of 2.5 µg Vetergesic (Ceva Animal Health). Surgery was performed on the right knee. An incision was made medial to the parapatellar ligament and the medial meniscotibial ligament (MMTL) fully severed (Figure 2.4). The joint capsule was closed using a Vicryl 6-0 round-bodied needle suture kit (Ethicon) and the dermal layer above closed using an Ethilon 5-0 reverse-cutting needle suture kit (Ethicon). Once recovered from anaesthesia, mice were returned to their home cage, administered with Vetergesic once daily for 3 days, and weighed daily. Left and right legs were harvested 12 weeks post-surgery, processed and sectioned as in sections 2.5.3.1 and 2.5.3.2 respectively.

For each sample, six sections from the same point across all joints were analysed using the OARSI scoring system (Glasson *et al.*, 2010) by two scorers. Scorers were blind to the genotypes of samples when scoring.

2.5.3 Histological analysis

2.5.3.1 Tissue processing

Mice aged 3 weeks and 3 months old were sacrificed as in section 2.5, legs and inguinal fat pads (IGFP) were dissected, and skin and excess muscle removed. Legs and IGFP were

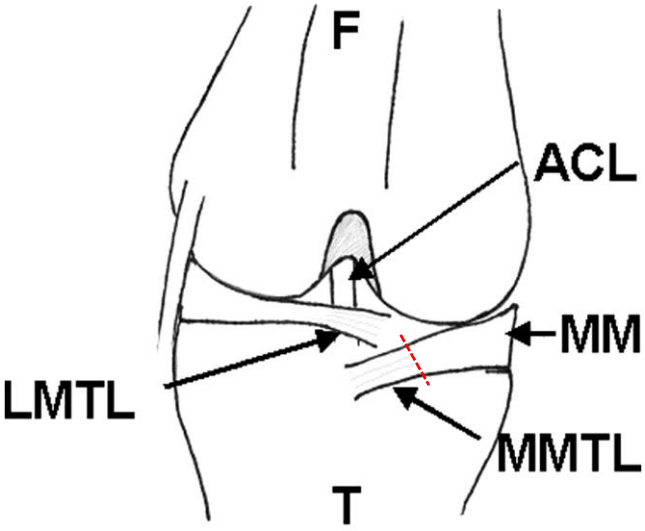

Figure 2.4. Destabilisation of the medial meniscus surgery. *In the destabilisation of the medial meniscus model, the medial meniscotibial ligament (MMTL) is surgically severed to induce osteoarthritis. In this diagram of a murine right knee joint, the femur (F), tibia (T), medial meniscus (MM), anterior cruciate ligament (ACL) and lateral meniscotibial ligament (LMTL) are also shown. Taken from Glasson, Blanchet and Morris, 2007.*

fixed in 10% (v/v) neutral buffered formalin (NBF) (HT501128, Sigma-Aldrich-Aldrich) for 24 hours at 4 °C and stored in 70% ethanol at 4 °C.

Legs from 3-week-old mice were decalcified in 14% (w/v) EDTA at room temperature for 7 days whereas 3-month aged legs were decalcified in 10% (w/v) formic acid (Thermo Scientific) for 48 hours at room temperature. Tissues were washed in running tap water for 1 hour prior to processing according to the protocol in Table 2.6. Legs were embedded in paraffin wax using a Microm EC 350 embedding centre. For 3-month aged mice, knees were embedded coronally for articular surface visualisation and for 3-week old mice, knees were embedded sagittally for growth plate visualisation.

Table 2.6. Tissue processing protocol.

Reagent	**Time**	**Temperature**
70% Ethanol	6 hours	Room temperature
90% Ethanol	45 minutes	Room temperature
95% Ethanol	45 minutes	Room temperature
100% Ethanol	45 minutes	Room temperature
100% Ethanol	45 minutes	Room temperature
100% Ethanol	45 minutes	Room temperature
Histoclear II*	30 minutes	Room temperature
Histoclear II	30 minutes	Room temperature
Histoclear II	30 minutes	Room temperature
Paraffin Wax**	Overnight	60 °C
Paraffin wax	1 hour	60 °C

**National Diagnostics **Paraplast, Sigma-Aldrich.*

2.5.3.2 Tissue sectioning

Paraffin embedded legs were sectioned using a Microm HM355S microtome and section transfer system with MX35 ultra blades (Thermo Scientific) and set at 42 °C. Embedded tissues were initially trimmed at 10 µm until the femoral condyles and tibial plateau became visible (Glasson *et al.*, 2010). Serial sections of 5 µm spanning 500 µm were collected across 25 Superfrost® Plus slides (Thermo Scientific), dried overnight at 37 °C and stored at room temperature.

2.5.3.3 Histological staining

Sections were stained with Weigert's Iron Haematoxylin (haematoxylin 0.5% w/v, ethanol 47.5% v/v, ferric chloride 0.58% w/v, HCl 0.5% v/v), Fast Green (0.06% w/v) and Safranin O (0.1% w/v) according to the protocol in Table 2.7. Stained sections were mounted with DPX New (Merck) under coverslips and airdried overnight at room temperature. Slides were

imaged using an Axioplan 2 brightfield microscope with an AxioCam HRc camera using AxioVision Digital Imaging Software (Zeiss) or Leica SCN400 slide scanner using the SCN400 Client (Leica).

Table 2.7. Haematoxylin, Fast Green and Safranin O staining protocol.

Reagent	**Time**
Histoclear II	5 minutes
Histoclear II	5 minutes
Ethanol 100%	5 minutes
Ethanol 90%	5 minutes
Ethanol 70%	5 minutes
Ethanol 50%	5 minutes
Distilled water	5 minutes
Haematoxylin	10 minutes
Distilled water	10 seconds
Acid Alcohol 0.5%	5 seconds
Running tap water	10 minutes
Fast green 0.06%	5 minutes
Acetic acid 1%	15 seconds
Safranin O 0.1%	5 minutes
Ethanol 95%	1 minute
Ethanol 100%	1 minute
Ethanol 100%	1 minute
Histoclear II	2 minutes
Histoclear II	2 minutes

2.5.3.4 Histological analyses

Imaged microscope slides were analysed using QuPath v. 0.3.2 (Bankhead *et al.*, 2017). Stain vector values for Safranin O, fast green and haematoxylin were set using slides from a control sample which were included in every staining batch. Analysis was performed on sections from comparable locations in respective joints. Tibial growth plates were selected by training a pixel classifier with control sample images whereas articular surfaces were selected manually using the wand tool.

2.5.4 X-ray analysis

2.5.4.1 X-ray imaging

P21 and 3-month aged legs were harvested, fixed, and stored in 70% ethanol as in section 2.5.2.1. Legs were oriented in the sagittal plane and imaged using an In-Vivo Xtreme imaging system (Bruker) with high resolution X-ray, 1.2 second exposure and using the magnification stage.

2.5.4.1.1 Femur measurement

X-ray images from 2.5.3.1 were analysed using ImageJ. To assess femur length, the distance from the greater trochanter to the medial condyle was measured and to assess femur width the diameter at the distal metaphysis was measured as in Figure 2.5.

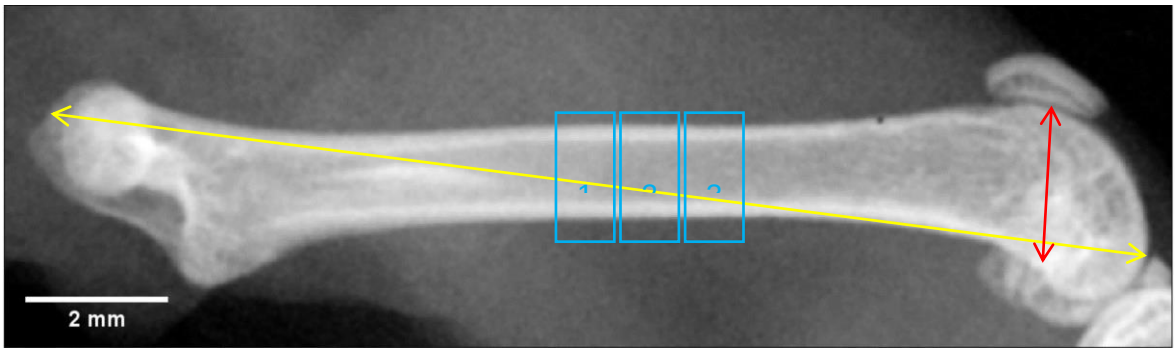

Figure 2.5. Representative 3-month aged femur x-ray. *Femur length and width in 3-week aged and 3-month aged mice was measured in x-ray images. Femur length was measured from the greater trochanter to the medial condyle (yellow line) and femur width was measured at the distal metaphysis (red line). For 3-month aged mice, bone density was measured using the Bruker Bone Density Software Module for three regions of interest (blue boxes) in the middle of the femur. Scale bar, 2 mm.*

2.5.4.1.2 Bone density analysis

Bone density and radius of X-rayed femurs was measured using Bruker Molecular Imaging Software v. 7.2.0.21122 with the Bruker Bone Density Software Module. Briefly, the Bone Density Software Module estimates long-bone mineralisation by modelling a cylindrical symmetry to an X-ray image and extracting the relevant parameters (Vizard *et al.*, 2010). Bone modelling assumes that the long bone has been X-rayed in the surrounding tissue. For 3-week aged femurs there was often insufficient tissue remaining after dissection to allow for reliable modelling, therefore only 3-month femurs were analysed. For bone density analysis, 3 standard size regions of interest (ROI) were generated in the middle of the femur (Figure 2.5) and mean values calculated. The chi-square value measures the quality of the cylindrical model fitting for each ROI. In line with the manufacturer's recommendation only ROIs with chi-square values between 8 and 80 were used for bone density analysis.

2.6 Statistical analysis

Relative expression data from qRT-PCR experiments was analysed using the $2^{-\Delta CT}$ method (Livak *et al.*, 2001) where CT is the threshold cycle and ΔCT = target gene CT - 18S rRNA (or U6 snRNA) CT.

Statistical analyses were performed using Microsoft Excel 2016 and Graphpad Prism 9. Data are presented as mean ± standard error (SE) unless otherwise stated. Data were checked for normality and transformed respectively where necessary prior to t-tests and ANOVAs. Differences between groups were analysed using a two-tailed Student's t-test,

one-way ANOVA with Tukey's post hoc test or two-way ANOVA with Sidak's post hoc test (* $p < 0.05$, ** $p < 0.01$, *** $p < 0.001$, **** $p < 0.0001$).

Chapter 3

Regulation of ADAMTS expression by microRNA-29

3 Regulation of ADAMTS expression by microRNA-29

3.1 Introduction

MiRNAs are able to target a plethora of mRNAs, often targeting multiple genes involved with related pathways or disease processes. Indeed normal animal development is dependent on miRNAs with global abolition of the miRNA processing enzyme Dicer being embryonic lethal in mice (Bernstein *et al.*, 2003). It is therefore not surprising that dysregulation of miRNA expression has been associated with a wide range of diseases including diabetes, heart disease, kidney disease and cancer (Paul *et al.*, 2017). Although the majority of miRNAs act intracellularly, miRNAs are also recognised a playing a key role in intercellular signalling. With this in mind, miRNAs are also rapidly emerging as potential biomarkers for a host of human diseases (Condrat *et al.*, 2020).

Dysregulation of miRNAs has been associated with OA (Iliopoulos *et al.*, 2008; Jones *et al.*, 2009; Díaz-Prado *et al.*, 2012; Balaskas *et al.*, 2017). A key miRNA implicated in OA is miR-140 which is reported to be down regulated in OA cartilage (Iliopoulos *et al.*, 2008; Miyaki *et al.*, 2009). MiR-140-5p has been shown to target several genes implicated in cartilage catabolism including *MMP13*, *ADAMTS5* and *IGFBP-5* (Tardif *et al.*, 2009). Therefore, whilst miR-140 knockout resulted in a premature OA-like phenotype, mice overexpressing miR-140 were protected from cartilage degradation in an antigen-induced arthritis model (Miyaki *et al.*, 2010).

Previous work in our lab by Dr. Linh Le suggested a potential role for the miR-29 family in OA. In human OA and murine DMM cartilage miR-29 was upregulated in diseased tissue and downregulated genes in DMM cartilage were concomitantly enriched for predicted miR-29 targets (Le *et al.*, 2016). Further experiments supported a potential role for miR-29 in OA. SOX9, NF-κB and TGF-β1 were found to negatively regulate the expression of miR-29 whereas IL-1 treatment of SW1353 upregulated miR-29 expression. Moreover, miR-29 and TGF-β appeared to act in a negative feedback loop with miR-29 repressing signalling, thereby inhibiting TGF-β1 reporter induction (Le *et al.*, 2016). Finally, several members of the ADAMTS family were shown to be directly targeted by miR-29, including *ADAMTS6*, *ADAMTS10*, *ADAMTS14*, *ADAMTS17*, *ADAMTS19* by miR-29 whereas expression of these genes was induced by TGF-β1 treatment (Le, 2015).

MiR-29 has been strongly implicated in OA based on previous work in our group and many miR-29 targets are known to play a role in the disease. In this chapter, the role of miR-29, in conjunction with TGF-β, in OA through the regulation the ADAMTS family will be further explored.

Aims

- Use existing datasets to identify ADAMTS genes potentially involved in OA.
- Identify which members of the ADAMTS family are regulated by miR-29.
- Investigate the effect of TGF-β1 stimulation on ADAMTS expression in primary human chondrocytes and chondrocyte cell lines.

3.2 Results

3.2.1 Bioinformatic analysis of existing datasets using SkeletalVis

SkeletalVis (phenome.manchester.ac.uk) is an online data portal developed by Soul *et al.* (2019), allowing the exploration and comparison of gene expression across 300 skeletal transcriptomics datasets. SkeletalVis both brings these datasets together, but also analyses them using a consistent pipeline, allowing more accurate comparison. To identify members of the ADAMTS family which maybe dysregulated in human and surgically induced murine models of OA, datasets from studies using comparable experimental conditions were analysed using SkeletalVis. For characteristics of the studies included in these analyses see Table 3.1.

For human OA analysis three studies were found which compared gene expression in joint-matched knee OA and healthy cartilage using either microarray or RNA-sequencing (Klinger *et al.*, 2013; Snelling *et al.*, 2014; Dunn *et al.*, 2016) (Figure 3.1). Studies utilising comparable tissues and methods were chosen to minimise variability in data. However, this approach does limit the number of studies analysed and the generalisability of results.

Across all three studies *ADAMTS1*, *ADAMTS2*, and *ADAMTS6* were consistently upregulated, whereas *ADAMTS3*, *ADAMTS13* and *ADAMTS20* were consistently downregulated. For *ADAMTS2*, *ADAMTS5*, *ADAMTS6* and *ADAMTS14*, expression was significantly upregulated ($q < 0.05$) in one study whereas no *ADAMTSs* were significantly downregulated. Expression data for *ADAMTS5* and *ADAMTS17* was only available in two of the datasets however their expression was upregulated in both. Similarly, expression data for *ADAMTS8* and *ADAMTS19* was only available in two of the datasets however their expression was downregulated in both.

For murine OA analysis three studies were found which compared gene expression in knee cartilage from DMM and sham surgery conditions after 2 weeks (Bateman *et al.*, 2013; Loeser *et al.*, 2013; Gardiner *et al.*, 2015) (Figure 3.2A) and two of which also after 8 weeks (Loeser *et al.*, 2013; Gardiner *et al.*, 2015) (Figure 3.2B).

Across all three studies at 2 weeks post-DMM *ADAMTS1*, *ADAMTS3*, *ADAMTS7*, *ADAMTS8*, *ADAMTS12*, *ADAMTS15* and *ADAMTS16* were consistently upregulated, whereas *ADAMTS18* was consistently down regulated. Expression data for *ADAMTS13* was only available in two of the datasets however its expression was downregulated in both. Expression of *ADAMTS5* and *ADAMTS12* was significantly upregulated in one study, whereas expression of *ADAMTS6* was significantly upregulated in two studies, and expression of *ADAMTS10*, *ADAMTS14* and *ADAMTS18* was significantly downregulated in one study. For the two studies with expression data at 8 weeks post-DMM *ADAMTS2*, *ADAMTS6*, *ADAMTS15* and *ADAMTS18* were consistently upregulated, whereas *ADAMTS1* was consistently downregulated. No *ADAMTSs* were significantly dysregulated in 8-week datasets.

Table 3.1. SkeletalVis study characteristics.

Model	Age (median)	Sample size (male / female)	Tissue	Platform	Study
HAC	64 years	10 (6 / 4)	Tibial plateau	Microarray	(Snelling *et al.*, 2014)
HAC	Not available	15 (ns)	Femoral condyle	Microarray	(Klinger *et al.*, 2013)
HAC	69.5 years	8 (5 / 3)	Femoral condyle	RNA-seq	(Dunn *et al.*, 2016)
2-weeks post-DMM	10-weeks	4 (4 / 0)	Whole knee	Microarray	(Bateman *et al.*, 2013)
2-weeks post-DMM	12-weeks	9 (9 / 0)	Tibial plateau	Microarray	(Loeser *et al.*, 2013)
2-weeks post-DMM	12-weeks	24 (24/0)	Tibial plateau	Microarray	(Gardiner *et al.*, 2015)

8-weeks post-DMM	12-weeks	9 (9 / 0)	Tibial plateau	Microarray	(Loeser *et al.*, 2013)
8-weeks post-DMM	12-weeks	24 (24/0)	Tibial plateau	Microarray	(Gardiner *et al.*, 2015)

ns (not stated)

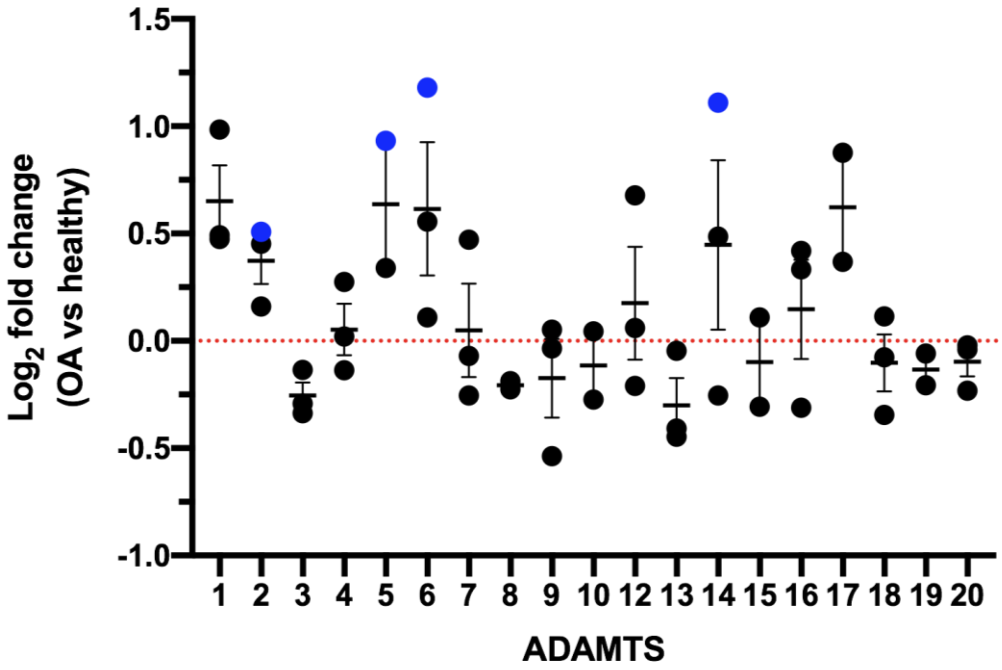

Figure 3.1. ADAMTS expression in human osteoarthritis. *Expression data from 3 joint-matched knee OA datasets were analysed using SkeletalVis. Log_2 fold change expression of ADAMTS genes in OA cartilage over healthy cartilage from the same knee was calculated. For data in blue adjusted p-value < 0.05. ADAMTS5, ADAMTS8, ADAMTS17 and ADAMTS19 n = 2, otherwise n = 3. Data presented as mean ± SEM.*

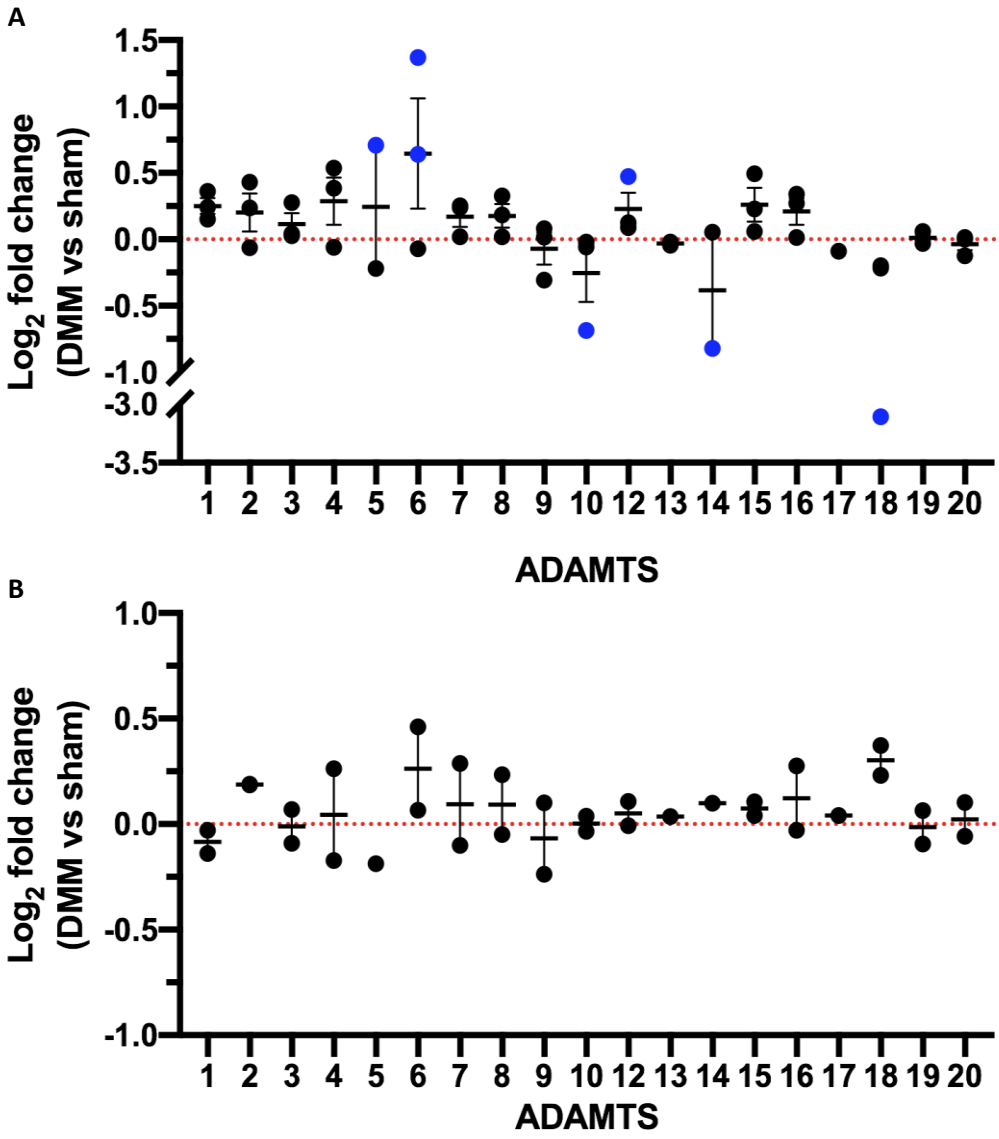

Figure 3.2. ADAMTS expression the DMM model of osteoarthritis. *Expression data from 3 murine DMM datasets 2 weeks post-surgery (A) and 2 murine DMM studies 8 weeks post-surgery (B) were analysed using SkeletalVis. Fold change expression of ADAMTS genes in knee cartilage from DMM over sham operated mice was calculated. For data in blue adjusted p-value < 0.05. 2 weeks post-surgery n = 2 for ADAMTS13, n = 1 for ADAMTS17, otherwise n = 3. 8 weeks post-surgery n = 1 for ADAMTS17, otherwise n = 2. Data presented as mean ± SEM.*

3.2.2 Identification of putative ADAMTS microRNA-29 targets

3.2.2.1 MicroRNA-29 target prediction

MiR-29 has previously been shown to regulate the expression of several members of the ADAMTS family including *ADAMTS7* (Du *et al.*, 2012), *ADAMTS6*, *ADAMTS10, ADAMTS14*, *ADAMTS17* and *ADAMTS19* (Le *et al.*, 2016). Given that dysregulation of miR-29 and several ADAMTSs have been associated with OA, the effect of miR-29 on ADAMTS expression was further investigated.

The miRabel miRNA target prediction tool (bioinfo.univ-rouen.fr/mirabel/) aims to improve the accuracy of miRNA target prediction by aggregating results from four prediction algorithms (miRanda, PITA, SVmicrO, and TargetScan) and generating a new miRabel score (Quillet *et al.*, 2020). To identify putative interactions between miR-29 and members of the ADAMTS family, miRabel was used to predict which of the ADAMTSs might be regulated by miR-29a-3p, miR-29b-3p and miR-29c-3p (Table 3.2).

For *ADAMTS7*, *ADAMTS9*, *ADAMTS10*, *ADAMTS14*, *ADAMTS17*, *ADAMTS18* and *ADAMTS19*, at least one algorithm predicted an interaction with miR-29 with a significant miRabel score (< 0.05). Only *ADAMTS4*, *ADAMTS8* and *ADAMTS12* were not predicted by any of the algorithms to be targeted by miR-29.

In addition to bioinformatic target prediction, the 3'-UTRs of all ADAMTSs were analysed for the miR-29 6mer seed sites (GGTGCT) (Table 3.2). Whilst 3'-UTRs of *ADAMTS1*, *ADAMTS3*, *ADAMTS4*, *ADAMTS8* and *ADAMTS13* contained no seed sites, the remaining ADAMTS all possessed at least one mir-29 6mer seed sites in their 3'-UTRs. Notably, not all ADAMTSs possessing miR-29 seed sites in their UTRs were predicted miR-29 targets.

Table 3.2. ADAMTS miR-29 target prediction.

Gene	miR-29a-3p		miR-29b-3p		miR-29c-3p		6-mer seed sites
	miRabel score	Algorithms	miRabel score	Algorithms	miRabel score	Algorithms	
ADAMTS1			0.964	M, S			0
ADAMTS2	0.975	S, T	0.975	S, T	0.975	S, T	7
ADAMTS3	0.967	M, S	0.968	M, S			0
ADAMTS4							0
ADAMTS5	0.086	P, M, S, T	0.1	P, M, S, T	0.116	P, M, S, T	2
ADAMTS6	0.117	P, M, S	0.102	P, M, S	0.104	P, M, S	1
ADAMTS7	0.001	P, M, S, T	0.001	P, M, S, T	0.001	P, M, S, T	1
ADAMTS8							0
ADAMTS9	0.001	P, M, S, T	0.001	P, M, S, T	0.001	P, M, S, T	3
ADAMTS10	0.005	P, M, S, T	0.009	P, M, S, T	0.005	P, M, S, T	1
ADAMTS12							5
ADAMTS13	0.773	M, S, T	0.788	M, S, T	0.777	M, S, T	0
ADAMTS14	0.033	P, M, S, T	0.059	P, M, S, T	0.043	P, M, S, T	4
ADAMTS15	0.987	T	0.985	T	0.987	T	5
ADAMTS16	0.446	P, M, S	0.878	P, M, S	0.867	P, M, S	2
ADAMTS17	0.001	P, M, S, T	0.001	P, M, S, T	0.001	P, M, S, T	5
ADAMTS18	0.009	P, M, S, T	0.008	P, M, S, T	0.006	P, M, S, T	1
ADAMTS19	0.01	P, M, S, T	0.023	P, M, S, T	0.018	P, M, S, T	2
ADAMTS20	0.964	T	0.963	T	0.963	T	2

PITA (P), miRanda (M), SVmicrO (S), TargetScan (T).

3.2.3 Members of the ADAMTS family are targeted by microRNA-29

3.2.3.1 MicroRNA-29 targets the 3'-UTRs of ADAMTSs

As previously mentioned, several members of the ADAMTS family have been shown to be regulated by miR-29. Multiple other ADAMTSs are predicted targets of miR-29 and/or contain one or more miR-29 seed sites in their 3'UTRs. To investigate whether miR-29 might directly regulate additional members of the ADAMTS family, the 3'UTRs of *ADAMTSs* which were predicted miR-29 targets and/or possessed at least one miR-29 seed site were cloned into the pmiRGLO luciferase reporter and cotransfected with miR-29b-3p mimic or negative control miRNA mimic in to DF1 cells for 48 hours. A reduction in luciferase activity with overexpression of miR-29b-3p indicated targeting of the 3'-UTR by miR-29.

MiR-29a, miR-29b and miR-29c share the same seed sequence and are predicted to target many of the same genes. Moreover mutual targeting of multiple genes has been demonstrated by previous work in our group (Le, 2015). In line with this and to reduce costs, it was deemed sufficient just to overexpress miR-29b-3p in experiments as this represented both miR-29 genomic loci and was likely to behave similarly to miR-29a and c.

The 3'UTR regions containing miR-29 seed sites of *ADAMTS2*, *ADAMTS5*, *ADAMTS7*, *ADAMTS9*, *ADAMTS12*, *ADAMTS15*, *ADAMTS16*, *ADAMTS18* and *ADAMTS20* were cloned downstream of the firefly luciferase reporter in pmiRGLO. 3'-UTR regions larger than 1000 bp were cloned as two regions into separate constructs for example ADAMTS2.1 and ADAMTS2.2. Le (2015) previously verified *ADAMTS6*, *ADAMTS10*, *ADAMTS14*, *ADAMTS17*, *ADAMTS19* as direct miR-29 targets, therefore luciferase assays for these were not repeated.

DF1 cells were transfected with 100 nM ADAMTS-3'UTR-pmiRGLO plasmid and either 50 nM miR-29b-3p mimic or 50 nM negative control mimic for 48 hours according to Le (2015) and Le *et al.* (2016). Transfection of miR-29b-3p mimic was confirmed by repression of a previously validated luciferase reporter plasmid (data not shown). Cells were then harvested and luciferase assays performed. Overexpression of miR-29b-3p significantly reduced luciferase activity for ADAMTS2.1, ADAMTS2.2, ADAMTS9, ADAMTS15.2, ADAMTS16, ADAMTS18 and ADAMTS20 3'-UTR reporters (Figure 3.3). Luciferase activity was also reduced by 0.59 and 0.77-fold for ADAMTS12.1 and ADAMTS12.2 3'-UTR constructs respectively, however this did not reach statistical significance.

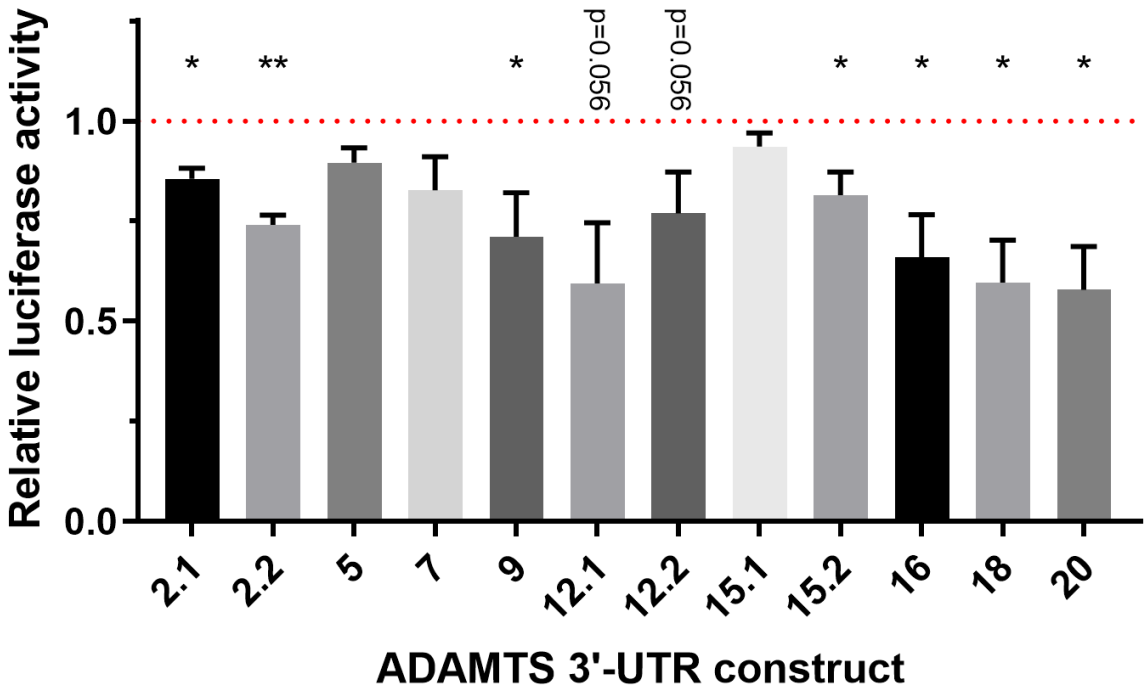

Figure 3.3. ADAMTS wild-type luciferase assays. *ADAMTS 3'-UTR luciferase reporter plasmids were contransfected into DF1 cells with miR-29b-3p or negative control miRNA mimic for 48 hours and luciferase assays were performed. Relative luciferase activity was normalised to Renilla luciferase and is presented as miR-29b-3p fold change over negative control. Data presented as mean ± SEM, n = 3, two-tailed unpaired t-test * p < 0.05, ** p < 0.01.*

3.2.3.2 Mutant luciferase assays

Overexpression of miR-29b-3p significantly reduced luciferase activity in multiple ADAMTS 3'-UTR-pmirGLO constructs. To verify that miR-29b was directly targeting the seed sites of respective 3'-UTRs, these seed sites were removed through mutagenesis and the luciferase assays repeated. Seed sites were mutated to either EcoR1, SalI or XbaI restriction sites to allow for confirmation of mutagenesis by restriction digest and were verified with sequencing.

Mutagenesis of miR-29 seed sites in ADAMTS2.1, ADAMTS2.2, ADAMTS9, ADAMTS12.1, ADAMTS12.2, ADAMTS15.2, ADAMTS16, ADAMTS18 and ADAMTS20 3'-UTR reporters rescued miR-29b-3p repression of luciferase activity (Figure 3.4). This confirmed that miR-29b was able to downregulate respective ADAMTS expression through direct binding to seed sites within the 3'-UTR. However, not all 3'-UTR reporters were completely rescued by seed site mutagenesis. Although to a far lesser extent, miR-29b-3p overexpression still significantly reduced luciferase activity in ADAMTS2.2 and ADAMTS16 reporters suggesting a degree of seed site-independent repression.

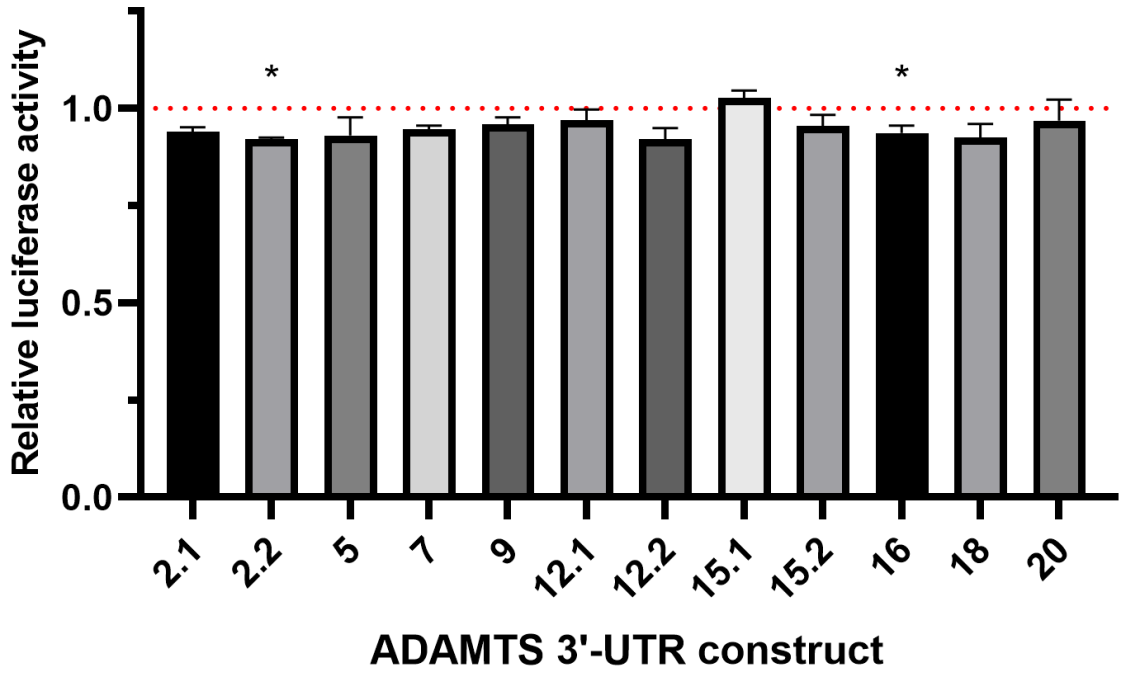

Figure 3.4. ADAMTS mutant luciferase assays. *Mutated ADAMTS 3'-UTR luciferase reporter plasmids were cotransfected into DF1 cells with miR-29b-3p or negative control miRNA mimic for 48 hours and luciferase assays were performed. Relative luciferase activity was normalised to Renilla luciferase and is presented as miR-29b-3p fold change over negative control miRNA mimic (red dotted line). Data presented as mean ± SEM, n = 3, two-tailed unpaired t-test * p < 0.05.*

3.2.3.3 Identification of non-functional miR-29-3p mimic

Subsequent experiments revealed that the batch of miR-29-3p miRCURY LNA mimic used for the mutant ADAMTS 3'-UTR assays (section 3.2.3.2) was not fully functional, despite reassurance from the manufacturer (Qiagen) that a yellow colour seen in the lyophilised mimic would not affect performance.

Repetition of the luciferase assay for the wild-type ADAMTS12.1 3'-UTR reporter using a fresh batch of miR-29b-3p mimic alongside that used in mutant ADAMTS 3'-UTR assays demonstrated that whilst the new batch repressed luciferase activity as in section 3.2.3.1, the older batch used in the mutant assays did not (Figure 3.5). This suggested that data from the mutated ADAMTS 3'-UTR may not be valid as the miR-29b-3p mimic used was not fully functional. Both wild-type and mutant luciferase assays for ADAMTS2.2 were repeated using the fresh batch of miR-29b-3p mimic to investigate whether seed site mutagenesis was indeed able to rescue significant miR-29b-3p repression (Figure 3.5). Although seed site mutagenesis rescued miR-29b-3p luciferase repression in the ADAMTS2.2 3'-UTR reporter, these assays would need to be repeated to confirm that seed mutagenesis was able to rescue miR-29b-3p repression in all ADAMTS 3'-UTR reporters - unfortunately the schedule did not leave enough time for repetition of these experiments within the current project.

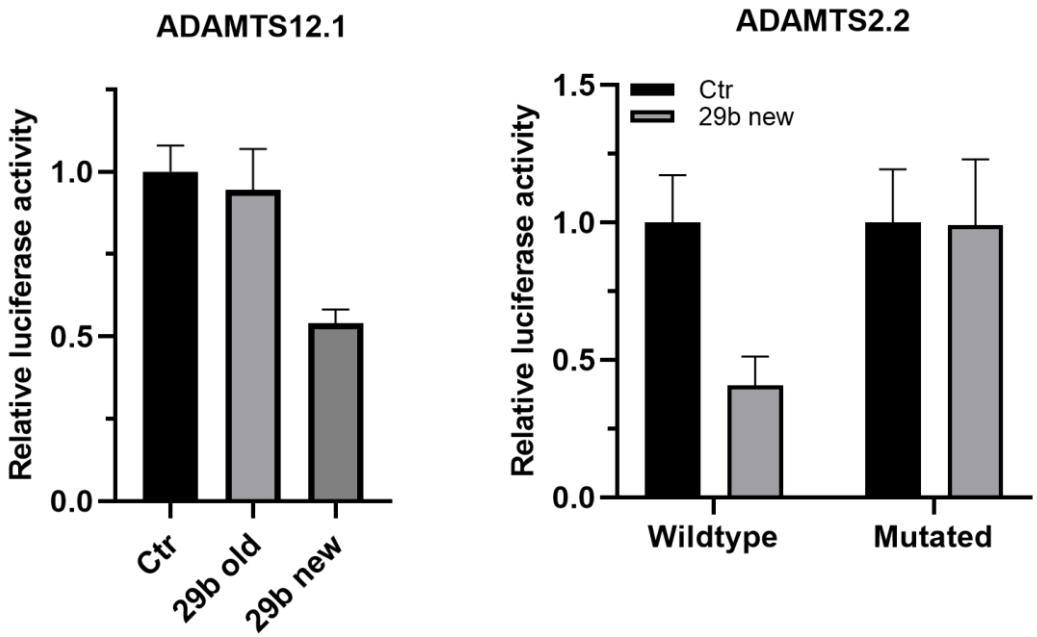

Figure 3.5. Non-functional miRNA-29b-3p mimic luciferase assays. *Luciferase assays were performed to compare the effect of two batches of miR-29b-3p mimic (29b old and 29b new) on wild-type ADAMTS12.1 3'-UTR luciferase reporter activity (A) and a fresh batch of miR-29b-3p mimic (29b new) on wild-type and mutated ADAMTS2.2 3'-UTR luciferase reporter activity (B). MiR-29b-3p mimic was compared to negative control miRNA mimic (ctr). Data presented as mean of 4 technical replicates ± SD, n = 1.*

3.2.3.4 ADAMTS expression is regulated by miR-29b in SW1353 cells

Members of the ADAMTS family showed evidence of dysregulation in OA and the ability to be directly regulated by miR-29b-3p in 3'-UTR luciferase reporter assays. To investigate the effect of miR-29 on the expression of ADAMTSs, SW1353 cells were transfected with 50 nM miR-29b-3p mimic for 48 hours and RNA was extracted. Whilst this experiment was initially performed with n = 3, subsequent identification of the non-functional miR-29b-3p batch described in section 3.2.3.3 suggested these data may be unreliable. Therefore, overexpression of miR-29b in SW1353 cells was repeated with n = 1 using the new functional miR-29b-3p batch.

In order to ensure that miRNA mimics were being effectively transfected into cells, miR-29b-3p mimic was transfected into SW1353 cells, expression of mature miR-29b was measured using qRT-PCR. Expression of mature miR-29b-3p was > 600-fold higher in cells transfected with miR-29b-3p mimic compared to the negative control (Figure 3.6) confirming efficient transfection of miRNA into cells.

Expression of all ADAMTS family members was also quantified using qRT-PCR in SW1353 cells and HACs. In SW1353 cells, *ADAMTS2*, *ADAMTS6*, *ADAMTS7*, *ADAMTS9*, *ADAMTS12*, *ADAMTS13*, *ADAMTS14* and *ADAMTS15* were substantially downregulated (> 20%) by miR-29b-3p transfection whilst expression of *ADAMTS1* and *ADAMTS16* appeared to be unregulated (Figure 3.6). Expression of *ADAMTS20* appeared to be

upregulated however standard deviation was high. *ADAMTS3*, *ADAMTS4*, *ADAMTS5*, *ADAMTS8*, *ADAMTS10*, *ADAMTS17*, *ADAMTS18* and *ADAMTS19* expression could not be reliably detected.

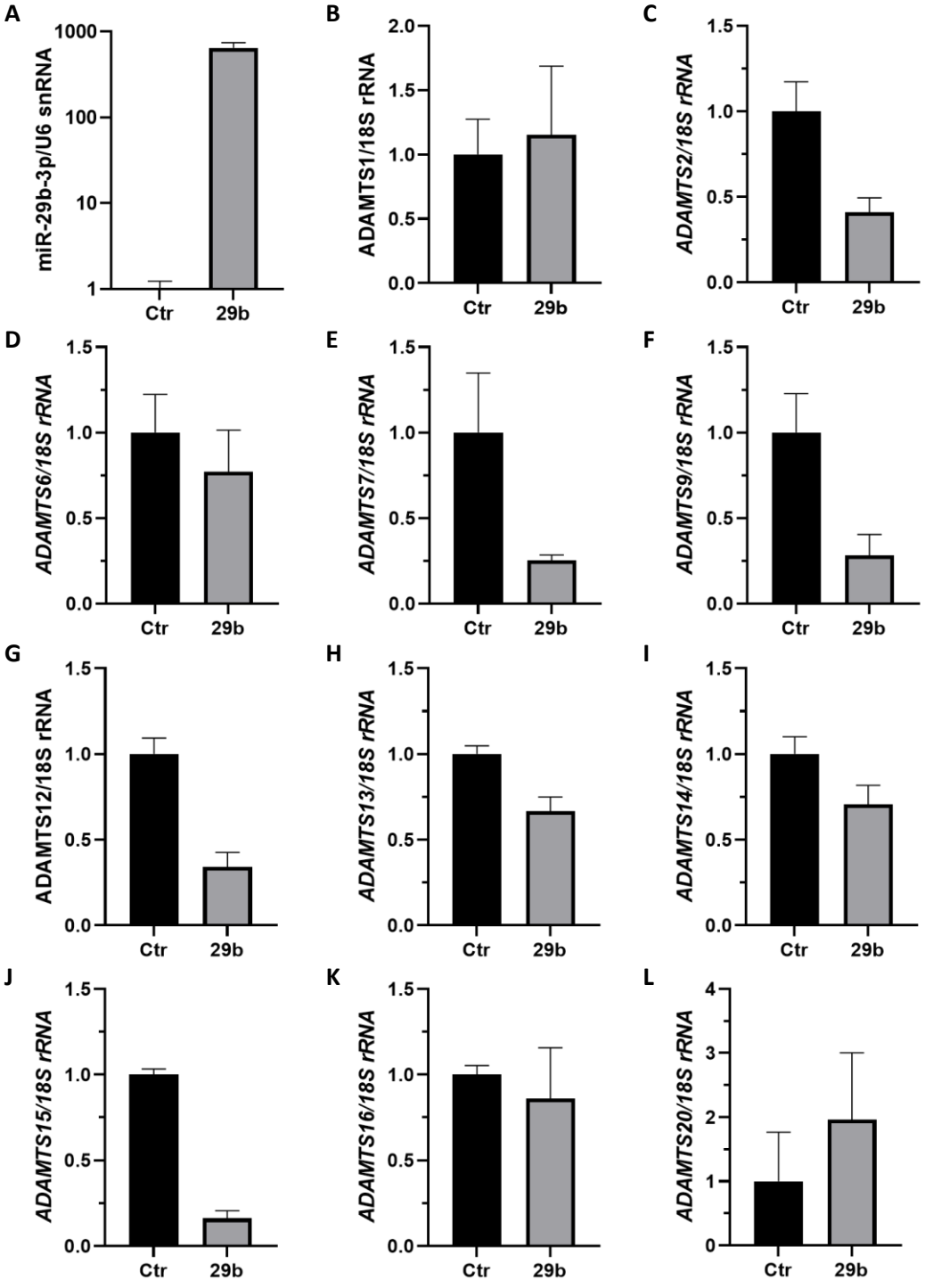

Figure 3.6. Effect of miRNA-29b overexpression on ADAMTS expression in SW1353 cells. *SW1353 cells were transfected with 50 nm miR-29b-3p mimic and negative control for 48 hours. Expression of mature miR-29b-3p (A) and ADAMTS1 (B), ADAMTS2 (C), ADAMTS6 (D), ADAMTS7 (E), ADAMTS9 (F), ADAMTS12 (G), ADAMTS13 (H), ADAMTS14 (I), ADAMTS15 (J), ADAMTS16 (K) and ADAMTS20 (L) were measured using qRT-PCR and normalised to U6 snRNA and 18S rRNA respectively. Data presented as mean of 3 technical replicates ± SD, n = 1.*

3.2.3.5 ADAMTS expression is regulated by miR-29b in primary chondrocytes

To verify efficient transfection of miRNA mimics, HACs were transfected with 50 nM FAM-tagged negative control miRCURY LNA miRNA mimic with increasing volumes of Lipofectamine 3000 reagent. Transfection efficiency was assessed by fluorescence microscopy with efficiency calculated as the proportion of cells showing fluorescein amidite (FAM) localisation. With all volumes of Lipofectamine FAM appeared to localise around the centre of cells (Figure 3.7A). Transfection efficiency increased from 61.6% with 0 µl Lipofectamine 3000 to 84.7% with 4 ul (Figure 3.7B).

In order to investigate whether miR-29 regulated ADAMTSs in a primary cell model, HACs were transfected with miR-29b-3p mimic for 48 hours and ADAMTS expression was measured using qRT-PCR (Figure 3.8). *ADAMTS12* was significantly downregulated by transfection with miR-29b-3p with *ADAMTS3*, *ADAMTS7*, and *ADAMTS15* being substantially (but not significantly) downregulated (> 20%). On the other hand, *ADAMTS1* and *ADAMTS4* were upregulated by 1.25-fold and 4.65-fold respectively however this failed to reach significance.

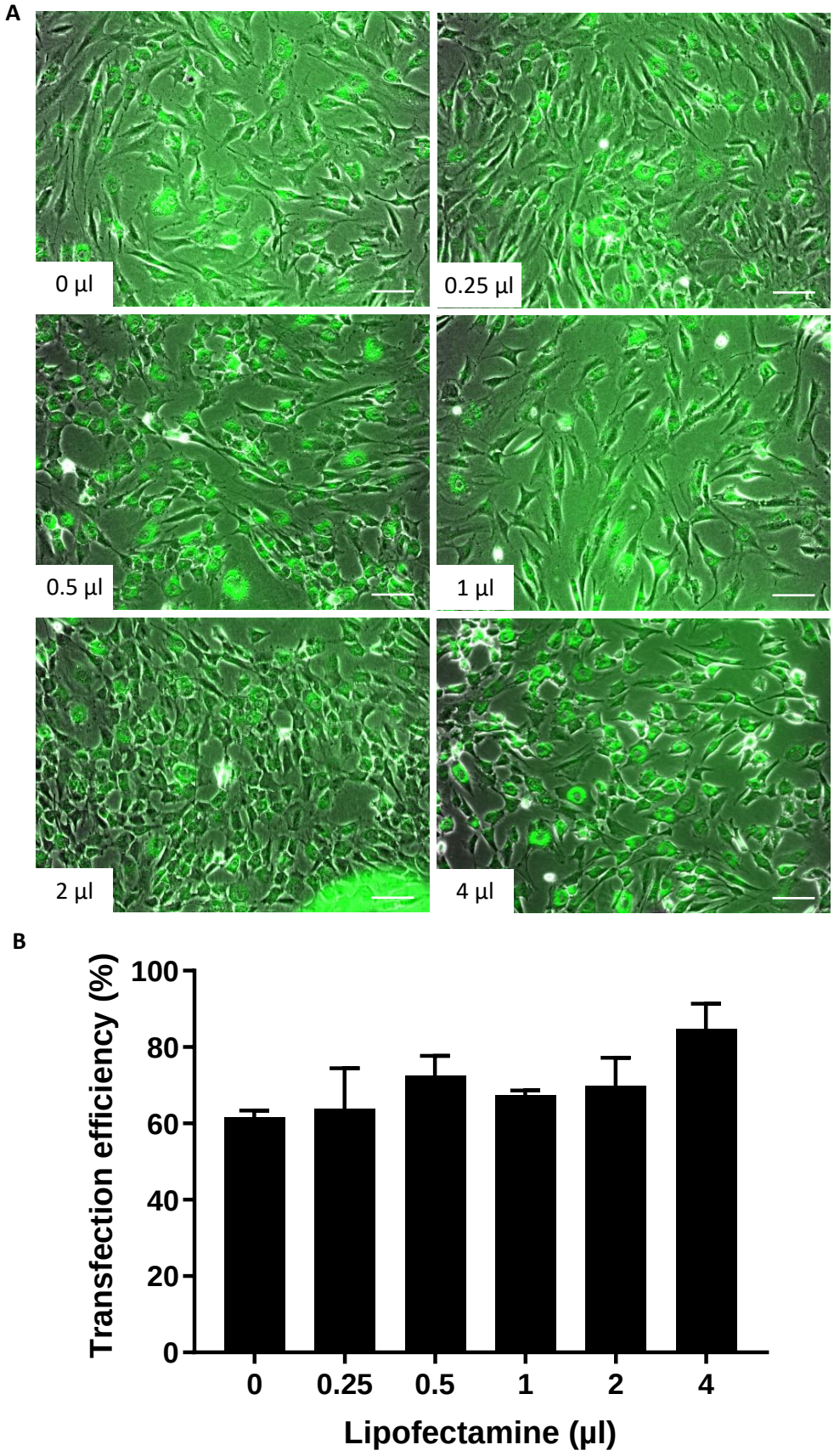

Figure 3.7. Transfection efficiency of miRNA mimics. *(A) Representative fluorescence microscope images of HACs transfected with 50 nM FAM-tagged negative control miRNA mimic and varying volumes of Lipofectamine 3000 reagent. Scale bar, 100 µm. (B) Transfection efficiency was calculated from the proportion of cells showing localisation of FAM. Data presented as as mean of 3 fields of view per well ± SD, n = 1.*

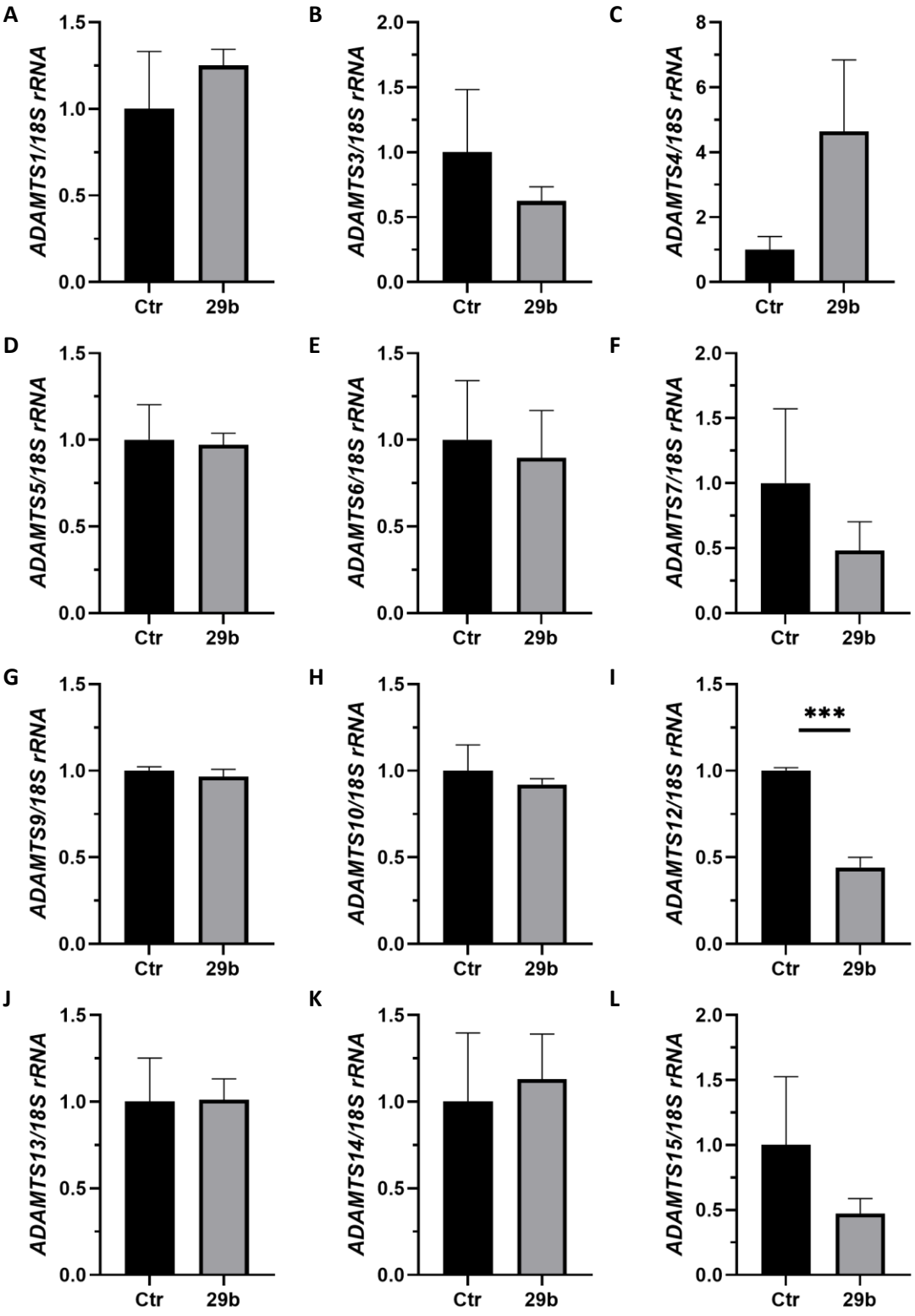

Figure 3.8. Effect of miRNA-29b overexpression on ADAMTS expression in human articular chondrocytes. *HACs were transfected with 50 nm miR-29b-3p mimic and negative control for 48 hours. Expression of ADAMTS1 (A), ADAMTS3 (B), ADAMTS4 (C), ADAMTS5 (D), ADAMTS6 (E), ADAMTS7 (F), ADAMTS9 (G), ADAMTS10 (H), ADAMTS12 (I), ADAMTS13 (J), ADAMTS14 (K) and ADAMTS15 (L) was measured using qRT-PCR and normalised to 18S rRNA. Data presented as mean ± SEM, n = 3, two-tailed unpaired t-test *** p < 0.001.*

3.2.3.6 Comparing miR-29b regulation of ADAMTS in primary and SW1353 cells

SW1353 is a chondrosarcoma cell line which is commonly used as a model for HACs which rely on access to human cartilage samples and yield a relatively limited number of chondrocytes. Moreover, *in vitro* proliferation of HACs leads to dedifferentiation and a loss of chondrocytic phenotype (Gebauer *et al.*, 2005). To assess how effectively SW1353 cells modelled ADAMTS expression in HACs, qRT-PCR data from both cell types transfected with miR-29b-3p were compared (Table 3.3). Expression of *ADAMTS1*, *ADAMTS6*, *ADAMTS7*, *ADAMTS9*, *ADAMTS12*, *ADAMTS13*, *ADAMTS14* and *ADAMTS15* was detectable in both SW1353 cells and HACs however expression of *ADAMTS8*, *ADAMTS17*, *ADAMTS18* and *ADAMTS19* could not be reliably detected in either cell type. On the other hand, *ADAMTS2*, *ADAMTS16* and *ADAMTS20* expression was only detected in SW1353 cells whereas *ADAMTS3*, *ADAMTS4*, *ADAMTS5* and *ADAMTS10* expression was only detected HACs.

In response to transfection with miR-29b-3p mimic, expression of *ADAMTS6*, *ADAMTS7*, *ADAMTS12* and *ADAMTS15* was downregulated and expression of *ADAMTS1* upregulated in SW1353 cells and HACs. Expression of *ADAMTS9* and *ADAMTS13* was downregulated in SW1353 cells and unaffected in HACs whereas expression of *ADAMTS14* was downregulated in SW1353 cells and upregulated in HACs.

Table 3.3. Regulation of ADAMTSs by miR-29: predicted targets, luciferase reporter repression and foldchange expression in SW1353 cells and HACs with miR-29b-3p overexpression

Gene	miRabel score < 0.05	3'-UTR luciferase repression	SW1353 cells	HACs
ADAMTS1	×	NA	1.2	1.3
ADAMTS2	×	✓	0.4	ND
ADAMTS3	×	×	ND	0.6
ADAMTS4	×	NA	ND	4.6
ADAMTS5	×	×	ND	1.0
ADAMTS6	×	✓*	0.8	0.9
ADAMTS7	✓	×	0.3	0.5
ADAMTS8	×	×	ND	ND
ADAMTS9	✓	✓	0.3	1.0
ADAMTS10	✓	✓*	ND	0.9
ADAMTS12	×	**	0.3	0.4***
ADAMTS13	×	NA	0.7	1.0
ADAMTS14	✓	✓*	0.7	1.1
ADAMTS15	×	✓	0.2	0.5
ADAMTS16	×	✓	0.9	ND
ADAMTS17	✓	✓*	ND	ND
ADAMTS18	✓	✓	ND	ND
ADAMTS19	✓	✓*	ND	ND
ADAMTS20	×	✓	2.0	ND

** Le 2015, ** p = 0.056, *** p < 0.001, NA (not assayed), ND (not detected)*

3.2.4 TGF-β1 regulation of ADAMTS

TGF-β signalling is known to play an important role in cartilage homeostasis. In line with this, dysregulation of TGF-β signalling has been found in OA cartilage along with SNPs in multiple TGF-β signalling components being associated with OA development (Verdier *et al.*, 2005; Tachmazidou *et al.*, 2019). Similarly to miR-29, TGF-β signalling has also been implicated in the regulation of ADAMTS expression in articular cartilage (Shen *et al.*, 2013).

Significantly, previous studies have found miR-29 may regulate TGF-β signalling and vice versa. Treatment of SW1353 cells and HACs with TGF-β1 was shown to downregulate the expression of miR-29 whereas transfection of SW1353 cells with a miR-29 mimic suppressed TGF-β induction of a TGF-β/Smad luciferase reporter (Le *et al.*, 2016).

To investigate whether miR-29 and TGF-β signalling may work together to regulate ADAMTS expression, the effect of TGF-β treatment in SW1353 cells and HACs on ADAMTS expression was assessed.

3.2.4.1 TGF-β1 stimulation of SW1353

To investigate the effect of TGF-β signalling on ADAMTS expression, SW1353 cells were treated with 5 ng/ml TGF-β1 for 8 or 24 hours and qRT-PCR was used to measure gene expression according to Le (2015). To confirm that cells were responding to TGF-β, expression of plasminogen activator inhibitor (PAI)-1, a well-known TGF-β inducible gene (Keeton *et al.*, 1991; Westerhausen *et al.*, 1991; Riccio *et al.*, 1992; Dennler *et al.*, 1998), was measured in TGF-β1 stimulated SW1353 cells. TGF-β1 treatment significantly upregulated *PAI-1* expression by 2.8 and 2.1-fold after 8 and 24 hours respectively (Figure 3.9).

The expression of ADAMTS family members was then measured in TGF-β1 treated SW1353 cells using qRT-PCR (Figure 3.9). *ADAMTS3*, *ADAMTS4*, *ADAMTS5*, *ADAMTS6*, *ADAMTS8*, *ADAMTS10*, *ADAMTS17*, *ADAMTS18*, *ADAMTS19*, *ADAMTS20* expression could not be reliably detected at the three time points across all three experiments and so the effect of TGF-β1 treatment on these genes in SW1353 cells could not be assessed. Expression of *ADAMTS9* in response to TGF-β1 treatment was significantly downregulated after 8 hours with a lesser, non-significant reduction still apparent after 24 hours. On the other hand, expression of *ADAMTS16* was significantly upregulated after 8 and 24 hours of TGF-β1 treatment. *ADAMTS15* expression was also upregulated after 8 and 24 hours however this did not reach statistical significance ($p = 0.615$ and $p = 0.051$ respectively).

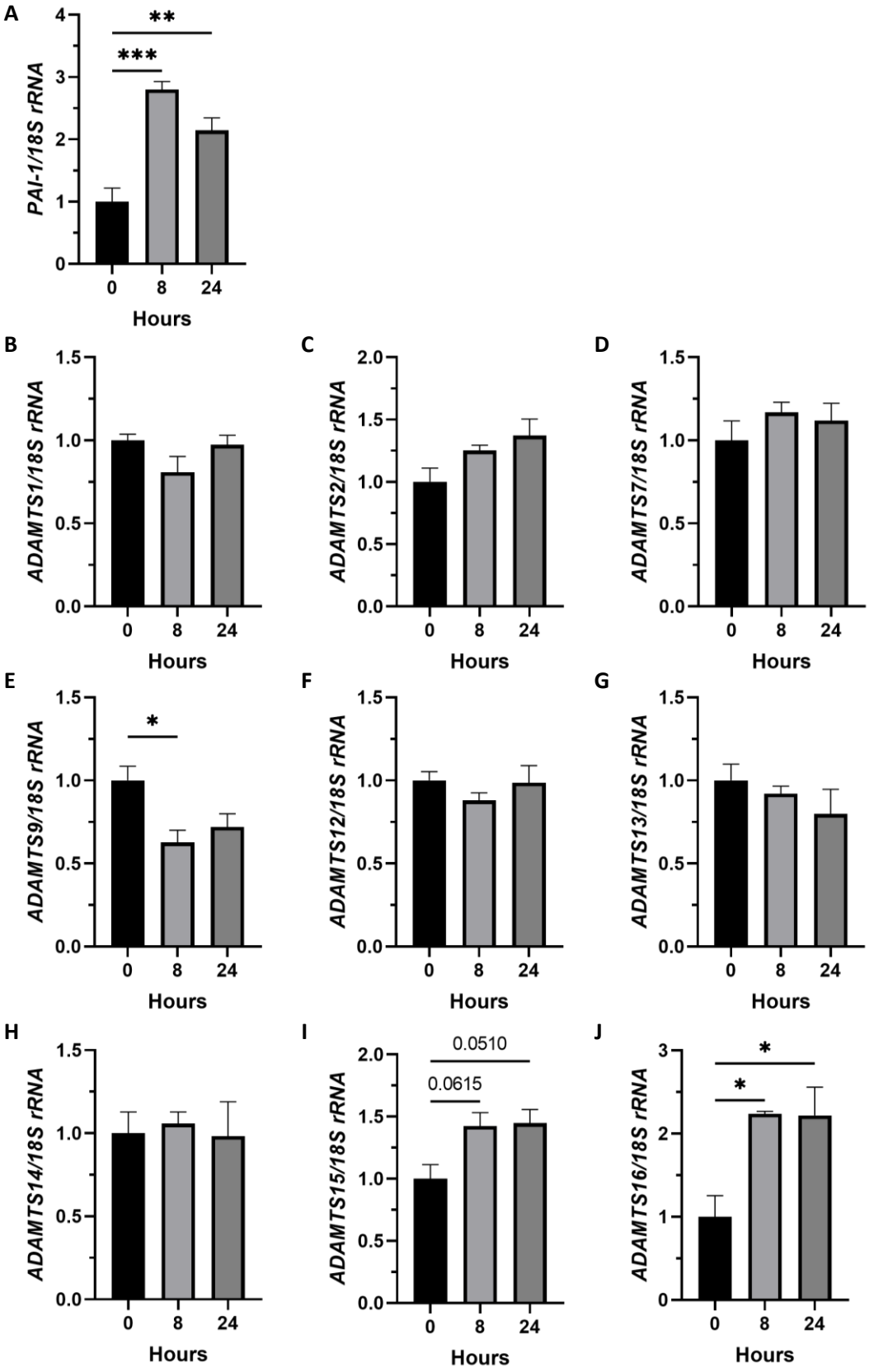

Figure 3.9. Effect of TGF-β1 stimulation on ADAMTS expression in SW1353 cells. *SW1353 cells were serum starved for 24 hours prior to treatment with 5 ng/ml TGF-β1 for 8 or 24 hours or vehicle control (4 mM HCl, 0.5% (w/v) BSA). PAI1 (A) and ADAMTS1 (B), ADAMTS2 (C), ADAMTS7 (D), ADAMTS9 (E), ADAMTS12 (F), ADAMTS13 (G), ADAMTS14 (H), ADAMTS15 (I) and ADAMTS16 (J) expression were measured using qRT-PCR and normalised 18S rRNA. Data presented as mean ± SEM, n = 3, one-way ANOVA with Dunnett's post hoc test, * p < 0.05, ** p < 0.01, *** p < 0.001.*

3.2.4.2 TGF-β1 stimulation of human primary chondrocytes

In order to investigate whether TGF-β signalling regulated ADAMTSs in a primary cell model. Although SW1353 cells grow quickly and can be passaged many times, HACs grow comparatively slowly with multiple passages resulting in dedifferentiation (Darling *et al.*, 2005). SW1353 cells demonstrated greater stimulation of PAI1 expression by TGF-β1 at 8 hours compared to 24 hours, therefore due to a limited number of cells, TGF-β1 treatment of HACs was performed for 8 hours. HACs were treated with 5 ng/ml TGF-β1 for 8 hours and qRT-PCR was used to measure gene expression. In line observations in SW1353 cells, *PAI-1* was significantly upregulated in HACs 8 hours after TGF-β1 treatment (Figure 3.10). However, whereas TGF-β1 treatment upregulated *PAI-1* expression by 2.8-fold in SW1353 cells, *PAI-1* was upregulated by 18.8-fold in HACs after 8 hours indicating a more robust response to TGF-β1 stimulation.

Expression of ADAMTSs was regulated more dramatically in HACs when compared to SW1353 cells in response to TGF-β1 treatment. *ADAMTS1*, *ADAMTS3*, *ADAMTS5*, *ADAMTS9*, *ADAMTS12*, *ADAMTS13*, *ADAMTS15, ADAMTS19* and *ADAMTS20* were significantly downregulated 8 hours after TGF-β1 treatment whereas *ADAMTS2*, *ADAMTS4*, *ADAMTS6*, *ADAMTS10* and *ADAMTS14* were significantly upregulated. TGF-β1 treatment did not significantly augment the expression of *ADAMTS7*.

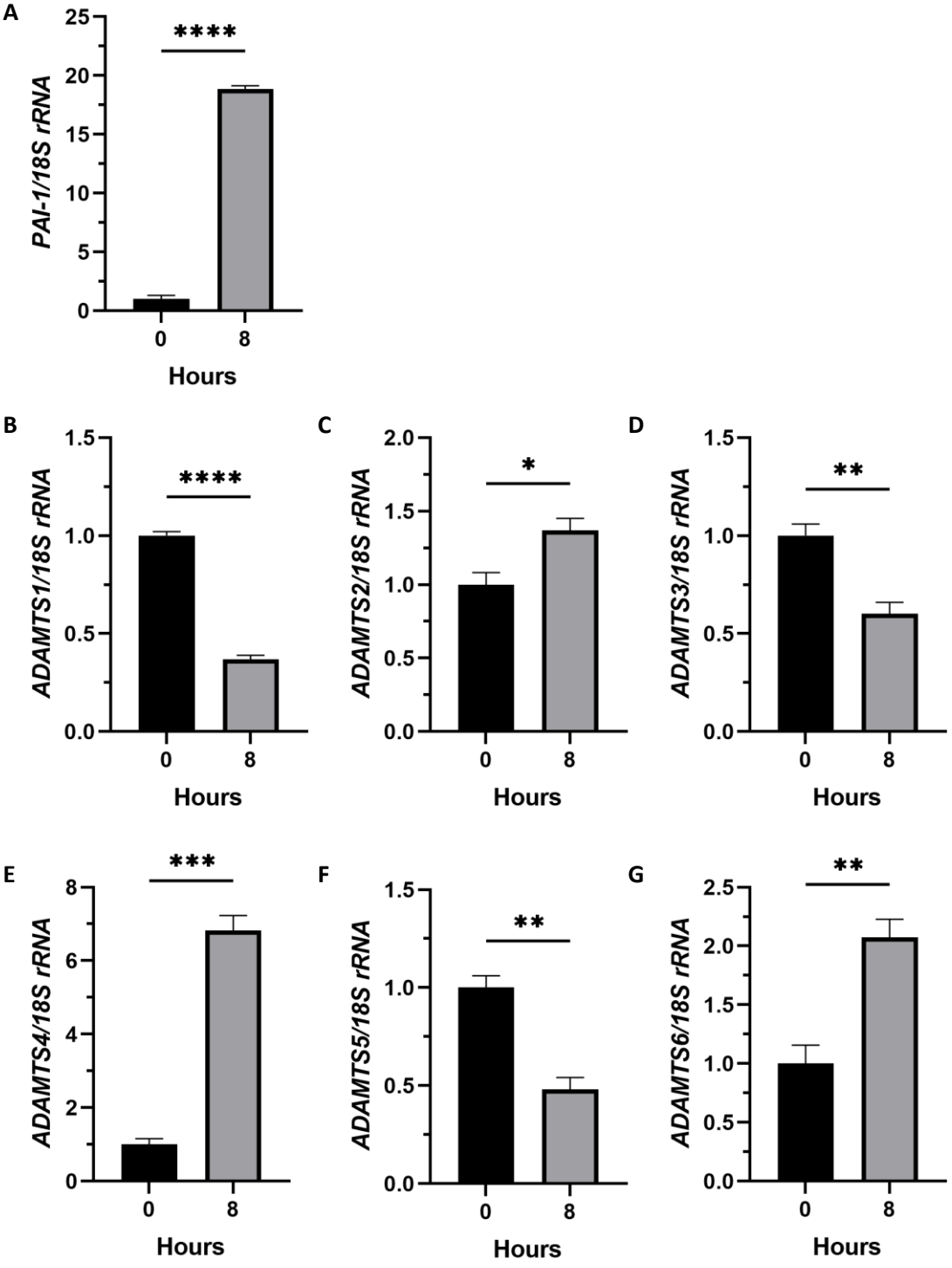
A
PAI-1/18S rRNA
****
Hours
B
ADAMTS1/18S rRNA
****
Hours
C
ADAMTS2/18S rRNA
*
Hours
D
ADAMTS3/18S rRNA
**
Hours
E
ADAMTS4/18S rRNA
***
Hours
F
ADAMTS5/18S rRNA
**
Hours
G
ADAMTS6/18S rRNA
**
Hours

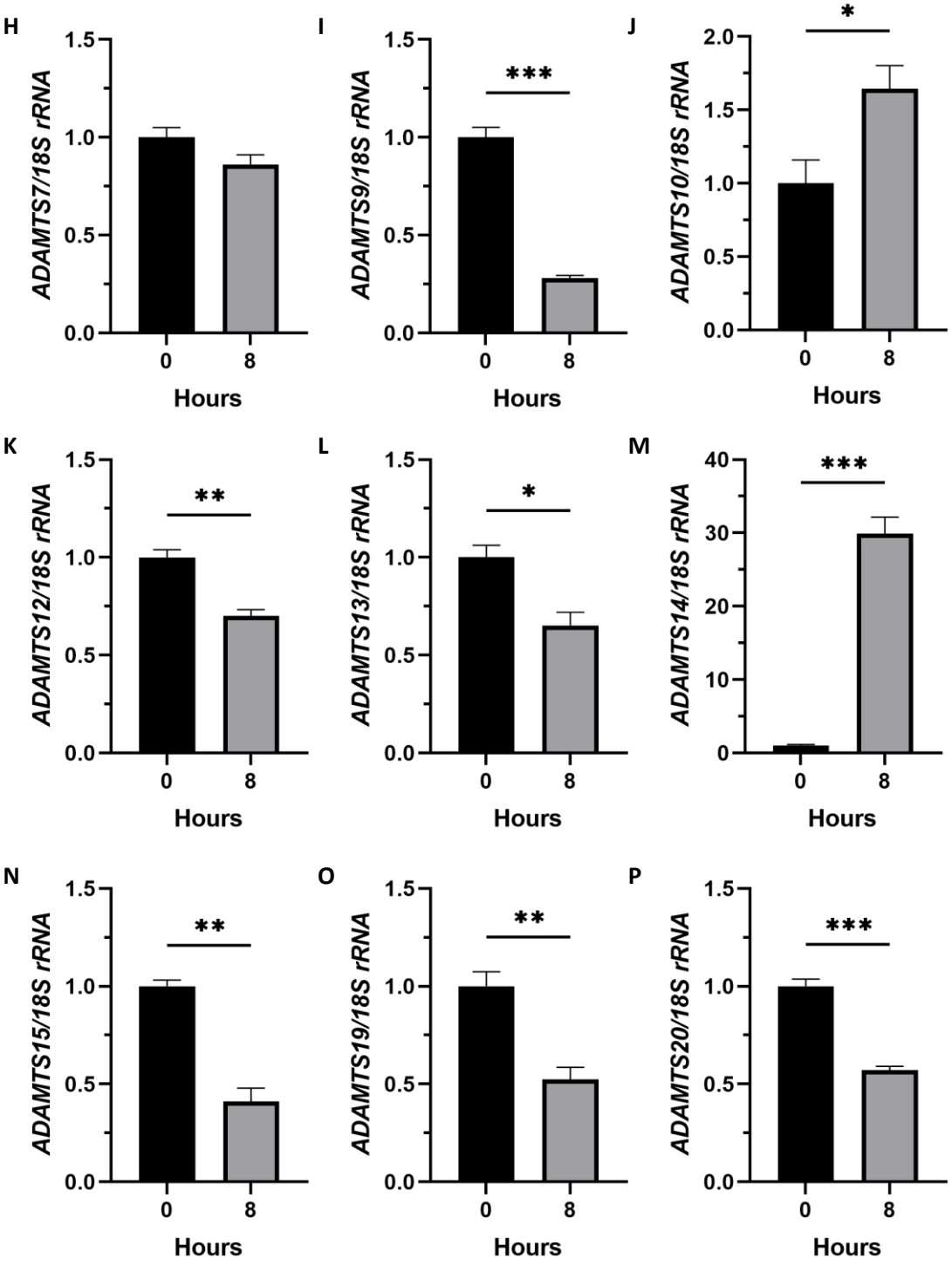

Figure 3.10. Effect of TGF-β1 stimulation on ADAMTS expression in human articular chondrocytes. *HACs were serum starved for 24 hours prior to treatment with 5 ng/ml TGF-β1 for 8 or vehicle control (4 mM HCl, 0.5% (w/v) BSA). PAI1 (A) and ADAMTS1 (B), ADAMTS2 (C), ADAMTS3 (D), ADAMTS4 (E), ADAMTS5 (F), ADAMTS6 (G), ADAMTS7 (H), ADAMTS9 (I), ADAMTS10 (J), ADAMTS12 (K), ADAMTS13 (L), ADAMTS14 (M), ADAMTS15 (N), ADAMTS (O) and ADAMTS20 (P) expression were measured using qRT-PCR and normalised 18S rRNA. Data presented as mean ± SEM, n = 3, two-tailed unpaired t-test, * p < 0.05, ** p < 0.01, *** p < 0.001, **** p < 0.0001.*

3.3 Discussion

The aim of this project was to establish whether the miR-29 family plays an important role in cartilage development and the pathogenesis of OA. Specifically, this chapter sought to identify members of the ADAMTS family which are regulated by miR-29 and TGF-β in cell lines and primary human chondrocytes.

Many members of the ADAMTS family have been implicated in OA with their ability to degrade a wide range of extracellular matrix components. Expression of the miR-29 family is dysregulated in OA and miR-29a, miR-29b and miR-29c have previously been shown to target multiple ADAMTSs alluding to a potentially important regulatory network (Le *et al.*, 2016). Finally, dysregulation of TGF-β signalling in OA is well documented (Blaney Davidson *et al.*, 2007; Shen *et al.*, 2014; Cherifi *et al.*, 2021) with TGF-β being known to regulate the expression of *ADAMTS4* and *ADAMTS5* (Moulharat *et al.*, 2004; Shen *et al.*, 2013; Cilek *et al.*, 2021) along with reciprocating negative regulation by miR-29 (Le *et al.*, 2016).

Using SkeletalVis, ADAMTS expression was analysed in transcriptomic datasets from three human OA, three 2-week DMM studies and two 8-week DMM studies. Broadly, overlap between human and murine OA studies was poor. Only *ADAMTS1* was consistently upregulated in human OA and 2-week DMM studies with *ADAMTS5* and *ADAMTS6* being significantly upregulated ($q < 0.05$) in at least one human and murine study. Whilst *ADAMTS2* and *ADAMTS6* were consistently upregulated in human and 8-week DMM studies, there was no overlap in ADAMTS downregulation between human OA and DMM studies.

One explanation for the poor overlap between human OA and DMM studies may lie in the relative age differences of these models. In human OA studies, tissue was taken from patients in their 60's, consistent with OA being a disease of old age. In contrast, DMM surgery was performed on 10-12-week-old mice and with tissue being harvested 1-8 weeks later. Given that 'old' mice, equivalent to humans aged 40-50 years, are 18-24 months old (Castanheira et al., 2021), studies using much younger mice may not accurately model the disease process. Consistent with this, DMM-induced OA has been found to be more severe in mice aged 12-months compared with 12-weeks, accompanied by the DE of 493 genes (Loeser et al., 2012).

Upregulation of *ADAMTS5* in OA cartilage has been shown previously and analysis using SkeletalVis is consistent with this (Song *et al.*, 2007). Analysis also showed upregulation of *ADAMTS1*, *ADAMTS2*, *ADAMTS6*, and *ADAMTS17*. Similarly to *ADAMTS4* and *ADAMTS5*, *ADAMTS1* is recognised as a proteoglycanase and thus upregulation in OA is

unsurprising, however not all studies corroborate this finding (Kevorkian *et al.*, 2004). Expression of *ADAMTS2* was upregulated across both human OA and murine DMM studies. *ADAMTS2* is a procollagen N-proteinase and as such, upregulation in OA has been suggested as a repair response to cartilage damage (C. Y.-Y. Yang *et al.*, 2017). On the other hand, expression of another procollagen N-proteinase, *ADAMTS3* was downregulated in human OA studies potentially representing a failure of ECM repair. Along with confirming changes in ADAMTS expression in OA which have been shown previously, analysis of existing transcriptomics datasets with SkeletalVis suggested the regulation of other ADAMTSs in OA which are less well characterised but may merit further investigation.

Bioinformatic analysis utilising the miRabel miRNA target prediction tool predicted miR-29 targeting of all ADAMTS family members except *ADAMTS4*, *ADAMTS8* and *ADAMTS12*. Moreover, significant miRabel scores (≤ 0.05) for *ADAMTS7*, *ADAMTS9*, *ADAMTS10*, *ADAMTS14*, *ADAMTS17*, *ADAMTS18* and *ADAMTS19* strongly suggested miR-29 interactions. Interestingly, whilst the presence of a 3'-UTR miR-29 seed site (6-mer) was necessary for a significant miRabel score, not all ADAMTS possessing 3'-UTR seed sites were predicted targets. Indeed, whilst *ADAMTS2* and *ADAMTS12* have seven and five 3'-UTR miR-29 seed sites respectively, neither were predicted targets of miR-29 highlighting the importance of features outside of the seed sequence in these algorithms.

Luciferase assays found downregulation of *ADAMTS2*, *ADAMTS9*, *ADAMTS12* ($p = 0.056$) *ADAMTS15*, *ADAMTS16*, *ADAMTS18* and *ADAMTS20* by miR-29b-3p. Although mutation of 3'-UTR seed sequences appeared to abolish miR-29 targeting, the subsequent identification of a non-functional mimic suggested these data may not be reliable. In light of this, repetition of these assays with a validated mimic will be needed to verify these data.

Overexpression of miR-29b-3p in SW1353 cells downregulated expression of *ADAMTS2*, *ADAMTS9*, *ADAMTS12* and *ADAMTS15* however because of the non-functioning mimic, these experiments were only completed for $n = 1$ and require further repeats for validation. In HACs overexpressing miR-29b-3p, *ADAMTS12* was significantly downregulated, in line with data from SW1353 experiments and luciferase assays. Therefore *ADAMTS12* was the most promising miR-29 target based on these experiments.

Adamts12 knockout mice are born healthy and have no overt phenotype (Hour *et al.*, 2010), as is the case for the closely related *Adamts7* (Bauer *et al.*, 2015). However double knockout of *Adamts12* and *Adamts7* results in heterotopic ossification of the hindlimb tendon, ligament and meniscal tissues after 4 months suggesting functional overlap between these two COMP degrading enzymes (Mead *et al.*, 2018). In fact, knockout of *Adamts7* resulted in compensatory upregulation of *Adamts12* in murine tendons and *vice versa* (Mead *et al.*, 2018). Expression of *ADAMTS12* has be shown to be upregulated in

OA and RA cartilage as well as RA synovium (Kevorkian *et al.*, 2004; Davidson *et al.*, 2006; Liu, 2009). ADAMTS12 is suggested to favour OA progression by degrading COMP. Fragments of the same size as those seen by *in vitro* ADAMTS12 COMP digestion were found in human OA cartilage and IL-1β and TNF-α upregulated ADAMTS12 expression (Luan *et al.*, 2008). On the other hand, inhibition of ADAMTS12 using antibodies, siRNA and the α2M competitive inhibitor reduced COMP degradation (Luan *et al.*, 2008).

In addition to COMP degradation, ADAMTS12 has also been implicated in inflammation in OA. In several models of inflammation including asthma, colitis, endotoxic sepsis, and pancreatitis, *Adamts12* knockout mice demonstrated an elevated inflammatory response (Moncada-Pazos *et al.*, 2012; Paulissen *et al.*, 2012). Moreover, in the collagen-induced arthritis model, *Adamts12* deficiency promoted inflammatory arthritis development with knockout mice showing increased paw swelling, cartilage loss, bone destruction and synovitis (Wei *et al.*, 2018). On the other hand, overexpression of *Adamts12 in vitro* attenuated IL-1β induction of inflammatory signalling pathways such as NF-κB, p38 and JNK via cleavage of CTGF (Wei *et al.*, 2018), whereas in OA synovial fibroblasts, IL-1β upregulated *ADAMTS12* expression (Pérez-García *et al.*, 2016). Therefore, ADAMTS12 not only contributes to OA development through degradation of COMP, but through its role as an inflammatory mediator.

Expression of *ADAMTS4* was also increased in HACs overexpressing miR-29b-3p by 4.6-fold although this was not statistically significant. Upregulation of *ADAMTS4* in OA has been associated with demethylation of specific CpG sites in the promoter region (Roach *et al.*, 2005; Cheung *et al.*, 2008) and miR-29 is widely recognised for its role in regulating components of the DNA methylation machinery (Amodio *et al.*, 2015; Memari *et al.*, 2018). Considering this, upregulation of *ADAMTS4* by miR-29 may be mediated through downregulation of *DNMT3A* and/or *DNMT3B* and subsequent hypomethylation of key CpGs within the *ADAMTS4* promoter. Future experiments exploring the methylation status of the *ADAMTS4* promoter with miR-29 overexpression would be needed to confirm this regulatory mechanism.

Putting together the data discussed above, miR-29 may regulate the expression some ADAMTSs (Table 3.3), although further investigation is needed. *ADAMTS9*, *ADAMTS10*, *ADAMTS14*, *ADAMTS17*, *ADAMTS18* and *ADAMTS20* were predicted miR-29 targets (miRabel score < 0.05) and the 3-UTRs of these genes were directly targeted by miR-29b-3p in this and previous studies in our group. In HACs overexpressing miR-29b, none of these genes were found to be significantly downregulated suggesting that targeting seen in luciferase assays may not be biologically significant. Whilst *ADAMTS7* was a predicted miR-29 target, luciferase assays found no evidence of a direct interaction. Conversely,

ADAMTS2, *ADAMTS6*, *ADAMTS12*, *ADAMTS15* and *ADAMTS16* were not predicted miR-29 targets, but luciferase assays in this and previous studies have suggested direct targeting. *ADAMTS12* showed evidence of direct targeting by miR-29 in luciferase assays ($p = 0.056$) although mutant assays would be needed to confirm this. Moreover, *ADAMTS12* was downregulated in SW1353 and HACs overexpressing miR-29b suggesting that miR-29 may regulate *ADAMTS12 in vivo*. MiRNA target prediction tools can be helpful in suggesting potential interactions and guiding experimental design. However, the data presented here demonstrate that such tools should not be relied upon and that any predicted interactions require experimental validation. Equally, genes that are not predicted miRNA targets may indeed to be targeted *in vivo*.

To investigate the effect of TGF-β signalling on ADAMTS expression, SW1353 cells and HACs were treated TGF-β1 (5 ng/ml). *PAI-1*, a well-known TGF-β inducible gene (Keeton *et al.*, 1991; Westerhausen *et al.*, 1991; Riccio *et al.*, 1992; Dennler *et al.*, 1998) was significantly upregulated in SW1353 cells and HACs after 8 hours. However, whilst *PAI-1* was upregulated by 2.8-fold in SW1353 cells, it was upregulated by 18.8-fold in HACs suggesting more robust activation of TGF-β signalling.

In SW1353 cells, TGF-β1 treatment significantly downregulated expression of *ADAMTS9* after 8 hours and significantly upregulated expression of *ADAMTS16* after both 8 and 24 hours. TGF-β1 treatment of HACs for 8 hours elicited a more substantial response than in SW1353. Whilst expression of *ADAMTS1*, *ADAMTS3*, *ADAMTS5*, *ADAMTS9*, *ADAMTS12*, *ADAMTS13*, *ADAMTS15, ADAMTS19* and *ADAMTS20* was significantly downregulated, expression of *ADAMTS2*, *ADAMTS4*, *ADAMTS6*, *ADAMTS10* and *ADAMTS14* was upregulated. These data are consistent with previous work in our group which found significant upregulation of *ADAMTS6*, *ADAMTS10* and *ADAMTS14* in response to TGF-β1 treatment in HACs (Le, 2015). Moreover, *ADAMTS10* and *ADAMTS14* were validated as direct targets of miR-29b (Le, 2015).

Interestingly, although TGF-β1 did increase expression of the aggrecan degrading *ADAMTS4*, in HACs TGF-β1 generally appeared to be chondroprotective. Expression of other proteoglycanase (*ADAMTS1, 9, 15 and 20*) and COMP-cleaving (*ADAMTS12*) enzymes was downregulated whereas expression of procollagen N-proteinases (*ADAMTS2* and *ADAMTS14*) was upregulated. Of note, *ADAMTS14* expression was upregulated by 30-fold, even more so than *PAI-1*. Upregulation of *ADAMTS14* has been reported in OA (Kevorkian *et al.*, 2004; Davidson *et al.*, 2006; Swingler *et al.*, 2009; Dunn *et al.*, 2016) and SNPs have been associated with increased risk of OA (Rodriguez-Lopez *et al.*, 2009; Poonpet *et al.*, 2013; Ma *et al.*, 2018). Whilst global knockout of *ADAMTS14* had no obvious consequences, simultaneous knockout of *ADAMTS2* resulted in skin lesions in aged mice

suggesting a collaborative function between these two procollagen N-proteinases (Dupont *et al.*, 2018). Therefore, as has been suggested for *ADAMTS2*, upregulation of *ADAMTS14* may represent an attempt to repair damaged cartilage.

An antagonistic relationship between miR-29 and TGF-β has previously been shown. Expression of miR-29a, miR-29b and miR-29c was negatively regulated by TGF-β1 in HACs, whereas overexpression of miR-29b-3p repressed a SMAD2/3/4 luciferase reporter along with TGF-β1 induction of *ADAMTS4* expression (Le *et al.*, 2016). With this in mind, it would be interesting to see if TGF-β1 represses miR-29 targeting of *ADAMTS12* or given that *ADAMTS12* was also negatively regulated by TGF-β1 in HACs, whether they may cooperate in negatively regulating *ADAMTS12*. *Vice versa*, it would also be interesting see whether transfection with miR-29b-3p counteracts TGF-β regulation of other ADAMTSs, for example the stark upregulation of *ADAMTS14* seen in HACs.

Analysis of existing datasets reenforced the importance of the ADAMTSs OA. MiR-29 was predicted, and subsequently demonstrated, to regulate the expression of several ADAMTSs in luciferase assays and cell models overexpressing miR-29b-3p with *ADAMTS12* being the most compelling direct target. TGF-β signalling was also found to regulate the expression several ADAMTS family members, broadly exerting a chondroprotective influence through the downregulation of ECM-degrading enzymes and upregulation of cartilage anabolic procollagen N-proteinases. Future experiments should seek to establish whether the regulation of ADAMTSs seen here is congruent with the reciprocal negative regulation between miR-29 and TGF-β observed previously. Whilst further work is needed to fully understand the interaction between miR-29, TGF-β and the ADAMTS family, therapies which augment miR-29 expression could target this regulatory network with the aim of preventing or even reversing OA progression.

Chapter 4

The effect of microRNA-29 on DNA methylation

4 The effect of microRNA-29 on DNA methylation

4.1 Introduction

DNA methylation involves the addition of a methyl group to a cytosine nucleotide forming 5-mC and is generally associated with transcriptional repression (Greenberg *et al.*, 2019). Dysregulation of DNA methylation is a well-known participant in many disease processes, most notably featuring in most types of cancer, however the role of DNA methylation in OA is less well studied.

Differential methylation has been observed in the promoters of key genes involved in OA pathogenesis including ADAMTSs and MMPs (Reynard, 2017; Miranda-Duarte, 2018). Upregulation of *ADAMTS4* in OA human chondrocytes was shown to be associated with demethylation of specific CpG sites within the promoter (Roach *et al.*, 2005; Cheung *et al.*, 2008). On the other hand, increased promoter methylation has been associated with reduced expression of *SOX9* in OA (Kim *et al.*, 2013). Moreover, genome-wide analyses have revealed distinct patterns of DNA methylation not only in healthy and OA cartilage, but also in cartilage from knee and hip joints (den Hollander *et al.*, 2014; Rushton *et al.*, 2014; Li *et al.*, 2018).

Components of the DNA methylation machinery are known to be regulated by miR-29 including DNMTs, TETs and TDG (Morita *et al.*, 2013; Kremer *et al.*, 2018). In lung cancer , expression of the miR-29 family was inversely correlated *DNMT3A* and *DNMT3B*. In the same study, miR-29 overexpression was shown to reduce global DNA methylation (Fabbri *et al.*, 2007). Conversely, brain-specific knockout of miR-29 increased *DNMT3A* expression and non-CG (CH) methylation (Swahari *et al.*, 2021). In fact, widespread recognition of the role miR-29 in regulating DNA methylation has led to miR-29 often being referred to as an ‘epi-miRNA’ (Amodio *et al.*, 2015; Memari *et al.*, 2018).

In the previous chapter, miR-29 was found to regulate the expression of members of the ADAMTS family in chondrocytes. *ADAMTS2*, *ADAMTS9*, *ADAMTS12*, *ADAMTS15*, *ADAMTS16*, *ADAMTS18* and *ADAMTS20* were downregulated in luciferase assays, *ADAMTS2*, *ADAMTS9*, *ADAMTS12* and *ADAMTS15* were downregulated in SW1353 cells transfected with miR-29b-3p mimic, and *ADAMTS12* was downregulated in HACs transfected with miR-29b-3p mimic. Overall, *ADAMTS12* was the most convincing miR-29 target identified. In this chapter, the interplay between miR-29 and DNA methylation in chondrocytes will be explored.

Aims

- Use existing datasets to identify if genes involved in DNA methylation are potentially implicated in OA.
- Assess whether genes involved in DNA methylation are regulated by miR-29.
- Investigate the effect of miR-29 overexpression on global DNA methylation.

4.2 Results

4.2.1 Bioinformatic analysis

4.2.1.1 Regulation of DNA methylation in OA

To investigate whether genes associated with DNA methylation were regulated in existing OA datasets, SkeletalVis was used to assess the expression of *DNMT1*, *DNMT3A*, *DNMT3B*, *TDG*, *TET1*, *TET2* and *TET3* in the same human OA and murine OA studies as in section 3.2.1.

For human OA, when comparing joint-matched knee OA and healthy cartilage across all three studies, expression of *DNMT3A*, *DNMT3B*, *TDG*, *TET1* and *TET2* was not consistently regulated. Expression data for *DNMT1* and *TET3* was only available in two of the datasets however *TET3* was upregulated in both (Figure 4.1A).

For murine OA studies, when comparing knee cartilage from DMM and sham surgery after 2 weeks (Figure 4.1B), *DNMT1*, *DNMT3A* and *DNMT3B* were not consistently regulated across all three studies. Similarly, although data for *TET1*, *TET2*, *TET3* and *TDG* was only available in two of the datasets, their expression was not consistently regulated. In studies looking at gene expression 8 weeks after DMM surgery (Figure 4.1C), *DNMT1* was upregulated in both datasets whereas *DNMT3A* and *DNMT3B* appeared to be unregulated. Data for *TET1*, *TET2*, *TET3* and *TDG* was only available from one of the studies and their expression appeared to be unregulated. Across all human and murine DMM studies, none of the aforementioned genes were significantly dysregulated.

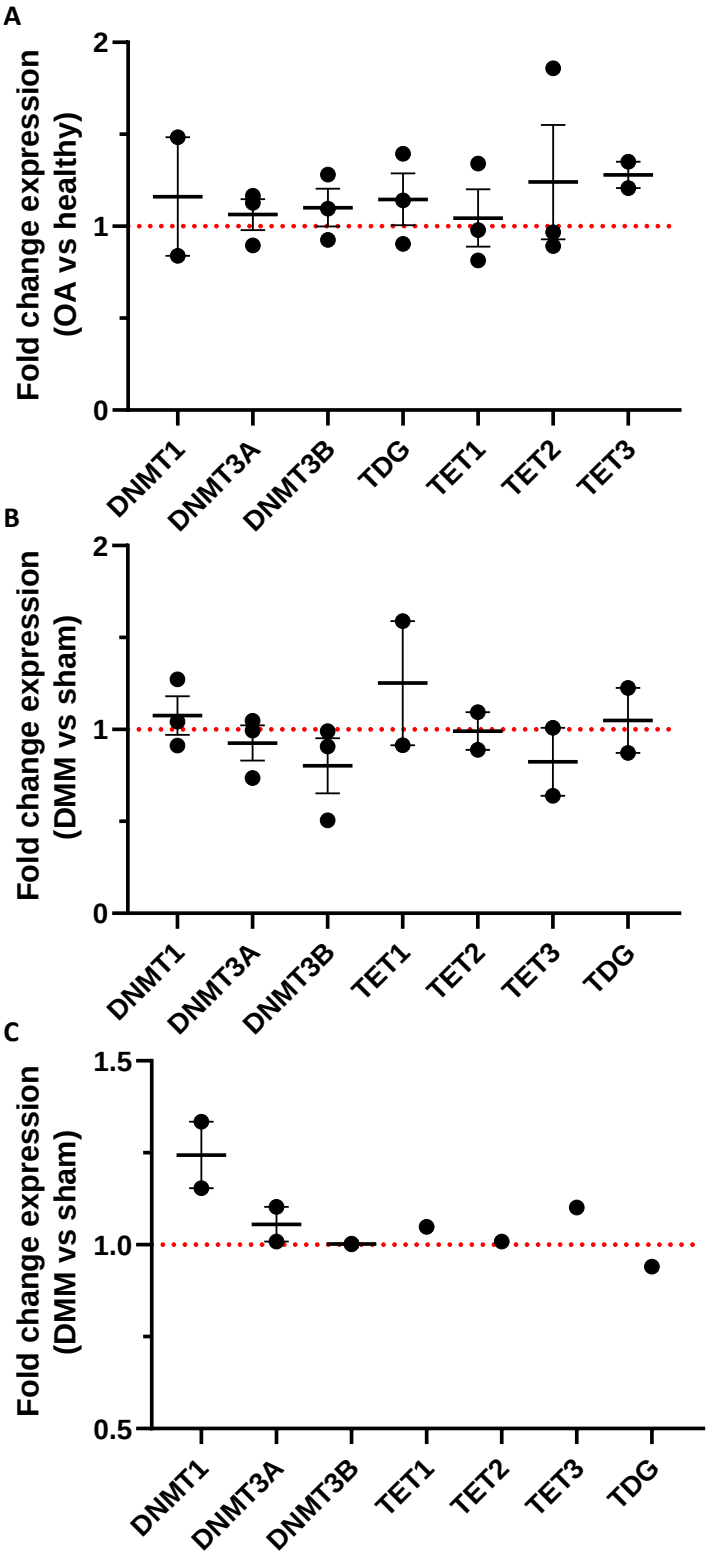

Figure 4.1. Expression of DNA methylation genes in DMM osteoarthritis model. *Expression data from 3 joint-matched human knee OA studies (A), 3 murine 2 weeks post-DMM studies (B) and 2 murine 8 weeks post-DMM studies (C) were analysed using SkeletalVis. Fold change expression of DNMT1, DNMT3A, DNMT3B, TET1, TET2, TET3 and TDG in OA knee cartilage over healthy cartilage (A) and in knee cartilage from DMM over sham operated mice was calculated. Data presented as mean ± SEM.*

4.2.1.2 Prediction of methylation gene targets of miR-29

Targeting of genes involved in epigenetic regulation by miR-29 is well documented. To identify if miR-29 might directly target genes involved in DNA methylation miRabel was used to predict putative miR-29 targets (Table 4.1).

For *DNMT3A, DNMT3B, TDG, TET1* and *TET2* PITA, miRanda, SVmicrO and TargetScan all predicted an interaction with miR-29 with a significant miRabel score (≤ 0.05). Despite containing 13 3'-UTR 6-mer seed sites and miRanda, SVmicrO and TargetScan predicting interaction with miR-29, miRabel scores for miR-29a-3p, miR-29b-3p and miR-29c-3p were all greater than 0.05. On the other hand, PITA and SVmicrO both predicted an interaction between miR-29 and *DNMT1* despite its 3'-UTR not possessing a 6-mer seed site however miRabel scores for all three miR-29 family members were high.

Table 4.1. Methylation gene miR-29 target prediction.

Gene	miR-29a-3p		miR-29b-3p		miR-29c-3p		6-mer seed sites
	miRabel score	**Algorithms**	**miRabel score**	**Algorithms**	**miRabel score**	**Algorithms**	
DNMT1	0.99461	P, S	0.99189	P, S	0.99378	P, S	0
DNMT3A	0.00386	P, M, S, T	0.00572	P, M, S, T	0.00348	P, M, S, T	15
DNMT3B	0.00091	P, M, S, T	0.00101	P, M, S, T	0.00108	P, M, S, T	3
TDG	0.00144	P, M, S, T	0.00072	P, M, S, T	0.00101	P, M, S, T	4
TET1	0.00052	P, M, S, T	0.00105	P, M, S, T	0.00118	P, M, S, T	5
TET2	0.00801	P, M, S, T	0.01152	P, M, S, T	0.00659	P, M, S, T	4
TET3	0.14166	M, S, T	0.1559	M, S, T	0.06659	M, S, T	13

PITA (P), miRanda (M), SVmicrO (S), TargetScan (T).

4.2.2 Effect of microRNA-29 overexpression on methylation expression

4.2.2.1 Methylation expression in microRNA-29 treated SW1353

Several genes involved in the regulation of DNA methylation were predicted to be direct targets of miR-29. To investigate whether miR-29 might regulate DNA methylation in chondrocytes, the expression of *DNMT1, DNMT3A, DNMT3B, TET1, TET2, TET3* and *TDG* was measured using qRT-PCR in SW1353 cells and HACs transfected with miR-29b-3p mimic or negative control for 48 hours (as in section 3.2.3.4).

In SW1353 cells, miR-29b-3p transfection downregulated the expression of *DNMT3A*, *TET1*, *TET2*, *TET3* and *TDG* by 0.51, 0.23, 0.32, 0.29 and 0.55-fold respectively suggesting these genes maybe directly targeted by miR-29 (Figure 4.2). Expression of *DNMT1* and *DNMT3B* did not appear to be regulated by miR-29b-3p transfection suggesting these may not be direct targets. As mentioned previously (section 3.2.3.4), these data only represent one biological repeat, therefore repeat experiments would be needed to validate these findings.

Similarly to SW1353 cells, miR-29b-3p transfection of HACs significantly downregulated the expression of *DNMT3A* and *TET2* (Figure 4.3). Expression of TDG was downregulated by 0.59-fold however this did not reach statistical significance ($p = 0.055$). *TET1* and *TET3* expression was reduced by 0.8 and 0.51-fold respectively however standard error was high, therefore these data may not be representative. Again, *DNMT1* and *DNMT3B* did not appear to be regulated by miR-29b-3p transfection.

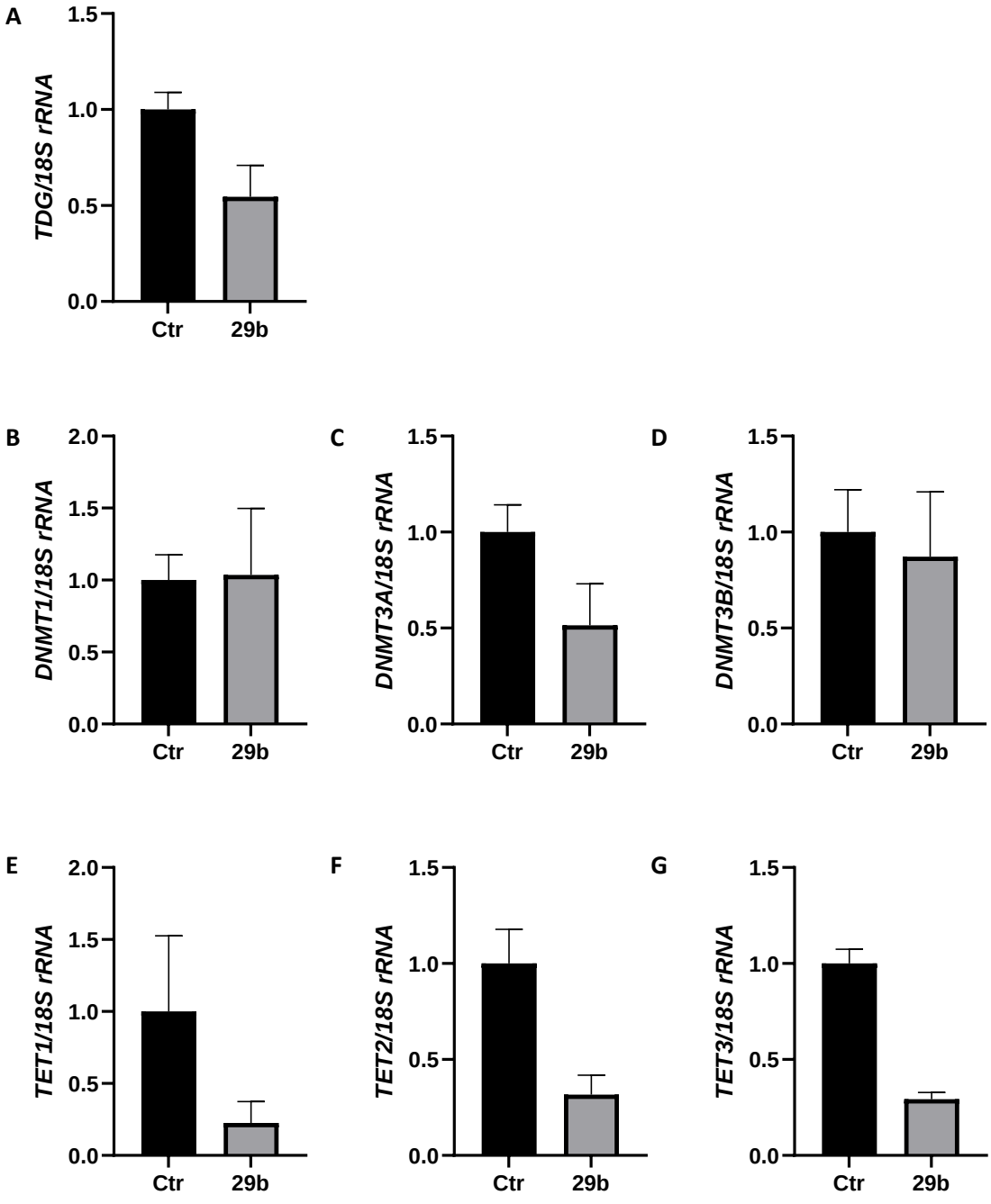

Figure 4.2. Effect of miRNA-29b overexpression on methylation gene expression in SW1353 cells. *SW1353 cells were transfected with 50 nM miR-29b-3p mimic and negative control for 48 hours. Expression of TDG (A), DNMT1 (B), DNMT3A (C), DNMT3B (D), TET1 (E), TET2 (F) and TET3 was measured using qRT-PCR and normalised to 18S rRNA. Data presented as mean of 3 technical replicates ± SD, n = 1.*

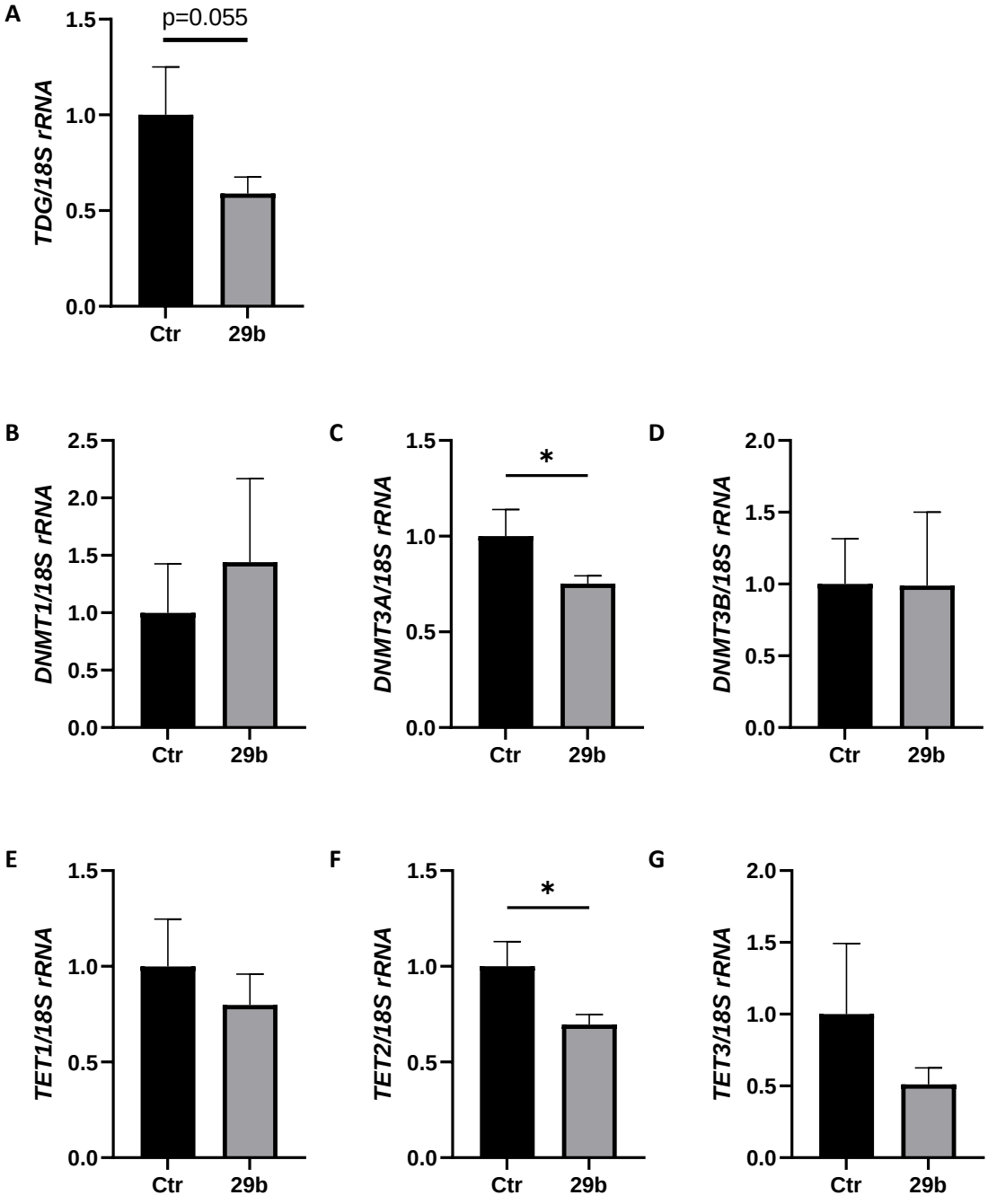

Figure 4.3. Effect of miRNA-29b overexpression on methylation gene expression in human articular chondrocytes. *HACs were transfected with 50 nm miR-29b-3p mimic and negative control for 48 hours. Expression of TDG (A), DNMT1 (B), DNMT3A (C), DNMT3B (D), TET1 (E), TET2 (F) and TET3 (G) was measured using qRT-PCR and normalised to 18S rRNA. Data presented as mean ± SEM, n =3, two-tailed unpaired t-test * p < 0.05.*

4.2.3 Effect of microRNA-29 on global DNA methylation

4.2.3.1 Dot blot

Overexpression of miR-29b-3p in SW1353 cells and HACs suggested that miR-29 may directly regulate several genes involved in DNA methylation. Specifically, *DNMT3A* is responsible for the *de novo* methylation of DNA whereas *TET1*, *TET2*, *TET3* and *TDG* are involved in the active demethylation of DNA. MiR-29 is upregulated in human OA hip cartilage (Le *et al.*, 2016), therefore, this may lead to the disruption of global DNA methylation in OA cartilage.

To investigate whether upregulation of miR-29 may dysregulate DNA methylation, SW1353 cells were transfected with 50 nM miR-29b-3p mimic or negative control, or treated with 5 µM 5-Aza (a positive control for global demethylation) or vehicle control (0.5% v/v DMSO). GDNA was extracted, and a dot blot assay performed to assess global DNA methylation in treated cells. Briefly, gDNA was spotted on a polyvinylidene fluoride (PVDF) membrane and relative methylation quantified using a 5-mC antibody (Figure 4.4A).

Treatment of SW1353 cells with 5-Aza significantly reduced global methylation by 0.25-fold relative to the vehicle control confirming that the assay was able to detect changes in methylation (Figure 4.4B). When compared a negative control mimic, overexpression of miR-29b-3p significantly reduced global methylation by 0.63-fold suggesting the upregulation of miR-29 may downregulate global DNA methylation in OA.

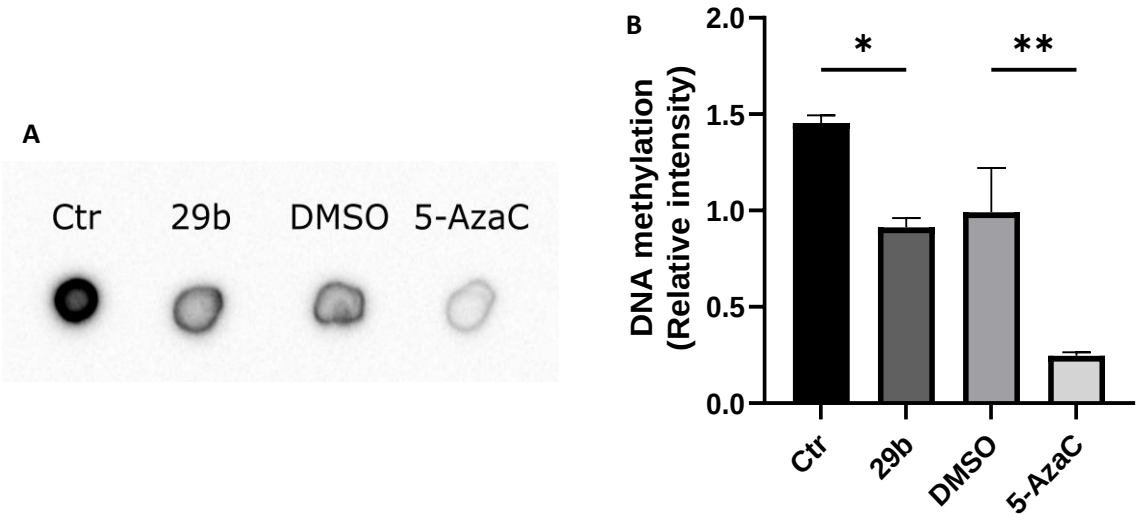

Figure 4.4. Dot blot analysis of 5-mC in miRNA-29 and 5-Aza in SW1353 cells. *(A) Genomic DNA from SW1353 cells treated with negative control (Ctr), miR-29b-3p mimic (29b), Vehicle control (DMSO) or 5-Aza control (5-AzaC) was blotted onto a PVDF membrane before incubation with a 5-mC primary antibody and HRP-conjugated secondary antibody and imaging (representative image, n = 3). (B) DNA methylation was quantified by measuring the integrated density of each dot. Data presented as mean ± SEM, n = 3, two-tailed unpaired t-test * p < 0.05, ** p < 0.01.*

4.2.3.2 Methylation array

MiR-29 was predicted to target several genes involved in the regulation of DNA methylation, with *DNMT3A* and *TET2* being significantly downregulated in response to miR-29b-3p overexpression in HACs. Overexpression of miR-29b-3p in SW1353 cells also significantly reduced 5-mC in a dot blot assay. To further investigate the effect of miR-29 on methylation, a methylation array was performed on SW1353 cells overexpressing miR-29b-3p.

SW1353 cells were transfected with miR-29b-3p mimic or negative control in quadruplicate and DNA and RNA extracted simultaneously. Expression of *TDG, DNMT3A, DNMT3B, TET1, TET2* and *TET3* was measured in the RNA using qRT-PCR. *TDG, DNMT3A, TET1, TET2 and TET3* were downregulated by 0.7, 0.47, 0.37, 0.35 and 0.36-fold respectively (Figure 4.5), consistent with previous data. Looking at the data in Figure 4.5, sample 1 for control treated (C1) and sample 4 for miR-29b-3p treated (M4) cells appeared to show the most consistent response to respective treatments and were chosen for methylation array analysis.

DNA from samples C1 and M4 were bisulfite treated and analysed using an Illumina Infinium MethylationEPIC BeadChip array for differentially methylated regions (DMR) in miR-29b-3p and control treated samples. Analysis of methylation array data found 125 CpG sites with greater than 10% differential methylation and seven CpG sites with greater than 20% differential methylation (Figure 4.6A). Overall, there were few notable DMRs with only DMRs within the tripartite motif containing 58 (*TRIM58*) and calcium voltage-gated channel auxiliary subunit beta 1 (*CACNB1*) genes differentially methylated by more than 10% (Figure 4.6B).

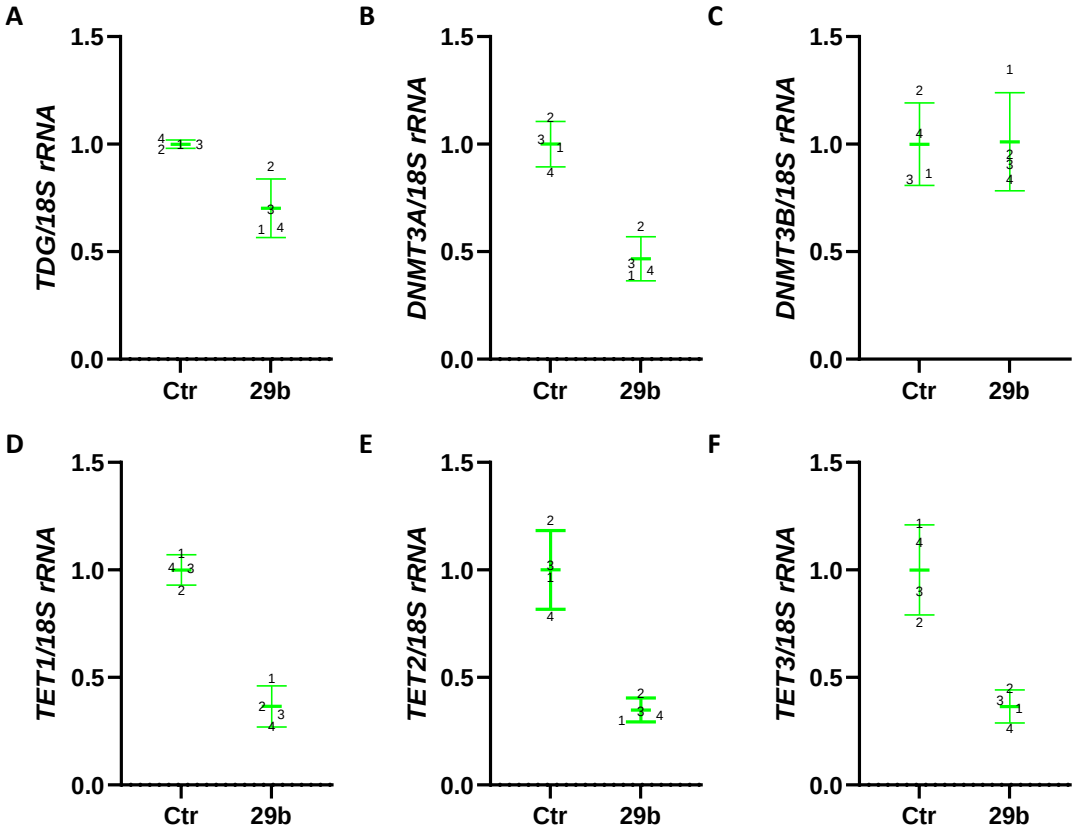

Figure 4.5. Expression of methylation genes in array samples. *Expression of TDG (A), DNMT3A (B), DNMT3B (C), TET1 (D), TET2 (E) and TET3 (F) was measured in RNA from miR-29b-3p (29b) and control mimic (Ctr) treated samples from the methylation array. Samples are labelled 1-4 for 29b and ctr. Expression measured using qRT-PCR and normalised to 18S rRNA. Data presented as mean of 4 technical replicates ± SD (green), n = 1.*

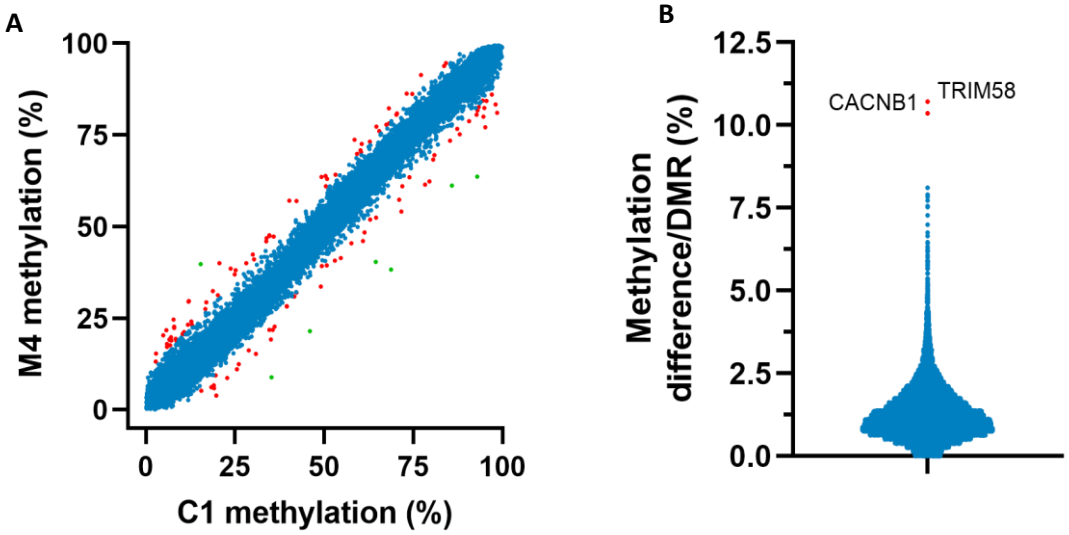

Figure 4.6. DNA methylation array of miRNA-29 treated SW1353 cells. *DNA methylation was measured in miR-29b1-3p and control mimic treated SW1353 cells using a Illumina Infinium MethylationEPIC BeadChip array. (A) Percentage methylation per CpG for the control treated sample was plotted against the miR-29b1-3p treated sample. CpGs with a difference of ≥ 20% are green and CpGs with a difference of ≥ 10% are in red. (B) Average methylation difference per DMR was calculated. DMRs in CACNB1 and TRIM58 (red) were differential methylated by ≥ 10%.*

4.2.3.3 Bisulfite PCR confirmation of array targets

Methylation array data from miR-29b-3p treated SW1353 cells found DMRs within the *TRIM58* and *CACNB1* genes. To verify whether the identified DMRs for *TRIM58* and *CACNB1* were indeed differentially methylated, gDNA from control samples C2, C3 and C4, and miR-29b-3p treated samples M1, M2 and M3 was analysed using bisulfite PCR pyrosequencing.

For the DMRs within *TRIM58* and *CACNB1*, DNA methylation was assessed at six and 11 CpGs respectively. Although in the DNA methylation array differential methylation was 10.4% and 10.7% for *TRIM58* and *CACNB1* respectively, bisulfite PCR pyrosequencing found differences of less than 2% (Figure 4.7).

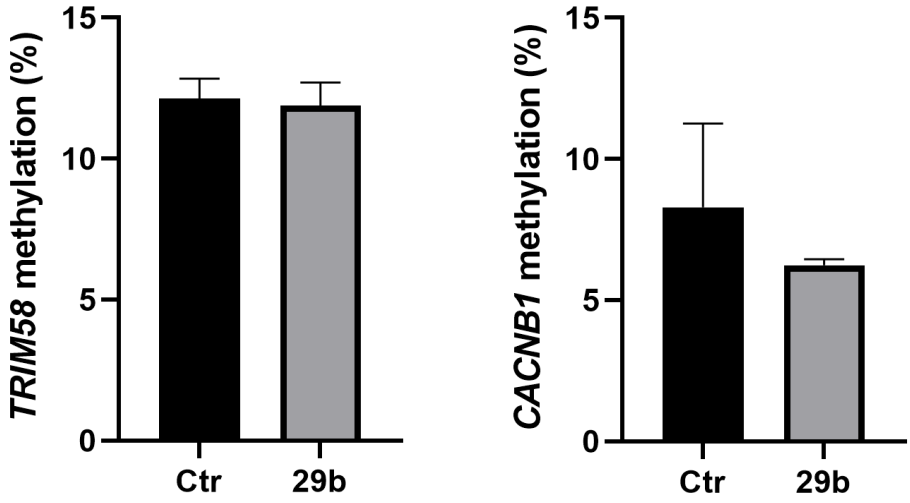

Figure 4.7. Bisulfite PCR pyrosequencing of miR-29 treated SW1353 cells. *DNA methylation was measured in miR-29b-3p (29b) and control (Ctr) treated SW1353 cells using bisulfite PCR pyrosequencing. Data presented as percentage methylation across 6 or 11 sites for TRIM58 and CACNB1 respectively from 3 technical replicates, mean ± SD, n = 1.*

4.3 Discussion

The importance of the miR-29 family in cartilage development and the pathogenesis of OA was further explored in this chapter. Specifically, the role of miR-29 in the regulation of DNA methylation in chondrocytes and OA was investigated by measuring the effect of miR-29b overexpression on the regulation of genes involved in the DNA methylation process.

There is increasing evidence of the potential role of DNA methylation in OA. Whilst changes in the expression of genes involved in DNA methylation have been reported in OA (Shen *et al.*, 2017), whether expression of these genes is a hallmark of OA remains to be seen. Evidence for specific patterns of global methylation and the potential significance of methylation at specific CpG sites is more widespread suggesting that the role of methylation in OA may be more subtle.

As previously discussed, the miR-29 family are recognised as 'epi-miRNAs' due to their widely reported roles in the regulation of multiple components of the DNA methylation machinery. Given that miR-29 and DNA methylation have both been implicated in OA, and that miR-29 is known to regulate DNA methylation in other disease contexts, the relationship between miR-29 and DNA methylation in chondrocytes, and more broadly OA was explored in this chapter.

The expression of *DNMT1*, *DNMT3A*, *DNMT3B*, *TDG*, *TET1*, *TET2* and *TET3* was assessed in existing OA datasets and analysed using SkeletalVis (Soul *et al.*, 2019). Broadly, no substantial differences were seen in the expression of these genes across joint-matched knee OA and murine DMM studies, although slight upregulation of *TET3* and *DNMT1* was observed in two OA and DMM datasets respectively. Upregulation of *DNMT1* by IL-1β has been reported (Akhtar *et al.*, 2013) however other studies have found no evidence of *DNMT1* upregulation in OA chondrocytes (Sesselmann *et al.*, 2009). Whilst *TET2* and *TET3* expression appeared to be unregulated, *TET1* was reported to be downregulated in OA chondrocytes (Taylor *et al.*, 2014).

The miR-29 family is already known to regulate the expression of genes involved in DNA methylation. Therefore, it is unsurprising that bioinformatic prediction of miR-29 targets identified putative interactions between all miR-29a-3p, miR-29b-3p and miR-29c-3p, and *DNMT3A*, *DNMT3B*, *TDG, TET1* and *TET2*. In light of this, the effect of miR-29b-3p overexpression in SW1353 cells and HACs on the expression of the aforementioned genes was assessed. Expression of *DNMT3A*, *TDG* and *TET2* was negatively regulated in response to miR-29b-3p overexpression in HACs. This is in line with previous studies showing direct targeting of *DNMT3A* and *TET2* by miR-29b (Garzon *et al.*, 2009; Takayama *et al.*, 2015). Given that these were small scale exploratory experiments, only miR-29b-3p

mimic was used. Future experiments should use both miR-29b-3p mimic and antagomir to fully investigate regulation of methylation-related genes in chondrocytes. Notably, not all predicted targets of miR-29 were downregulated highlighting the importance of experimental validation of miRNA-target predictions.

Given that miR-29b-3p appeared to regulate the expression of genes involved in DNA methylation, the effect of miR-29b on global methylation was assessed. Dot blot analysis of gDNA from miR-29b-3p overexpressing SW1353 cells suggested that upregulation of miR-29 was associated with a significant decrease in global methylation. However, methylation array data failed to replicate these data with only seven CpG sites showing greater than 20% differential methylation and only two DMRs being differentially methylated by more than 10% overall – *TRIM58* and *CACNB1*. *TRIM58* is an E3 ubiquitin protein ligase implicated as a tumour suppressor with aberrant promoter methylation being associated with poor prognosis in liver and lung cancer (Qiu *et al.*, 2016; Kajiura *et al.*, 2017). *CACNB1* is a voltage dependent calcium channel associated with T cell function and excitation and contraction coupling in skeletal muscle (Rima *et al.*, 2016; Erdogmus *et al.*, 2022). Both *TRIM58* and *CACNB1* are significantly upregulated in human OA subchondral bone and downregulated in human OA cartilage in microarray data analysed using SkeletalVis however no major role for either gene in OA is known. Moreover, subsequent analysis of the DMRs located within *TRIM58* and *CACNB1* did not recapitulate the differences in methylation observed in the methylation array.

There may be several explanations as to why regulation of *DNMT3A* and *TET2*, and the reduction in global methylation seen with miR-29b-3p overexpression were not corroborated by methylation array. Firstly, changes in the expression of *DNMT3A* are only likely to impact *de novo* methylation. Given that SW1353 is a terminally differentiated cell line, reducing the capacity for the *de novo* methylation may have little biological significance. Moreover, as a chondrosarcoma cell line, global DNA methylation patterns in SW1353 cells have likely already been drastically altered during oncogenic transformation. In addition, given that *DNMT3A* is associated DNA methylation whereas *TET2* is associated demethylation, it is possible that downregulation of both simultaneously cancels out any effects on global DNA methylation.

Recent work by Swahari *et al.* (2021) may suggest an alternative explanation. Brain-specific knockout of miR-29 in mice resulted in a concomitant increase in *DNMT3A* expression with miR-29 being shown to directly regulate *DNMT3A*. Interestingly, whilst global CG methylation was largely unaffected, a significant increase in CH methylation was observed. CH methylation is significantly less common than CG methylation with high resolution assays needed to distinguish CH methylation from CG methylation (Ziller *et al.*, 2011; He

et al., 2015). Only CpG methylation was analysed in these data. Therefore, whilst global CpG methylation patterns were not altered by miR-29 overexpression in SW1353 cells, differences may be seen in CH methylation. Further analysis of the methylation array data from this project may clarify whether this is the case.

Overall, the experiments in the chapter contribute to the importance of the miR-29b family in cartilage development and OA pathogenesis. The role of DNA methylation has become more apparent in recent years (Reynard, 2017; Miranda-Duarte, 2018) and miR-29 is already well known to regulate many genes associated with DNA methylation (Morita *et al.*, 2013; Kremer *et al.*, 2018). In this chapter, miR-29 was shown to downregulate expression of *DNMT3A*, *TDG* and *TET2* in HACs, and reduce global 5-mC levels in SW1353 cells suggesting a potentially important role in the regulation of DNA methylation in chondrocytes. Despite this, further investigation utilising a methylation array failed to corroborate these findings.

Future experiments should aim to clarify the effect of miR-29b overexpression on DNA methylation in primary chondrocytes in order to overcome the aforementioned limitations of studies utilising SW1353 cells. Moreover, complimentary experiments utilising either a miR-29b antagomir or knockout model should be implemented to further elucidate the biological significance of potential regulatory interactions. It will be important for therapies aimed at augmenting miR-29 to take account of the potential benefits or drawbacks of accompanying changes in DNA methylation.

Chapter 5

Generation and analysis of microRNA-29 knockout mouse model

5 Generation and analysis of a microRNA-29 knockout mouse model

5.1 Introduction

The miR-29 family has been implicated in OA through previous research in our lab as well as in this thesis (Le *et al.*, 2016). Members of the ADAMTS family were found to be regulated by miR-29 as well as by TGF-β signalling, which is negatively regulated by, and negatively regulates miR-29. Moreover, as the role of DNA methylation in OA is increasingly being recognised, the recognition of miR-29 as an epi-miRNA may be pertinent to its role in OA.

Global knockout of the miR-29 family is lethal with mice deficient for both the *miR-29ab1* and *miR-29b2c* loci dying within 42 days. MiR-29 knockout mice are smaller, weigh less, develop kyphosis and display a severe neurological phenotype characterised by severe ataxia (Cushing *et al.*, 2015; Dooley *et al.*, 2016; Caravia *et al.*, 2018; Swahari *et al.*, 2021). Knockout of only the *miR-29ab1* locus results in a similar, albeit less severe phenotype, characterised again by smaller size, reduced weight, kyphosis, ataxia and premature death by 28-30 weeks of age (Papadopoulou *et al.*, 2015; Dooley *et al.*, 2016; Caravia *et al.*, 2018). In contrast, mice lacking only the *miR-29b2c* cluster are generally healthy with slight reductions in body weight reported at most (Kauffman *et al.*, 2015; Dooley *et al.*, 2016; Sassi *et al.*, 2017; Caravia *et al.*, 2018).

Development of OA generally occurs in later life and as such, experiments using mouse models to study OA *in vivo* typically use adult mice to better model the disease process (Samvelyan *et al.*, 2020). The severely shortened lifespan conferred by global knockout of miR-29 would limit the age at which knockout animals could be studied for joint and potential OA development. Moreover, with a range of phenotypes reported in miR-29 knockout mice, delineating the effect of miR-29 knockout in the joint from coexisting and potentially confounding phenotypes may be difficult. For example, obesity is a widely recognised risk factor for OA (Blagojevic *et al.*, 2010; Apold *et al.*, 2014; Raud *et al.*, 2020) and Dooley *et al.* (2016) report protection from diet-induced obesity and reduced overall body weight in miR-29 knockout mice.

Cartilage-specific knockout of miR-29 may overcome the aforementioned complications associated with global knockout. Many cartilage-specific knockout mouse models exist and these have been used to study to the role of a wide range of genes in cartilage development, homeostasis and disease (Kanakis *et al.*, 2021). In models utilising the Cre-*loxP* system, expression of Cre recombinase is under the control of a cartilage-specific promoter (e.g., *COL2A1*) and thus, *loxP* recombination and deletion of the intervening sequence occurs only where the promoter is expressed. Moreover, to avoid embryonic lethality brought about

by the deletion of genes critical during early development, inducible Cre-*loxP* systems have been developed which allow not only spatial, but temporal control of gene deletion. In the Cre-ERT system, administration of tamoxifen relieves cytoplasmic sequestration of Cre recombinase allowing nuclear localisation and subsequent recombination of *loxP* sites (Feil *et al.*, 1996).

To further explore the role the miR-29 family in cartilage and OA development, mice possessing a cartilage-specific knockout of the *miR-29ab1* and *miR-29b2c* loci, both independently and simultaneously were generated. In this chapter, the effect of miR-29 knockout in these mice will be investigated using molecular and histological analyses.

Aims

- Generate a mouse model possessing cartilage-specific knockout of *miR-29ab1*, *miR-29b2c* and both loci together.
- Verify cartilage-specific knockout of miR-29 expression.
- Assess the effect of miR-29 knockout on the expression of cartilage and OA-related genes using mRNA-seq.
- Explore the effect of miR-29 knockout during cartilage development and in OA.

5.2 Results

5.2.1 Generation of a cartilage-specific microRNA-29 knockout model

Given that global knockout of miR-29 is lethal, to investigate the effect knockout in OA, a strategy to knockout miR-29 specifically in cartilage was pursued. The Cre-*loxP* system is a widely used tool enabling tissue-specific and inducible knockout of one or more genes with a high degree of precision. Therefore, to generate a cartilage-specific knockout of miR-29, the aim was to cross a cartilage-specific Cre mouse to mice possessing floxed *miR-29ab1* and *miR-29b2c* loci.

5.2.1.1 *Acan-creERT2* mice

Initially, the plan was to achieve cartilage-specific miR-29 knockout using the *acan-creERT2* inducible mouse generated by Cascio *et al.* (2014). In order to generate *acan-creERT2* mice, *acan-creERT2*$^{+/0}$*:CTGF*$^{fl/fl}$ (Poulet *et al.*, 2016) were crossed with C57BL/6 to generate *acan-creERT2*$^{+/0}$*:CTGF*$^{wt/fl}$ mice. These mice were further crossed to C57BL/6 mice to produce *acan-creERT2* mice.

Subsequent to breeding of the *acan-creERT2* mouse, communication from Prof. George Bou-Gharios indicated that not all chondrocytes in these mice were expressing the transgene leading to poor tissue-specific knockout (also discussed in Kanakis *et al.*, 2021). Therefore, an alternative breeding strategy was pursued using a *col2a1-cre* mouse.

5.2.1.2 MicroRNA-29 knockout breeding

5.2.1.2.1 *Col2a1-cre* mice

Given that cartilage-specific knockout of miR-29 was unlikely to be complete using the *acan-creERT2* mouse, the *col2a1-cre* mouse was chosen instead. *Col2a1*-cre mice possess a Cre recombinase under the control of a *Col2a1* promoter (Sakai *et al.*, 2001). Use of a *col2a1-cre* transgene to successfully drive cartilage-specific knockout is well reported (Staal *et al.*, 2014; Dudek *et al.*, 2016; Valverde-Franco *et al.*, 2016; Almonte-Becerril *et al.*, 2018). Although the *col2a1-cre* mouse lacked an inducible promoter, it appeared more likely to produce reliable cartilage-specific knockout of miR-29.

5.2.1.2.1.1 Optimisation of genotyping

Genotyping of *col2a1-cre* was initially performed using a touchdown PCR protocol with 45 (10 followed by 35 cycles) amplification cycles, however, as seen in Figure 5.1, this resulted in false positives in known wild-type mice, indicating non-specific amplification. Optimisation of the number of cycles for the second amplification step was undertaken to prevent false positives in *col2a1-cre* genotyping. Touch down PCR was performed with a second amplification of 25, 20, 15 and 10 cycles. At 20 cycles, a bright band at 450 bp could be seen with the known wild-type mouse showing no band (Figure 5.1).

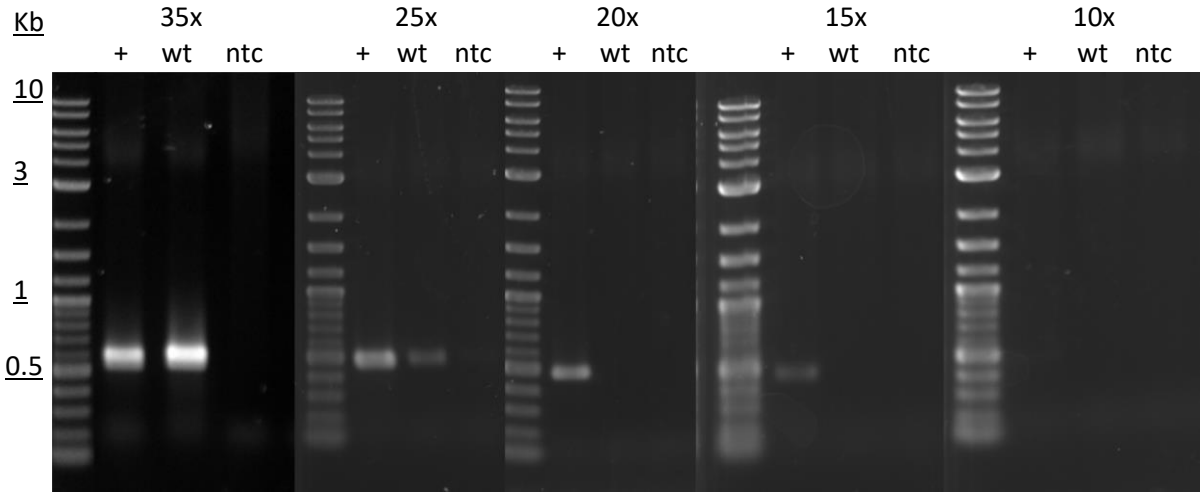

Figure 5.1. Optimisation of col2a1-cre genotyping PCR. *Touch down PCR was used to genotype known positive (+) and negative (wt) col2a1-cre mice initially with 35 cycles (35x) of the second amplification stage. At 35 cycles, known col2a1-cre negative mice showed a band at 450 bp indicating non-specific amplification. Optimisation was undertaken with the second amplification stage being performed for 25, 20, 15 and 10 cycles to improve the specificity of the assay. ntc = no template control.*

5.2.1.2.2 Breeding of single knockout mice

As previously discussed, the miR-29 family are expressed from two separate loci; *miR-29a* and *miR-29b1* are expressed from chromosome 7, whereas *miR-29b2* and *miR-29c* are expressed from chromosome 1. The breeding scheme in Figure 5.2 was undertaken to generate a mouse in which either the *miR-29ab1* or *miR-29b2c* is knocked out in the cartilage. *MiR-29ab1*$^{fl/fl}$ and *miR-29b2c*$^{fl/fl}$ mice were crossed with *col2a1-cre* mice to produce *miR-29ab1*$^{fl/fl}$*:col2a1-cre* and *miR-29b2c*$^{fl/fl}$*:col2a1-cre* mice respectively (referred to as AB1-KO and B2C-KO mice respectively). Offspring were genotyped by PCR for either the *miR-29ab1* or *miR-29b2c* floxed locus and the *col2a1-cre* transgene as in Figure 5.3.

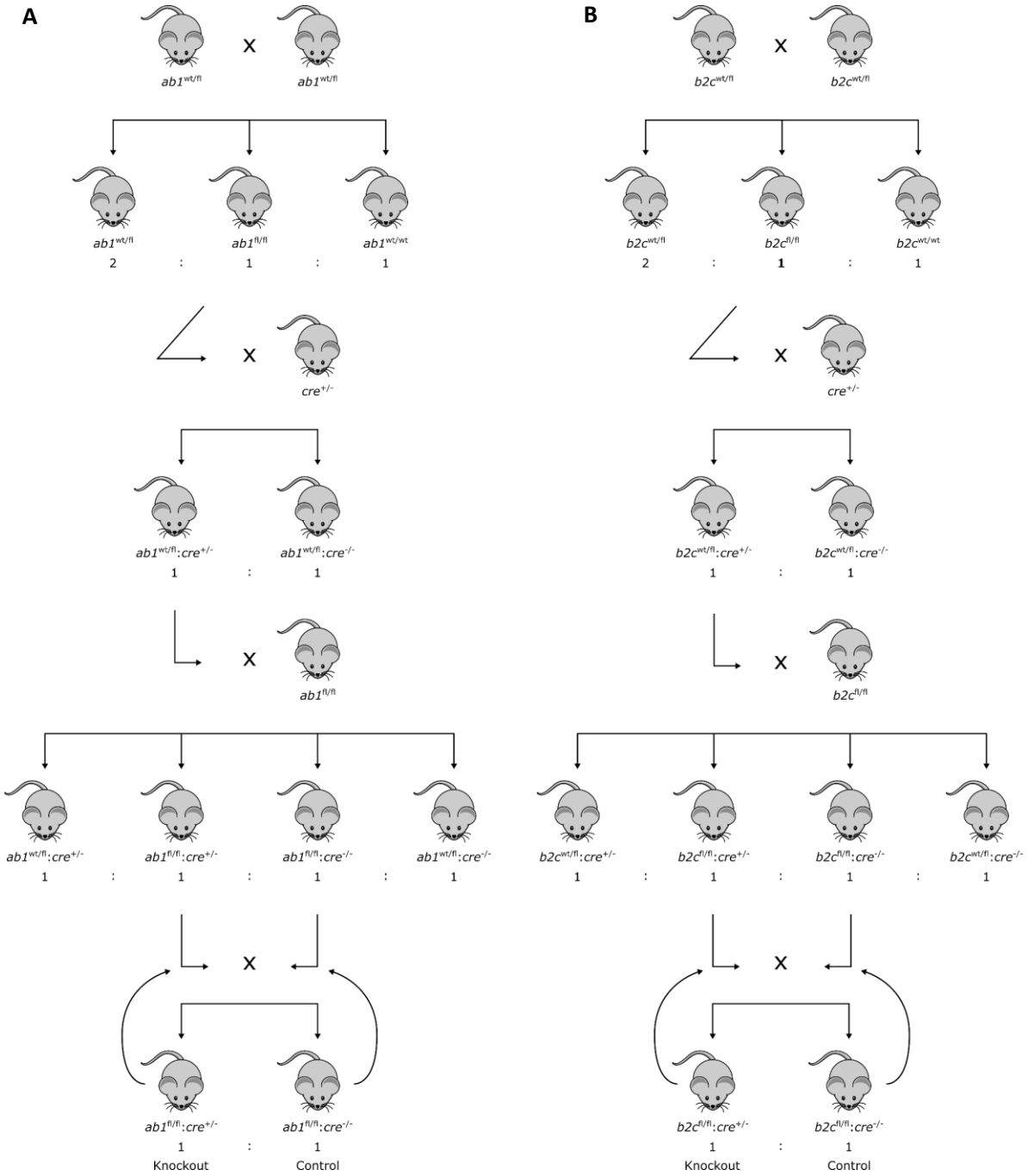

Figure 5.2. MiRNA single knockout breeding scheme. *To generate a cartilage-specific knockout of miR-29ab1 (A) or miR-29b2c (B) individually, heterozygous floxed mice (wt/fl) were crossed to produce homozygous floxed (fl/fl) offspring. Homozygous floxed mice were crossed with heterozygous col2a1-cre mice ($cre^{+/-}$) to produce $wt/fl:cre^{+/-}$ offspring. Finally, $wt/fl:cre^{+/-}$ mice were crossed with $fl/fl:cre^{-/-}$ mice to produce single knockout ($fl/fl:cre^{+/-}$) and control ($fl/fl:cre^{-/-}$) mice. Single knockout colonies were maintained by crossing male knockout with female control mice. Predicted mendelian ratios of offspring are given below each new generation.*

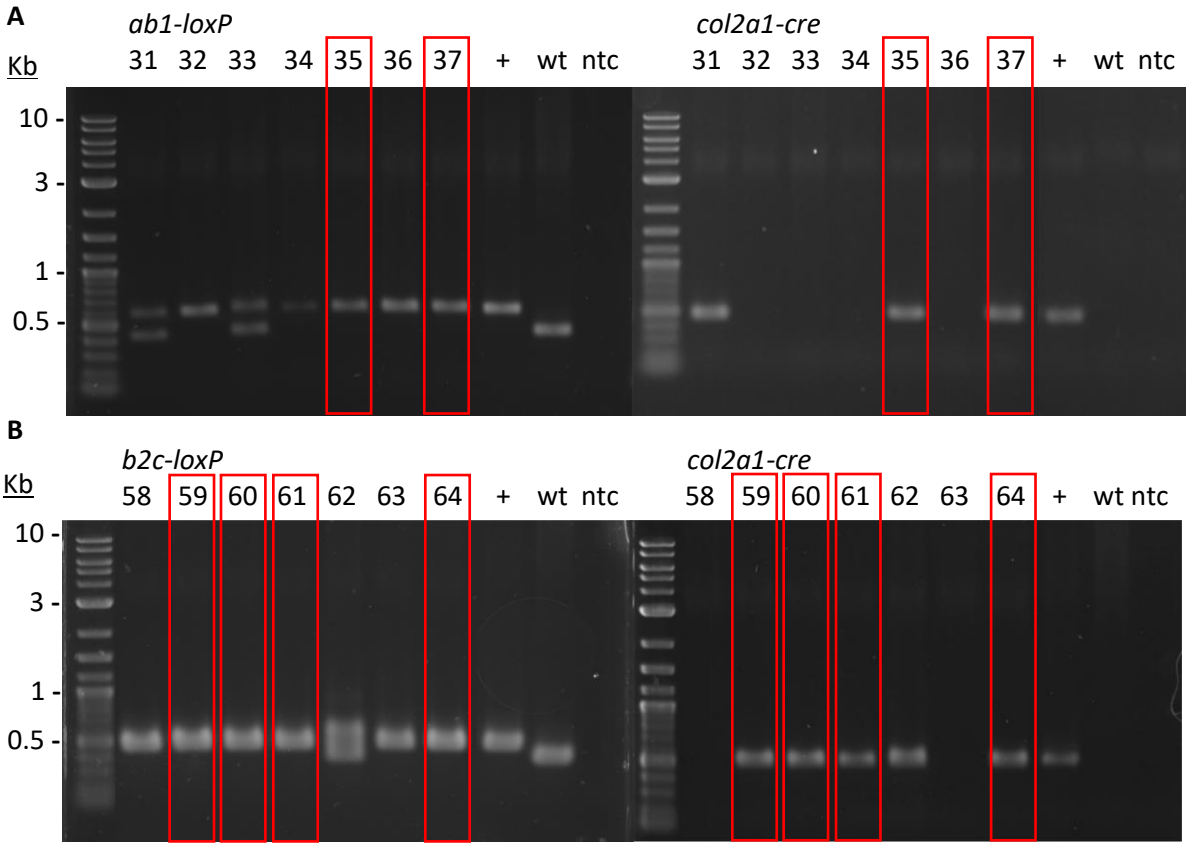

Figure 5.3. Single knockout mouse example genotyping PCR. *Offspring from the miR-29ab1 (A) and miR-29b2c (B) knockout breeding scheme were genotyped for the miR-29ab1 and miR-29b2c floxed loci respectively along with col2a1-cre. Mice that possessed the homozygous floxed miR-29ab1 or miR-29b2c locus and hemizygous col2a1-cre are highlighted in red. Positive control mice (+) showed the homozygous floxed miR-29ab1 (581 bp) and miR-29b2c (447 bp) bands respectively along with the hemizygous col2a1-cre (450 bp) band. Wild-type mice (wt) showed the homozygous wild-type miR-29ab1 (419 bp) and miR-29b2c (354 bp) bands respectively along with no col2a1-cre band. ntc = no template control.*

5.2.1.2.3 Breeding of double knockout mice

Given that miR-29 is expressed from both the *miR-29ab1* and *miR-29b2c* loci, knocking out either locus individually was unlikely to demonstrate the full effect of miR-29 knockout. Moreover, it was possible that the knocking out of one locus may cause upregulation of the other to compensate. Therefore, the breeding scheme in Figure 5.4 was undertaken to generate a mouse in which the *miR-29ab1* and *miR-29b2c* loci were knocked out simultaneously in the cartilage. Initially, *miR-29ab1*$^{fl/fl}$ and *miR-29b2c*$^{fl/fl}$ were crossed to produce *miR-29ab1*$^{fl/fl}$*:miR-29b2c*$^{fl/fl}$ in which both miR-29 loci were floxed. Following this, *miR-29ab1*$^{fl/fl}$*:miR-29b2c*$^{fl/fl}$ mice were crossed with B2C-KO mice to produce offspring possessing both the *miR-29ab1* and *miR-29b2c* floxed loci along with the *col2a1-cre* transgene (referred to as DKO mice). Offspring were genotyped by PCR for the *miR-29ab1* and *miR-29b2c* floxed locus, and the *col2a1-cre* transgene as in Figure 5.5.

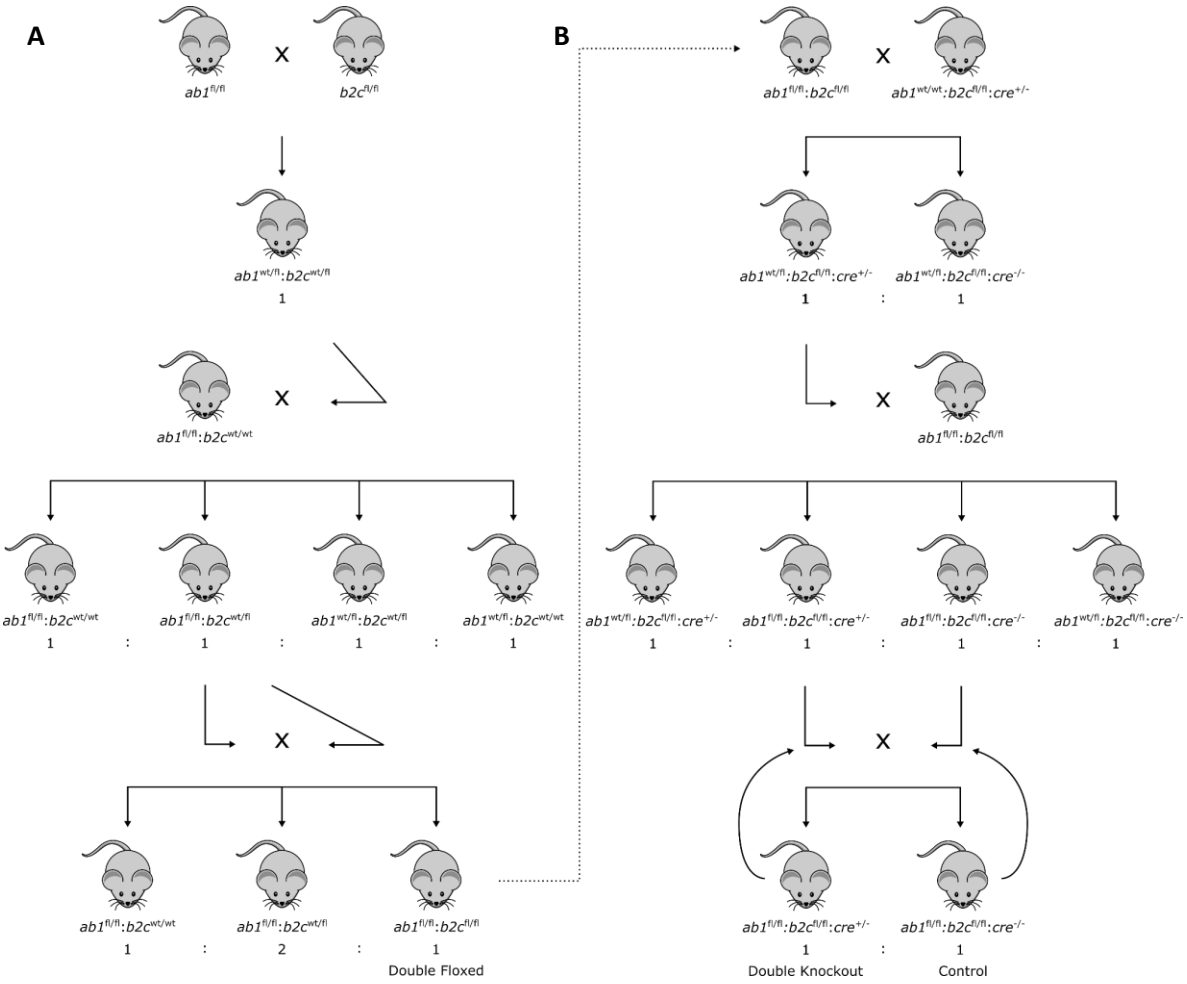

Figure 5.4. MiRNA-29 double knockout breeding scheme. *(A) To generate double floxed mice, homozygous miR-29ab1 ($ab1^{fl/fl}$) and miR-29b2c ($b2c^{fl/fl}$) floxed mice were crossed. Subsequent selection and crossing of offspring produced double floxed ($ab1^{fl/fl}:b2c^{fl/fl}$). (B) To generate a cartilage-specific knockout of miR-29ab1 and miR-29b2c simultaneously, $ab1^{fl/fl}:b2c^{fl/fl}$ and $b2c^{fl/fl}:cre^{+/-}$ knockout mice were crossed. Subsequent selection and crossing of offspring produced double knockout ($ab1^{fl/fl}:b2c^{fl/fl}:cre^{+/-}$) and control ($ab1^{fl/fl}:b2c^{fl/fl}:cre^{-/-}$) mice. Double knockout colonies were maintained by crossing knockout male and control female mice. Predicted mendelian ratios of offspring are given below each new generation.*

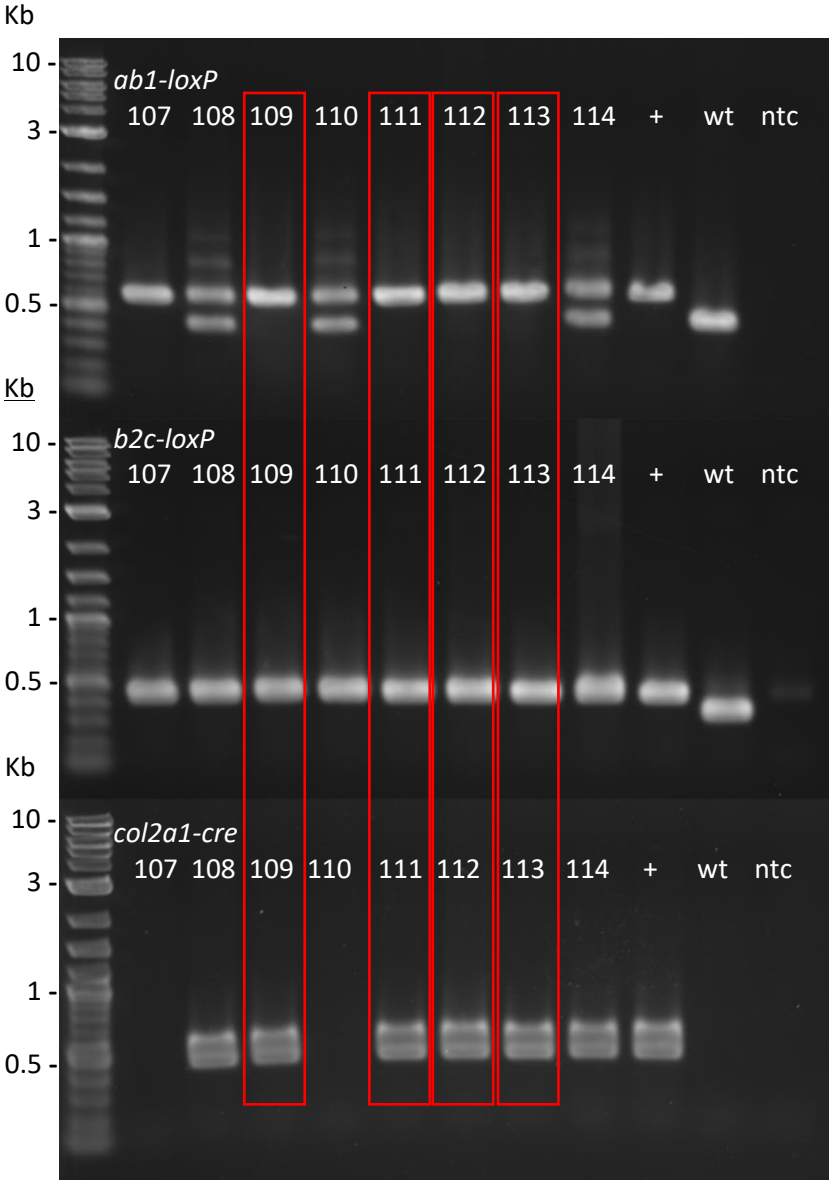

Figure 5.5. Double knockout mouse example genotyping PCR. *Offspring from the double knockout breeding scheme were genotyped for the miR-29ab1 and miR-29b2c floxed loci along with col2a1-cre. Mice that possessed the homozygous floxed miR-29ab1 and miR-29b2c locus, and hemizygous col2a1-cre are highlighted in red. Positive control mice (+) showed the homozygous floxed miR-29ab1 (581 bp) and miR-29b2c (447 bp) bands along with the col2a1-cre (450 bp) band. Wild-type mice (wt) showed the homozygous wild-type miR-29ab1 (419 bp) and miR-29b2c (354 bp) bands along with no col2a1-cre band. ntc = no template control.*

5.2.2 Confirmation of microRNA-29 knockout

The breeding strategy to generate a cartilage-specific knockout of the *miR-29ab1* and *miR-29b2c* loci both independently and simultaneously was successful. To verify that knockout was indeed cartilage-specific, PCR of gDNA and qRT-PCR of RNA extracted from knockout mouse tissues was used to confirm cartilage-specific deletion of miR-29 genomic loci and reduction in miR-29 expression respectively.

5.2.2.1 Confirming gDNA microRNA-29 knockout

By using *col2a1-cre*, knockout of miR-29 should be achieved predominantly in cartilage - specifically in chondrocytes (Sakai *et al.*, 2001). To verify this, gDNA was extracted from femoral head cartilage (hip), ear biopsies and liver tissue from P21 knockout and control mice. Primers were designed to flank the floxed miR-29 loci and PCR was used to look for genomic deletion of *miR-29ab1* and *miR-29b2c*.

For AB1-KO mice, liver samples had a single band at ~1350 bp representing the intact *miR-29ab1* locus whereas ear samples also showed a second band at ~650 bp representing *loxP* recombination and deletion of the *miR-29ab1* locus (Figure 5.6A). Hip cartilage samples showed the same two bands (~1350 bp and ~650 bp) as ear samples, however the lower band was notably brighter relative to the larger one suggesting a greater level of knockout. Control mice showed a single band at 1350 bp for hip (PCR for Ctr1 failed), ear and liver samples representing the intact *miR-29ab1* locus.

Similarly, for B2C-KO mice, liver samples had a single band at ~2000 bp (PCR for KO3 failed) representing the intact *miR-29b2c* locus whereas ear samples also showed a second band at ~700 bp representing the deletion of the *miR-29b2c* locus (Figure 5.6B). Hip cartilage samples only showed the lower band (PCR for KO3 failed) suggesting a greater level of knockout compared to ear samples. Control mice showed a single band at ~2000 bp.

DKO mice were assayed for the *miR-29ab1* and *miR-29b2c* floxed loci. For all hip cartilage samples, *miR-29ab1* and *miR-29b2c* PCRs failed - this was presumed to be because of a failed DNA extraction. For the *miR-29ab1* PCR in DKO1, the liver sample showed one band at ~1350 bp whereas the ear sample showed a second band at ~650 bp. Control samples showed a single band at ~1350 bp. For the *miR-29b2c* PCR in DKO1, the liver sample showed one band at ~2000 bp whereas the ear sample showed a second band at 700 bp. Control samples showed a single band at ~2000 bp (Figure 5.6C).

For all PCR reactions across all samples, bands in liver gDNA appeared to be ~200 bp larger than in ear and hip samples. GDNA from all samples was extracted using the Phire Tissue Direct PCR kit which, while facilitating DNA extraction in approximately 10 minutes, does not produce purified and contaminant free DNA. To investigate whether DNA binding contaminants might explain this discrepancy, PCR was also performed on liver gDNA extracted using TRIzol™ reagent. Bands from PCR performed on TRIzol™ Reagent extracted samples appeared at the expected size in gel electrophoresis compared to Phire extracted samples suggesting that TRIzol™ extraction may remove contaminants causing retardation of PCR bands.

Finally, to verify that the higher and lower bands seen in *miR-29ab1* and *miR-29b2c* PCRs (Figure 5.6) represented the intact and deleted loci respectively, these bands were purified and sequenced. Sequencing data showed that for *miR-29ab1* and *miR-29b2c* loci, the larger bands seen in knockout PCRs represented the respective full loci flanked by *loxP* sites (Figure 5.7). For the smaller bands, sequencing of both loci showed the presence of just one *loxP* site confirming *loxP* recombination and deletion of the *miR-29ab1* and *miR-29b2c* loci.

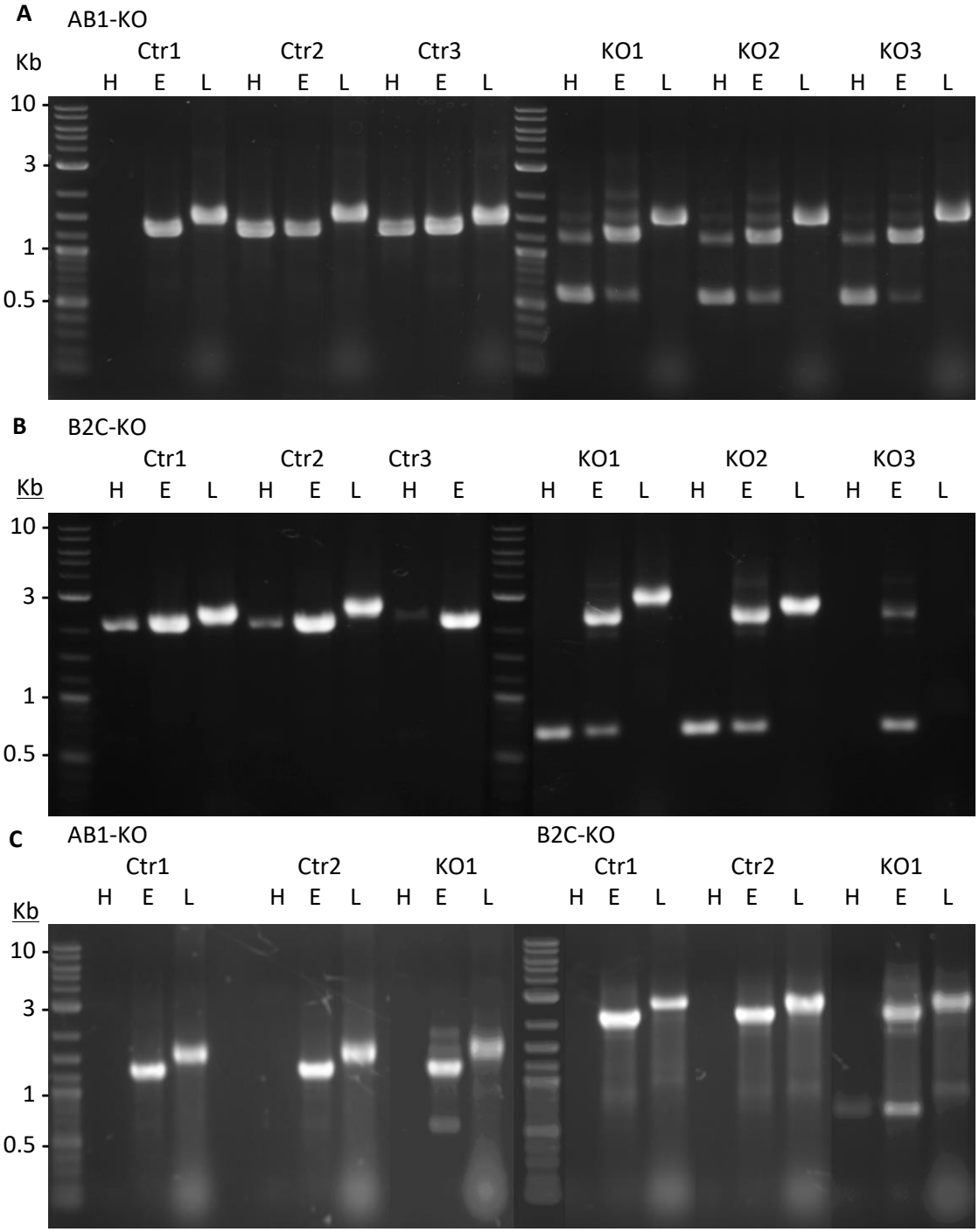

Figure 5.6. Confirmation of miRNA-29 genomic knockout. *Primers were designed to flank the loxP sites of the miR-29ab1 and miR-29b2c floxed loci. Genomic DNA was extracted from femoral head cartilage (H), ear biopsies (E) and liver (L) of P21 AB1-KO, B2C-KO, DKO and respective control (Ctr) mice. PCR was used to amplify the miR-29ab1 locus in AB1-KO mice (A), the miR-29b2c locus in B2C-KO mice (B) and both loci in DKO mice (C). For the miR-29ab1 locus wild-type band is ~1350 bp and knockout band is ~650 bp. For the miR-29b2c locus wild-type band is ~2000 bp and knockout band is ~700 bp.*

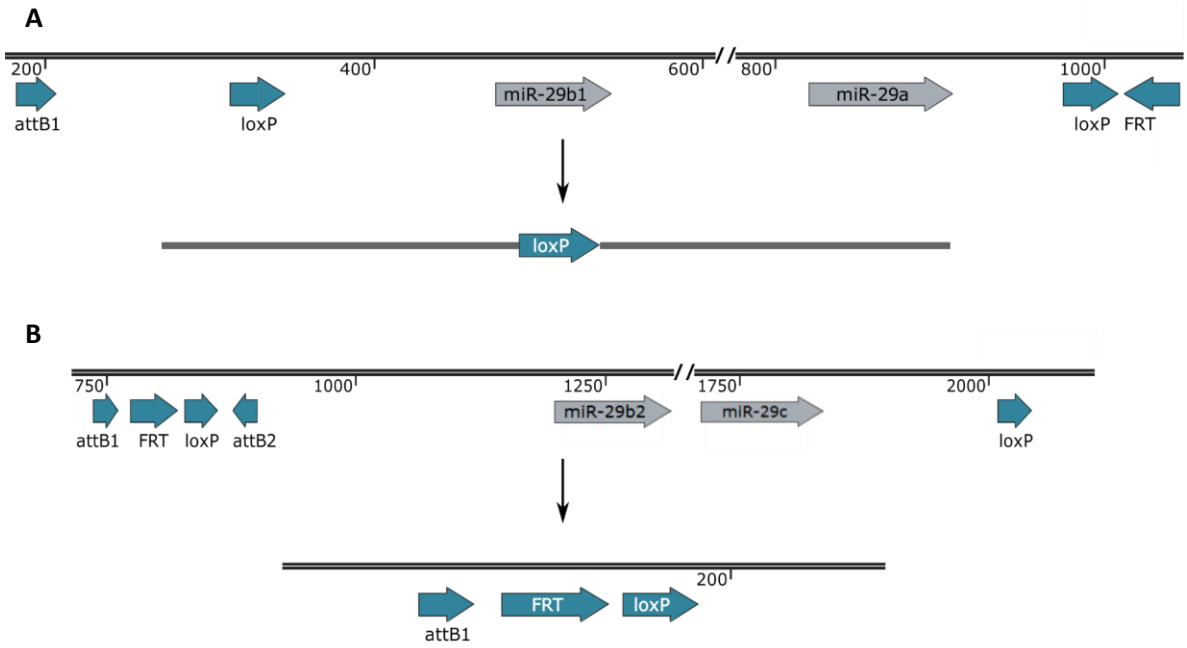

Figure 5.7. Sequencing of miRNA-29 knockout. *Products from miR-29ab1 (A) and miR-29b2c (B) knockout PCRs were purified and sequenced. Sequencing data for the larger products of both miR-29ab1 and miR-29b2c PCRs showed the intact loci flanked by loxP sites. For the smaller products of both, PCRs showed loxP recombination and deletion of the miR-29ab1 and miR-29b2c loci. Figure generated using SnapGene viewer version 5.0.6.*

5.2.2.2 Expression of microRNA-29 in knockout animals

Tissue-specific knockout of miR-29 in AB1-KO, B2C-KO and DKO animals was confirmed by PCR and sequence analysis of gDNA from knockout animals. It was important to confirm that expression of miR-29 was also reduced in the cartilage of knockout animals. To investigate this, cartilage from the femoral heads of P21 knockout and control mice was harvested and RNA was extracted using the mirVana™ miRNA Isolation Kit which is designed to retain small RNAs during total RNA extraction. Femoral head cartilage was chosen because it was easy to harvest compared to knee cartilage, provided a relatively high RNA yield and could be harvested from legs being used for histological analysis thereby minimising the number of animals used for experiments.

To assess the purity of hip cartilage harvested from knockout and control animals, and ensure cartilage was largely free of subchondral bone, the expression of cartilage and bone marker genes was measured in cartilage and femoral bone samples. For AB1-KO, B2C-KO and DKO hip cartilage, expression of tartrate-resistant acid phosphatase (*Trap*) was significantly lower when compared to femoral bone suggesting little contamination with subchondral bone (Figure 5.8). On the other hand, expression of *Acan* and *Col2a1* was significantly higher in hip cartilage from AB1-KO, B2C-KO and DKO mice compared to femoral bone again suggesting little bone contamination and implying high cartilage purity.

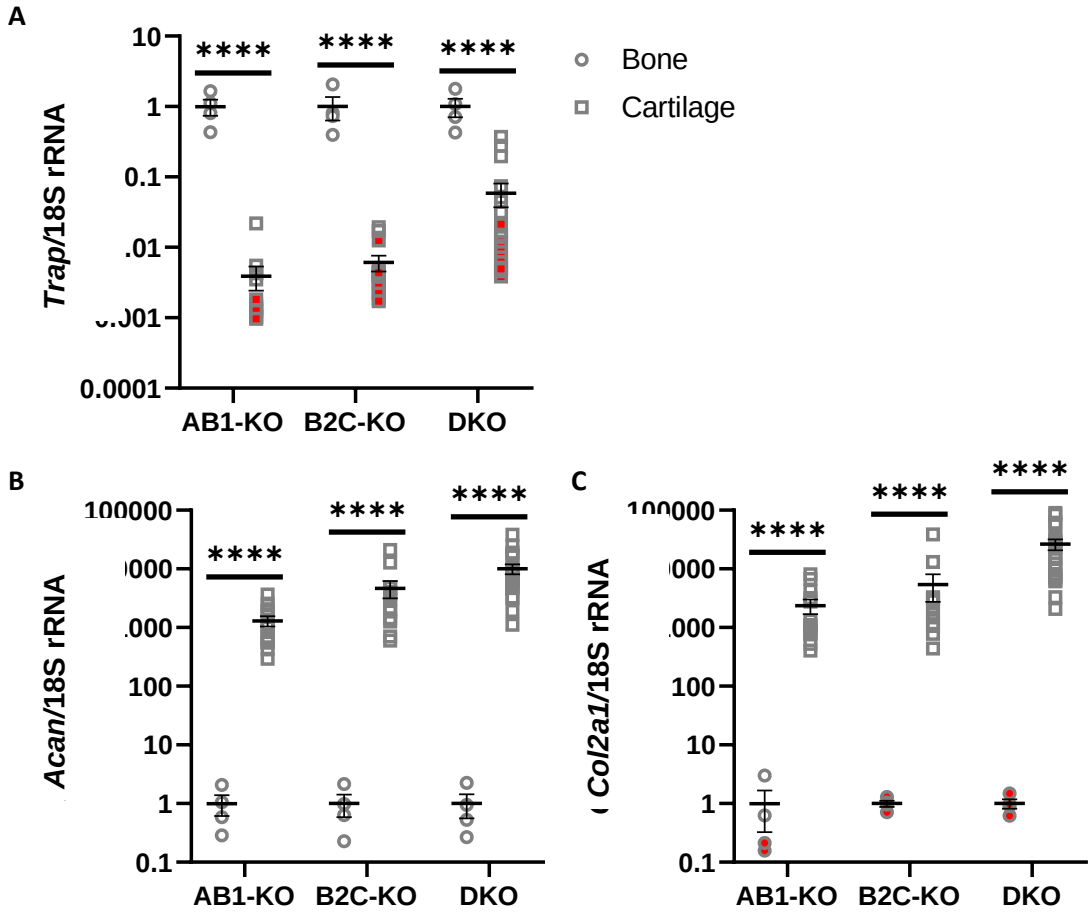

Figure 5.8. Expression of cartilage and bone markers in knockout hip cartilage. *Femoral head cartilage was harvested from P21 AB1-KO, B2C-KO and DKO mice and RNA was extracted. The expression of Trap (A), Acan (B) and Col2a1 (C) was measured in cartilage and wild-type femoral bone (femur) RNA using qRT-PCR and normalised to 18S rRNA to assess cartilage purity. AB1-KO n = 14, B2C-KO n = 14, DKO n = 21, femoral bone n = 4. Data presented as mean ± SEM, two-tailed unpaired t-test **** p < 0.0001. CT values for samples in red were set to 40 as expression was not detected after 40 cycles.*

5.2.2.2.1 Quantification of mature microRNA-29

To confirm miR-29 expression was reduced in the cartilage of knockout animals, expression of mature miR-29a, miR-29b and miR-29c transcripts was measured using TaqMan MicroRNA Assays (TMA). TMAs utilise a miRNA-specific reverse transcription primer and TaqMan probe and PCR primer set to quantify the expression of mature miRNA transcripts. TMAs also allow for the pooling of reverse transcription primers to facilitate the measurement of multiple mature miRNAs from a single reverse transcription reaction.

RNA extracted from AB1-KO P21 hip cartilage was reverse transcribed using a primer pool containing miR-29a, miR-29b, miR-29c and U6 snRNA as an endogenous control. Expression of mature miR-29a, miR-29b and miR-29c was measured using qRT-PCR and normalised to U6 snRNA.

Consistent with AB1-KO mice demonstrating genomic knockout of the *miR-29ab1* locus, expression of mature miR-29a and miR-29b was significantly reduced in knockout hip cartilage compared to littermate controls (Figure 5.9A). However, although the *miR-29b2c* was intact in AB1-KO mice, expression of miR-29c also appeared to be significantly reduced in knockout cartilage. One explanation for this could be that due to the high sequence similarity of mature miR-29a, miR-29b and miR-29c, pooling of reverse transcription primers resulted in cross reactivity of these primers and loss of specificity in the PCR reaction.

To investigate whether pooling of reverse transcription primers was leading to a loss of specificity in mature miR-29 qRT-PCR, separate reverse transcription reactions were performed for miR-29a, miR-29b and miR-29c. Similarly to the samples reverse transcribed using the primer pool, expression of miR-29a, miR-29b and miR-29c was significantly reduced in AB1-KO hip cartilage when compared to littermate controls (Figure 5.9B). Therefore, it was not the pooling of reverse transcription primers that was leading to cross reactivity between TMAs.

In the cartilage of AB1-KO cartilage, expression of miR-29a and miR-29b should be reduced whereas expression of miR-29c should be unaffected. However, expression of miR-29a, miR-29b and miR-29c was reduced when measured with TMAs. TMAs are advertised as allowing for “single-base discrimination of homologous family members” however the data in Figure 5.9 suggested this may not be the case. To further troubleshoot this issue, data were shared with the manufacturer. Bioinformatic analysis of TMAs for miR-29a, miR-29b and miR-29c revealed significant cross reactivity between the assays for miR-29a and miR-29c. This cross reactivity explained the apparent reduced expression of miR-29c in AB1-KO cartilage.

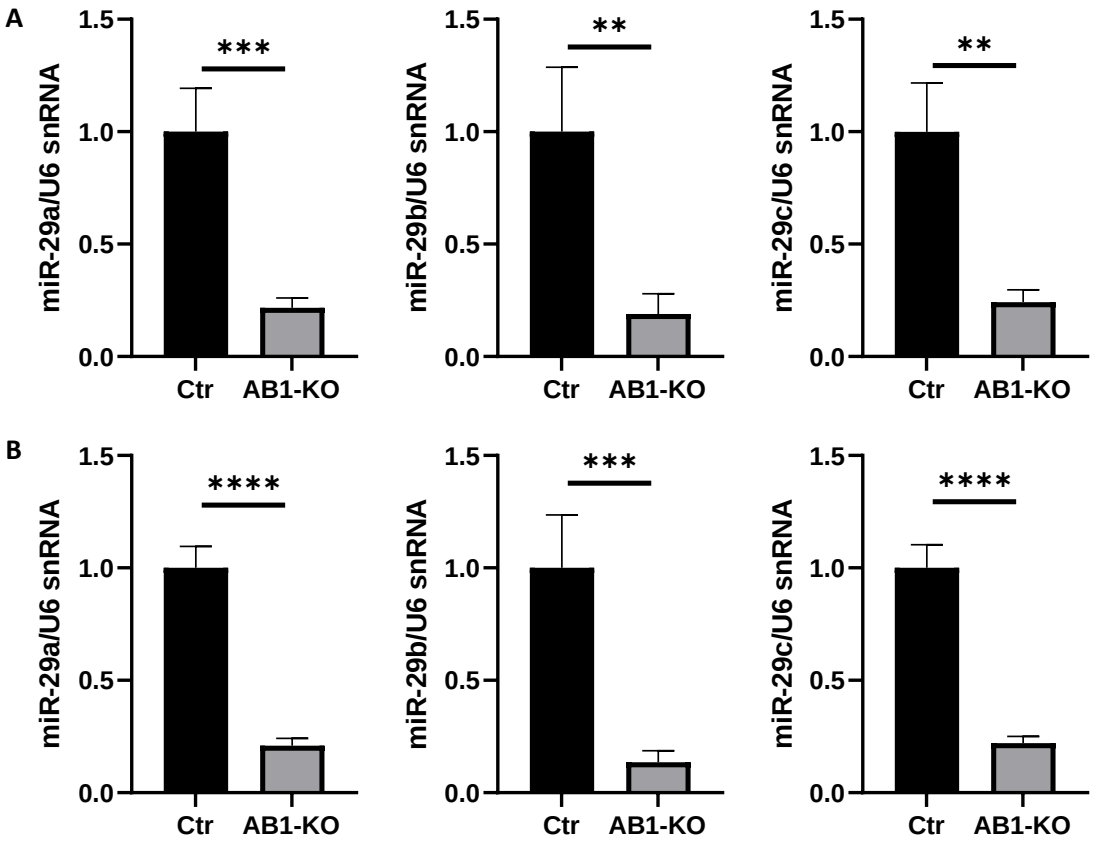

Figure 5.9. Expression of mature miRNA-29 in AB1-KO cartilage. *Expression of mature miR-29a, miR-29b and miR-29c was measured in RNA from P21 AB1-KO and control (Ctr) femoral head cartilage using TaqMan MicroRNA Assays. Reverse transcription was performed using a primer pool of miR-29a, miR-29b and miR-29c primers (A) or a separate reaction for each primer (B) to assess primer cross reactivity. Expression was measured using qRT-PCR and normalised to U6 snRNA. Data presented as mean ± SEM, n ≥ 7, two-tailed unpaired t-test ** p < 0.01, *** p < 0.001, **** p < 0.0001.*

5.2.2.2.2 Quantification of microRNA-29 primary transcripts

Given that TMAs were not able to effectively discriminate between mature miR-29a and miR-29c, an alternative strategy was required to verify respective reduced of expression of miR-29a, miR-29b and miR-29c in miR-29 knockout mice. Using the Universal Probe Library, qRT-PCR assays were designed to amplify the primary transcripts of *miR-29a*, *miR-29b1*, *miR-29b2* and *miR-29c*.

Expression of *miR-29a*, *miR-29b1*, *miR-29b2* and *miR-29c* was measured in RNA from AB1-KO, B2C-KO and DKO hip cartilage using the primary transcript qRT-PCR assays. In hip cartilage from AB1-KO mice expression of miR-29a and miR-29b1 primary transcripts was significantly reduced compared to littermate controls, whereas expression of miR-29b2 and miR-29c primary transcripts was not significantly different (Figure 5.10A). On the other hand, in B2C-KO cartilage, expression of miR-29b2 and miR-29c primary transcripts was significantly reduced compared to littermate controls whereas expression of miR-29a and miR-29b1 was not significantly different (Figure 5.10B). Finally, in hip cartilage from DKO mice, expression of miR-29a, miR-29b1, miR-29b2 and miR-29c transcripts was significantly reduced compared to littermate controls (Figure 5.10C).

Consistent with the respective genotypes of these mice, and with the data from genomic knockout PCRs, these data demonstrate knockout of the *miR-29ab1* and *miR-29b2c* loci, independently and simultaneously in AB1-KO, B2C-KO and DKO mice respectively. Moreover, in contrast to TMAs, primary transcript qRT-PCR were able to discriminate between the expression of *miR-29a*, *miR-29b1*, *miR-29b2* and *miR-29c*.

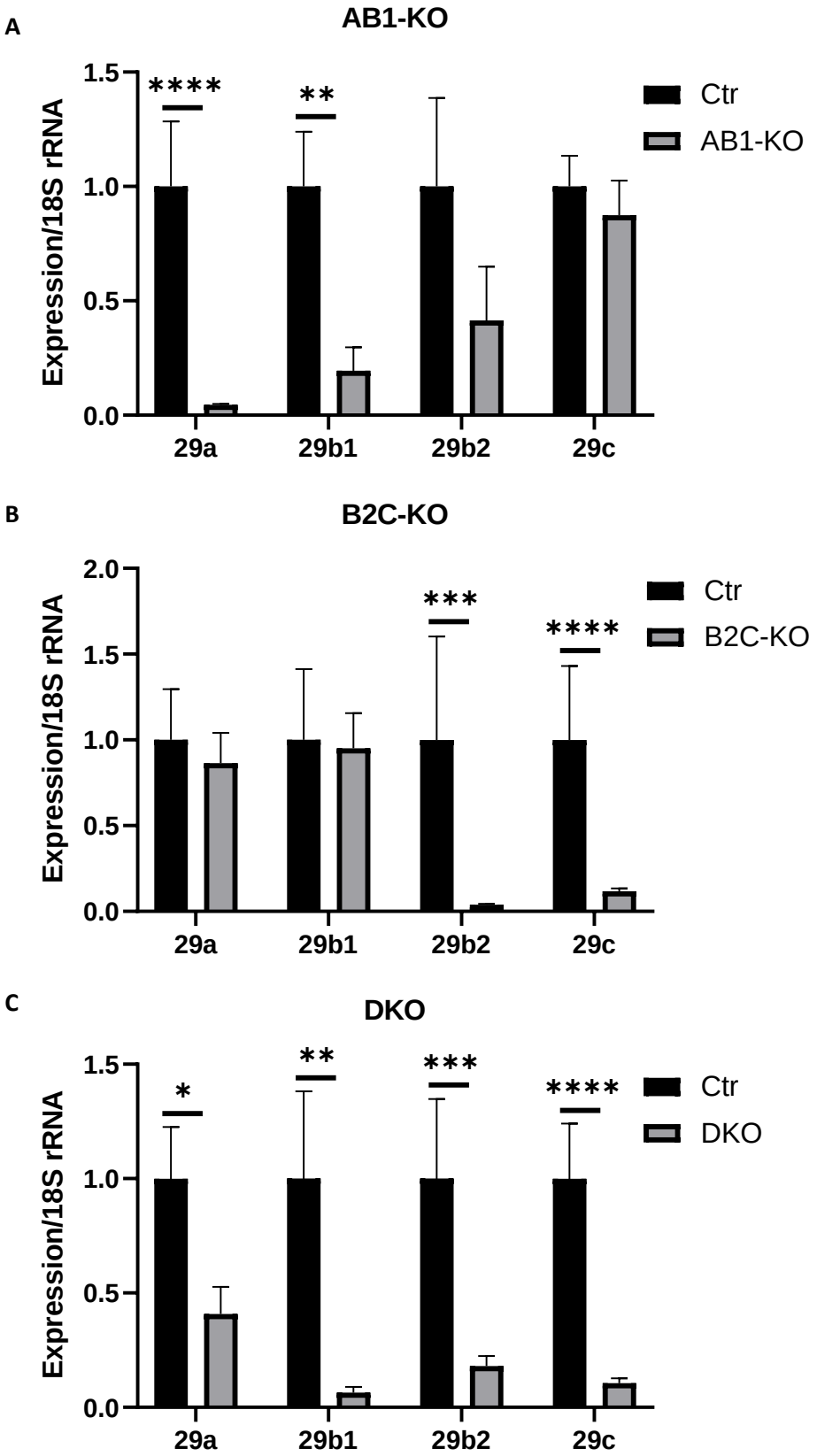

Figure 5.10. Expression of mature miRNA-29 in AB1-KO cartilage. *Expression of miR-29a, miR-29b1, miR-29b2 and miR-29c primary transcripts was measured in RNA from P21 AB1-KO (A), B2C-KO (B), DKO (C) and respective control (Ctr) femoral head cartilage using primary transcript qRT-PCR assays and normalised to 18S rRNA. Data presented as mean ± SEM, for AB1-KO and B2C-KO n = 7, for DKO n ≥ 10, two-tailed unpaired t-test * p < 0.05, ** p < 0.01, *** p < 0.001, **** p < 0.0001.*

5.2.3 MicroRNA-29 double knockout mice mRNA-sequencing

Identifying miRNA regulatory networks is complicated with miRNAs often targeting many mRNAs and mRNAs often possessing many miRNA binding sites. Global analysis of expression changes in response to miRNAs can be used to elucidate their function. To further investigate the role of miR-29 in articular cartilage, mRNA-seq was used assess the effect of miR-29 knockout on global gene expression.

5.2.3.1 Sample quality

Cartilage was harvested from the femoral heads of six DKO and six control 3-week-old male mice and total RNA was extracted. To assess the purity of harvested cartilage, expression of *Trap*, *Acan* and *Col2a1* was measured by qRT-PCR as in section 5.2.2.2. Expression of *Trap* was significantly downregulated in RNA from DKO and littermate control cartilage compared to femur whereas expression of *Acan* and *Col2a1* was significantly upregulated (Figure 5.11). Furthermore, there was no significant difference in *Trap*, *Acan* and *Col2a1* expression between DKO and littermate control mice suggesting samples were of equal purity.

Sample quality was assessed prior to mRNA-seq. Following quality control by Novogene for RNA quantity and RIN (see Table 5.1), the following samples were selected for mRNA-seq: Ctr-2, Ctr-3, Ctr-4, Ctr-5, DKO-2, DKO-4, DKO-5 and DKO-6.

Table 5.1. Novogene mRNA-seq quality control

Sample	Total RNA (g)	RIN
DKO-1	0.297	3
DKO-2	0.403	4.2
DKO-3	0.442	6.7
DKO-4	0.574	4.8
DKO-5	0.338	3.8
DKO-6	0.077	1
Ctr-1	0.494	3.6
Ctr-2	0.492	6.5
Ctr-3	0.533	2.7
Ctr-4	0.612	6.7
Ctr-5	0.408	3.7
Ctr-6	0.484	3.8

Underlined samples selected for mRNA-seq

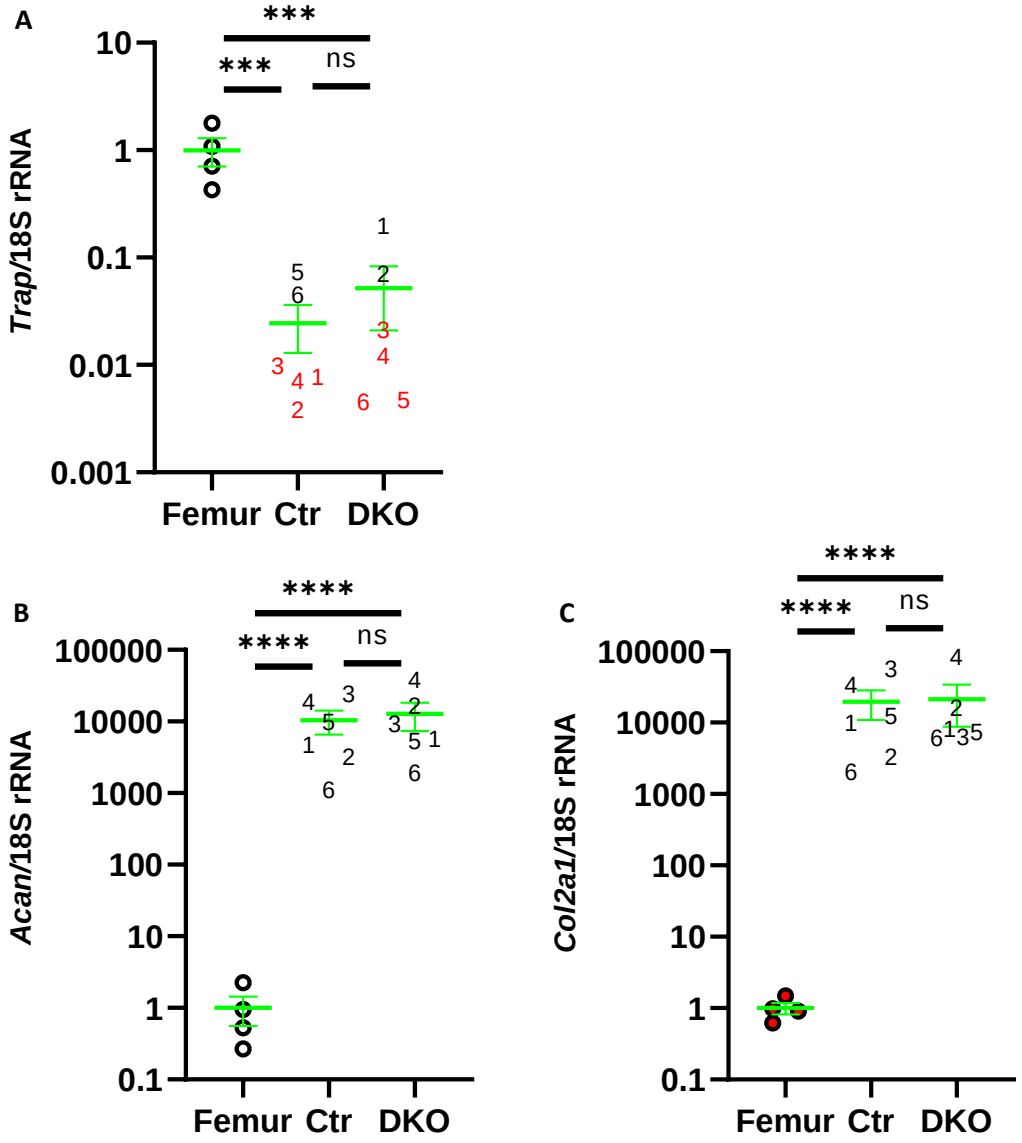

Figure 5.11. Expression of cartilage and bone markers in mRNA-seq samples. *Femoral head cartilage was harvested from 3-week-old male DKO mice and RNA was extracted. The expression of Trap (A), Acan (B) and Col2a1 (C). was measured in DKO and littermate control (Ctr) cartilage, and wild-type femoral bone (femur) RNA using qRT-PCR and normalised to 18S rRNA to assess cartilage purity. DKO n = 6, Ctr n = 6, femur n = 4. Data presented as mean ± SEM, one-way ANOVA *** p < 0.001, **** p < 0.0001. CT values for samples in red were set to 40 as expression was not detected after 40 cycles.*

5.2.3.2 Analysis of mRNA-sequencing data

Analysis of the mRNA-seq data using principal component analysis (PCA) showed that control samples clustered together. Whilst two DKO samples clustered separately, the remaining two DKO samples clustered more closely with the controls (Figure 5.12A). When analysing the data including all four DKO samples there were 60 differentially expressed (DE) genes (34 upregulated, 26 downregulated, $q \leq 0.05$) (Figure 5.12B and Appendix table 4). However, when the two DKO samples which clustered with the control samples were excluded from the analysis, there were 1324 DE genes (683 upregulated, 641 downregulated, $q \leq 0.05$) (Figure 5.12C and Appendix table 5). In a similar study, Swahari *et al.* (2021) found DE of 2,823 genes with brain-specific knockout of miR-29 consistent with the DE of 1324 genes seen in here with the omission of the two DKO samples which clustered with controls. Of the genes 34 upregulated genes identified in the analysis of all four DKO samples, 30 overlapped with upregulated genes identified in the analysis omitting the two DKO samples which clustered with the controls.

Gene ontology (GO) analysis of significantly upregulated genes in the two separately clustering DKO (compared to control) revealed enrichment for 845 terms across molecular functions (MF), biological processes (BP) and cellular components (CC) as well as being enriched for many Kyoto Encyclopaedia of Genes and Genomes (KEGG), Reactome (REAC), WikiPathways (WP), Transcription Factor Database (TF), Comprehensive Resource of Mammalian Protein Complexes (CORUM) and Human Phenotype Ontology (HP) terms (Figure 5.12C) (Raudvere *et al.*, 2019).

Among the enriched GO terms in DKO cartilage were extracellular matrix, extracellular matrix binding and collagen-containing extracellular matrix with significantly upregulated genes including *Adamts2*, *Adamts4*, *Mmp9*, *Mmp13*, *Mmp15*, *Mmp16, Col1a1*, *Col1a2* and *Col8a1* (Table 5.2). GO terms were also enriched for cellular response to TGF-β stimulus and response to TGF-β with *Tgfbr1*, *Col1a1* and *Col1a2* being amongst the significantly upregulated genes (Table 5.3). Finally, enriched human phenotype ontologies included endochondral bone-related terms including increased bone mineral density, osteopetrosis, abnormal diaphysis morphology, abnormality of bone mineral density and tibial bowing (Table 5.4).

Further analysis of significantly upregulated genes enriched for extracellular matrix, extracellular matrix binding and collagen-containing extracellular matrix showed that Ctr and DKO samples grouped separately with hierarchical clustering across all three groups (Figure 5.13, Figure 5.14 and Figure 5.15). Within extracellular matrix and collagen-containing extracellular matrix enriched genes *Col1a1* and *Col2a1* were highly differentially expressed and grouped closely with hierarchical clustering (Figure 5.13 and Figure 5.15).

On the other hand, expression of *Adamts2* and *Adamts4* was comparatively moderate and with distant clustering suggesting that DE may be mediated through different regulatory mechanisms.

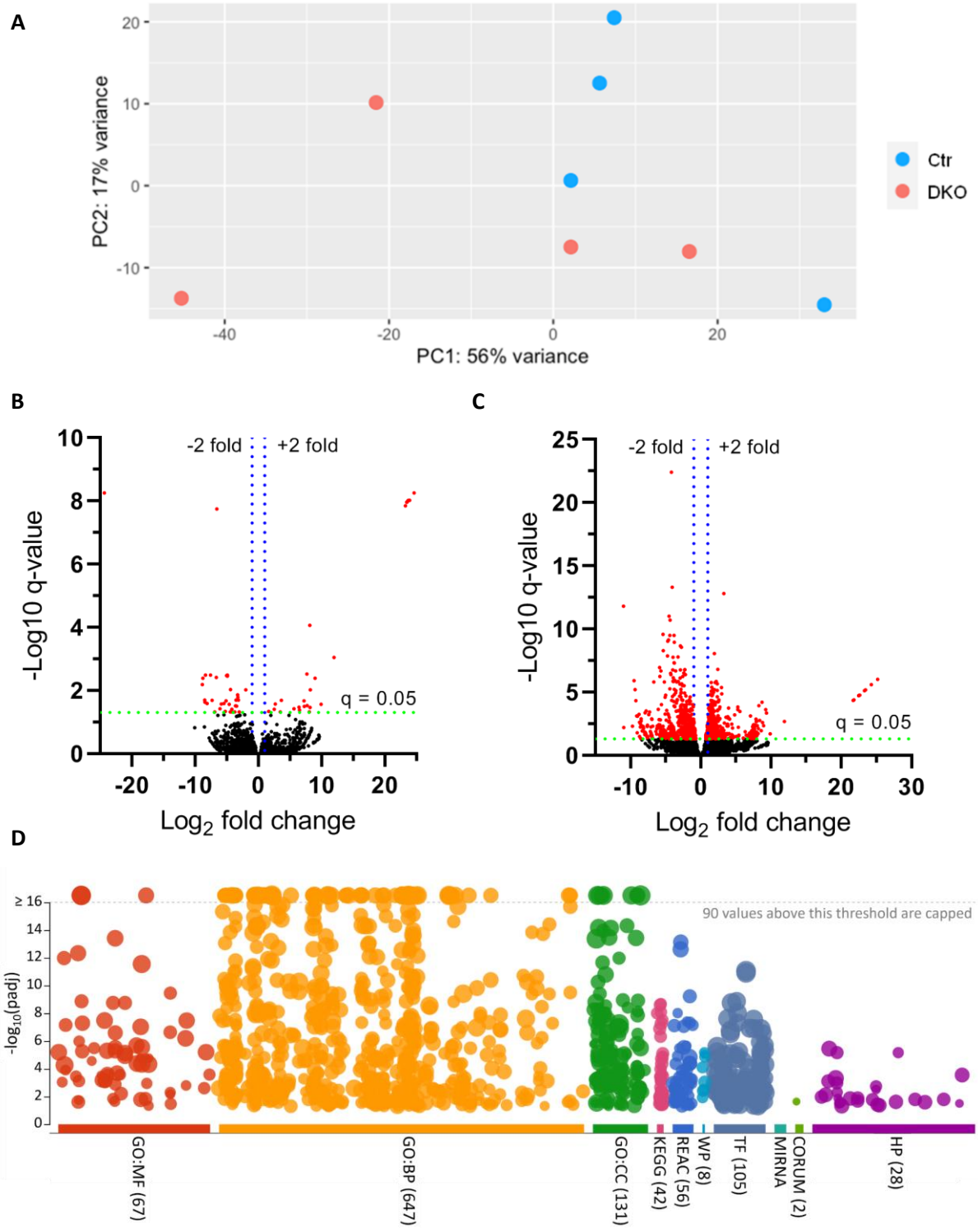

Figure 5.12. Analysis of double knockout mRNA-seq data. *(A) Principal component (PC) analysis of miR-29 DKO mRNA-seq data showed that whilst two DKO samples clustered separately from Ctr samples, two DKO samples clustered more closely with control (Ctr) samples. (B) Volcano plot of mRNA-seq data showing log_2 fold change in expression plotted against -log_{10} q-value for analysis including (B) and excluding (C) DKO samples which grouped with Ctr samples. Significantly differentially expressed genes (q ≤ 0.05) in red. (D) GO analysis of upregulated genes (q ≤ 0.05) (excluding the DKO samples which clustered with Ctr) in Figure C showed enrichment for hundreds of gene ontologies (GO) as well as KEGG, REAC, WP, TF, CORIUM and HP ontologies. Analysis performed using g:Profiler (Raudvere et al., 2019).*

Table 5.2. Significantly upregulated genes (q ≤ 0.05) in miR-29 DKO cartilage with enrichment for extracellular matrix gene ontologies.

Gene Ontology	Gene
Extracellular matrix GO: 0031012	*Cthrc1, Olfml2b, Dcn, Cpz, Angpt4, Mmp16, Ccbe1, Mmp15, Wnt4, Angpt2, Lox, Adamts2, Col8a1, Emid1, Gpc1, Lgals9, Fbln2, Lingo3, Adamts4, Atrnl1, Adam10, S100a11, Serpine2, Ptprz1, Col1a2, Spn, Timp1, Sema6d, Cstb, Ctsc, Col1a1, Ccn4, Mmp9, Mmp13, Tnc, Dmp1*
Extracellular matrix binding GO:0050840	*Olfml2b, Dcn, Plekha2, Gpc1, Fbln2, Spp1, Itgb3, Itga2, Dmp1*
Collagen-containing extracellular matrix GO: 0062023	*Dcn, Angpt4, Angpt2, Lox, Adamts2, Col8a1, Emid1, Gpc1, Lgals9, Fbln2, Adamts4, Atrnl1, Adam10, S100a11, Serpine2, Ptprz1, Col1a2, Spn, Timp1, Sema6d, Cstb, Ctsc, Col1a1, Mmp9, Tnc*

Table 5.3. Significantly upregulated genes (q ≤ 0.05) in miR-29 DKO cartilage with enrichment for TGF-β gene ontologies.

Gene Ontology	Gene
Cellular response to TGF-β stimulus GO: 0071560	*Cldn1, Cx3cr1, Lrg1, Wnt4, Lox, Tgfbr1, Hsp90ab1, Actr3, Zfp36l1, Cldn5, Cdh5, Pdgfa, Hpgd, Fyn, Ptprk, Col1a2, Col1a1, Zeb2*
Response to TGF-β GO: 0071559	*Cldn1, Cx3cr1, Lrg1, Wnt4, Lox, Tgfbr1, Hsp90ab1, Actr3, Zfp36l1, Cldn5, Cdh5, Pdgfa, Hpgd, Fyn, Ptprk, Col1a2, Col1a1, Zeb2*

Table 5.4. Significantly upregulated genes (q ≤ 0.05) in miR-29 DKO cartilage with enrichment for endochondral-related human phenotype ontologies.

Human Phenotype Ontology	Gene
Increased bone mineral density HP: 0011001	*Car2, Fermt3, Ostm1, Ncf1, Fam111a, Sost, Dlx3, Cldn13, Csf1r, Tnfrsf11a, Gja1, Phex, Lrp4, Snx10, Ctsk, Acp5, Dmp1*
Osteopetrosis HP: 0011002	*Car2, Fermt3, Ostm1, Csf1r, Tnfrsf11a, Gja1, Snx10*
Abnormal diaphysis morphology HP: 0000940	*Car2, Satb2, Ncf1, Antxr2, Fam111a, Sost, Arsb, Ifih1, B2m, Glb1, Cldn13, Tnfrsf11a, Hpgd, Vdr, Lifr, Gja1, Col1a2, Sgms2, Phex, Col1a1, Sh3pxd2b, Lrp4, Snx10, Zeb2, Mmp9, Mmp13, Acp5, Dmp1*
Abnormality of bone mineral density HP: 0004348	*Il12a, Car2, Fermt3, Sp7, Ostm1, Satb2, Ncf1, Ctnnb1, Spib, Antxr2, Fam111a, Adamts2, Sost, Il12rb1, Ifih1, Dlx3, Glb1, Cldn13, Psat1, Csf1r, Cdkn1a, Tnfrsf11a, Hpgd, Pls3, Vdr, Runx1, Lifr, Ifitm5, Gja1, Col1a2, Sgms2, Phex, Col1a1, Tyrobp, Sh3pxd2b, Lrp4, Snx10, Syk, Ctsk, Dusp6, Mmp13, Acp5, Dmp1*
Tibial bowing HP: 0002982	*Satb2, Vdr, Lifr, Col1a2, Phex, Col1a1, Mmp13, Dmp1*

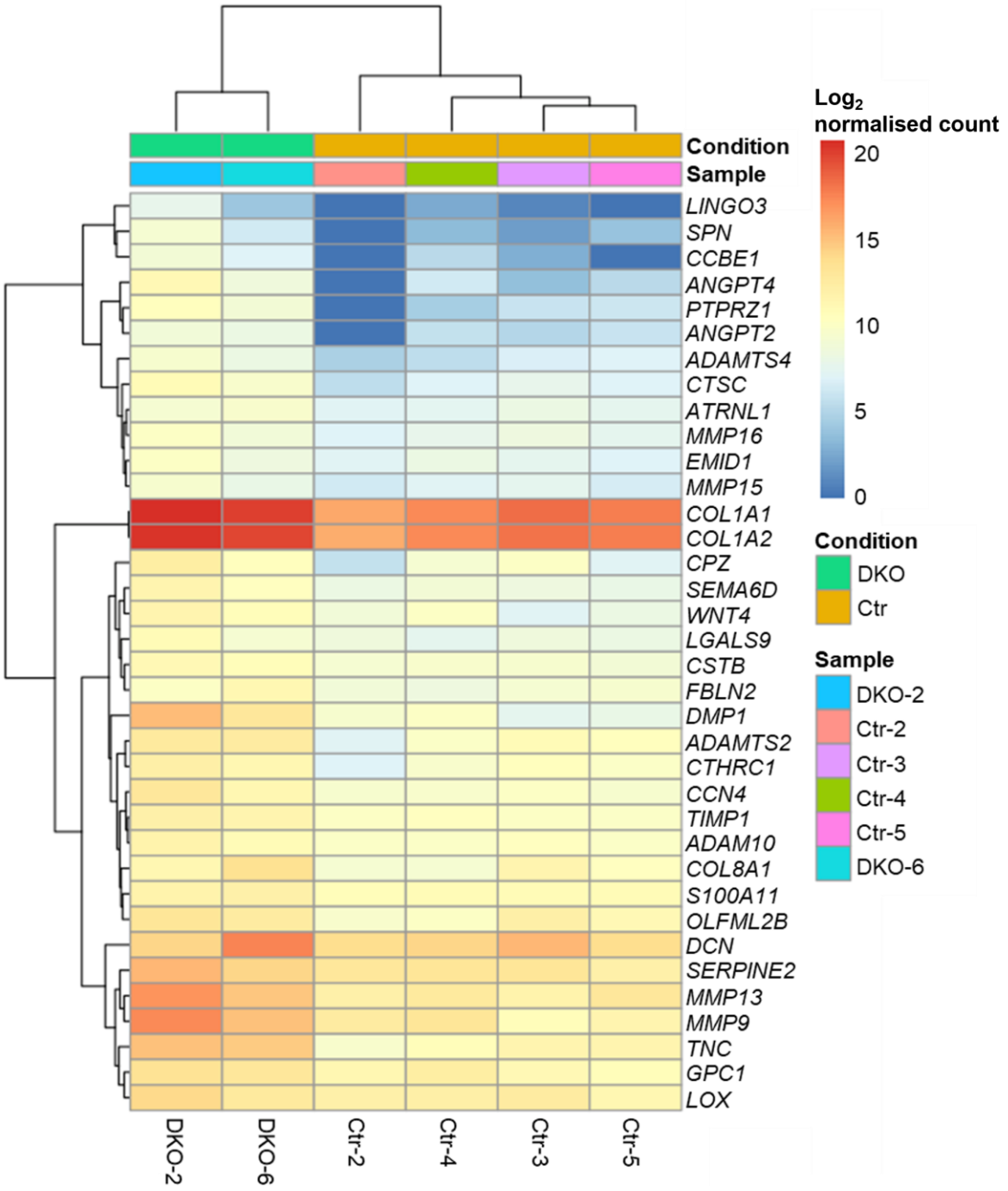

Figure 5.13. Enrichment of extracellular matrix genes in mRNA-seq data. *A hierarchical clustering heat map of significantly upregulated genes (q ≤ 0.05) enriched for the extracellular matrix gene ontology (GO: 0031012). Hierarchical clustering was performed using DESeq2. Log_2 normalised count data is presented as low (0) to high (20) scaled from blue to red respectively.*

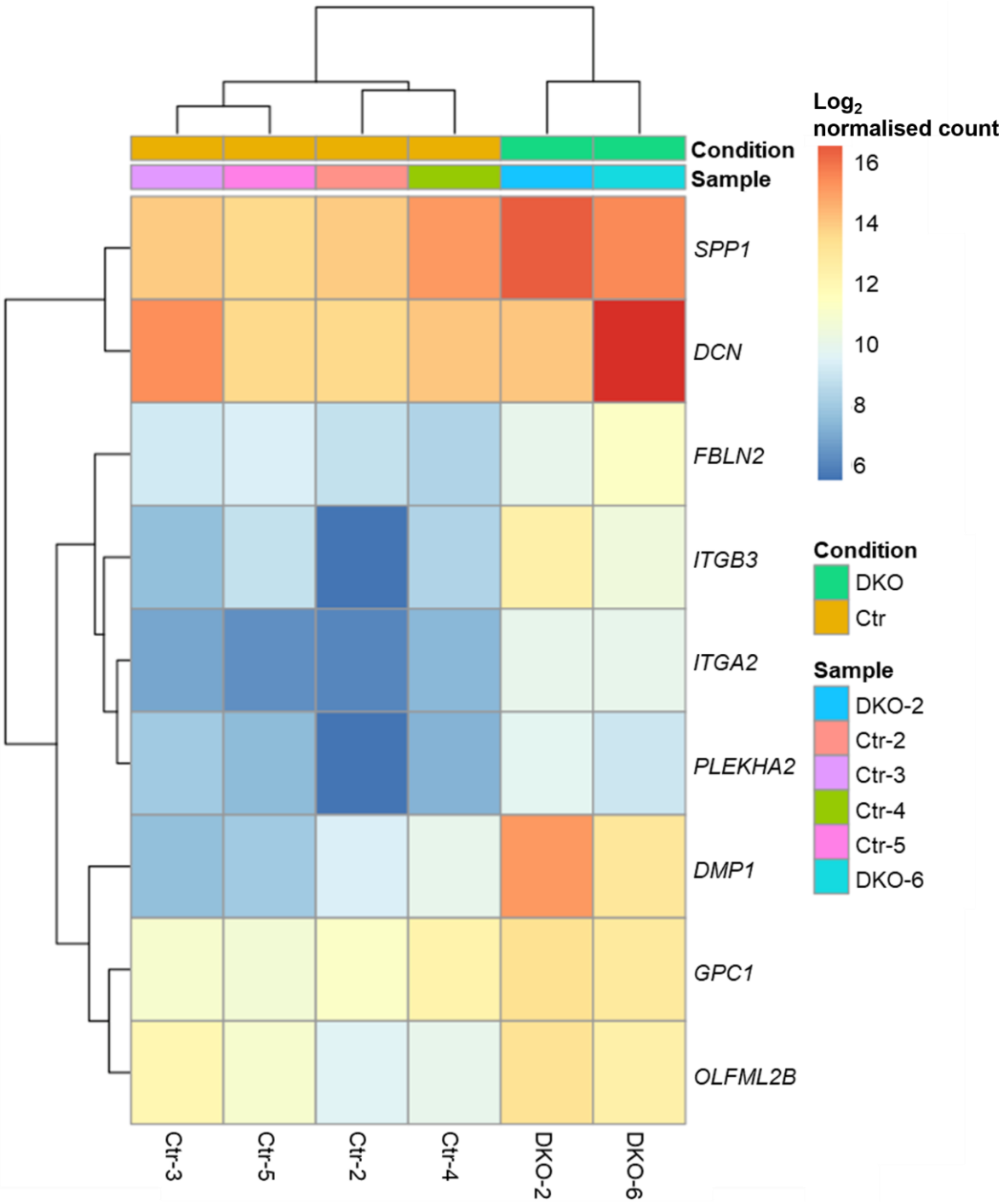

Figure 5.14. Enrichment of extracellular matrix binding genes in mRNA-seq data. *A hierarchical clustering heat map of significantly upregulated genes (q ≤ 0.05) enriched for the extracellular matrix binding gene ontology (GO: 0050840). Hierarchical clustering was performed using DESeq2. Log$_2$ normalised count data is presented as low (6) to high (16) scaled from blue to red respectively.*

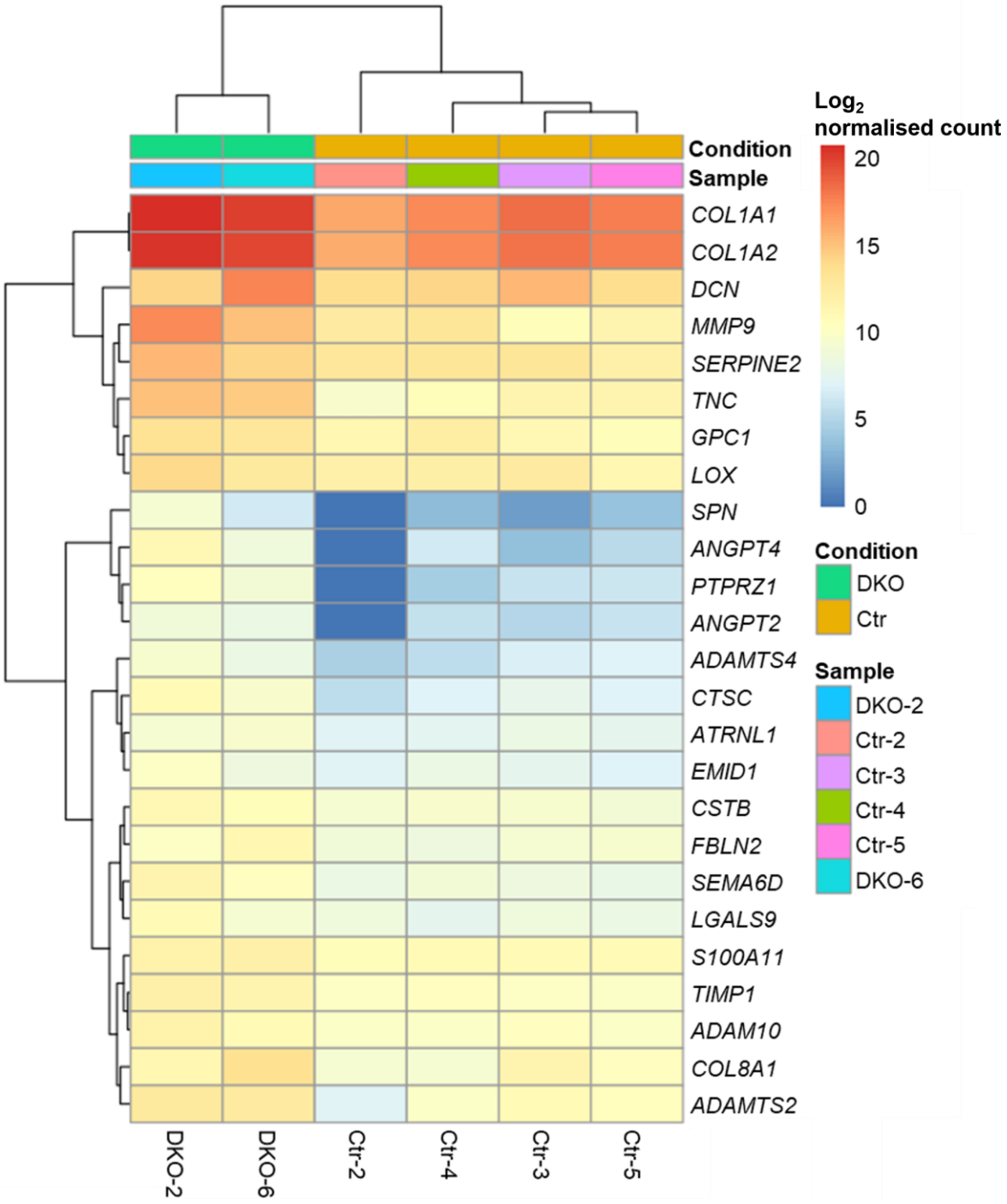

Figure 5.15. Enrichment of collagen-containing extracellular matrix genes in mRNA-seq data. *A hierarchical clustering heat map of significantly upregulated genes ($q \leq 0.05$) enriched for the collagen-containing extracellular matrix gene ontology (GO: 0062023). Hierarchical clustering was performed using DESeq2. Log_2 normalised count data is presented as low (0) to high (20) scaled from blue to red respectively.*

5.2.3.2.1 ADAMTS expression in microRNA-29 double knockout mice

As discussed in chapter 3, members of the ADAMTS family showed evidence of being regulated by miR-29. Luciferase reporter assays suggested direct targeting of *ADAMTS2*, *ADAMTS9*, *ADAMTS15*, *ADAMTS16*, *ADAMTS18* and *ADAMTS20* by miR-29b-3p and transfection of HACs with miR-29b-3p downregulated expression of *ADAMTS12*.

To further investigate whether miR-29 regulated members of the ADAMTS family *in vivo*, ADAMTS expression was analysed in DKO mRNA-seq data (Figure 5.16). In hip cartilage from 3-week aged DKO mice expression of *Adamts2* and *Adamts4* was significantly upregulated ($q \leq 0.05$) compared with littermate controls. On the other hand, expression of *Adamts3*, *Adamts6* and *Adamts10* was significantly downregulated ($q \leq 0.05$) in DKO cartilage compared with littermate controls. Expression of *Adamts8*, *Adamts13* and *Adamts19* was not reliably detected.

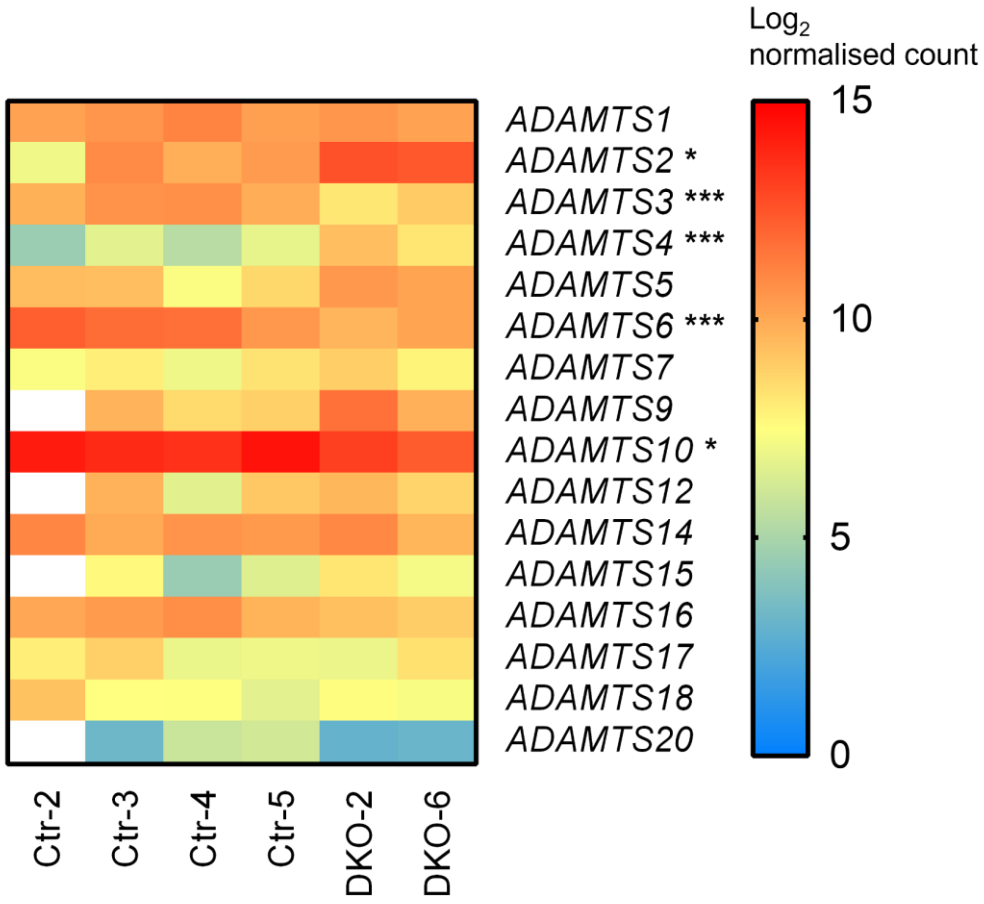

Figure 5.16. ADAMTS expression in miRNA-29 double knockout hip cartilage. *Heatmap of ADAMTS expression in hip cartilage from 3-week aged miR-29 DKO and littermate control mice. Log_2 normalised count data is presented as low (0) to high (15) scaled from blue to red respectively. Wald test with multiple test correction was performed using DESeq2, * padj < 0.05, *** padj < 0.001.*

5.2.3.2.2 Expression of DNA methylation genes microRNA-29 double knockout mice

Several genes involved in the regulation of DNA methylation are predicted targets of miR-29. As discussed in chapter 4, *DNMT3A* and *TET2* were downregulated in SW1353 cells and HACs by miR-29b-3p. Moreover, transfection of SW1353 cells with a miR-29b-3p mimic significantly reduced global methylation.

To assess whether DNA methylation was dysregulated in miR-29 DKO hip cartilage, expression of *Tdg*, *Dnmt1*, *Dnmt3a*, *Dnmt3b*, *Tet1*, *Tet2* and *Tet3* was analysed in DKO mRNA-seq data (Figure 5.17). No significant difference in expression of these genes was seen between DKO and littermate control hip cartilage. However, on average expression of *Dnmt3b* and *Tet2* was downregulated by 0.51 and 0.7-fold respectively whereas expression of *Tdg* was upregulated by 1.26-fold.

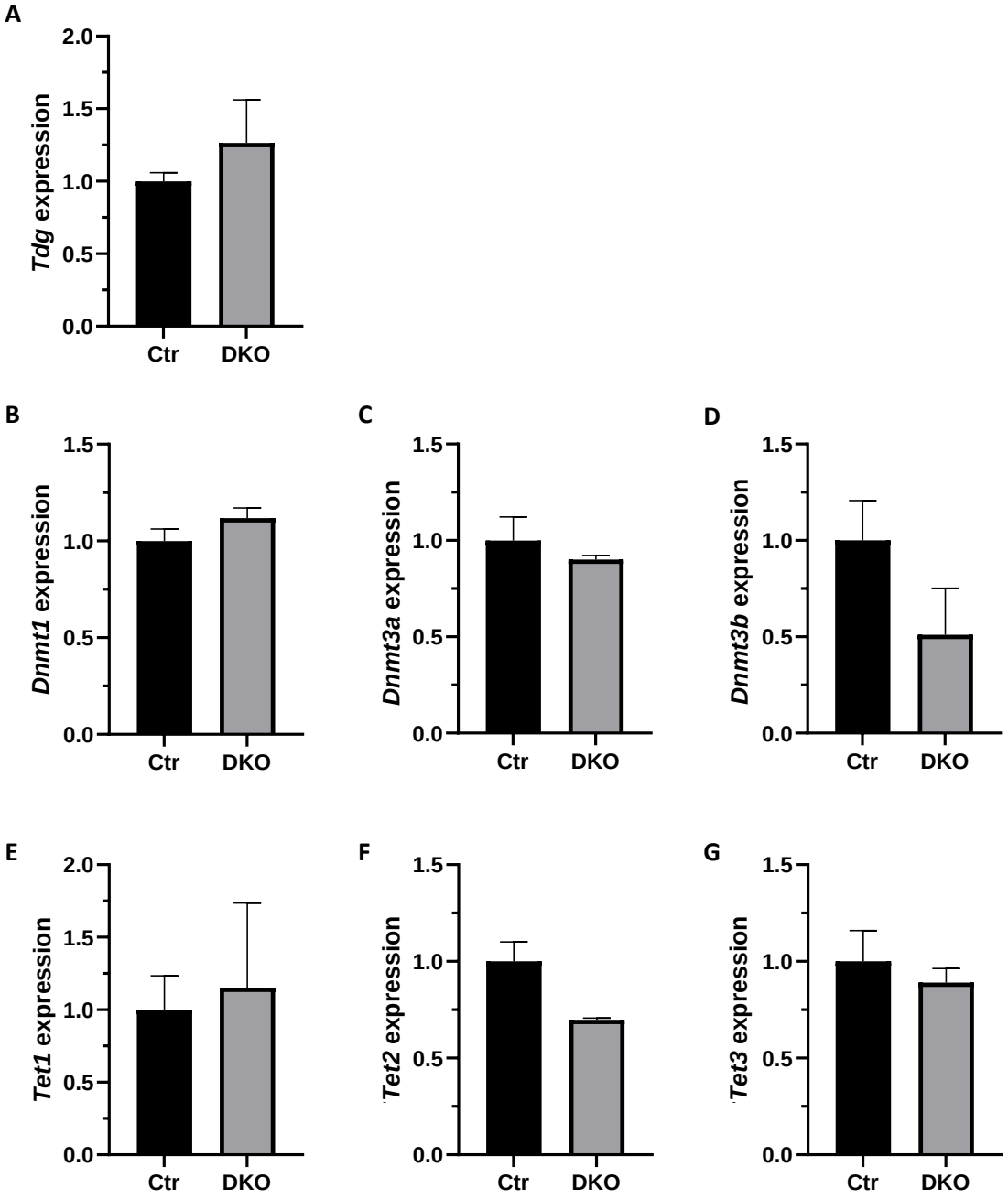

Figure 5.17. Expression of DNA methylation genes in miRNA-29 double knockout hip cartilage. *Expression of Tdg (A), Dnmt1 (B), Dnmt3a (C), Dnmt3b (D), Tet1 (E), Tet2 (F) and Tet3 (G) was analysed in mRNA-seq data for hip cartilage from 3-week aged miR-29 DKO and littermate control mice, n ≥ 2. Data presented as mean ± SEM fold change of normalised counts.*

5.2.3.2.3 Upregulation of a predicted lncRNA

Analysis of significantly upregulated genes (q ≤ 0.05) in DKO samples identified *Gm27019* as being upregulated by over 50-fold in DKO samples compared with controls (Figure 5.18A). To verify upregulation of *Gm27019* in miR-29 DKO cartilage, primers were designed to amplify the *Gm27019* transcript and qRT-PCR was used to measure expression in hip cartilage samples from 3-week aged DKO and littermate controls (as in section 5.2.2.2). Expression of *Gm27019* was significantly upregulated in DKO samples compared with littermate controls by 17.5-fold when measured using qRT-PCR (Figure 5.18B).

Gm27019 is a predicted long non-coding RNA (lncRNA) located directly upstream of the *miR-29b1* gene and overlapping by two base pairs. To investigate why *Gm27019* was upregulated by miR-29 knockout, the genomic sequence for *Gm27019* (ENSMUST00000183056.2) was aligned with genomic sequencing data from DKO mice. Analysis of this aligned sequence showed that the *loxP* site upstream of the *miR-29ab1* locus was located within the 3' end of *Gm27019* (Figure 5.18C). Genomic sequencing data from DKO cartilage showed that *loxP* recombination of the *loxP* sites at the *miR-29ab1* locus resulted 3' deletion in the *Gm27019* gene (Figure 5.18D). Therefore, *Gm27019* upregulation as a result of miR-29 knockout may result from the deletion of a 3' negative regulatory sequence.

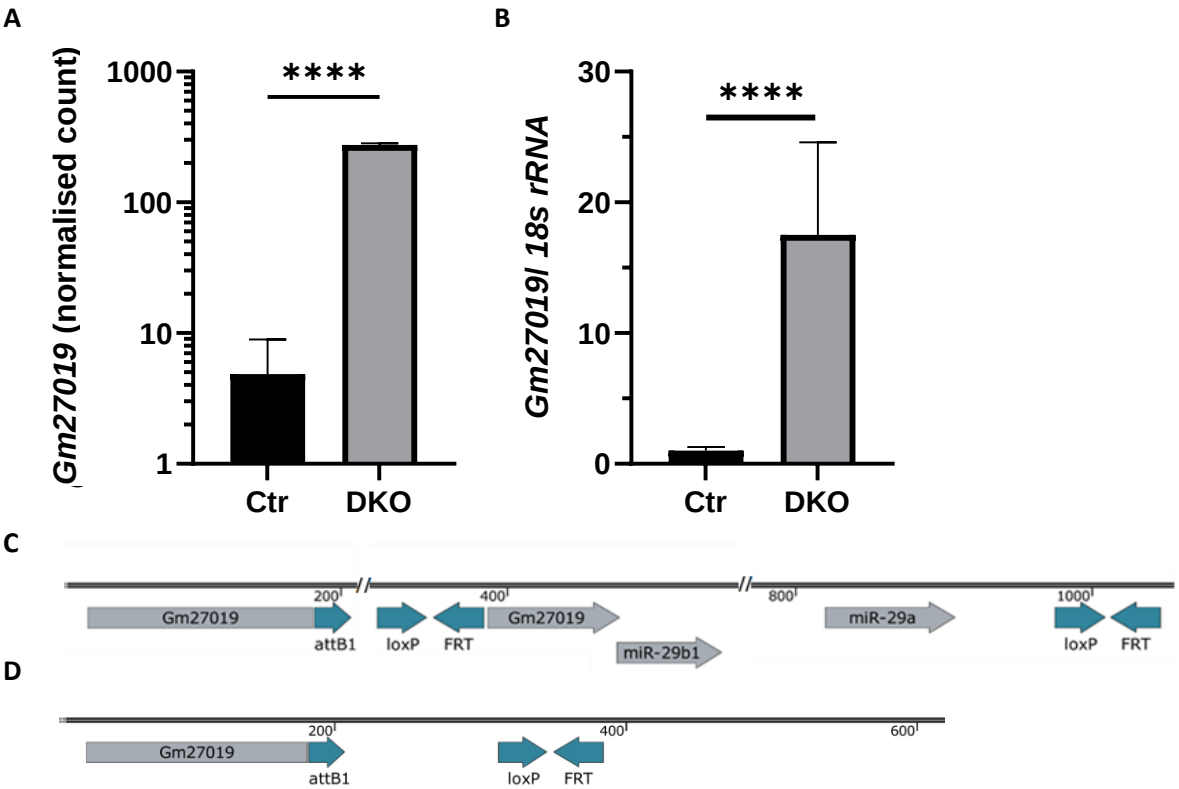

Figure 5.18. Upregulation of Gm27019 in miRNA-29 DKO hip cartilage. *(A) Analysis of mRNA-seq data found that Gm27019 was significantly upregulated in hip cartilage from 3-week aged DKO mice compared to littermate controls (Ctr) (n ≤ 2). (B) Upregulation of Gm27019 in DKO cartilage was confirmed using qRT-PCR (n ≥ 9). (C) Genomic sequencing data from DKO mice showed that the loxP site upstream of the miR-29ab1 locus was located within the Gm27019 gene. (D) Sequencing of gDNA from DKO cartilage showed that loxP recombination resulted in a deletion in Gm27019. (A and B) Data presented as mean ± SEM, two-tailed unpaired t-test **** p < 0.0001.*

5.2.4 Characterisation of micoRNA-29 knockout mice

By crossing *miR-29ab1* and *miR-29b2c* floxed mice with *col2a1-cre* mice, cartilage-specific AB1-KO, B2C-KO and DKO mice were generated. Knockout mice demonstrated no obvious developmental abnormalities at birth compared to littermates. Significantly, in contrast to global miR-29 knockout mice (Cushing *et al.*, 2015; Swahari *et al.*, 2021), cartilage-specific double knockout mice did not die by 6 weeks of age allowing investigation of the effect of miR-29 in the cartilage past this relatively young age.

Although double knockout mice survived past 6 weeks of age, by 18 weeks of age (95% CI; 14.4, 22.3), knockout mice demonstrated repetitive and excessive grooming behaviour, ultimately leading to self-inflicted ulcerative skin lesions that necessitated culling of the animal (n = 10). This phenotype was not seen in littermate controls. In light of this, ageing experiments past 12 weeks could not be performed and the number of animals available for DMM studies was extremely limited.

5.2.4.1 Litter ratios of knockout mice

Although knockout mice were born phenotypically normal, it was possible that miR-29 knockout may reduce prenatal survival. To assess whether cartilage-specific knockout of miR-29 had any influence on foetal viability the proportion of control and knockout animals per litter was compared.

When comparing the proportion of wild-type and knockout animals per litter from AB1-KO breeding pairs, the proportion of knockout mice per litter was significantly lower than wild-type littermates at 44% (Figure 5.19A). Similarly, in DKO breeding pairs, the proportion of knockout mice per litter was also significantly lower than wild-type littermates at 39% (Figure 5.19C). In contrast, in B2C breeding pairs, the proportion of knockout mice per little was significantly higher than wild-type littermates at 59% (Figure 5.19B). These data suggest AB1 and DKO mice have may have reduced foetal viability whereas in B2C-KO mice, foetal viability may be increased.

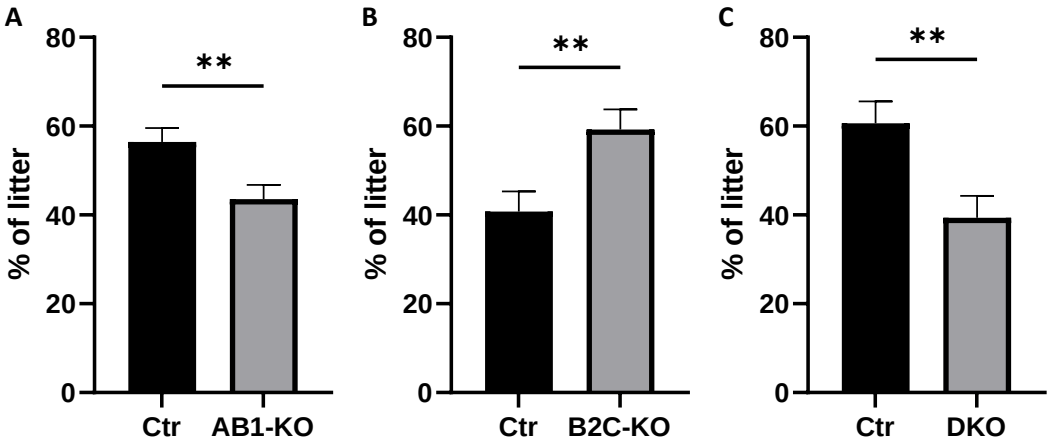

Figure 5.19. Proportions of miRNA-29 knockout mice per litter. *The percentage of knockout and wild-type (Ctr) mice born per litter for AB1-KO (A), B2C-KO (B), and DKO (C) breeding pairs was calculated. Data presented as mean ± SEM, AB1-KO n = 29, B2C-KO n = 16, DKO n = 22, two-tailed unpaired t-test ** p < 0.01.*

5.2.4.2 Gross body weight of knockout mice

Cartilage-specific knockout of *miR-29ab1* with and without simultaneous knockout of *miR-29b2c* significantly reduced foetal viability. To investigate whether knockout mice developed normally AB1-KO, B2C-KO and DKO mice were weighed at 3 weeks and 12 weeks of age and compared to littermate controls.

At 3 weeks of age AB1-KO, B2C-KO and DKO mice were not significantly different in weight to littermate controls although, on average knockout weighed less than controls across all three strains (Figure 5.20A). At 12 weeks of age, both AB1-KO and DKO mice weighed significantly less than littermate controls whereas no significant difference was seen in B2C-KO mice (Figure 5.20B). For AB1-KO, knockout mice weighed on average 4.4% less than control littermates whereas for DKO, this weight difference was more dramatic with knockout mice weighing 8.8% less than control littermates.

Given that knockout of miR-29 in AB1-KO and DKO mice was cartilage-specific, a difference in weight may represent a delay in skeletal development, however this weight difference could also be explained by reduced food intake if animals are stressed or less able to compete for food due to miR-29 knockout. If the latter explanation was the case, knockout animals may have reduced body fat. To see if this was the case, inguinal fat IGFPs were harvested from 3-month AB1-KO and DKO mice and weighed. When IGFP weight was normalised to overall weight, ABI-KO and DKO mice were not significantly different to littermate controls (Figure 5.20C) suggesting body fat was unaffected by miR-29 knockout.

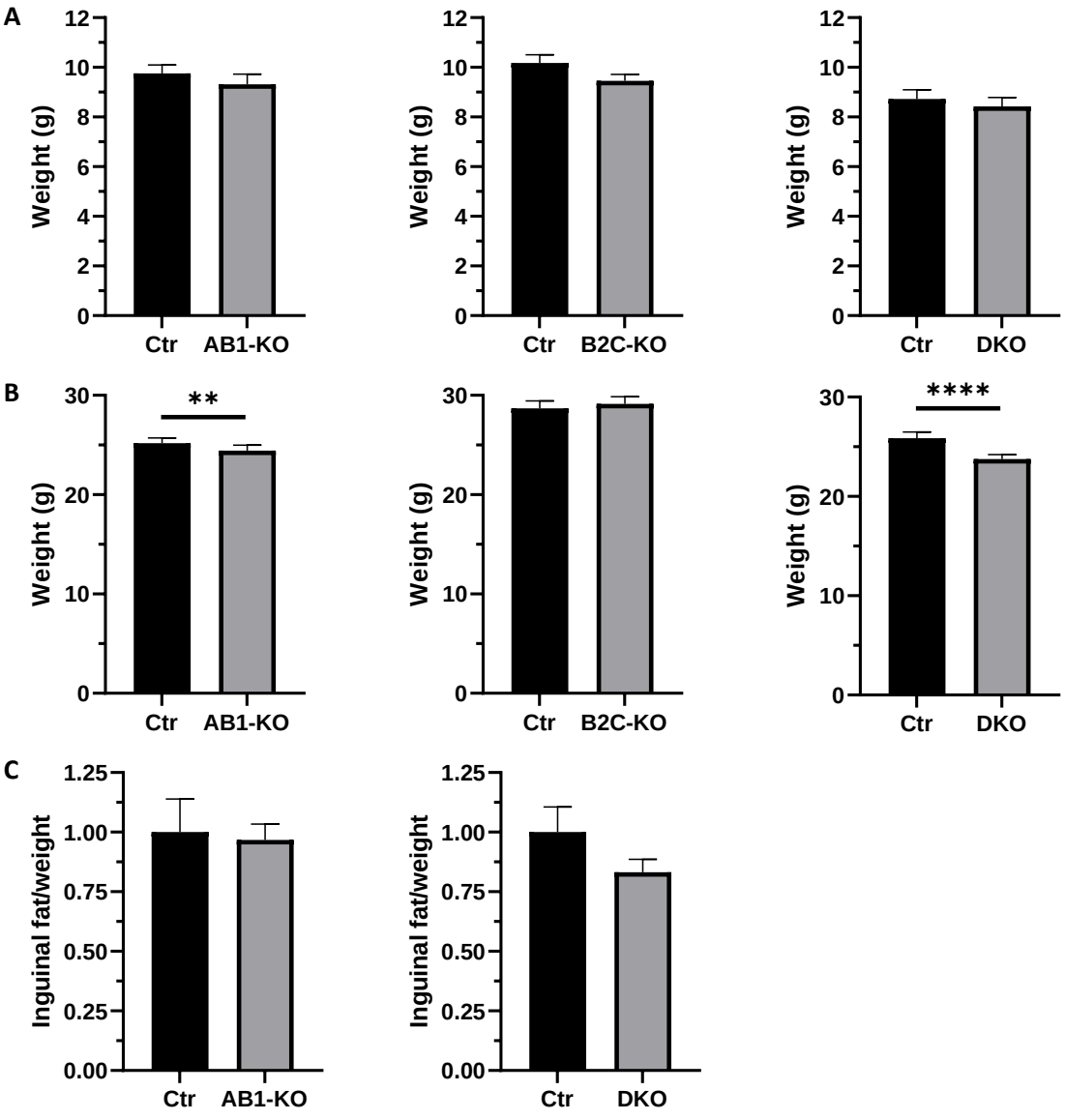

Figure 5.20. Weights of miRNA-29 knockout mice. *AB1-KO, B2C-KO, DKO and littermate control mice were weighed at aged 3-weeks (A) and 12-weeks (B) and compared with littermate controls (Ctr). (C) Inguinal fat was harvested from 3-month AB1-KO and DKO mice, weighed, normalised to overall animal weight, and compared with littermate controls (Ctr). For body weight AB1-KO 3-weeks n ≥ 24, AB1-KO 12-weeks n ≥ 34, B2C-KO 3-weeks n ≥ 20, B2C-KO 12-weeks n ≥ 15, DKO 3-weeks n ≥ 9 and DKO 12-weeks n ≥ 17. For inguinal fat weight AB1-KO n ≥ 5, DKO n ≥ 7. Data presented as mean ± SEM, two-way ANOVA was used to control for sex differences, ** p < 0.01, **** p < 0.0001.*

5.2.4.3 Femur length in knockout mice

In AB1-KO and DKO mice, cartilage-specific knockout of miR-29 lead to a significant reduction in weight at 12 weeks of age. One hypothesis for this reduced weight could be delayed skeletal development. To investigate whether miR-29 knockout mice showed signs of delayed skeletal development, AB1-KO, B2C-KO and DKO legs were analysed using X-ray and the length and width of femoral bones was measured.

The length of femurs (greater trochanter to the medial condyle) was measured from X-ray images of legs from 3-week and 12-week aged mice. At 3 weeks of age mean femur length was shorter in AB1-KO, B2C-KO and DKO mice by 4%, 7.1% and 2.2% respectively however this difference only reached significance for B2C-KO (Figure 5.21A). At 12 weeks of age, femur length was significantly shorter in AB1-KO, B2C-KO and DKO mice at 3.8%, 4.7% and 4.9% respectively (Figure 5.21B).

In addition to measuring the length of femurs in knockout mice, the width of femurs was measured across the distal femoral growth plate. At 3 weeks of age there was no significant difference in the width of femurs in AB1-KO, B2C-KO and DKO mice compared to littermate controls (Figure 5.22A). Similarly, there was no significant difference in the width of femurs in AB1-KO, B2C-KO and DKO mice (Figure 5.22B).

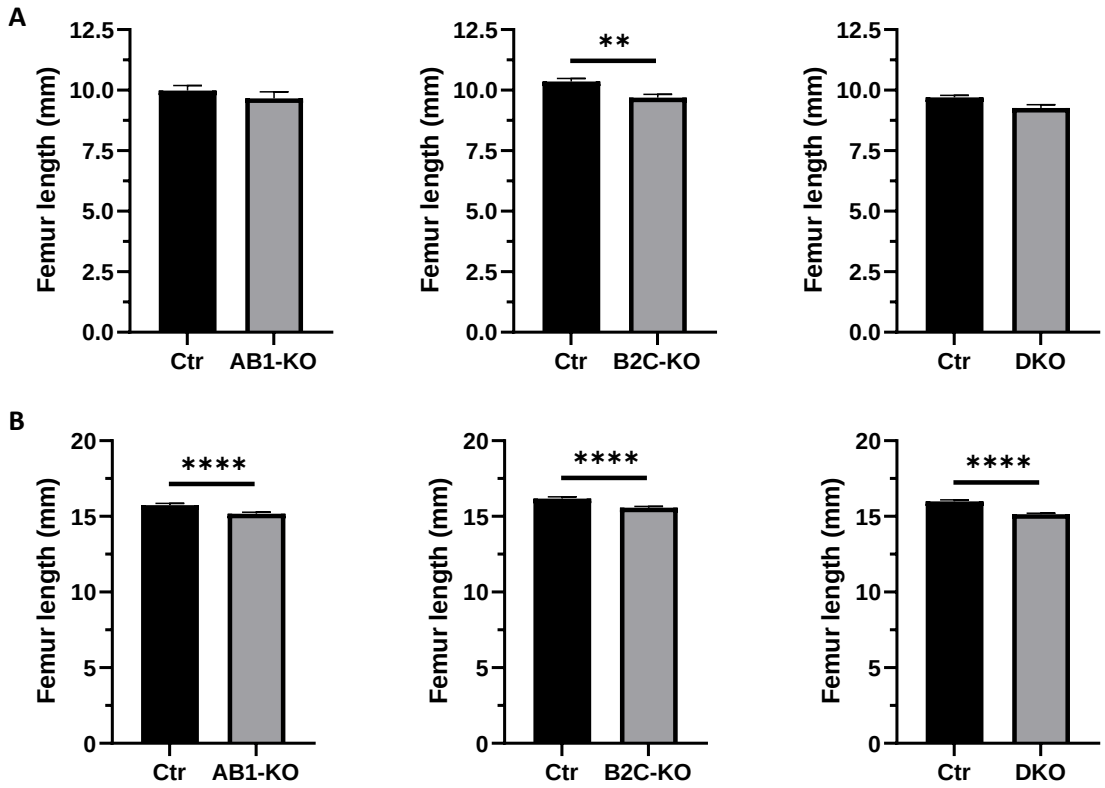

Figure 5.21. Femur length of miRNA-29 knockout mice. *Femur length was measured in X-ray images of AB1-KO, B2C-KO, DKO and littermate control mice aged 3-weeks (A) and 12-weeks (B). AB1-KO 3-weeks n ≥ 6, AB1-KO 12-weeks n ≥ 15, B2C-KO 3-weeks n ≥ 8, B2C-KO 12-weeks n ≥ 12, DKO 3-weeks n ≥ 9 and DKO 12-weeks n ≥ 16. Data presented as mean ± SEM, two-way ANOVA was used to control for sex differences, ** p < 0.01, **** p < 0.0001.*

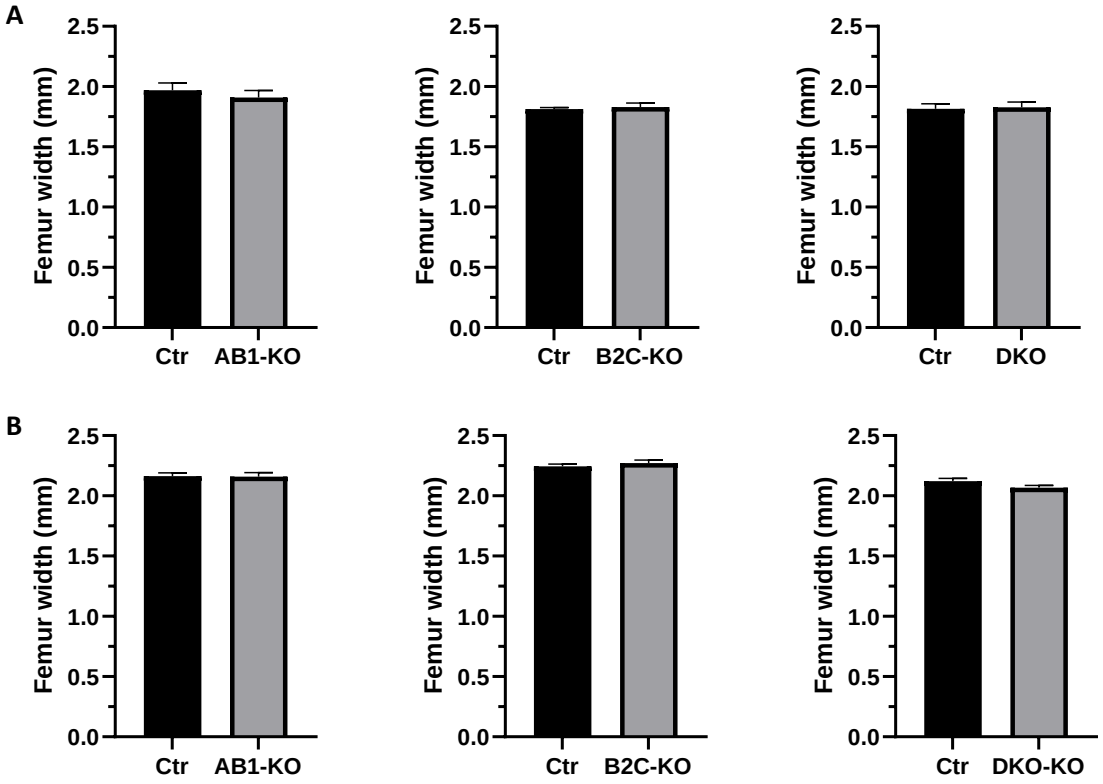

Figure 5.22. Femur width of miRNA-29 knockout mice. *Femur width was measured in X-ray images of AB1-KO, B2C-KO, DKO and littermate control (Ctr) mice aged 3-weeks (A) and 12-weeks (B). AB1-KO 3-weeks n ≥ 7, AB1-KO 12-weeks n ≥ 17, B2C-KO 3-weeks n ≥ 8, B2C-KO 12-weeks n ≥ 12, DKO 3-weeks n ≥ 9 and DKO 12-weeks n ≥ 16. Data presented as mean ± SEM.*

5.2.4.4 Bone density in knockout mice

X-ray images taken with the Bruker In-Vivo Xtreme imaging system can be analysed for bone density using the Bruker Bone Density Software Module. By modelling a cylindrical symmetry to long-bones, the Bone Density Software Module is able to estimate bone density from 2D X-ray images generating results reportedly comparable to dual-energy X-ray absorptiometry (DEXA) and microCT methodologies (Vizard *et al.*, 2010; Sasser *et al.*, 2012).

Accurate bone density measurement of long-bones relies on sufficient surrounding tissue being present, however insufficient tissue remained after dissection of legs from 3-week aged mice. Bone density was measured in the femurs of 12-week aged AB1-KO, B2C-KO and DKO mice using the Bone Density Software Module from three ROIs in the middle of the bone. For AB1-KO, B2C-KO and DKO mice there was no significant difference in bone density compared with littermate controls (Figure 5.23A). Bone radius measurements are also generated from bone modelling. Similarly to bone density, there was no significant difference in femur radius for AB1-KO, B2C-KO and DKO mice compared with littermate controls (Figure 5.23B).

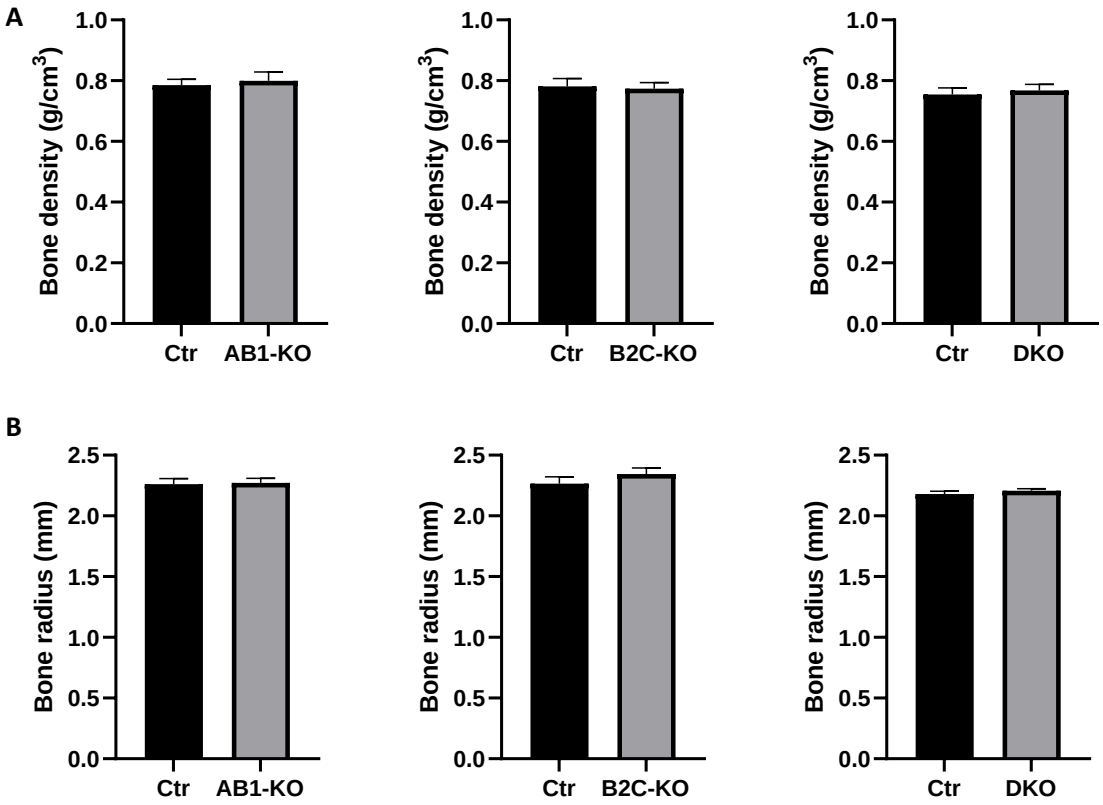

Figure 5.23. Bone density and radius of miRNA-29 knockout mice. *Bone density (A) and radius (B) was measured in femurs from AB1-KO, B2C-KO, DKO and littermate control mice aged 12-weeks using the Bruker Bone Density Software Module. AB1-KO n ≥ 14, B2C-KO n ≥ 12, DKO n ≥ 17. Data presented as mean ± SEM.*

5.2.5 Histological analysis of microRNA-29 knockout mice

Legs from 3-week aged AB1-KO (19 in total), B2C-KO (13 in total) and DKO (17 in total) mice were harvested with the aim of sectioning in the sagittal plane and staining with Safranin O and Fast Green in order to assess growth plate development. Given that AB1-KO, B2C-KO and DKO mice demonstrated significantly shorter femurs at 3-months of age, it was plausible that dysregulation within the growth plate during development was a contributing factor.

Harvested legs were fixed in 10% NBF before being stored in 70% ethanol. Colleagues at Newcastle University had significant expertise and experience in histological processing of mouse legs in addition to having access to automated tissue processing and slide imaging facilities. In light of this, our collaborators kindly volunteered to perform histological analyses on AB1-KO (19 in total), B2C-KO (13 in total) and DKO (17 in total) 3-week aged mice in addition to DKO 3-month mice (20 in total). Unfortunately, a combination of difficulties associated with the COVID-19 pandemic and personal circumstances conspired to prevent the processing and analysis of these samples being completed by colleagues at Newcastle University. For DKO 3-month aged mice, one knockout and one control sample were processed at UEA and four slides from each analysed, however clearly any differences between these samples will require validation with more samples.

It is hoped that histological analysis of growth plates in 3-week aged AB1-KO, B2C-KO and DKO mice along with joint and growth plate structure in 3-month aged DKO mice will shed light on the processes contributing the reduced weight and femur length observed in miR-29 knockout mice. Unfortunately, these analyses are now beyond the scope of this project, however the aim is to publish and disseminate the findings of these experiments once they are completed.

5.2.5.1 Histological analysis of 3-month aged joints

5.2.5.1.1 Optimisation of decalcification protocol

Typically, mouse legs are decalcified using EDTA or formic acid (Glasson *et al.*, 2010). Whilst EDTA decalcification is optimal for preserving antigenicity, decalcification with formic acid is vastly less time consuming with incubation times measured in hours compared to days and weeks for EDTA (H. Liu *et al.*, 2017).

Legs from 3-month aged mice were decalcified using 14% EDTA for 14 days or 10% formic acid for 48 hours before sectioning and staining for Safranin O and fast green. Compared to legs decalcified with formic acid, Safranin O staining in EDTA decalcified samples was less intense, less consistent and appeared washed out, particularly in the tibial growth plate (Figure 5.24). Given more consistent staining performance and significantly reduced incubation time, formic acid was selected as the decalcification method for 3-month aged joints.

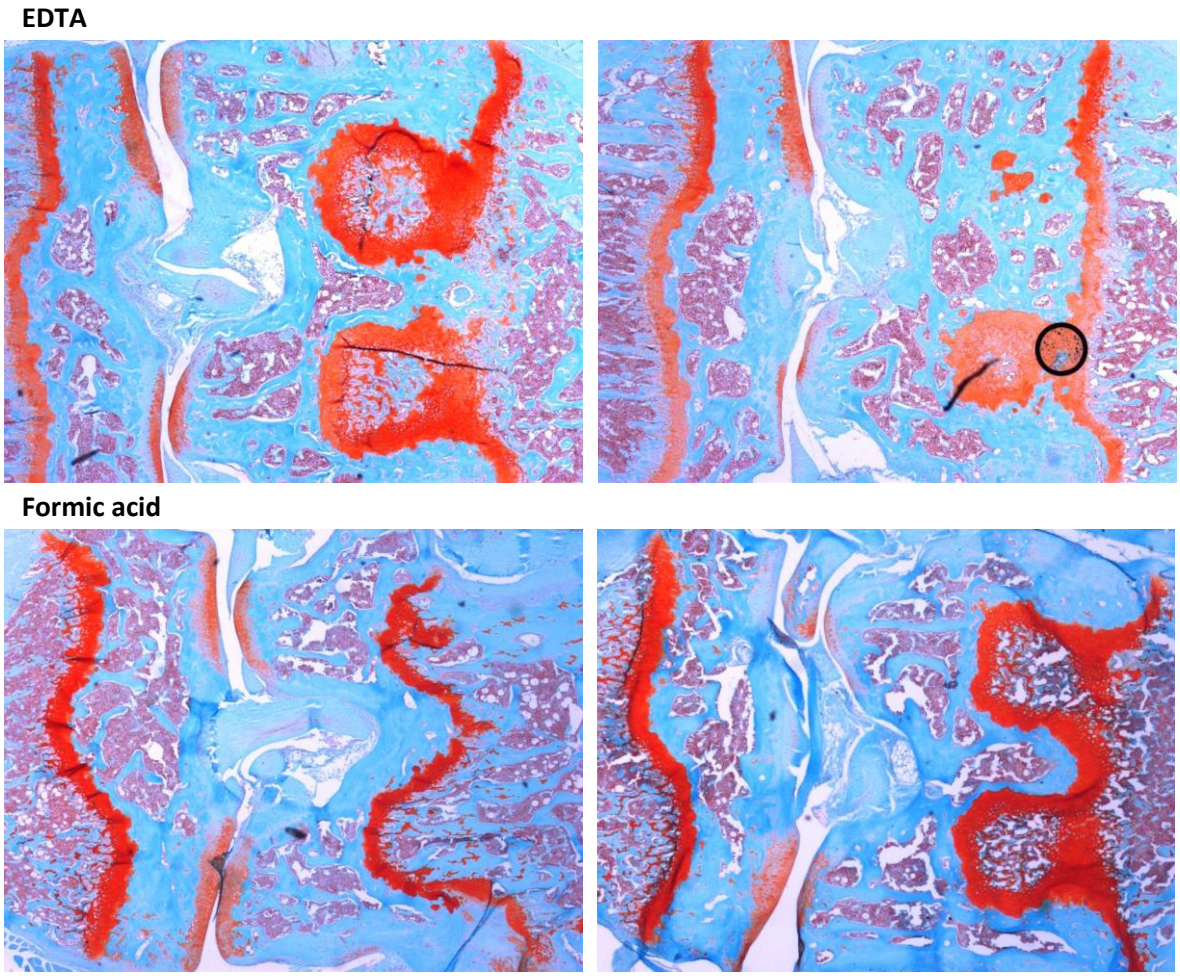

Figure 5.24. Decalcification of 3-month aged mouse legs. *Legs were harvested from 3-month aged mice and fixed in 10% NBF for 24 hours prior decalcification using with 14% EDTA for 14 days or 10% formic acid for 48 hours. Legs were sectioned at 5 µm, stained with Safranin O and Fast Green, and imaged at 5x magnification. Representative images presented, n = 2.*

5.2.5.1.2 Analysis of articular surfaces

In order to investigate the effect of miR-29 knockout on osteoarthritis, the articular surfaces of 3-month aged AB1-KO, B2C-KO and DKO were compared. Sections at comparable locations within the knee joint - as judged by the appearance of the femoral condyles - were selected for analysis. Visibly, no overt differences were observable in the articular surface integrity, size or Safranin O staining intensity for AB1-KO and B2C-KO samples compared with controls whereas DKO samples appeared to show reduced Safranin O staining (Figure 5.25).

To further investigate potential differences between miR-29 knockout and control articular surfaces Safranin O staining intensity, articular surface area and articular cartilage depth were measured using QuPath. For AB1-KO and B2C-KO samples, no significant differences were measured in Safranin O staining, articular surface area or articular cartilage depth (Figure 5.26). For DKO samples, little difference was seen in articular

surface area or cartilage depth. A reduction of 38% was seen in Safranin O staining intensity in DKO compared to control however standard deviation was high and more samples would need to be analysed to verify this difference.

Clustering of chondrocytes is a hallmark of OA with increased numbers and sizes of clusters of chondrocytes present in OA cartilage (Lotz *et al.*, 2010). With this in mind, cell number, size and organisation were assessed in the articular cartilage of 3-month aged AB1-KO, B2C-KO and DKO mice. No significant difference in cell number or average cell area was observed between AB1-KO, B2C-KO and DKO, and control articular cartilage (Figure 5.27A and Figure 5.27B). To assess whether cells were more likely to cluster, Delaunay cluster analysis was used to measure the average number of cells within 10 µm of each detected cell. No significant differences cell count, cell area or cell clustering were observed in any of the miR-29 knockout mice compared with controls (Figure 5.27C).

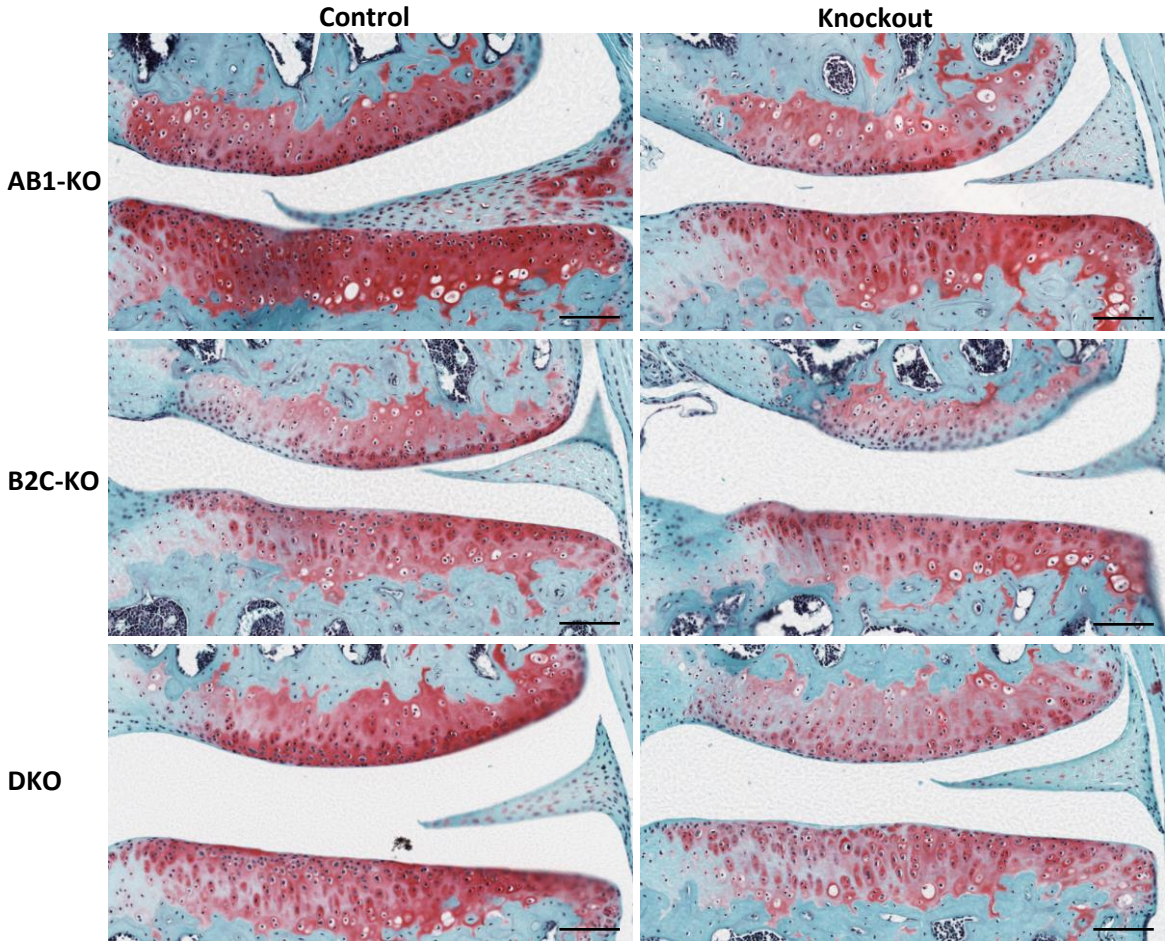

Figure 5.25. Histological analysis of miRNA-29 knockout articular cartilage. *Knee joints from AB1-KO, B2C-KO, DKO and littermate control mice were decalcified in 10% (v/v) formic acid prior to tissue processing, embedding in paraffin wax and coronal sectioning at 5 µm. Sections were stained with Safranin O, Fast Green and haematoxylin and imaged at 15x magnification. Representative images of lateral femoral and tibial condyles. Scale bar, 100 µm.*

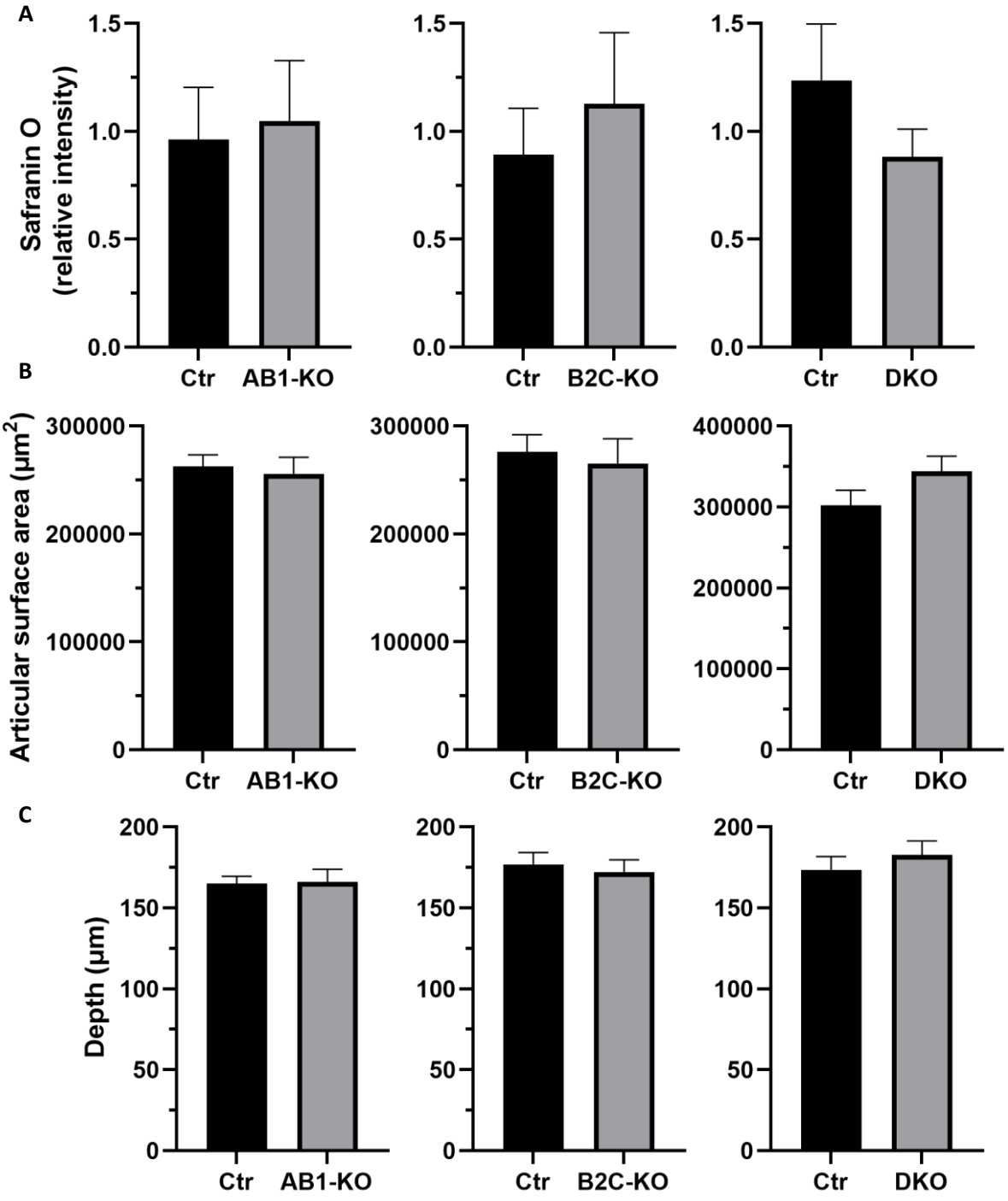

Figure 5.26. Quantification miRNA-29 knockout articular cartilage histological analysis. *Safranin O staining intensity (A), articular surface area (B) and articular cartilage depth (C) were measured in knee articular cartilage from AB1-KO, B2C-KO and DKO mice. For Safranin O staining relative intensity was normalised within staining batches to account for variations in staining. Articular cartilage depth was measured as the minimum Feret (or caliper) diameter of the selected articular surface. For AB1-KO and B2C-KO n ≥ 8 and n ≥ 6 respectively, data presented as mean ± SEM. For DKO n = 1, data presented as mean ± SD of 4 slides.*

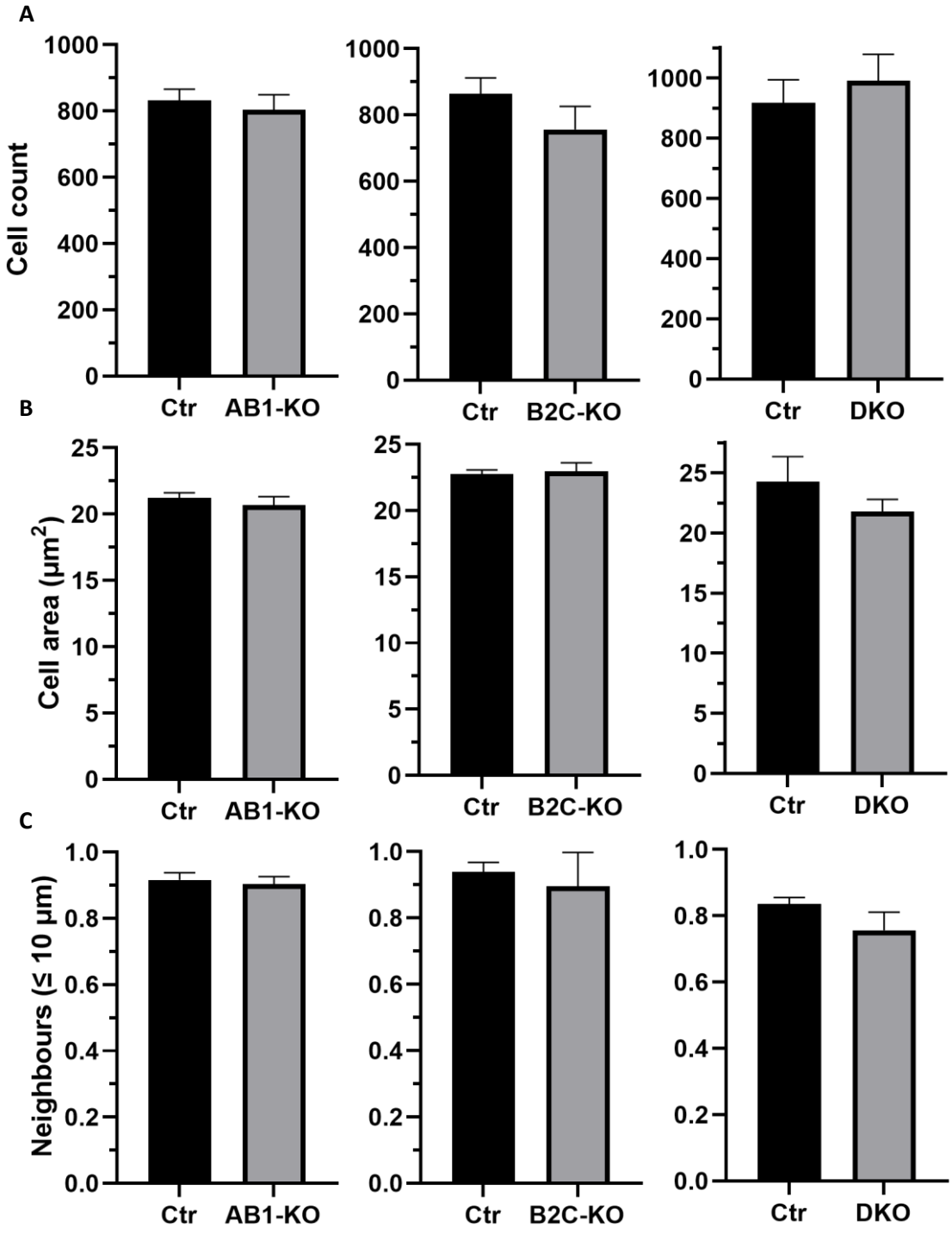

Figure 5.27. MiRNA-29 knockout articular cartilage chondrocyte analysis. *Cell count (A), cell area (B) and number of neighbouring cells (C) were measured in knee articular cartilage from AB1-KO, B2C-KO and DKO mice. For cell counts the total number of cells across the 4 articular surfaces was measured. The number of neighbouring cells for each detected cell was calculated using Delaunay cluster analysis with a neighbouring cell being within 10 µm. For AB1-KO and B2C-KO n ≥ 8 and n ≥ 6 respectively, data presented as mean ± SEM. For DKO n = 1, data presented as mean ± SD of 4 slides.*

5.2.5.1.3 Automating growth plate selection

Legs from 3-month aged AB1-KO, B2C-KO and DKO mice were harvested and decalcified using 10% formic acid for 48 hours prior to tissue processing. Legs were sectioned in the coronal plane and stained with Safranin O, Fast Green and haematoxylin. Whole slide images were analysed using the open source QuPath software package (Bankhead *et al.*, 2017) which facilitated the generation of automated scripts for batch processing of microscope images. For tibial growth plate (TGP) measurements, control images were used to train a pixel classifier (PC) to recognise and select TGPs in experimental images. Once trained, the growth plate PC was able to select regions of interest reliably and automatically around growth plates for further analysis (Figure 5.28A). Moreover, because the PC was blind to the genotype of samples, growth plate selection was less likely to be biased.

To validate to this approach, TGP from four AB1-KO and control mice were selected manually or using the trained pixel classifier from six slides, each containing four sections, representing 24 sections per sample and totalling 96 sections for AB1-KO and control groups. Visibly, manual and PC growth plate selections were comparable (Figure 5.28A). The area of manual growth plate selections showed a strong significant positive correlation with PC selections ($p < 0.0001$) (Figure 5.28B) and the difference between normalised areas was not significantly different from 0 (one sample t-test).

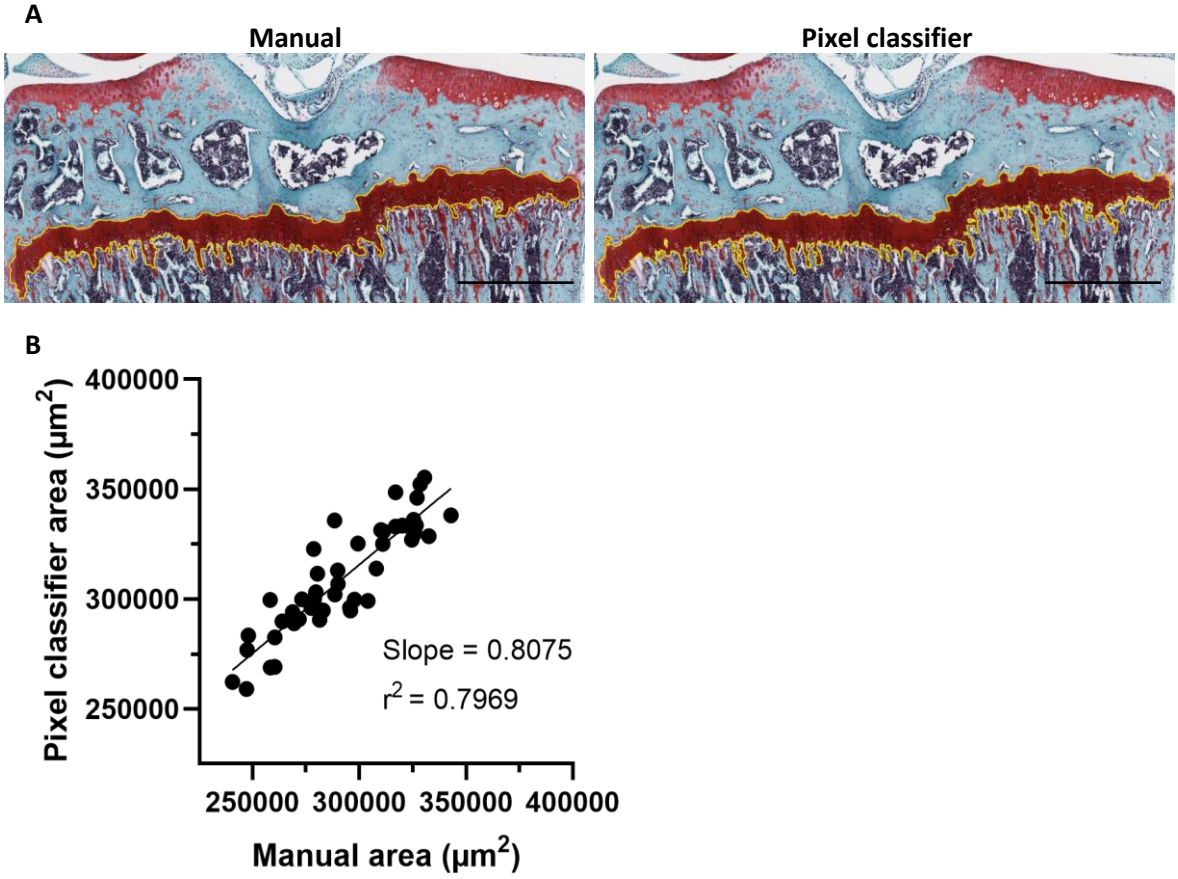

Figure 5.28. Tibial growth pixel classifier optimisation. *(A) Using QuPath, tibial growth plates in Safranin O, Fast Green and haematoxylin stained 3-month aged AB1-KO knee sections (n = 96) were selected manually or using a trained pixel classifier. Representative images shown, scale bar 500 µm. (B) Mean growth plate area per slide was compared in manual and pixel classifier selected growth plate selections and strong positive correlation was observed (r^2 = 0.7969).*

5.2.5.2 Analysis of growth plates

At 3-months of age, AB1-KO and DKO mice weighed significantly less and AB1-KO, B2C-KO and DKO mice had significantly shorter femurs than littermate controls. Multiple studies have found that growth plate disorganisation can lead to the development of shorter long bones (Karaplis *et al.*, 1994; Akiyama *et al.*, 2004; Später *et al.*, 2006). To assess whether this might be the case in miR-29 knockout mice, tibial growth plates in AB1-KO, B2C-KO and DKO were analysed.

As discussed in section 5.2.4.1.3, regions of interest around tibial growth plates in AB1-KO, B2C-KO and DKO mice were selected using a trained pixel classifier in QuPath. Visibly, no overt differences were observed in the growth plates of AB1-KO, B2C-KO and DKO mice (Figure 5.29). To further investigate whether there was any difference in the growth plates of miR-29 knockout mice at 3 months, Safranin O intensity, total area and depth were measured. For Safranin O intensity and growth plate area there was no significant difference between miR-29 knockout and control mice (Figure 5.30A and Figure 5.30B). However, AB1-KO mice had significantly deeper tibial growth plates compared with controls (Figure 5.30C). Moreover, DKO mice also appeared to have deeper tibial growth plates on average, although this would need to be verified in more samples.

To assess cellular organisation within the tibial growth plate cell number, size and organisation were assessed. No significant differences were found in miR-29 knockout mice for cell area or number of neighbouring cells based on Delaunay cluster analysis (Figure 5.31B and Figure 5.31C). Whilst no significant difference in cell count was seen in AB1-KO and B2C-KO mice, DKO mice had on average ~20% few cells when compared to controls (Figure 5.31A). As before, due to DKO samples only representing one animal per group this would require verification with more samples.

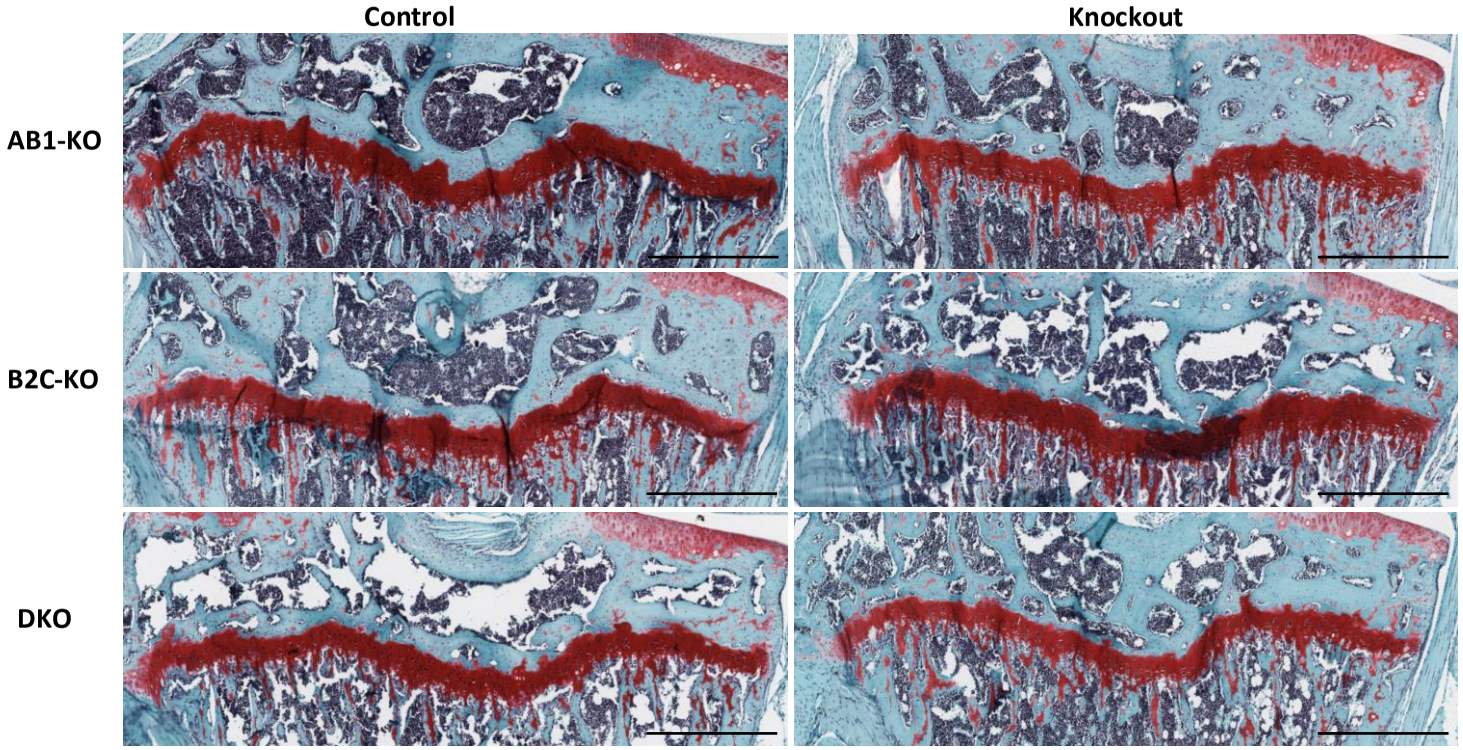

Figure 5.29. Histological analysis of miRNA-29 knockout tibial growth plate. *Knee joints from AB1-KO, B2C-KO, DKO and littermate control mice were decalcified in 10% (v/v) formic acid prior to tissue processing, embedding in paraffin wax and coronal sectioning at 5 µm. Sections were stained with Safranin O, Fast Green and haematoxylin and imaged at 15x magnification. Representative images of tibial growth plates. Scale bar, 500 µm.*

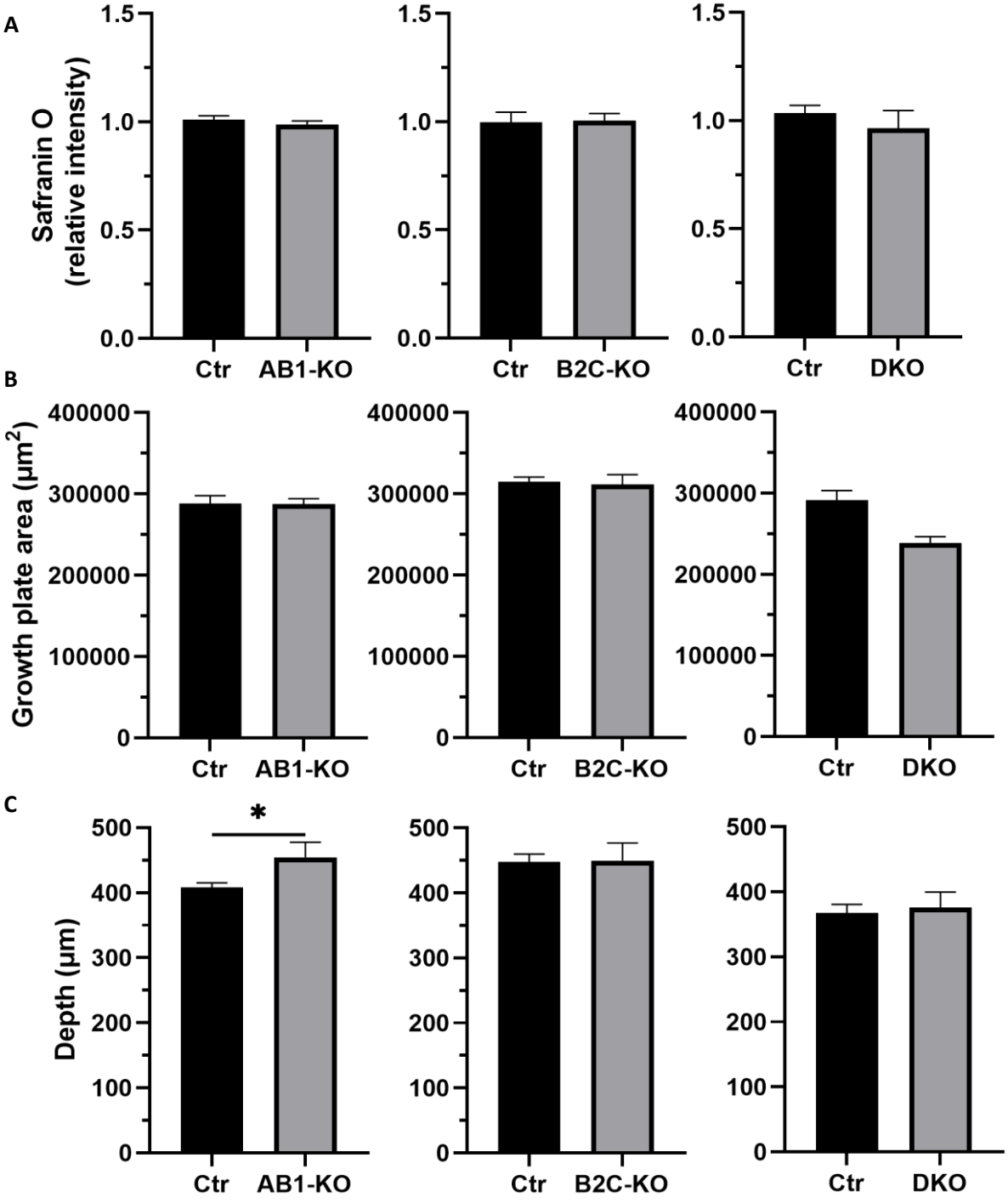

Figure 5.30. Quantification of miRNA-29 knockout tibial growth plate histological analysis. *Safranin O staining intensity (A), tibial growth plate area (B) and tibial growth plate depth (C) were measured in knee articular cartilage from AB1-KO, B2C-KO and DKO mice. For Safranin O staining relative intensity was normalised within staining batches to account for variations in staining. Growth plate depth was measured as the minimum Feret (or caliper) diameter of the selected growth plate. For AB1-KO and B2C-KO n ≥ 8 and n ≥ 6 respectively, data presented as mean ± SEM. For DKO n = 1, data presented as mean ± SD of 4 slides.*

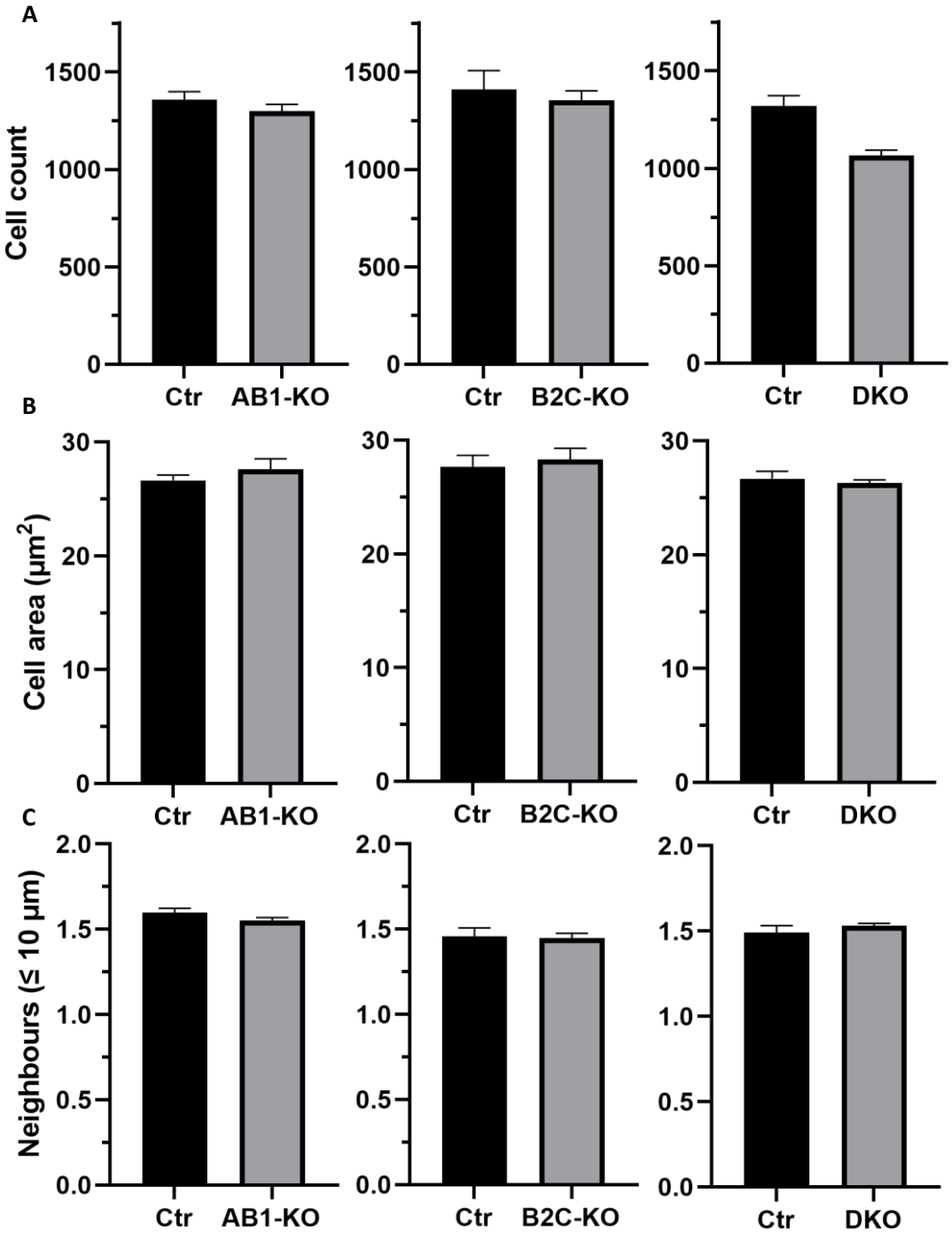

Figure 5.31. MiRNA-29 knockout tibial growth plate chondrocyte analysis. *Cell count (A), cell area (B) and number of neighbouring cells (C) were measured in tibial growth plates from AB1-KO, B2C-KO and DKO mice. The number of neighbouring cells for each detected cell was calculated using Delaunay cluster analysis with a neighbouring cell being within 10 µm. For AB1-KO and B2C-KO n ≥ 8 and n ≥ 6 respectively, data presented as mean ± SEM. For DKO n = 1, data presented as mean ± SD of 4 slides.*

5.2.5.3 Destabilisation of the medial meniscus

To evaluate the effect of miR-29 knockout on OA progression, the aim was to perform DMM and sham surgery on 12-week aged DKO and control mice and compare OA severity across these groups. However, several issues severely limited the number of animals available for DMM surgery. Due to the COVID-19 pandemic, all mouse colonies had to vastly reduced in order to allow for the maintenance of lines during the initial lockdown period by technical staff. In addition, the excessive grooming phenotype described in section 5.2.3 conspired further to limit the number of animals available for OA modelling.

Firstly, the eventual need to cull excessively grooming animals around 18 weeks of age greatly limited the breeding capacity of the DKO colony and thus the ability to increase the size of the colony. Secondly, DMM surgery is typically performed on mice aged 10 to 12 weeks of age with harvesting of legs for histological analysis at 6 to 10 weeks post-surgery (Blease *et al.*, 2018). Therefore, because of the excessive grooming phenotype, animals were unlikely to survive the full length of the DMM experiment before needing to be culled. Indeed, several animals designated for DMM surgery had to be culled before this could take place and several more required culling prior to completion of the experiment. In light of the above limitations, DMM experiments were only completed on one DKO and two control animals with no sham surgery performed. Therefore, data from these experiments are unlikely to provide a full representation of the effect of miR-29 knockout in the DMM model. Nonetheless, histological analysis was performed on these animals with the aim of provisionally highlighting potential differences.

DMM surgery was performed on the right legs of one DKO and two littermate control animals aged 12 weeks (± 1 week), legs were harvested 10 weeks later, fixed and decalcified using 10% formic acid for 48 hours. Legs were then processed and sectioned as previously described (Figure 5.32). In lieu of sham controls, unoperated left legs were also processed and analysed. Whilst not controlling for any differences observed as a result of merely opening the joint capsule, analysis of unoperated legs would at least indicate if OA induction had been successful.

For DMM and unoperated legs, six sections per animal were analysed using the OARSI scoring system (Glasson *et al.*, 2010) to assess OA progression in the lateral femoral condyle (LFC), lateral tibial plateau (LTP), medial femoral condyle (MFC) and medial tibial plateau (MTP). For each section, the mean of score from two scorers was taken. Safranin O staining was broadly less intense than in other analyses (see section 5.2.5.1.2) suggesting staining may not have been as effective. Mean OARSI scores for all three animals across all four joint quadrants were higher in DMM operated legs compared to

unoperated controls indicating that surgery had successfully induced some OA-like changes (Figure 5.33). When comparing OARSI scores between DKO and control DMM operated legs, mean scores were higher for DKO sections in all fout joint quadrants however standard deviation was also high (Figure 5.33). Whilst potentially indicating that miR-29 knockout may have a negative effect on OA progression, experiments would need to be performed using more animals to confirm this.

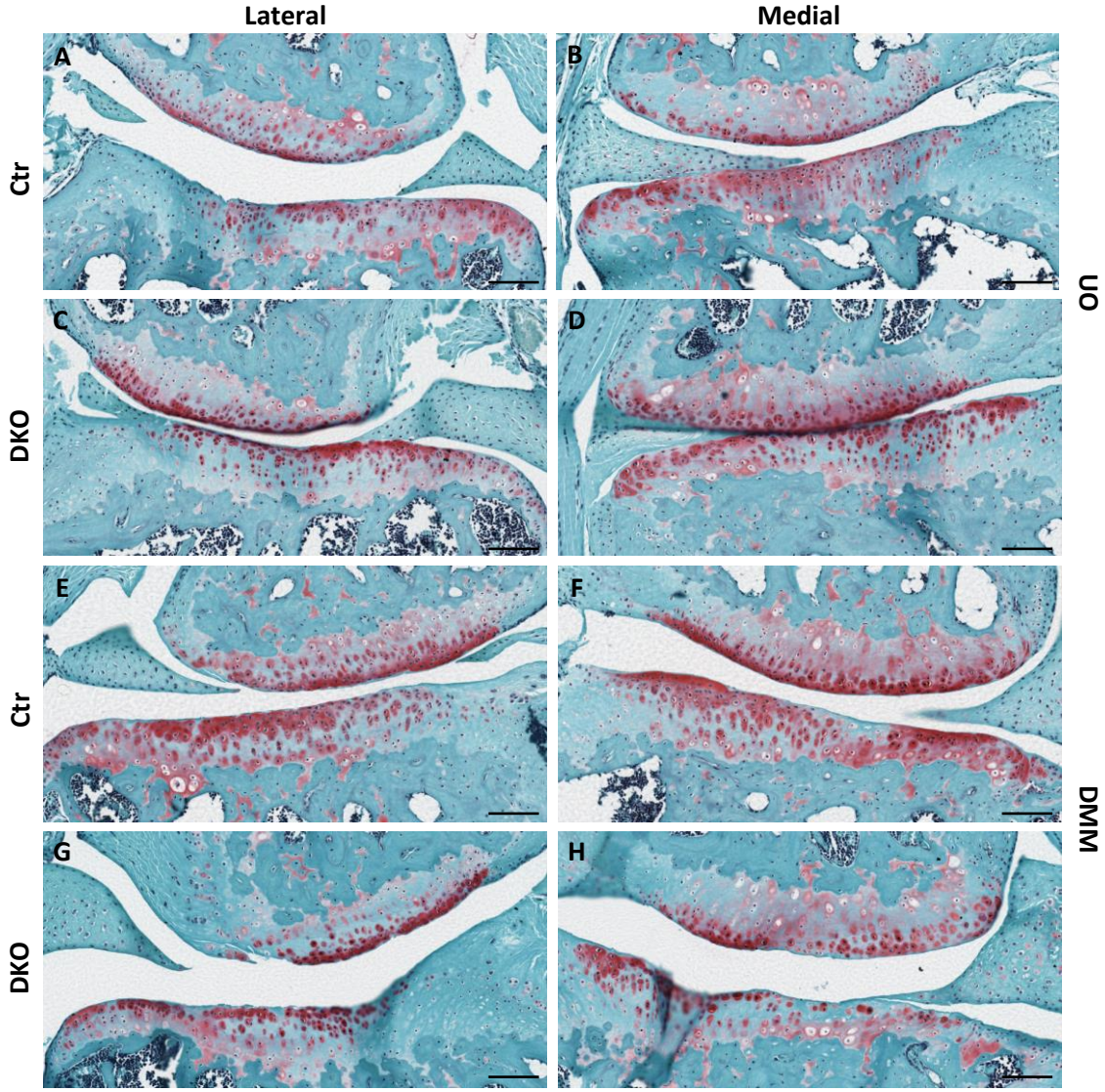

Figure 5.32. Histological analysis of miRNA-29 knockout DMM surgery. *DMM surgery was performed on 1 DKO and 2 control mice. DMM and unoperated (UO) were sectioned and stained with Safranin O, Fast Green and haematoxylin and imaged at 15x magnification. Representative images of femoral condyle (top) and tibial plateau (bottom) shown. OA-like damage was assessed using the OARSI scoring system. First score is femoral condyle, second score is tibial plateau; (A) 0, 1; (B) 0.5, 0; (C) 0, 0.5; (D) 0, 1; (E) 1, 1; (F) 0, 0.5; (G) 0.5, 1; (H) 2, 0.5. Scale bar, 100 µm.*

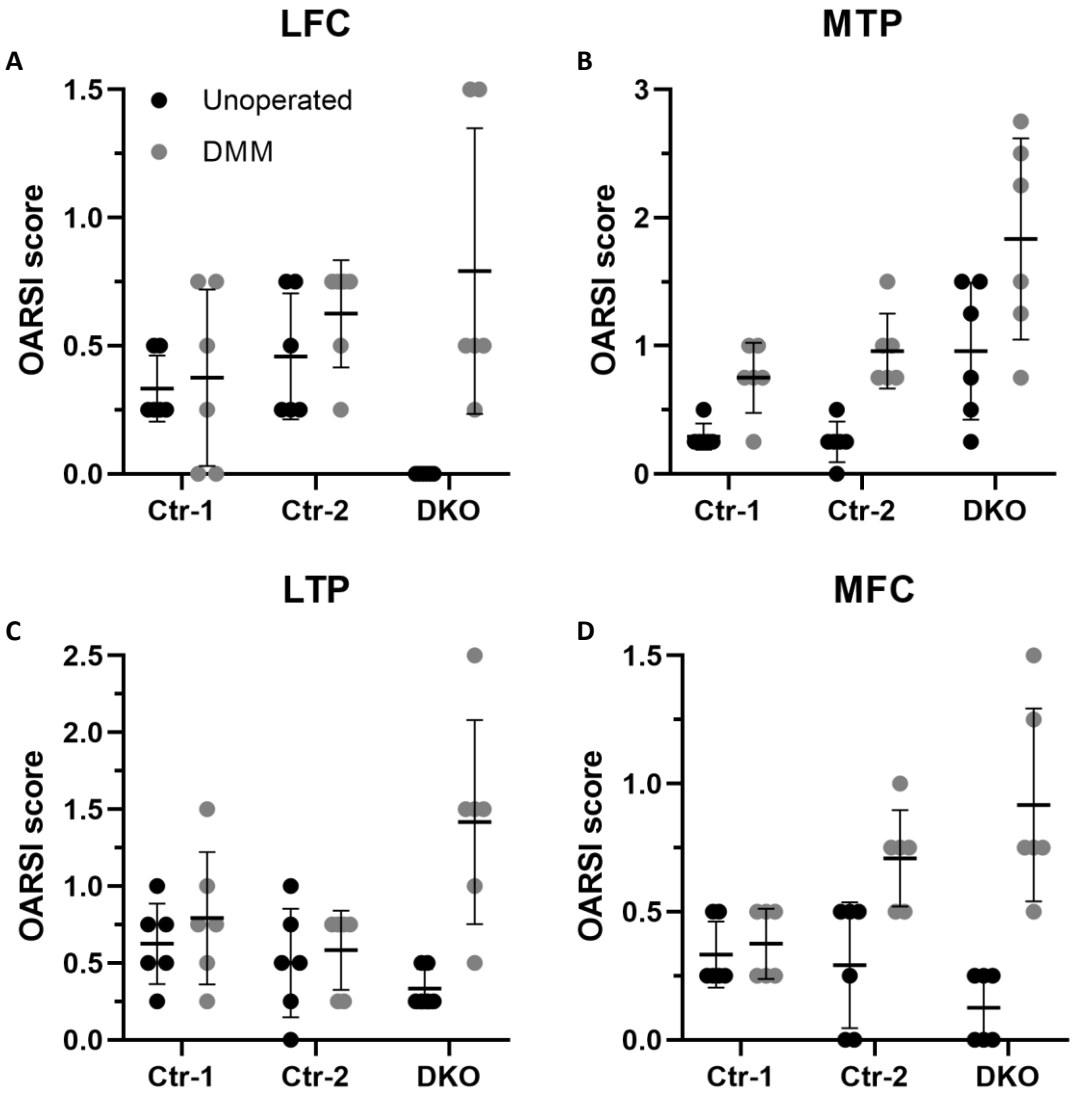

Figure 5.33. OARSI scoring of DKO DMM joints. *Histological sections from DMM operated and unoperated legs taken from 1 DKO and 2 control (Ctr) mice were analysed using OARSI scoring. Scoring was performed across 6 sections for the lateral femoral condyle (LFC) (A), medial tibial plateau (MTP) (B), lateral tibial plateau (LTP) (C) and medial femoral condyle (MFC) (D) quadrants. Mean score from 2 scorers was taken. Data presented as mean ± SD.*

5.3 Discussion

In previous chapters the role of miR-29 in cartilage and OA was investigated in the SW1353 cell line and primary human chondrocytes. To further explore the importance of the miR-29 family in cartilage development and OA pathogenesis, miR-29 knockout mouse models were generated, and the effect of this knockout was studied.

Whilst the initial plan was to use the *acan-creERT2* mouse to facilitate cartilage-specific and inducible miR-29 knockout, subsequent communication with Prof. George Bou-Gharios (also see Kanakis *et al.*, 2021) suggested this may not be the most effective system to use. In light of this, an alternative breeding scheme utilising the *col2a1-cre* mouse (Sakai *et al.*, 2001) was pursued. The breeding scheme was successfully carried out and mice possessing cartilage-specific knockout of *miR-29ab1* (AB1-KO), *miR-29b2c* (B2C-KO), and both loci together (DKO) were generated.

MiR-29 knockout mice were born healthy and demonstrated no obvious differences compared to littermate controls. Although some studies have found no difference in the birth rate of miR-29 knockout mice (Cushing *et al.*, 2015; Dooley *et al.*, 2016; Swahari *et al.*, 2021) others have reported global knockout birth rates as low as 1% and birth rates for *miR-29ab1* deficient mice of 10% (Kauffman *et al.*, 2015; Sassi *et al.*, 2017). Cartilage-specific knockout of miR-29 resulted in a significant reduction in birth rate for AB1-KO and DKO compared to littermate controls (44% and 39% respectively) whereas B2C-KO mice were born at increased rate. Increased birth rate in *miR-29b2c* deficient mice has not been shown previously whereas the phenotype of *miR-29ab1* deficiency is exacerbated by simultaneous loss of *miR-29b2c* (Dooley *et al.*, 2016; Caravia *et al.*, 2018).

To confirm knockout of miR-29 in articular cartilage, expression of miR-29a, miR-29b and miR-29c was measured in hip cartilage from 3-week-old knockout mice. Quantification of miR-29 in AB1-KO mice found that contrary to the manufacturer's claims, these assays were not able to discriminate between miR-29a and miR-29c. Therefore, qRT-PCR assays were designed to measure the expression of *miR-29a*, *miR-29b1*, *miR-29b2* and *miR-29c* primary transcripts. Along with DNA sequencing data, analysis of miR-29 primary transcript expression confirmed reduced expression of *miR-29a* and *miR-29b1* in AB1-KO cartilage, *miR-29b2* and *miR-29c* in B2C-KO cartilage, and all four primary transcripts in DKO cartilage.

Given that miR-29 was found to regulate the expression of several ADAMTSs along with genes involved in DNA methylation, the transcriptome of hip cartilage from 3-week-old DKO mice was analysed using mRNA-seq. Expression of the bone marker *Trap* was significantly lower in harvested cartilage compared to femoral bone, whereas expression of the cartilage

markers *Acan* and *Col2a1* was significantly higher indicating that harvested cartilage tissue was largely free of contaminating bone. Initial analysis of mRNA-seq data using PCA identified two DKO samples which clustered with control samples (DKO-4 and DKO-5) and two which clustered separately (DKO-2 and DKO-6). Further analysis including DKO-4 and DKO-5 only identified 60 DE genes whereas analysis excluding these samples identified 1324. To maximise the number of targets identified, DKO-4 and DKO-5 were excluded from further analyses. Identified targets would require future validation using qRT-PCR however this strategy avoided missing potentially important interactions.

GO analysis of significantly upregulated genes ($q \leq 0.05$) found enrichment for 845 terms. Enriched GO terms included extracellular matrix, extracellular matrix binding and collagen-containing extracellular matrix. Within these ontologies, upregulated genes included several MMPs and ADAMTs. *Mmp13* and *Mmp9* were upregulated in DKO cartilage and *MMP13* is considered the primary collagenase in OA (Troeberg *et al.*, 2012) with overexpression inducing OA-like cartilage damage in mice (Neuhold *et al.*, 2001). Although *Mmp13* is not a predicted target of miR-29, it was found to be downregulated in the synovial tissue of miR-29a overexpressing mice (Ko *et al.*, 2017). *MMP9* has been shown to be upregulated in OA, however its role in OA is less well understood (Zeng *et al.*, 2015).

Data in previous chapters suggested miR-29 may regulate members of the ADAMTS family. Analysis of mRNA-seq data from DKO hip cartilage identified significant DE of *Adamts2*, *Adamts3*, *Adamts4*, *Adamts6* and *Adamts10*. *Adamts12* was the most convincing miR-29 target in previous chapters however expression was not significantly regulated in DKO hip cartilage. Significantly, whilst experiments suggesting miR-29 targeting of *ADAMTS12* were conducted in human cells, mRNA-seq was performed on murine cells. Therefore, this apparent discrepancy may be explained sequence differences or alternative splicing of *ADAMTS12* between humans and mice. Future experiments could utilise luciferase assays to clarify if miR-29 is able to directly target the 3'-UTR of murine *ADAMTS12*.

Adamts3 expression was significantly downregulated in DKO hip cartilage consistent with *Adamts3* not being a predicted miR-29 target. On the other hand, *Adamts2* was upregulated in DKO cartilage, consistent with miR-29b negatively regulating expression in SW1353 cells and targeting its 3'UTR in luciferase assays. Expression of *Adamts4* was also upregulated in DKO cartilage, however distant hierarchical clustering from *Adamts2* suggested regulation may occur via a different mechanism.

ADAMTS4 is not predicted to be a miR-29 target but is known to be upregulated by hypomethylation of specific CpGs within its promoter (Roach *et al.*, 2005; Cheung *et al.*, 2008). The *de novo* DNA methyltransferases *DNMT3A* and *DNMT3B* are directly targeted

by miR-29b (Garzon *et al.*, 2009) however in this case, miR-29 knockout would be expected to increase *ADAMTS4* promoter methylation. Moreover, neither *Dnmt3a* nor *Dnmt3b* were differentially expressed in DKO cartilage. Regulation of *ADAMTS4* by miR-29 may not be so straightforward. For example, regulation of *DNMT1* by miR-29b was shown to function through targeting of the *DNMT1* transactivator *SP1* (Garzon *et al.*, 2009). Bisulfite PCR of the *Adamts4* promoter may elucidate the mechanism of regulation in DKO cartilage.

Upregulated genes in DKO cartilage were also enriched for cellular response to TGF-β stimulus and response to TGF-β ontologies. Specifically, *Tgfbr1* was significantly upregulated in response to miR-29 knockout consistent with the previously observed negative feedback loop (Le *et al.*, 2016). MiR-29 is not predicted to target *TGFBR1* however miR-29b has been shown to downregulate expression of *TGF-β1*, *TGF-β2* and *TGF-β3* in HEK293 and HTM cell lines (Luna *et al.*, 2011; Haidong Wang *et al.*, 2019). Therefore, miR-29 may modulate *TGFBR1* by regulating expression of its ligands (Yan *et al.*, 2017). Consistent with this hypothesis, *Tgf-β1*, *Tgf-β2* and *Tgf-β3* were all upregulated in mRNA-seq data from DKO cartilage however none statistically significantly. Additionally, congruent with the fibrotic role of TGF-β, *Col1a1* and *Col2a1* were also significantly upregulated in DKO hip cartilage.

Counterintuitively, knockout of miR-29 upregulated the expression of *Gm27019* (a predicted lncRNA directly upstream of *miR-29b1*) by more than 50-fold, with upregulation verified by qRT-PCR. Analysis of genomic sequencing data from DKO cartilage revealed that *loxP* recombination resulted in a 114 bp 3' deletion in the *Gm27019* gene. Removal of a negative regulatory site may explain upregulation of *Gm27019*. In fact, the 3' deleted region in *Gm27019* contains several predicted transcription factor binding sites as well as being a predicted target of miR-7684-3p. Recently, the lncRNA *NONMMUT055714* was found to act as a sponge for miR-7684-5p (Wei *et al.*, 2021), therefore miR-7684-3p may interact similarly with *Gm27019*. The role of *GM27019* is not well studied however one study found that expression of *GM27019* was reduced at days three and six during osteoblast differentiation (Khayal *et al.*, 2018). In comparison to global knockout of both miR-29 loci, cartilage-specific knockout mice survived past 6 weeks of age. Of note was the observation of repetitive grooming behaviour seen around 18 weeks of age, culminating in severe skin lesions and eventual culling of the animal. Initially, this phenotype was hypothesised to be a result of spontaneous ulcerative dermatitis, a syndrome often seen in aged C57BL/6 mice (Brayton, 2007). However, contrary to this hypothesis, observations of excessive grooming were confined to DKO mice with no instances seen in littermate controls. Recently, Swahari *et al.* (2021) reported ulcerative skin lesions as a result of excessive grooming in brain-specific (Nestin-Cre) miR-29 knockout mice at 20 days. Although *Col2a1* expression is

largely confined to chondrogenic tissues (Sakai *et al.*, 2001), transient expression has been also been shown in other tissues including the brain (Cheah *et al.*, 1991; Long *et al.*, 2001). In light of this, the observed excessive grooming phenotype may represent transient Cre expression in the brain, and thus mild but biologically significant knockdown of miR-29. Quantification of miR-29 expression in the brains of DKO mice would confirm this.

In-line with previous findings (Cushing *et al.*, 2015; Caravia *et al.*, 2018), AB1-KO and DKO mice weighed significantly less than littermate controls at 12 weeks with a greater difference seen in DKO mice. Global deficiency of the *miR-29ab1* locus has been found to reduce white adipose tissue (Dooley *et al.*, 2016; Caravia *et al.*, 2018) although no significant difference in relative inguinal fat weight was seen in AB1-KO or DKO mice. At 12-weeks old, AB1-KO, B2C-KO and DKO had significantly shorter femurs compared to controls suggesting a potential explanation for the observed weight difference. Multiple studies have reported retarded growth in miR-29 knockout mice (Cushing *et al.*, 2015; Sassi *et al.*, 2017; Swahari *et al.*, 2021) although none have investigated the length of long bones. No difference was seen in the width or bone density of femurs in 12-week-old mice. Analysis of mRNA-seq data however did reveal that upregulated genes were enriched for endochondral-related human phenotype ontologies including abnormal diaphysis morphology, osteopetrosis, abnormality of bone mineral density and tibial bowing. Future work looking at growth plate structure, particularly during earlier stages of skeletal development may elucidate the underlying cause of the shorter long bones seen in miR-29 knockout mice. Legs from 3-week aged miR-29 knockout mice have been harvested and are awaiting histological analyses by colleagues at Newcastle University. Findings from these analyses will be published once completed.

To assess the effect of miR-29 knockout on joint development, knees from AB1-KO, B2C-KO and DKO mice were analysed using histology. Knees from 3-week aged mice as well as more 12-week aged mice were harvested in anticipation of histological analyses being completed by colleagues at Newcastle University however the effects of the COVID-19 pandemic and personal challenges prohibited these analyses. Nonetheless, knees from 12-week aged AB1-KO and B2C-KO mice, along with one DKO and control mouse were processed, sectioned and stained with Safranin O, Fast Green and haematoxylin for histological analysis.

Histological analyses of the articular surfaces from AB1-KO and B2C-KO mice found no significant differences in Safranin O staining, articular surface area or cellular organisation. Safranin O staining was significantly reduced in the articular surfaces of the DKO mouse compared with the littermate control. Though, this finding would need to be verified in a larger sample size. These data are however consistent with the upregulation of *MMP13* and *ADAMTS4* seen in mRNA-seq data from DKO cartilage. Expression of *MMP13* and *ADAMTS4* is increased in OA cartilage (Reboul *et al.*, 1996; Naito *et al.*, 2007) whereas knockdown of *MMP13* and *ADAMTS4* has been shown to reduce cartilage degradation in a murine DMM model and human cartilage explants respectively (Song *et al.*, 2007; Little *et al.*, 2009).

The tibial growth plates of miR-29 knockout mice were also examined in histological sections. Using QuPath (Bankhead *et al.*, 2017) a pixel classifier was trained to reliably and accurately draw regions of interest around tibial growth plates allowing for automation and genotype-blind analysis of samples. Growth plate measurements generated from automated analyses correlated well with manual analyses and were not significantly different highlighting the utility such tools in histological analyses. No significant differences were seen in Safranin O staining, growth plate area or cellular organisation in AB1-KO and B2C-KO tibial growth plates. Growth plate depth was significantly increased in AB1-KO mice suggesting potential dysregulation however as no other differences were seen, further investigation is needed to clarify the cause of this. In DKO sections, growth plate area and cell count were notably reduced however again, further analyses would be needed to verify this finding.

Finally, to investigate the effect of miR-29 knockout on OA development, DMM surgery was performed on DKO mice to induce OA. Due to limiting factors on colony size caused by both the COVID-19 pandemic and the excessive grooming phenotype seen in aged DKO mice, DMM studies were only completed for one experimental and two control animals. Compared to unoperated knees, OARSI scores in DMM operated knees were higher across all four joint quadrants indicating the DMM successfully induced OA-like changes. When comparing DKO to littermate controls, OARSI scores were higher across all four joint quadrants, although standard deviation was also high suggesting aggravation of OA progression. Increased OA progression is consistent with the decreased Safranin O staining seen in the articular cartilage of aged mice, as well as the increased expression of *Mmp13* and *Adamts4* seen 3-week-old DKO hip cartilage. Whilst further experiments using more animals and performing sham surgery will be needed to verify these data, the initial finding that miR-29 knockout may worsen OA progression may inform future experiments.

The data in this chapter support the hypothesis that the miR-29 family plays an important role in cartilage development and OA pathogenesis. In hip cartilage, miR-29 knockout resulted in the DE of 1324 genes, many of which are implicated in cartilage development and OA. Furthermore, preliminary histological analyses of aged and DMM operated DKO knees suggested miR-29 knockout may significantly impact joint development and exacerbate OA development. It will be interesting to see if future work corroborates these findings.

Chapter 6

Discussion and future directions

6 Discussion and future directions

OA is a progressive and debilitating degenerative joint disease affecting an estimated 8.5 million people in the UK alone (Versus Arthritis, 2021). Despite this, therapeutic interventions are largely limited to pain killers in the short-term and joint replacement at the end point of the disease. The underlying factors leading to the development of OA pathogenesis are complex and often difficult to identify. However, OA is broadly characterised by an imbalance in cartilage anabolism and catabolism, ultimately leading to the loss of articular cartilage in synovial joints. Cartilage anabolism is driven through the synthesis of structural components including collagens and proteoglycans, whereas cartilage catabolism is mediated by ECM degrading enzymes such as those in the MMP and ADAMTSs families.

MiRNAs play a critical role in the regulation of gene expression and as such, dysregulation of miRNAs in OA is well documented, with many being differentially expressed in OA cartilage (Iliopoulos *et al.*, 2008; Jones *et al.*, 2009; Díaz-Prado *et al.*, 2012; Balaskas *et al.*, 2017). Previous work in our group highlighted the potential importance of the miR-29 family in OA. This project sought to further elucidate the role miR-29 in OA. In SW1353 cells and human primary chondrocytes regulation of the ADAMTS metalloproteinase family by miR-29 and TGF-β was investigated. MiR-29 is recognised a key epi-miRNA, therefore the effect of miR-29 overexpression on DNA methylation in chondrocytes was also explored. Finally, to study the role of miR-29 in cartilage and OA development, cartilage-specific miR-29 knockout models were generated, and the effect of miR-29 knockout analysed using mRNA-seq and histology.

6.1 Analysis of existing transcriptomic datasets

SkeletalVis (Soul *et al.*, 2019) was used to identify ADAMTSs, as well as genes involved with DNA methylation, which may be dysregulated in OA. SkeletalVis allows for the combined analysis of transcriptomics datasets with a consistent pipeline, facilitating comparisons across studies. In the studies analysed here, the proteoglycanases *ADAMTS1*, *ADAMTS4* and *ADAMTS5* were upregulated, consistent with the cartilage degradation seen in OA. The procollagen N-proteinase *ADAMTS2* was also upregulated potentially representing an attempt to repair damaged cartilage (C. Y.-Y. Yang *et al.*, 2017). No substantial differences were observed in the expression of DNA methylation related genes. Slight upregulation of *DNMT1* and *TET1* in OA was seen, however these differences are not reported in the literature. Data from DNA methylation studies is not currently available on SkeletalVis however this would be a useful addition. Moreover, the inclusion of

microRNA datasets would further improve the utility of this tool in identifying putative regulatory networks.

Analyses like these are easily performed with SkeletalVis and may be useful for identifying potentially important research avenues for wet-lab experiments. SkeletalVis is a valuable tool, allowing for the interrogation of gene expression changes across multiple existing transcriptomics datasets. Despite this, more fundamental differences in experimental design, such as the joint articular cartilage is harvested from, whether control samples are taken from the same or different patients, and the methodology used to measure gene expression still limit comparisons across studies.

6.2 MicroRNA-29 as an epi-miRNA in chondrocytes

DNA methylation is rapidly emerging as an important regulatory mechanism in chondrocytes and OA more broadly with distinct changes in global methylation being identified in OA (den Hollander *et al.*, 2014; Fernández-Tajes *et al.*, 2014; Jeffries *et al.*, 2014; Rushton *et al.*, 2014; Wu *et al.*, 2020). MiR-29 is known to regulate components of the DNA methylation machinery in many disease contexts and as such, is recognised as one of the major epi-miRNAs (Kwon *et al.*, 2018; Memari *et al.*, 2018). Specifically, by analysing the expression of miRNAs and mRNAs across more than 3000 tumours from 11 human cancers, Jacobsen *et al*. (2013) identified regulation of active DNA methylation pathways by the miR-29 family. Similarly, dysregulation of DNA methylation pathways was recently observed in a murine miR-29 knockout model (Swahari *et al.*, 2021) suggesting conservation of this regulatory pathway, at least between humans and mice. In light of this, the role of miR-29 in the regulation of DNA methylation in chondrocytes was explored.

All miR-29 family members were predicted to target genes involved in the regulation of DNA methylation. In HACs, overexpression of miR-29b-3p downregulated expression of *TDG* ($p = 0.055$), *DNMT3A* and *TET2*. Whilst *DNMT3A* is responsible for *de novo* methylation, *TET2* and *TDG* have roles in demethylation (Greenberg *et al.*, 2019). Expression of *DNMT3A* has been found to be upregulated in OA cartilage whereas expression of *TET2* appeared to be unregulated (Taylor *et al.*, 2014; Wu *et al.*, 2017). DE of *TDG* in OA has not been reported however miR-29a, miR-29b and miR-29c have been shown to directly regulate *TDG* in cancer cell lines (Morita *et al.*, 2013). More recently, expression of *miR-29b* and *DNMT3B* was found to be negatively correlated in OA chondrocytes with upregulation of *DNMT3B* being associated with increased methylation at a *miR-29b* promoter region (Dou *et al.*, 2020). However, despite the regulation of DNA methylation-related genes by miR-29 *in vitro*, mRNA-seq data failed to show any significant differences in the expression of these genes in DKO cartilage. This may represent a difference in the regulation of these genes

between humans and mice. It will be interesting to see if the same is seen with qRT-PCR analysis of these genes.

Reduced expression of *DNMT3A*, *TET2* and *TDG* in response to miR-29b overexpression would be expected to result global changes in DNA methylation. Analysis of global methylation in SW1353 cells indicated that miR-29b-3p overexpression significantly reduced 5-mC levels however methylation array and bisulfite PCR failed to replicate this observation. As previously discussed, this may represent the fact that SW1353 is a terminally differentiated chondrosarcoma cell line and thus, global methylation may already have been dramatically altered during oncogenic transformation. Moreover, miR-29 has been shown to regulate global levels of CH (but not CG) methylation (Swahari *et al.*, 2021). Further analysis of the methylation array data collected in this study may find that CH methylation was similarly regulated in response to miR-29b-3p overexpression in SW1353 cells.

Whilst these data suggest that miR-29 may plan an important role in regulating DNA methylation in chondrocytes and cartilage more broadly, future experiments should focus on using primary human chondrocytes and *in vivo* models to explore this relationship. Moreover, it would be interesting to see the effect of miR-29 knockout on global DNA methylation patterns in DKO cartilage as well as differentially expressed genes that are not directly targeted by miR-29.

6.3 General observations of microRNA-29 knockout mice

The breeding scheme to generate mice with cartilage-specific knockout of the *miR-29ab1* and *miR-29b2c* loci both independently, and simultaneously was successful. Cartilage-specific knockout of miR-29 was confirmed both at the genomic and mRNA level for respective mice. AB1-KO, B2C-KO and DKO mice were born apparently healthy and did not demonstrate any of the deleterious phenotypes previously shown in global miR-29 knockout mice, neither did they suffer from premature death (Cushing *et al.*, 2015; Dooley *et al.*, 2016; Caravia *et al.*, 2018).

The effect of miR-29 knockout on birth rates is inconclusive with differing reports, however in this study AB1-KO and DKO mice were born at significantly lower rates compared to littermate controls with DKO birth rates being lower than AB1-KO (Cushing *et al.*, 2015; Kauffman *et al.*, 2015; Dooley *et al.*, 2016; Sassi *et al.*, 2017; Swahari *et al.*, 2021). DKO mice demonstrated an excessive grooming phenotype which has been reported recently in brain-specific miR-29 knockout mice (Swahari *et al.*, 2021). Whilst in *col2a1-cre* mice, knockout is reported to be largely confined to chondrogenic tissues (Sakai *et al.*, 2001), expression has been reported in other tissues including in the brain (Cheah *et al.*, 1991;

Long *et al.*, 2001) suggesting subtle but biologically significant knockdown of miR-29 in the brains of DKO mice. With this in mind, future experiments should consider the use of an inducible system such as *col2a1-ERT2* (Chen *et al.*, 2007). Not only would this reduce problems associated with *col2a1* expression in the brain during development, but postnatal knockout of miR-29 may better represent the progressive changes in gene expression seen in OA disease development.

By 12 weeks of age AB1-KO and DKO mice weighed significantly less than littermate controls, again with this difference being more pronounced in DKO mice. Moreover, the femurs of AB1-KO, B2C-KO and DKO mice were significantly shorter however no differences were seen in femur width or bone density. Reduced femur length in other mouse models has been shown to result from growth plate disorganisation (Gualeni *et al.*, 2013; Hung *et al.*, 2019). Growth plates were analysed in histological sections from 12-week aged miR-29 knockout mice. Little difference was seen in the growth plates of miR-29 knockout mice compared to littermate controls, however in AB1-KO mice growth plate depth was significantly increased whereas growth plate area and cell count was reduced in DKO growth plates (n = 1).

GO analysis of upregulated genes in mRNA-seq data from 3-week aged DKO cartilage found enrichment of genes associated with abnormal diaphysis morphology and tibial bowing. Therefore, changes in gene expression with the potential to cause abnormal bone growth were detectable early in development and analysis of growth plates in younger mice may allude to the cause of the shorter femurs seen in miR-29 knockout mice. For example, expression of *Adamts10* was significantly reduced in DKO cartilage and 4-week aged *Adamts10* mutant mice were found to have shorter femurs as a result of shorter resting and expanded hypertrophic zones in the growth plate (Mularczyk *et al.*, 2018). As previously mentioned, legs from 3-week and more 12-week aged miR-29 knockout mice have been harvested and are awaiting analysis by colleagues at Newcastle University. It will be interesting to see if the observed changes in 12-week DKO growth plates persist with the analysis of a larger sample size. Furthermore, analysis of growth plate morphology and organisation in the growth plates of 3-week aged mice will hopefully elucidate the underlying cause of shorter femurs in miR-29 knockout mice.

6.4 MicroRNA-29 in cartilage

Our group has previously identified the miR-29 family as playing a potentially important role in OA. MiR-29a, miR-29b and miR-29c were upregulated in human OA cartilage as well as mouse models of OA and were shown to regulate the expression of genes associated with OA whilst being predicted to target many more (Le *et al.*, 2016). In this project, the role of miR-29 in cartilage and implicit implications for OA were further explored using *in vitro* and *in vivo* models.

MiR-29 was previously shown to negatively regulate the expression of *ADAMTS6*, *ADAMTS10*, *ADAMTS14* and *ADAMTS19* by directly targeting the 3'-UTRs of these genes (Le, 2015). In this study, whilst expression of *ADAMTS14* was downregulated by miR-29b-3p overexpression in SW1353 cells (n =1), expression of *ADAMTS10* and *ADAMTS14* was not regulated in HACs whereas expression of *ADAMTS19* was not reliably detected. This may represent the inherent heterogeneity of primary chondrocytes. In addition, whilst previous experiments used double-stranded RNA mimics, this study utilised LNA miRNA mimics which are designed to prevent activity in the passenger strand. In fact, whilst *ADAMTS6* is a predicted target of miR-29b-3p, miR-29b-1-5p is also predicted to target *ADAMTS6*. Therefore, differing responses to miR-29b overexpression may be due to differences in experimental approach.

Expression of *ADAMTS12* was downregulated in SW1353 cells and HACs in response to overexpression of miR-29b-3p. Additionally, miR-29b-3p significantly reduced luciferase activity in an *ADAMTS12* 3'-UTR reporter suggesting direct targeting. *ADAMTS12* was upregulated by 1.6-fold in mRNA-seq data from DKO hip cartilage but this was not significant. *ADAMTS12* is known to degrade COMP and is upregulated in OA (Liu *et al.*, 2006) and thus, targeting of *ADAMTS12* by miR-29 may represent an attempt to prevent cartilage degradation.

Consistent with a role for miR-29 in cartilage, GO analysis of upregulated genes in DKO cartilage found enrichment for extracellular matrix, extracellular matrix binding and collagen-containing extracellular matrix ontologies. Upregulated genes included *Adamts4* and *Mmp13*, metalloproteinases that are well-known for their roles in cartilage degradation during OA (Troeberg *et al.*, 2012). Expression of *Adamts2* was upregulated in mRNA-seq data whereas *Adamts3* was downregulated. Whilst expression of *ADAMTS2* was not reliably detected in miR-29b-3p transfected HACs, miR-29b-3p did negatively regulate *ADAMTS2* in SW1353s and in 3'-UTR in luciferase assays. On the other hand, *ADAMTS3* expression was not detected in SW1353 cells but expression was detected in HACs. *ADAMTS2* and *ADAMTS3* are both procollagen N-proteinases and upregulation in OA has

been suggested as an attempt to repair cartilage damage caused by OA (C. Y.-Y. Yang *et al.*, 2017). The primary substrates of these may allude further to their role in OA. Whilst ADAMTS2 activity is associated with type-1 collagen maturation in skin, bones, tendons and aorta, ADAMTS3 expression is higher in chondrocytes and is associated with type-2 collagen processing (Colige *et al.*, 1997; Fernandes *et al.*, 2001; Bekhouche *et al.*, 2015). Therefore, upregulation of ADAMTS2 may promote cartilage fibrosis by increased processing of type-1 collagen, with a concomitant reduction in type-2 collagen production due to downregulation of ADAMTS3. Similarly, *Adamts10* was also downregulated in DKO cartilage. While less is known about the role of *ADAMTS10* in cartilage, *ADAMTS10* has been shown to promote fibrillin-1 deposition in fibroblasts (Kutz *et al.*, 2011). Not only do fibrillins contribute to the elasticity of the ECM (Mithieux *et al.*, 2005), they have been found to regulate the bioavailability of TGF-β by binding to latent TGF-β protein complexes (Ramirez *et al.*, 2009). TGF-β1 also significantly upregulated *ADAMTS10* expression in HACs though, so where *ADAMTS10* fits in the miR-29-TGF-β regulatory network remains unclear.

GO analysis of mRNA-seq data from DKO cartilage found enrichment for upregulated genes associated with cellular response to TGF-β and response to TGF-β. Specifically, expression of *Tgfbr1* was upregulated by 2.4-fold, and expression of *Col1a1* and *Col1a2* was upregulated by 7.2 and 6.3-fold respectively. Increased TGF-β signalling is associated with the induction of fibrosis in synovial tissues and in articular cartilage (van Beuningen *et al.*, 1998; Scharstuhl *et al.*, 2003; Xue *et al.*, 2016). Increased type-1 collagen content in articular cartilage compromises structural integrity, increasing stiffness and decreasing durability (Rim *et al.*, 2020). Consistent with the simultaneous upregulation of *Tfgbr1*, *Col1a1* and *Col1a2* seen in DKO cartilage, TGF-β1 treatment has been shown to upregulate *COL1A1* expression in human and murine synovia (Remst *et al.*, 2014) whereas *SMAD7* overexpression inhibited TGF-β induced synovial fibrosis (Blaney Davidson *et al.*, 2006). In addition, *Mmp9* was upregulated in DKO cartilage and is known to activate latent TGF-β thus promoting TGF-β signalling (Yu *et al.*, 2000).

These data point to upregulation of TGF-β signalling and associated fibrosis in the cartilage of miR-29 knockout mice. In line with this, TGF-β1 stimulation of primary human chondrocytes significantly upregulated expression of *ADAMTS2* and *ADAMTS4* whereas expression of *ADAMTS3* was significantly downregulated. TGF-β1 stimulation resulted in a 30-fold increase in *ADAMTS14* expression whereas previous work in our group has found significant downregulation by miR-29b (Le, 2015). Little is known about the role of *ADAMTS14* in cartilage however it has been shown to cleave procollagen-1 suggesting it may contribute to fibrosis (Colige *et al.*, 2002). Nonetheless, *Adamts14* did not appear to

be significantly regulated in DKO cartilage. Overall, these data are consistent with previous data showing that miR-29 negatively regulates TGF-β signalling in chondrocytes (Le *et al.*, 2016). Congruent with the role of miR-29 knockout in tissue fibrosis suggested here, Dey *et al.* (2021) recently demonstrated that upregulation of TGF-β signalling as a result of pancreas-specific knockout of the *miR-29ab1* cluster contributed to fibrosis in acute pancreatitis.

In light of increased expression of profibrotic genes, along with enrichment of upregulated genes associated with TGF-β signalling, cartilage-specific knockout of miR-29 would be expected to lead to cartilage fibrosis and increased OA progression. Histological analysis of 12-week aged AB1-KO and B2C-KO knees found no significant difference in articular cartilage however Safranin O staining in DKO articular cartilage was reduced by 38%. Moreover, OARSI scoring of sections from DKO and control DMM knees indicated increased development OA-like damage. Whilst histological analyses of DKO knees were only completed for n = 1, these data suggest that miR-29 knockout may promote the development of OA via an increase in TGF-β induced fibrosis.

Future work will further seek to validate reduced staining and worse OA progression in DKO mice in a larger sample size. For DMM studies, sham operated controls also need to be included in analyses to ensure that any differences seen are not merely a result of opening the joint capsule. Finally, future DMM experiments will need to consider the excessive grooming phenotype seen in aged DKO mice. DMM surgery may be performed in younger mice to reduce the likelihood of this phenotype presenting during experiments. Alternatively, the use of an inducible *Cre-loxP* system may prevent unwanted knockout in the brain eliminating this phenotype all together.

In the model presented here (Figure 6.1), knockout of miR-29 aggravates OA progression through the upregulation of TGF-β signalling and concomitant development of fibrosis. On the other hand, overexpression of miR-29 may prevent cartilage fibrosis, thus protecting against OA. Specifically, downregulation of TGF-β signalling by miR-29 would inhibit upregulation of the profibrotic factors collagen I, ADAMTS2 and ADAMTS4 with a further contribution from the potential direct targeting of ADAMTS2. Moreover, targeting of MMP13 and MMP9 would protect against cartilage degradation. On the other hand, negative of regulation of TGF-β would be expected to increase ADAMTS3 expression and thus collagen II processing and ultimately cartilage repair. Therefore, augmentation of miR-29 in the joint may represent a promising OA therapy.

Recently, in a murine unilateral anterior crossbite model of temporomandibular OA, Sun *et al.* (2020) found intraarticular injection of an aptamer-agomiR-29b protected against

cartilage degradation, promoted expression of the anabolic genes *Col2a1* and *Acan*, and reduced expression of the anabolic genes *Mmp3* and *Mmp13* whereas aptamer-antagomiR-29b had the opposite effect. Moreover, overexpression of miR-29b using a bone marrow mesenchymal stem cell (BMSC)-specific aptamer specifically targeted agomiR-29b to BMSCs whilst having little effect on miR-29b levels in monocytes, macrophages or preosteoclasts demonstrating the potential of such a system in targeted miRNA-based therapies.

Not only does work by Sun *et al*. (2020) demonstrate beneficial regulation of OA-related pathways by miR-29, highly specific targeting of miR-29 overexpression to BMSCs demonstrates the potential to avoid off target effects of such a therapeutic strategy. This is pertinent given the neurological phenotype of miR-29 knockout mice observed in this study, and more severely by Swahari *et al.* (2021) with brain-specific knockout.

Speaking more broadly, miRNA therapeutics have attracted a lot attention in recent years. Specifically, their pleiotropic nature could enable the modulation of multiple targets or pathways within a disease process. Despite this promise, only a few miRNA-based therapies have made it to clinical trials thus far, with development of efficient administration routes, *in vivo* stability, and tissue and target specificity representing major challenges (Diener *et al.*, 2022). The importance of addressing these challenges is highlighted by the phase 1 study of a miR-34a mimic as potential solid tumour therapeutic in which four patient fatalities were observed as a result of immune-related adverse events (Hong *et al.*, 2020). Whether these immune responses were specific to miR-34a or a non-specific inflammatory effect is yet to be determined.

Traditional delivery methods for miRNA therapeutics include local or intravenous injection with inhalation being explored for respiratory diseases (Chow *et al.*, 2020). More recently, novel approaches such as continuous release from implanted 3D matrices have been explored (Diener *et al.*, 2022). Efficient delivery of therapeutic miRNAs to target tissues or cells can be achieved by various methods. Whereas liposomes were used in the aforementioned miR-34a study to facilitate intracellular delivery (Hong *et al.*, 2020), other delivery methods such as aptamer conjugates may facilitate more targeted delivery (Diener *et al.*, 2022). Aptamers are specifically designed nucleic acids capable of binding to molecular structures such as cell surface receptors and can therefore be targeted to specific cell types (J. Zhou *et al.*, 2017). As previously discussed, such approaches have been shown to facilitate highly target-specific delivery of miRNA therapeutics including for miR-29 (Sun *et al.*, 2020). Given the potential of miRNA-based therapies, and miR-29 specifically, it is exciting to see a miR-29 therapy currently in the stages of clinical development.

Local injection of TenoMiR (ClinicalTrials.gov Identifier: NCT04670289), a miR-29a mimic, has been found to improve tendon healing in murine and equine models of tendinopathy by downregulation of biomechanically inferior type-3 collagen (Millar *et al.*, 2015; Watts *et al.*, 2017). The use of TenoMir in the treatment of tennis elbow is currently being evaluated in a phase 1 clinical trial and if successful, may pave the way for the use of miR-29 mimics in other diseases. Based on the emerging role of miR-29 in mediating fibrosis in OA demonstrated in this project, local administration of a miR-29 mimic may slow or even reverse cartilage damage in patients with OA, slowing disease progression and potentially improving prognosis. Future experiments exploring the effects of intra-articular injection of miR-29 mimic in mouse models of OA will shed light on whether miR-29 augmentation may be efficacious treatment.

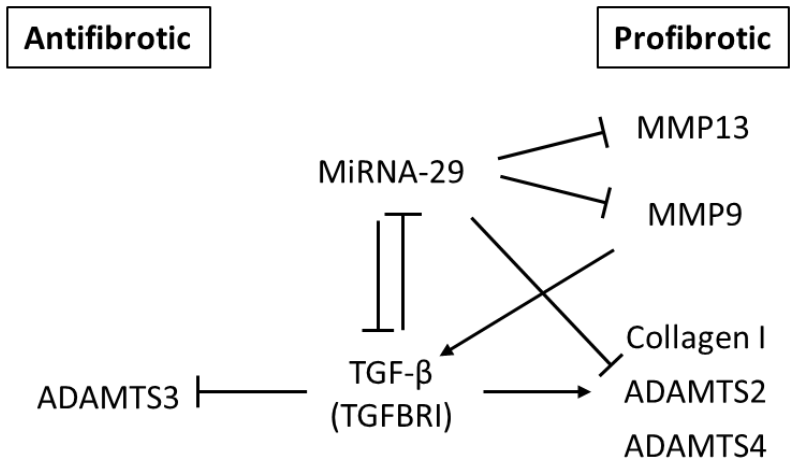

Figure 6.1. Model of the role of miRNA-29 in cartilage fibrosis. *Schematic of the proposed regulatory network in which miR-29 prevents cartilage fibrosis by negatively regulating TGF-β signalling, in part via MMP9, as well as reducing cartilage degradation through negative regulation of MMP13.*

References

Ahluwalia, J.K. *et al.* (2008) 'Human cellular microRNA hsa-miR-29a interferes with viral nef protein expression and HIV-1 replication', *Retrovirology*, 5(1), p. 117. Available at: https://doi.org/10.1186/1742-4690-5-117.

Ahmed, A.S. *et al.* (2018) 'Activation of NF-κB in synovium versus cartilage from patients with advanced knee osteoarthritis: a potential contributor to inflammatory aspects of disease progression', *The Journal of Immunology*, 201(7), pp. 1918–1927. Available at: https://doi.org/10.4049/jimmunol.1800486.

Aitken, D. *et al.* (2018) 'A randomised double-blind placebo-controlled crossover trial of HUMira (adalimumab) for erosive hand osteoarthritis – the HUMOR trial', *Osteoarthritis and Cartilage*, 26(7), pp. 880–887. Available at: https://doi.org/10.1016/j.joca.2018.02.899.

Akhtar, N. and Haqqi, T.M. (2013) 'In human chondrocytes DNMT-1 plays a key role in the expression of several genes associated with the pathogenesis of osteoarthritis (OA)', *Osteoarthritis and Cartilage*, 21, pp. S35–S36. Available at: https://doi.org/10.1016/j.joca.2013.02.094.

Akiyama, H. *et al.* (2002) 'The transcription factor Sox9 has essential roles in successive steps of the chondrocyte differentiation pathway and is required for expression of Sox5 and Sox6', *Genes and Development*, 16(21), pp. 2813–2828. Available at: https://doi.org/10.1101/gad.1017802.

Akiyama, H. *et al.* (2004) 'Interactions between Sox9 and β-catenin control chondrocyte differentiation', *Genes and Development*, 18(9), pp. 1072–1087. Available at: https://doi.org/10.1101/gad.1171104.

Akkiraju, H. and Nohe, A. (2015) 'Role of chondrocytes in cartilage formation, progression of osteoarthritis and cartilage regeneration', *Journal of Developmental Biology*, 3(4), pp. 177–192. Available at: https://doi.org/10.3390/jdb3040177.

Alexopoulos, L.G. *et al.* (2009) 'Developmental and osteoarthritic changes in Col6a1-knockout mice: Biomechanics of type VI collagen in the cartilage pericellular matrix', *Arthritis and Rheumatism*, 60(3), pp. 771–779. Available at: https://doi.org/10.1002/art.24293.

Alizadeh, M. *et al.* (2019) 'The potential role of miR-29 in health and cancer diagnosis, prognosis, and therapy', *Journal of Cellular Physiology*, 234(11), pp. 19280–19297. Available at: https://doi.org/10.1002/jcp.28607.

Almonte-Becerril, M. *et al.* (2018) 'Genetic abrogation of the fibronectin-α5β1 integrin interaction in articular cartilage aggravates osteoarthritis in mice', *PLOS ONE*, 13(6), p. e0198559. Available at: https://doi.org/10.1371/journal.pone.0198559.

Amodio, N. *et al.* (2015) 'miR-29s: A family of epi-miRNAs with therapeutic implications in hematologic malignancies', *Oncotarget*, 6(15), pp. 12837–12861. Available at: https://doi.org/10.18632/oncotarget.3805.

Anders, S., Pyl, P.T. and Huber, W. (2015) 'HTSeq-A Python framework to work with high-throughput sequencing data', *Bioinformatics*, 31(2), pp. 166–169. Available at: https://doi.org/10.1093/bioinformatics/btu638.

Andhare, R.A. *et al.* (2009) 'Hyaluronan promotes the chondrocyte response to BMP-7', *Osteoarthritis and Cartilage*, 17(7), pp. 906–916. Available at: https://doi.org/10.1016/j.joca.2008.12.007.

Apold, H. *et al.* (2014) 'Risk factors for knee replacement due to primary osteoarthritis, a population based, prospective cohort study of 315,495 individuals', *BMC Musculoskeletal Disorders*, 15(1), p. 217. Available at: https://doi.org/10.1186/1471-2474-15-217.

Archer, C.W. and Francis-West, P. (2003) 'The chondrocyte', *The International Journal of Biochemistry & Cell Biology*, 35(4), pp. 401–404. Available at: https://doi.org/10.1016/s1357-2725(02)00301-1.

Åsvold, B.O. *et al.* (2014) 'Causal associations of tobacco smoking with cardiovascular risk factors: A Mendelian randomization analysis of the HUNT study in Norway', *International Journal of Epidemiology*, 43(5), pp. 1458–1470. Available at: https://doi.org/10.1093/ije/dyu113.

Baek, D. *et al.* (2018) 'Inhibition of miR-449a promotes cartilage regeneration and prevents progression of osteoarthritis in in vivo rat models', *Molecular Therapy - Nucleic Acids*, 13, pp. 322–333. Available at: https://doi.org/10.1016/j.omtn.2018.09.015.

Bakker, A.C. *et al.* (2001) 'Overexpression of active TGF-beta-1 in the murine knee joint: evidence for synovial-layer-dependent chondro-osteophyte formation', *Osteoarthritis and Cartilage*, 9(2), pp. 128–136. Available at: https://doi.org/10.1053/joca.2000.0368.

Balaskas, P. *et al.* (2017) 'MicroRNA profiling in cartilage ageing', *International Journal of Genomics*, 2017, p. 2713725. Available at: https://doi.org/10.1155/2017/2713725.

Bankhead, P. *et al.* (2017) 'QuPath: Open source software for digital pathology image analysis', *Scientific Reports*, 7(1), p. 16878. Available at: https://doi.org/10.1038/s41598-017-17204-5.

Barland, P., Novikoff, A.B. and Hamerman, D. (1962) 'Electron microscopy of the human synovial membrane', *Journal of Cell Biology*, 14(2), pp. 207–220. Available at: https://doi.org/10.1083/jcb.14.2.207.

Barter, M.J. *et al.* (2015) 'Genome-wide microRNA and gene analysis of mesenchymal stem cell chondrogenesis identifies an essential role and multiple targets for miR-140-5p', *Stem Cells*, 33(11), pp. 3266–3280. Available at: https://doi.org/10.1002/stem.2093.

Bateman, J.F. *et al.* (2013) 'Transcriptomics of wild-type mice and mice lacking adamts-5 activity identifies genes involved in osteoarthritis initiation and cartilage destruction', *Arthritis and Rheumatism*, 65(6), pp. 1547–1560. Available at: https://doi.org/10.1002/art.37900.

Bau, B. *et al.* (2002) 'Relative messenger RNA expression profiling of collagenases and aggrecanases in human articular chondrocytes in vivo and in vitro.', *Arthritis and Rheumatism*, 46(10), pp. 2648–2657. Available at: https://doi.org/10.1002/art.10531.

Baudart, P. *et al.* (2017) 'Association between osteoarthritis and dyslipidaemia: a systematic literature review and meta-analysis', *RMD Open*, 3(2), p. e000442. Available at: https://doi.org/10.1136/rmdopen-2017-000442.

Bauer, R.C. *et al.* (2015) 'Knockout of Adamts7, a novel coronary artery disease locus in humans, reduces atherosclerosis in mice', *Circulation*, 131(13), pp. 1202–1213. Available at: https://doi.org/10.1161/CIRCULATIONAHA.114.012669.

Baugé, C. *et al.* (2011) 'Modulation of transforming growth factor beta signalling pathway genes by transforming growth factor beta in human osteoarthritic chondrocytes: Involvement of Sp1 in both early and late response cells to transforming growth factor beta', *Arthritis Research and Therapy*, 13(1), p. R23. Available at: https://doi.org/10.1186/ar3247.

Baugé, C. *et al.* (2014) 'Regulation and role of TGFβ signaling pathway in aging and osteoarthritis joints', *Aging and Disease*, 5(6), pp. 394–405. Available at: https://doi.org/10.14336/AD.2014.0500394.

Bazzini, A.A., Lee, M.T. and Giraldez, A.J. (2012) 'Ribosome profiling shows that miR-430 reduces translation before causing mRNA decay in Zebrafish', *Science*, 336(6078), pp. 233–237. Available at: https://doi.org/10.1126/science.1215704.

Bekhouche, M. and Colige, A. (2015) 'The procollagen N-proteinases ADAMTS2, 3 and 14 in pathophysiology', *Matrix Biology*, 44–46, pp. 46–53. Available at:

https://doi.org/10.1016/j.matbio.2015.04.001.

Berendsen, A.D. and Olsen, B.R. (2015) 'Bone development', *Bone*, 80, pp. 14–18. Available at: https://doi.org/10.1016/j.bone.2015.04.035.

Bernstein, E. *et al.* (2001) 'Role for a bidentate ribonuclease in the initiation step of RNA interference', *Nature*, 409(6818), pp. 363–366. Available at: https://doi.org/10.1038/35053110.

Bernstein, E. *et al.* (2003) 'Dicer is essential for mouse development', *Nature Genetics*, 35(3), pp. 215–217. Available at: https://doi.org/10.1038/ng1253.

Bestor, T.H. (2000) 'The DNA methyltransferases of mammals', *Human Molecular Genetics*, 9(16), pp. 2395–2402. Available at: https://doi.org/10.1093/hmg/9.16.2395.

van Beuningen, H.M. *et al.* (1998) 'Differential effects of local application of BMP-2 or TGF-beta 1 on both articular cartilage composition and osteophyte formation.', *Osteoarthritis and Cartilage*, 6(5), pp. 306–317. Available at: https://doi.org/10.1053/joca.1998.0129.

van Beuningen, H.M. *et al.* (2000) 'Osteoarthritis-like changes in the murine knee joint resulting from intra-articular transforming growth factor-β injections', *Osteoarthritis and Cartilage*, 8(1), pp. 25–33. Available at: https://doi.org/10.1053/joca.1999.0267.

Bhosale, A.M. and Richardson, J.B. (2008) 'Articular cartilage: structure, injuries and review of management', *British Medical Bulletin*, 87(1), pp. 77–95. Available at: https://doi.org/10.1093/bmb/ldn025.

Bi, W. *et al.* (1999) 'Sox9 is required for cartilage formation', *Nature Genetics*, 22(1), pp. 85–89. Available at: https://doi.org/10.1038/8792.

Bidanset, D.J. *et al.* (1992) 'Binding of the proteoglycan decorin to collagen type VI.', *Journal of Biological Chemistry*, 267(8), pp. 5250–5256. Available at: https://doi.org/https://doi.org/10.1016/S0021-9258(18)42759-7.

Bielajew, B.J., Hu, J.C. and Athanasiou, K.A. (2020) 'Collagen: quantification, biomechanics and role of minor subtypes in cartilage', *Nature Reviews Materials*, 5(10), pp. 730–747. Available at: https://doi.org/10.1038/s41578-020-0213-1.

Billinghurst, R.C. *et al.* (1997) 'Enhanced cleavage of type II collagen by collagenases in osteoarthritic articular cartilage', *Journal of Clinical Investigation*, 99(7), pp. 1534–1545. Available at: https://doi.org/10.1172/JCI119316.

Bird, A. (2007) 'Perceptions of epigenetics', *Nature*, 447(7143), pp. 396–398. Available at: https://doi.org/10.1038/nature05913.

Blagojevic, M. *et al.* (2010) 'Risk factors for onset of osteoarthritis of the knee in older adults: a systematic review and meta-analysis', *Osteoarthritis and Cartilage*, 18(1), pp. 24–33. Available at: https://doi.org/10.1016/j.joca.2009.08.010.

Blaney Davidson, E.N. *et al.* (2006) 'TGF β-induced cartilage repair is maintained but fibrosis is blocked in the presence of Smad7', *Arthritis Research & Therapy*, 8(3), p. R65. Available at: https://doi.org/10.1186/ar1931.

Blaney Davidson, E.N., van der Kraan, P.M. and van den Berg, W.B. (2007) 'TGF-β and osteoarthritis', *Osteoarthritis and Cartilage*, 15(6), pp. 597–604. Available at: https://doi.org/10.1016/j.joca.2007.02.005.

Blease, A. *et al.* (2018) 'Studying osteoarthritis pathogenesis in mice.', *Current Protocols in Mouse Biology*, 8(4), p. e50. Available at: https://doi.org/10.1002/cpmo.50.

Blom, A.B. *et al.* (2009) 'Involvement of the Wnt signaling pathway in experimental and human osteoarthritis: prominent role of Wnt-induced signaling protein 1', *Arthritis and Rheumatism*, 60(2), pp. 501–512. Available at: https://doi.org/10.1002/art.24247.

Bo, N. *et al.* (2012) 'Early cartilage degeneration in a rat experimental model of developmental dysplasia of the hip', *Connective Tissue Research*, 53(6), pp. 513–520. Available at: https://doi.org/10.3109/03008207.2012.700346.

Bohnsack, M.T., Czaplinski, K. and Görlich, D. (2004) 'Exportin 5 is a RanGTP-dependent dsRNA-binding protein that mediates nuclear export of pre-miRNAs', *RNA*, 10(2), pp. 185–191. Available at: https://doi.org/10.1261/rna.5167604.

Bonde, H. V, Talman, M.L.M. and Kofoed, H. (2005) 'The area of the tidemark in osteoarthritis – a three-dimensional stereological study in 21 patients', *APMIS*, 113(5), pp. 349–352. Available at: https://doi.org/https://doi.org/10.1111/j.1600-0463.2005.apm_113506.x.

Borden, P. *et al.* (1996) 'Cytokine control of interstitial collagenase and collagenase-3 gene expression in human chondrocytes', *Journal of Biological Chemistry*, 271(38), pp. 23577–23581. Available at: https://doi.org/10.1074/jbc.271.38.23577.

Borgonio Cuadra, V.M. *et al.* (2014) 'Altered expression of circulating microRNA in plasma of patients with primary osteoarthritis and in silico analysis of their pathways', *PLOS ONE*, 9(6), pp. 20–25. Available at: https://doi.org/10.1371/journal.pone.0097690.

Bourc'his, D. *et al.* (2001) 'Dnmt3L and the establishment of maternal genomic imprints.', *Science*, 294(5551), pp. 2536–2539. Available at: https://doi.org/10.1126/science.1065848.

Boyce, M.K. *et al.* (2013) 'Non-terminal animal model of post-traumatic osteoarthritis induced by acute joint injury', *Osteoarthritis and Cartilage*, 21(5), pp. 746–755. Available at: https://doi.org/10.1016/j.joca.2013.02.653.

Brayton, C. (2007) 'Spontaneous diseases in commonly used mouse strains', in J.G. Fox et al. (eds) *American College of Laboratory Animal Medicine*, pp. 623–717. Available at: https://doi.org/https://doi.org/10.1016/B978-012369454-6/50053-4.

Brown, C., Toth, A. and Magnussen, R. (2011) 'Clinical benefits of intra-articular anakinra for persistent knee effusion.', *The Journal of Knee Surgery*, 24(1), pp. 61–65. Available at: https://doi.org/10.1055/s-0031-1275398.

Brown, T.D. *et al.* (2006) 'Posttraumatic osteoarthritis: a first estimate of incidence, prevalence, and burden of disease', in *Journal of Orthopaedic Trauma*, pp. 739–744. Available at: https://doi.org/10.1097/01.bot.0000246468.80635.ef.

Bruckner, P. and van der Rest, M. (1994) 'Structure and function of cartilage collagens', *Microscopy Research and Technique*, 28(5), pp. 378–384. Available at: https://doi.org/https://doi.org/10.1002/jemt.1070280504.

Buckwalter, J.A. *et al.* (2005) 'Articular cartilage and osteoarthritis', *Instructional Course Lectures*, 54(4860), pp. 465–480. Available at: https://doi.org/10.1136/bmj.1.4860.506.

Cain, S.A. *et al.* (2016) 'ADAMTS-10 and -6 differentially regulate cell-cell junctions and focal adhesions', *Scientific Reports*, 6, p. 35956. Available at: https://doi.org/10.1038/srep35956.

Calce, S.E. *et al.* (2018) 'The relationship of age, activity, and body size on osteoarthritis in weight-bearing skeletal regions', *International Journal of Paleopathology*, 22, pp. 45–53. Available at: https://doi.org/10.1016/j.ijpp.2018.04.001.

Caravia, X.M. *et al.* (2018) 'The microRNA-29/PGC1α regulatory axis is critical for metabolic control of cardiac function', *PLOS Biology*, 16(10), pp. 1–26. Available at: https://doi.org/10.1371/journal.pbio.2006247.

Carlos Rodríguez-Manzaneque, J. *et al.* (2002) 'ADAMTS1 cleaves aggrecan at multiple sites and is differentially inhibited by metalloproteinase inhibitors', *Biochemical and Biophysical Research Communications*, 293(1), pp. 501–508. Available at: https://doi.org/10.1016/S0006-291X(02)00254-1.

Cascio, L. Lo *et al.* (2014) 'Generation of a mouse line harboring a bi-transgene expressing luciferase and tamoxifen-activatable creERT2 recombinase in cartilage', *Genesis*, 52(2), pp. 110–119. Available at: https://doi.org/10.1002/dvg.22734.

Castanheira, C.I.G.D. *et al.* (2021) 'Mouse microRNA signatures in joint ageing and post-traumatic osteoarthritis', *Osteoarthritis and Cartilage Open*, 3(4), p. 100186. Available at: https://doi.org/https://doi.org/10.1016/j.ocarto.2021.100186.

Chang, T.-C. *et al.* (2008) 'Widespread microRNA repression by Myc contributes to tumorigenesis', *Nature Genetics*, 40(1), pp. 43–50. Available at: https://doi.org/10.1038/ng.2007.30.

Cheah, K.S. *et al.* (1991) 'Expression of the mouse alpha 1(II) collagen gene is not restricted to cartilage during development', *Development*, 111(4), pp. 945–953. Available at: https://doi.org/10.1242/dev.111.4.945.

Cheleschi, S. *et al.* (2019) 'MicroRNA mediate visfatin and resistin induction of oxidative stress in human osteoarthritic synovial fibroblasts via NF-κB pathway', *International Journal of Molecular Sciences*, p. 5200. Available at: https://doi.org/10.3390/ijms20205200.

Chen, B. *et al.* (2019) 'Prenatal nicotine exposure increases osteoarthritis susceptibility in male elderly offspring rats via low-function programming of the TGFβ signaling pathway', *Toxicology Letters*, 314(June), pp. 18–26. Available at: https://doi.org/10.1016/j.toxlet.2019.06.010.

Chen, J. *et al.* (2017) 'Efficacy and safety of tanezumab on osteoarthritis knee and hip pains: a meta-analysis of randomized controlled trials', *Pain Medicine*, 18(2), pp. 374–385. Available at: https://doi.org/10.1093/pm/pnw262.

Chen, L. *et al.* (2017) 'MiR-29b-3p promotes chondrocyte apoptosis and facilitates the occurrence and development of osteoarthritis by targeting PGRN', *Journal of Cellular and Molecular Medicine*, 21(12), pp. 3347–3359. Available at: https://doi.org/https://doi.org/10.1111/jcmm.13237.

Chen, M. *et al.* (2007) 'Generation of a transgenic mouse model with chondrocyte-specific and tamoxifen-inducible expression of Cre recombinase.', *Genesis*, 45(1), pp. 44–50. Available at: https://doi.org/10.1002/dvg.20261.

Chen, W. *et al.* (2016) 'MicroRNA-381 regulates chondrocyte hypertrophy by inhibiting histone deacetylase 4 expression', *International Journal of Molecular Sciences*, 17(9), p. 1377. Available at: https://doi.org/10.3390/ijms17091377.

Cheon, H. *et al.* (2002) 'Increased expression of pro-inflammatory cytokines and metalloproteinase-1 by TGF-β1 in synovial fibroblasts from rheumatoid arthritis and normal individuals', *Clinical and Experimental Immunology*, 127(3), pp. 547–552. Available at: https://doi.org/10.1046/j.1365-2249.2002.01785.x.

Cherifi, C., Monteagudo, S. and Lories, R.J. (2021) 'Promising targets for therapy of osteoarthritis: a review on the Wnt and TGF-β signalling pathways', *Therapeutic Advances in Musculoskeletal Disease*, 13, p. 1759720X211006959. Available at: https://doi.org/10.1177/1759720X211006959.

Cheung, K.S.C. *et al.* (2008) 'Expression of ADAMTS-4 by chondrocytes in the surface zone of human osteoarthritic cartilage is regulated by epigenetic DNA de-methylation', *Rheumatology International*, 29(5), pp. 525–534. Available at: https://doi.org/10.1007/s00296-008-0744-z.

Chevalier, X. *et al.* (2009) 'Intraarticular injection of anakinra in osteoarthritis of the knee: A multicenter, randomized, double-blind, placebo-controlled study', *Arthritis Care and Research*, 61(3), pp. 344–352. Available at: https://doi.org/10.1002/art.24096.

Chevalier, X. *et al.* (2014) 'Adalimumab in patients with hand osteoarthritis refractory to

analgesics and NSAIDs: a randomised, multicentre, double-blind, placebo-controlled trial', *Annals of the Rheumatic Diseases*, 74(9), pp. 1697–1705. Available at: https://doi.org/10.1136/annrheumdis-2014-205348.

Chia, S.L. *et al.* (2009) 'Fibroblast growth factor 2 is an intrinsic chondroprotective agent that suppresses ADAMTS-5 and delays cartilage degradation in murine osteoarthritis', *Arthritis and Rheumatism*, 60(7), pp. 2019–2027. Available at: https://doi.org/10.1002/art.24654.

Choi, M.-C.C. *et al.* (2018) 'Alleviation of murine osteoarthritis by cartilage-specific deletion of IκBζ', *Arthritis and Rheumatology*, 70(9), pp. 1440–1449. Available at: https://doi.org/10.1002/art.40514.

Chow, M.Y.T., Qiu, Y. and Lam, J.K.W. (2020) 'Inhaled RNA therapy: from promise to reality', *Trends in Pharmacological Sciences*, 41(10), pp. 715–729. Available at: https://doi.org/https://doi.org/10.1016/j.tips.2020.08.002.

Cicuttini, F.M. and Wluka, A.E. (2014) 'Is OA a mechanical or systemic disease?', *Nature Reviews Rheumatology*, pp. 515–516. Available at: https://doi.org/10.1038/nrrheum.2014.114.

Cilek, M.Z. *et al.* (2021) 'Synergistic upregulation of ADAMTS4 (aggrecanase-1) by cytokines and its suppression in knee osteoarthritic synovial fibroblasts', *Laboratory Investigation*, 102(1), pp. 102–111. Available at: https://doi.org/10.1038/s41374-021-00685-4.

Cohen, S.B. *et al.* (2011) 'A randomized, double-blind study of AMG 108 (a fully human monoclonal antibody to IL-1R1) in patients with osteoarthritis of the knee', *Arthritis Research and Therapy*, 13(4), p. R125. Available at: https://doi.org/10.1186/ar3430.

Colige, A. *et al.* (1997) 'cDNA cloning and expression of bovine procollagen I N-proteinase: A new member of the superfamily of zinc-metalloproteinases with binding sites for cells and other matrix components', *Proceedings of the National Academy of Sciences of the United States of America*, 94(6), pp. 2374–2379. Available at: https://doi.org/10.1073/pnas.94.6.2374.

Colige, A. *et al.* (1999) 'Human Ehlers-Danlos syndrome type VII C and bovine dermatosparaxis are caused by mutations in the procollagen I N-proteinase gene', *The American Journal of Human Genetics*, 65(2), pp. 308–317. Available at: https://doi.org/https://doi.org/10.1086/302504.

Colige, A. *et al.* (2002) 'Cloning and characterization of ADAMTS-14, a novel ADAMTS displaying high homology with ADAMTS-2 and ADAMTS-3', *Journal of Biological Chemistry*, 277(8), pp. 5756–5766. Available at: https://doi.org/10.1074/jbc.M105601200.

Collins-racie, L.A. *et al.* (2004) 'ADAMTS-8 exhibits aggrecanase activity and is expressed in human articular cartilage', *Matrix Biology*, 23(4), pp. 219–230. Available at: https://doi.org/10.1016/j.matbio.2004.05.004.

Condrat, C.E. *et al.* (2020) 'miRNAs as biomarkers in disease: latest findings regarding their role in diagnosis and prognosis', *Cells*, 9(2), p. 276. Available at: https://doi.org/10.3390/cells9020276.

Cong, L., Zhu, Y. and Tu, G. (2017) 'A bioinformatic analysis of microRNAs role in osteoarthritis', *Osteoarthritis and Cartilage*, 25(8), pp. 1362–1371. Available at: https://doi.org/10.1016/j.joca.2017.03.012.

Cordes, K.R. *et al.* (2009) 'MiR-145 and miR-143 regulate smooth muscle cell fate and plasticity', *Nature*, 460(7256), pp. 705–710. Available at: https://doi.org/10.1038/nature08195.

Corr, M. (2008) 'Wnt-beta-catenin signaling in the pathogenesis of osteoarthritis', *Nature*

Clinical Practice Rheumatology, pp. 550–556. Available at: https://doi.org/10.1038/ncprheum0904.

Coutinho de Almeida, R. *et al.* (2019) 'RNA sequencing data integration reveals an miRNA interactome of osteoarthritis cartilage', *Annals of the Rheumatic Diseases*, 78(2), pp. 270–277. Available at: https://doi.org/10.1136/annrheumdis-2018-213882.

Cushing, L. *et al.* (2011) 'miR-29 is a major regulator of genes associated with pulmonary fibrosis', *American Journal of Respiratory Cell and Molecular Biology*, 45(2), pp. 287–294. Available at: https://doi.org/10.1165/rcmb.2010-0323OC.

Cushing, L. *et al.* (2015) 'Disruption of miR-29 leads to aberrant differentiation of smooth muscle cells selectively associated with distal lung vasculature', *PLOS Genetics*, 11(5), pp. e1005238–e1005238. Available at: https://doi.org/10.1371/journal.pgen.1005238.

Dancevic, C.M. *et al.* (2013) 'Biosynthesis and expression of a disintegrin-like and metalloproteinase domain with thrombospondin-1 repeats-15: A novel versican-cleaving proteoglycanase', *Journal of Biological Chemistry*, 288(52), pp. 37267–37276. Available at: https://doi.org/10.1074/jbc.M112.418624.

Darling, E.M. and Athanasiou, K.A. (2005) 'Rapid phenotypic changes in passaged articular chondrocyte subpopulations.', *Journal of Orthopaedic Research*, 23(2), pp. 425–432. Available at: https://doi.org/10.1016/j.orthres.2004.08.008.

Davidson, R.K. *et al.* (2006) 'Expression profiling of metalloproteinases and their inhibitors in synovium and cartilage', *Arthritis Research and Therapy*, 8(4), pp. 1–10. Available at: https://doi.org/10.1186/ar2013.

Deng, Z. *et al.* (2017) 'MicroRNA-29: a crucial player in fibrotic disease', *Molecular Diagnosis and Therapy*, 21(3), pp. 285–294. Available at: https://doi.org/10.1007/s40291-016-0253-9.

Denli, A.M. *et al.* (2004) 'Processing of primary microRNAs by the Microprocessor complex', *Nature*, 432(7014), pp. 231–235. Available at: https://doi.org/10.1038/nature03049.

Dennler, S. *et al.* (1998) 'Direct binding of Smad3 and Smad4 to critical TGFβ-inducible elements in the promoter of human plasminogen activator inhibitor-type 1 gene', *EMBO Journal*, 17(11), pp. 3091–3100. Available at: https://doi.org/10.1093/emboj/17.11.3091.

Dey, S. *et al.* (2021) 'Loss of miR-29a/b1 promotes inflammation and fibrosis in acute pancreatitis', *JCI Insight*, 6(19), p. e149539. Available at: https://doi.org/10.1172/jci.insight.149539.

Dharap, A. *et al.* (2013) 'MicroRNA miR-324-3p induces promoter-mediated expression of RelA gene', *PLOS ONE*, 8(11), pp. 4–8. Available at: https://doi.org/10.1371/journal.pone.0079467.

Díaz-Prado, S. *et al.* (2012) 'Characterization of microRNA expression profiles in normal and osteoarthritic human chondrocytes', *BMC Musculoskeletal Disorders*, 13(1), p. 144. Available at: https://doi.org/10.1186/1471-2474-13-144.

Dickhut, A. *et al.* (2008) 'Correlation of COL10A1 induction during chondrogenesis of mesenchymal stem cells with demethylation of two CpG sites in the COL10A1 promoter.', *Arthritis and Rheumatism*, 58(9), pp. 2743–2753. Available at: https://doi.org/10.1002/art.23736.

Diener, C., Keller, A. and Meese, E. (2022) 'Emerging concepts of miRNA therapeutics: from cells to clinic', *Trends in Genetics*, 38(6), pp. 613–626. Available at: https://doi.org/https://doi.org/10.1016/j.tig.2022.02.006.

Ding, C. *et al.* (2007) 'Association between leptin, body composition, sex and knee cartilage morphology in older adults: the Tasmanian older adult cohort (TASOAC) study', *Annals of the Rheumatic Diseases*, 67(9), pp. 1256–1261. Available at:

https://doi.org/10.1136/ard.2007.082651.

Djuranovic, S., Nahvi, A. and Green, R. (2012) 'miRNA-mediated gene silencing by translational repression followed by mRNA deadenylation and decay', *Science*, 336(6078), pp. 237–240. Available at: https://doi.org/10.1126/science.1215691.

Dooley, J. *et al.* (2016) 'The microRNA-29 family dictates the balance between homeostatic and pathological glucose handling in diabetes and obesity', *Diabetes*, 65(1), pp. 53–61. Available at: https://doi.org/10.2337/db15-0770.

Doß, F. *et al.* (2007) 'Elevated IL-6 levels in the synovial fluid of osteoarthritis patients stem from plasma cells', *Scandinavian Journal of Rheumatology*, 36(2), pp. 136–139. Available at: https://doi.org/10.1080/03009740701250785.

Dou, P. *et al.* (2020) 'Downregulation of microRNA-29b by DNMT3B decelerates chondrocyte apoptosis and the progression of osteoarthritis via PTHLH/CDK4/RUNX2 axis.', *Aging*, 13(5), pp. 7676–7690. Available at: https://doi.org/10.18632/aging.103778.

Drake, R.L. *et al.* (2009) *Gray's Anatomy for Students*.

Du, Y. *et al.* (2012) 'Upregulation of a disintegrin and metalloproteinase with thrombospondin motifs-7 by miR-29 repression mediates vascular smooth muscle calcification', *Arteriosclerosis, Thrombosis, and Vascular Biology*, 32(11), pp. 2580–2588. Available at: https://doi.org/10.1161/atvbaha.112.300206.

Dubé, C.E. *et al.* (2016) 'The relationship between smoking and knee osteoarthritis in the Osteoarthritis Initiative', *Osteoarthritis and Cartilage*, 24(3), pp. 465–472. Available at: https://doi.org/https://doi.org/10.1016/j.joca.2015.09.015.

Dudek, M. *et al.* (2016) 'The chondrocyte clock gene Bmal1 controls cartilage homeostasis and integrity', *The Journal of Clinical Investigation*, 126(1), pp. 365–376. Available at: https://doi.org/10.1172/JCI82755.

Dudhia, J. *et al.* (1996) 'Studies on the G3 domain of aggrecan from human cartilage', *Annals of the New York Academy of Sciences*, 785(1), pp. 245–247. Available at: https://doi.org/10.1111/j.1749-6632.1996.tb56273.x.

Dudhia, J. (2005) 'Aggrecan, aging and assembly in articular cartilage', *Cellular and Molecular Life Sciences*, pp. 2241–2256. Available at: https://doi.org/10.1007/s00018-005-5217-x.

Dumond, H. *et al.* (2003) 'Evidence for a key role of leptin in osteoarthritis', *Arthritis and Rheumatism*, 48(11), pp. 3118–3129. Available at: https://doi.org/10.1002/art.11303.

Dunn, S.L. *et al.* (2016) 'Gene expression changes in damaged osteoarthritic cartilage identify a signature of non-chondrogenic and mechanical responses', *Osteoarthritis and Cartilage*, 24(8), pp. 1431–1440. Available at: https://doi.org/10.1016/j.joca.2016.03.007.

Dupont, L. *et al.* (2018) 'Spontaneous atopic dermatitis due to immune dysregulation in mice lacking Adamts2 and 14', *Matrix Biology*, 70, pp. 140–157. Available at: https://doi.org/10.1016/j.matbio.2018.04.002.

Economics, O. (2010) 'The economic costs of arthritis for the UK economy', *Final Report, March* [Preprint]. Available at: http://www.oxfordeconomics.com/my-oxford/projects/128882.

Eichhorn, S.W. *et al.* (2014) 'MRNA destabilization is the dominant effect of mammalian microRNAs by the time substantial repression ensues', *Molecular Cell*, 56(1), pp. 104–115. Available at: https://doi.org/10.1016/j.molcel.2014.08.028.

Erdogmus, S. *et al.* (2022) 'Cavβ1 regulates T cell expansion and apoptosis independently of voltage-gated Ca2+ channel function', *Nature Communications*, 13(1), p. 2033. Available at: https://doi.org/10.1038/s41467-022-29725-3.

Eyre, D. (2002) ‘Collagen of articular cartilage’, *Arthritis Research & Therapy*, 4(1), pp. 30–35. Available at: https://www.ncbi.nlm.nih.gov/pubmed/11879535.

Ezura, Y. *et al.* (2009) ‘Methylation status of CpG islands in the promoter regions of signature genes during chondrogenesis of human synovium-derived mesenchymal stem cells.’, *Arthritis and Rheumatism*, 60(5), pp. 1416–1426. Available at: https://doi.org/10.1002/art.24472.

Fabbri, M. *et al.* (2007) ‘MicroRNA-29 family reverts aberrant methylation in lung cancer by targeting DNA methyltransferases 3A and 3B’, *Proceedings of the National Academy of Sciences*, 104(40), pp. 15805–15810. Available at: https://doi.org/10.1073/pnas.0707628104.

Farahat, M.N. *et al.* (1993) ‘Cytokine expression in synovial membranes of patients with rheumatoid arthritis and osteoarthritis’, *Annals of the Rheumatic Diseases*, 52(12), pp. 870–875. Available at: https://doi.org/10.1136/ard.52.12.870.

Fässler, R. *et al.* (1994) ‘Mice lacking alpha 1 (IX) collagen develop noninflammatory degenerative joint disease.’, *Proceedings of the National Academy of Sciences of the United States of America*, 91(11), pp. 5070–4. Available at: https://doi.org/10.1073/pnas.91.11.5070.

Feil, R. *et al.* (1996) ‘Ligand-activated site-specific recombination in mice.’, *Proceedings of the National Academy of Sciences of the United States of America*, 93(20), pp. 10887–10890. Available at: https://doi.org/10.1073/pnas.93.20.10887.

Felson, D.T. and Zhang, Y. (2015) ‘Smoking and osteoarthritis: a review of the evidence and its implications’, *Osteoarthritis and Cartilage*, 23(3), pp. 331–333. Available at: https://doi.org/10.1016/j.joca.2014.11.022.

Fernandes, J. *et al.* (1999) ‘In vivo transfer of interleukin-1 receptor antagonist gene in osteoarthritic rabbit knee joints. Prevention of osteoarthritis progression’, *American Journal of Pathology*, 154(4), pp. 1159–1169. Available at: https://doi.org/10.1016/S0002-9440(10)65368-0.

Fernandes, R.J. *et al.* (2001) ‘Procollagen II amino propeptide processing by ADAMTS-3: insights on dermatosparaxis’, *Journal of Biological Chemistry*, 276(34), pp. 31502–31509. Available at: https://doi.org/https://doi.org/10.1074/jbc.M103466200.

Fernández-Tajes, J. *et al.* (2014) ‘Genome-wide DNA methylation analysis of articular chondrocytes reveals a cluster of osteoarthritic patients’, *Annals of the Rheumatic Diseases*, 73(4), pp. 668–677. Available at: https://doi.org/10.1136/annrheumdis-2012-202783.

Fernández, M.P., Young, M.F. and Sobel, M.E. (1985) ‘Methylation of type II and type I collagen genes in differentiated and dedifferentiated chondrocytes.’, *The Journal of Biological Chemistry*, 260(4), pp. 2374–2378.

Fleischmann, R.M. *et al.* (2019) ‘A phase II trial of lutikizumab, an anti–interleukin-1α/β dual variable domain immunoglobulin, in knee osteoarthritis patients with synovitis’, *Arthritis and Rheumatology*, 71(7), pp. 1056–1069. Available at: https://doi.org/10.1002/art.40840.

Forman, J.J. and Coller, H.A. (2010) ‘The code within the code: microRNAs target coding regions’, *Cell Cycle*, 9(8), pp. 1533–1541. Available at: https://doi.org/10.4161/cc.9.8.11202.

Forman, J.J., Legesse-Miller, A. and Coller, H.A. (2008) ‘A search for conserved sequences in coding regions reveals that the let-7 microRNA targets Dicer within its coding sequence’, *Proceedings of the National Academy of Sciences of the United States of America*, 105(39), pp. 14879–14884. Available at: https://doi.org/10.1073/pnas.0803230105.

Fosang, A.J. *et al.* (1992) ‘The interglobular domain of cartilage aggrecan is cleaved by

PUMP, gelatinases, and cathepsin B', *Journal of Biological Chemistry*, 267(27), pp. 19470–19474. Available at: https://www.scopus.com/record/display.uri?eid=2-s2.0-0026701977&origin=inward&txGid=ba09890e62c92fc009acff3d548e3942 (Accessed: 17 April 2018).

Fosang, A.J. *et al.* (1996) 'Degradation of cartilage aggrecan by collagenase-3 (MMP-13)', *FEBS Letters*, 380(1–2), pp. 17–20. Available at: https://doi.org/10.1016/0014-5793(95)01539-6.

Friedman, R.C. *et al.* (2009) 'Most mammalian mRNAs are conserved targets of microRNAs', *Genome Research*, 19(1), pp. 92–105. Available at: https://doi.org/10.1101/gr.082701.108.

Fujikawa, K. *et al.* (2001) 'Purification of human von Willebrand factor-cleaving protease and its identification as a new member of the metalloproteinase family.', *Blood*, 98(6), pp. 1662–1666. Available at: https://doi.org/10.1182/blood.v98.6.1662.

Furuya, M. *et al.* (2018) 'Direct cell-cell contact between mature osteoblasts and osteoclasts dynamically controls their functions in vivo', *Nature Communications*, 9(1), p. 300. Available at: https://doi.org/10.1038/s41467-017-02541-w.

Gallo, A. *et al.* (2012) 'The majority of microRNAs detectable in serum and saliva is concentrated in exosomes', *PLOS ONE*, 7(3), p. e30679. Available at: https://doi.org/10.1371/journal.pone.0030679.

Gao, Y.H. *et al.* (2020) 'An update on the association between metabolic syndrome and osteoarthritis and on the potential role of leptin in osteoarthritis', *Cytokine*, 129(February), p. 155043. Available at: https://doi.org/10.1016/j.cyto.2020.155043.

Gardiner, M.D. *et al.* (2015) 'Transcriptional analysis of micro-dissected articular cartilage in post-traumatic murine osteoarthritis', *Osteoarthritis and Cartilage*, 23(4), pp. 616–628. Available at: https://doi.org/10.1016/j.joca.2014.12.014.

Garzon, R. *et al.* (2009) 'MicroRNA-29b induces global DNA hypomethylation and tumor suppressor gene reexpression in acute myeloid leukemia by targeting directly DNMT3A and 3B and indirectly DNMT1', *Blood*, 113(25), pp. 6411–6418. Available at: https://doi.org/10.1182/blood-2008-07-170589.

Gebauer, M. *et al.* (2005) 'Comparison of the chondrosarcoma cell line SW1353 with primary human adult articular chondrocytes with regard to their gene expression profile and reactivity to IL-1β', *Osteoarthritis and Cartilage*, 13(8), pp. 697–708. Available at: https://doi.org/10.1016/j.joca.2005.04.004.

Gendron, C. *et al.* (2007) 'Proteolytic activities of human ADAMTS-5: comparative studies with ADAMTS-4.', *Journal of Biological Chemistry*, 282(25), pp. 18294–18306. Available at: https://doi.org/10.1074/jbc.M701523200.

Geyer, M. *et al.* (2009) 'Differential transcriptome analysis of intraarticular lesional vs intact cartilage reveals new candidate genes in osteoarthritis pathophysiology.', *Osteoarthritis and Cartilage*, 17(3), pp. 328–335. Available at: https://doi.org/10.1016/j.joca.2008.07.010.

Ghouri, A. and Conaghan, P.G. (2021) 'Prospects for therapies in osteoarthritis', *Calcified Tissue International*, 109, pp. 339–350. Available at: https://doi.org/10.1007/s00223-020-00672-9.

Glasson, S.S. *et al.* (2005) 'Deletion of active ADAMTS5 prevents cartilage degradation in a murine model of osteoarthritis', *Nature*, 434(7033), pp. 644–648. Available at: https://doi.org/10.1038/nature03369.

Glasson, S.S. *et al.* (2010) 'The OARSI histopathology initiative - recommendations for histological assessments of osteoarthritis in the mouse', *Osteoarthritis and Cartilage*, 18(SUPPL. 3), pp. S17–S23. Available at: https://doi.org/10.1016/j.joca.2010.05.025.

Glasson, S.S., Blanchet, T.J. and Morris, E.A. (2007) 'The surgical destabilization of the medial meniscus (DMM) model of osteoarthritis in the 129/SvEv mouse', *Osteoarthritis and Cartilage*, 15(9), pp. 1061–1069. Available at: https://doi.org/10.1016/j.joca.2007.03.006.

Goldring, M.B. *et al.* (1994) 'Interleukin-1 beta-modulated gene expression in immortalized human chondrocytes.', *Journal of Clinical Investigation*, 94(6), pp. 2307–2316. Available at: https://doi.org/10.1172/JCI117595.

Goldring, M.B. and Marcu, K.B. (2009) 'Cartilage homeostasis in health and rheumatic diseases', *Arthritis Research & Therapy*, 11(3), p. 224. Available at: https://doi.org/10.1186/ar2592.

Goldring, M.B., Tsuchimochi, K. and Ijiri, K. (2006) 'The control of chondrogenesis', *Journal of Cellular Biochemistry*, 97(1), pp. 33–44. Available at: https://doi.org/10.1002/jcb.20652.

Goldring, S.R. and Goldring, M.B. (2017) 'Biology of the normal joint', in *Kelley and Firestein's Textbook of Rheumatology*, pp. 1–19. Available at: https://doi.org/10.1016/b978-0-323-31696-5.00001-2.

Gopalakrishnan, K. *et al.* (2012) 'Targeted disruption of Adamts16 gene in a rat genetic model of hypertension', *Proceedings of the National Academy of Sciences of the United States of America*, 109(50), pp. 20555–20559. Available at: https://doi.org/10.1073/pnas.1211290109.

Grall, F. *et al.* (2003) 'Responses to the proinflammatory cytokines interleukin-1 and tumor necrosis factor α in cells derived from rheumatoid synovium and other joint tissues involve nuclear factor κB-mediated induction of the Ets transcription factor ESE-1', *Arthritis and Rheumatism*, 48(5), pp. 1249–1260. Available at: https://doi.org/10.1002/art.10942.

Greenberg, M.V.C. and Bourc'his, D. (2019) 'The diverse roles of DNA methylation in mammalian development and disease', *Nature Reviews Molecular Cell Biology*, 20(10), pp. 590–607. Available at: https://doi.org/10.1038/s41580-019-0159-6.

Griffin, T.M. *et al.* (2009) 'Extreme obesity due to impaired leptin signaling in mice does not cause knee osteoarthritis', *Arthritis and Rheumatism*, 60(10), pp. 2935–2944. Available at: https://doi.org/10.1002/art.24854.

Grotle, M. *et al.* (2008) 'Obesity and osteoarthritis in knee, hip and/or hand: An epidemiological study in the general population with 10 years follow-up', *BMC Musculoskeletal Disorders*, 9(1), p. 132. Available at: https://doi.org/10.1186/1471-2474-9-132.

Gu, Q. *et al.* (2015) 'Effects of nicotine on a rat model of early stage osteoarthritis', *International Journal of Clinical and Experimental Pathology*, 8(4), pp. 3602–3612.

Gu, R. *et al.* (2016) 'MicroRNA-9 regulates the development of knee osteoarthritis through the NF-kappaB1 pathway in chondrocytes', *Medicine*, 95(36), p. e4315. Available at: https://doi.org/10.1097/MD.0000000000004315.

Gualeni, B. *et al.* (2013) 'A novel transgenic mouse model of growth plate dysplasia reveals that decreased chondrocyte proliferation due to chronic ER stress is a key factor in reduced bone growth', *Disease Models & Mechanisms*, 6(6), pp. 1414–1425. Available at: https://doi.org/10.1242/dmm.013342.

Guérit, D. *et al.* (2014) 'FOXO3A regulation by miRNA-29a controls chondrogenic cifferentiation of mesenchymal stem cells and cartilage formation', *Stem Cells and Development*, 23(11), pp. 1195–1205. Available at: https://doi.org/10.1089/scd.2013.0463.

Guilak, F. *et al.* (1994) 'Mechanical and biochemical changes in the superficial zone of articular cartilage in canine experimental osteoarthritis.', *Journal of Orthopaedic Research : Official Publication of the Orthopaedic Research Society*, 12(4), pp. 474–484. Available at: https://doi.org/10.1002/jor.1100120404.

Gullahorn, L., Lippiello, L. and Karpman, R. (2005) 'Smoking and osteoarthritis: Differential effect of nicotine on human chondrocyte glycosaminoglycan and collagen synthesis', *Osteoarthritis and Cartilage*, 13(10), pp. 942–943. Available at: https://doi.org/10.1016/j.joca.2005.03.001.

Guo, H. *et al.* (2010) 'Mammalian microRNAs predominantly act to decrease target mRNA levels', *Nature*, 466(7308), pp. 835–840. Available at: https://doi.org/10.1038/nature09267.

Guo, L. and Lu, Z. (2010) 'The fate of miRNA* strand through evolutionary analysis: Implication for degradation as merely carrier strand or potential regulatory molecule?', *PLOS ONE*, 5(6), pp. 1–9. Available at: https://doi.org/10.1371/journal.pone.0011387.

Ha, M. and Kim, V.N. (2014) 'Regulation of microRNA biogenesis', *Nature Reviews Molecular Cell Biology*, 15(8), pp. 509–524. Available at: https://doi.org/10.1038/nrm3838.

Hammond, S.M. *et al.* (2001) 'Argonaute2, a link between genetic and biochemical analyses of RNAi', *Science*, 293(5532), pp. 1146–1150. Available at: https://doi.org/10.1126/science.1064023.

Han, Y. and Lefebvre, V. (2008) 'L-Sox5 and Sox6 drive expression of the aggrecan gene in cartilage by securing binding of Sox9 to a far-upstream enhancer', *Molecular and Cellular Biology*, 28(16), pp. 4999–5013. Available at: https://doi.org/10.1128/MCB.00695-08.

Hardingham, T.E. and Fosang, A.J. (1992) 'Proteoglycans: many forms and many functions', *The FASEB Journal*, 6(3), pp. 861–870. Available at: https://doi.org/https://doi.org/10.1096/fasebj.6.3.1740236.

Harfe, B.D. *et al.* (2005) 'The RNaseIII enzyme Dicer is required for morphogenesis but not patterning of the vertebrate limb', *Proceedings of the National Academy of Sciences*, 102(31), pp. 10898–10903. Available at: https://doi.org/10.1073/pnas.0504834102.

Hascall, V.C. and Heinegård, D. (1974) 'Aggregation of cartilage proteoglycans: I. the role of hyaluronic acid', *Journal of Biological Chemistry*, 249(13), pp. 4232–4241. Available at: https://doi.org/10.1016/S0021-9258(19)42507-6.

He, B. and Jiang, D. (2020) 'HOTAIR-induced apoptosis is mediated by sponging miR-130a-3p to repress chondrocyte autophagy in knee osteoarthritis', *Cell Biology International*, 44(2), pp. 524–535. Available at: https://doi.org/https://doi.org/10.1002/cbin.11253.

He, Y. *et al.* (2012) 'The potential of microRNAs in liver fibrosis', *Cellular Signalling*, 24(12), pp. 2268–2272. Available at: https://doi.org/https://doi.org/10.1016/j.cellsig.2012.07.023.

He, Y. *et al.* (2014) 'Type X collagen levels are elevated in serum from human osteoarthritis patients and associated with biomarkers of cartilage degradation and inflammation', *BMC Musculoskeletal Disorders*, 15(1), pp. 1–10. Available at: https://doi.org/10.1186/1471-2474-15-309.

He, Y. and Ecker, J.R. (2015) 'Non-CG methylation in the human genome.', *Annual Review of Genomics and Human Genetics*, 16, pp. 55–77. Available at: https://doi.org/10.1146/annurev-genom-090413-025437.

Heinegård, D. and Saxne, T. (2011) 'The role of the cartilage matrix in osteoarthritis', *Nature Reviews Rheumatology*, 7(1), pp. 50–56. Available at: https://doi.org/10.1038/nrrheum.2010.198.

Henderson, B. and Pettipher, E.R. (1989) 'Arthritogenic actions of recombinant IL-1 and tumour necrosis factor alpha in the rabbit: evidence for synergistic interactions between cytokines in vivo.', *Clinical and Experimental Immunology*, 75(2), pp. 306–310. Available at: http://www.ncbi.nlm.nih.gov/pubmed/2784740 (Accessed: 3 May 2018).

Hinck, A.P. (2012) 'Structural studies of the TGF-βs and their receptors - Insights into evolution of the TGF-β superfamily', *FEBS Letters*, 586(14), pp. 1860–1870. Available at:

https://doi.org/10.1016/j.febslet.2012.05.028.

Hirano, F. *et al.* (1998) 'Functional interference of Sp1 and NF-κB through the same DNA binding site', *Molecular and Cellular Biology*, 18(3), pp. 1266–1274. Available at: https://doi.org/10.1128/MCB.18.3.1266.

den Hollander, W. *et al.* (2014) 'Knee and hip articular cartilage have distinct epigenomic landscapes: implications for future cartilage regeneration approaches', *Annals of the Rheumatic Diseases*, 73(12), pp. 2208–2212. Available at: https://doi.org/10.1136/annrheumdis-2014-205980.

Holmberg, S., Thelin, A. and Thelin, N. (2005) 'Knee osteoarthritis and body mass index: A population-based case-control study', *Scandinavian Journal of Rheumatology*, 34(1), pp. 59–64. Available at: https://doi.org/10.1080/03009740510017922.

Holmes, D.F. *et al.* (2018) 'Collagen fibril assembly and function', *Current Topics in Developmental Biology*. Edited by E.S. Litscher and P.M.B.T.-C.T. in D.B. Wassarman, 130, pp. 107–142. Available at: https://doi.org/10.1016/bs.ctdb.2018.02.004.

Hong, D.S. *et al.* (2020) 'Phase 1 study of MRX34, a liposomal miR-34a mimic, in patients with advanced solid tumours', *British Journal of Cancer*, 122(11), pp. 1630–1637. Available at: https://doi.org/10.1038/s41416-020-0802-1.

Horton, W.A. (1996) 'Progress in human chondrodysplasias: molecular genetics', *Annals of the New York Academy of Sciences*, 785(1), pp. 150–159. Available at: https://doi.org/10.1111/j.1749-6632.1996.tb56253.x.

Houard, X., Goldring, M.B. and Berenbaum, F. (2013) 'Homeostatic mechanisms in articular cartilage and role of inflammation in osteoarthritis', *Current Rheumatology Reports*, 15(11), p. 375. Available at: https://doi.org/10.1007/s11926-013-0375-6.

El Hour, M. *et al.* (2010) 'Higher sensitivity of Adamts12-deficient mice to tumor growth and angiogenesis', *Oncogene*, 29(20), pp. 3025–3032. Available at: https://doi.org/10.1038/onc.2010.49.

Hour, M. El *et al.* (2010) 'Higher sensitivity of Adamts12 -deficient mice to tumor growth and angiogenesis', *Oncogene*, pp. 3025–3032. Available at: https://doi.org/10.1038/onc.2010.49.

Howe, K.L. *et al.* (2021) 'Ensembl 2021', *Nucleic Acids Research*, 49(D1), pp. D884–D891. Available at: https://doi.org/10.1093/nar/gkaa942.

Huang, J. *et al.* (2019) 'The microRNAs miR-204 and miR-211 maintain joint homeostasis and protect against osteoarthritis progression', *Nature Communications*, 10(1), p. 2876. Available at: https://doi.org/10.1038/s41467-019-10753-5.

Hügle, T. and Geurts, J. (2017) 'What drives osteoarthritis? - synovial versus subchondral bone pathology', *Rheumatology*, 56(9), pp. 1461–1471. Available at: https://doi.org/10.1093/rheumatology/kew389.

Hui, A.Y. *et al.* (2012) 'A systems biology approach to synovial joint lubrication in health, injury, and disease', *Wiley Interdisciplinary Reviews: Systems Biology and Medicine*, 4(1), pp. 15–37. Available at: https://doi.org/10.1002/wsbm.157.

Hui, W. *et al.* (2012) 'Leptin produced by joint white adipose tissue induces cartilage degradation via upregulation and activation of matrix metalloproteinases', *Annals of the Rheumatic Diseases*, 71(3), pp. 455–462. Available at: https://doi.org/10.1136/annrheumdis-2011-200372.

Hung, J. *et al.* (2019) 'Leptin-deficient mice have altered three-dimensional growth plate histomorphometry', *Diabetology & Metabolic Syndrome*, 11(1), p. 8. Available at: https://doi.org/10.1186/s13098-019-0402-5.

Hunter, D.J. and Bierma-Zeinstra, S. (2019) 'Osteoarthritis', *The Lancet*, 393(10182), pp. 1745–1759. Available at: https://doi.org/10.1016/s0140-6736(19)30417-9.

Huntzinger, E. and Izaurralde, E. (2011) 'Gene silencing by microRNAs: contributions of translational repression and mRNA decay', *Nature Reviews Genetics*, 12(2), pp. 99–110. Available at: https://doi.org/10.1038/nrg2936.

Hutvágner, G. *et al.* (2001) 'A cellular function for the RNA-interference enzyme dicer in the maturation of the let-7 small temporal RNA', *Science*, 293(5531), pp. 834–838. Available at: https://doi.org/10.1126/science.1062961.

Hwang, H.-W., Wentzel, E.A. and Mendell, J.T. (2007) 'A hexanucleotide element directs microRNA nuclear import', *Science*, 315(5808), pp. 97–100. Available at: https://doi.org/10.1126/science.1136235.

Iliopoulos, D. *et al.* (2008) 'Integrative microRNA and proteomic approaches identify novel osteoarthritis genes and their collaborative metabolic and inflammatory networks', *PLOS ONE*. Edited by S. Koutsopoulos, 3(11), pp. e3740–e3740. Available at: https://doi.org/10.1371/journal.pone.0003740.

Imagawa, K. *et al.* (2014) 'Association of reduced type IX collagen gene expression in human osteoarthritic chondrocytes with epigenetic silencing by DNA hypermethylation', *Arthritis & Rheumatology*, 66(11), pp. 3040–3051. Available at: https://doi.org/https://doi.org/10.1002/art.38774.

Imhof, H. *et al.* (2000) 'Subchondral bone and cartilage disease: a rediscovered functional unit', *Investigative Radiology*, 35(10), pp. 581–588. Available at: https://doi.org/10.1097/00004424-200010000-00004.

Ingolia, N.T. *et al.* (2009) 'Genome-wide analysis in vivo of translation with nucleotide resolution using ribosome profiling', *Science*, 324(5924), pp. 218–223. Available at: https://doi.org/10.1126/science.1168978.

Ismail, H.M. *et al.* (2015) 'Interleukin-1 acts via the JNK-2 signaling pathway to induce aggrecan degradation by human chondrocytes', *Arthritis and Rheumatology*, 67(7), pp. 1826–1836. Available at: https://doi.org/10.1002/art.39099.

Jacobsen, A. *et al.* (2013) 'Analysis of microRNA-target interactions across diverse cancer types', *Nature Structural & Molecular Biology*, 20(11), pp. 1325–1332. Available at: https://doi.org/10.1038/nsmb.2678.

Janssen, L. *et al.* (2016) 'ADAMTS3 activity is mandatory for embryonic lymphangiogenesis and regulates placental angiogenesis', *Angiogenesis*, 19(1), pp. 53–65. Available at: https://doi.org/10.1007/s10456-015-9488-z.

Järvholm, B. *et al.* (2005) 'Age, bodyweight, smoking habits and the risk of severe osteoarthritis in the hip and knee in men', *European Journal of Epidemiology*, 20(6), pp. 537–542. Available at: https://doi.org/10.1007/s10654-005-4263-x.

Jeansonne, B.G. *et al.* (1979) 'Cell-to-cell communication of osteoblasts.', *Journal of Dental Research*, 58(4), pp. 1415–1423. Available at: https://doi.org/10.1177/00220345790580042101.

Jeffries, M.A. *et al.* (2014) 'Genome-wide DNA methylation study identifies significant epigenomic changes in osteoarthritic cartilage', *Arthritis & Rheumatology*, 66(10), pp. 2804–2815. Available at: https://doi.org/https://doi.org/10.1002/art.38762.

Jiang, H. *et al.* (2014) 'Diverse roles of miR-29 in cancer (Review)', *Oncology Reports*, 31(4), pp. 1509–1516. Available at: https://doi.org/10.3892/or.2014.3036.

Johnsen, M. B. *et al.* (2017) 'The causal role of smoking on the risk of hip or knee replacement due to primary osteoarthritis: a Mendelian randomisation analysis of the HUNT study', *Osteoarthritis and Cartilage*, 25(6), pp. 817–823. Available at:

https://doi.org/10.1016/j.joca.2016.12.021.

Johnsen, Marianne Bakke *et al.* (2017) 'The mediating effect of body mass index on the relationship between smoking and hip or knee replacement due to primary osteoarthritis. A population-based cohort study (the HUNT Study)', *PLOS ONE*. Edited by Y. Wang, 12(12), pp. e0190288–e0190288. Available at: https://doi.org/10.1371/journal.pone.0190288.

Johnsen, M.B. *et al.* (2019) 'The association between smoking and knee osteoarthritis in a cohort of Danish patients undergoing knee arthroscopy', *BMC Musculoskeletal Disorders*, 20(1), pp. 1–6. Available at: https://doi.org/10.1186/s12891-019-2518-z.

Jones, S.W. *et al.* (2009) 'The identification of differentially expressed microRNA in osteoarthritic tissue that modulate the production of TNF-α and MMP13', *Osteoarthritis and Cartilage*, 17(4), pp. 464–472. Available at: https://doi.org/https://doi.org/10.1016/j.joca.2008.09.012.

Jordan, J.M. *et al.* (2009) 'Prevalence of hip symptoms and radiographic and symptomatic hip osteoarthritis in African Americans and Caucasians: The Johnston County osteoarthritis project', *Journal of Rheumatology*, 36(4), pp. 809–815. Available at: https://doi.org/10.3899/jrheum.080677.

Kajiura, K. *et al.* (2017) 'Frequent silencing of the candidate tumor suppressor TRIM58 by promoter methylation in early-stage lung adenocarcinoma.', *Oncotarget*, 8(2), pp. 2890–2905. Available at: https://doi.org/10.18632/oncotarget.13761.

Kamekura, S. *et al.* (2005) 'Osteoarthritis development in novel experimental mouse models induced by knee joint instability', *Osteoarthritis and Cartilage*, 13(7), pp. 632–641. Available at: https://doi.org/10.1016/j.joca.2005.03.004.

Kanakis, I. *et al.* (2021) 'Cartilage-specific Cre recombinase transgenes/alleles in the mouse', in *Chondrocytes: Methods and Protocols*, pp. 23–38. Available at: https://doi.org/10.1007/978-1-0716-1119-7_3.

Kang, L. *et al.* (2016) 'MicroRNA-23a-3p promotes the development of osteoarthritis by directly targeting SMAD3 in chondrocytes.', *Biochemical and Biophysical Research Communications*, 478(1), pp. 467–473. Available at: https://doi.org/10.1016/j.bbrc.2016.06.071.

Karaplis, A.C. *et al.* (1994) 'Lethal skeletal dysplasia from targeted disruption of the parathyroid hormone-related peptide gene.', *Genes & Development*, 8(3), pp. 277–289. Available at: https://doi.org/10.1101/gad.8.3.277.

Karlsen, T.A. *et al.* (2014) 'microRNA-140 targets RALA and regulates chondrogenic differentiation of human mesenchymal stem cells by translational enhancement of SOX9 and ACAN.', *Stem Cells and Development*, 23(3), pp. 290–304. Available at: https://doi.org/10.1089/scd.2013.0209.

Karlsson, C. *et al.* (2010) 'Genome-wide expression profiling reveals new candidate genes associated with osteoarthritis', *Osteoarthritis and Cartilage*, 18(4), pp. 581–592. Available at: https://doi.org/https://doi.org/10.1016/j.joca.2009.12.002.

Karsdal, M.A. *et al.* (2008) 'Cartilage degradation is fully reversible in the presence of aggrecanase but not matrix metalloproteinase activity', *Arthritis Research & Therapy*, 10(3), pp. R63–R63. Available at: https://doi.org/10.1186/ar2434.

Kauffman, L. *et al.* (2015) 'Gradual rarefaction of hematopoietic precursors and atrophy in a depleted microRNA 29a, b and c environment', *PLOS ONE*, 10(7), p. e0131981. Available at: https://doi.org/10.1371/journal.pone.0131981. Retracted due to concerns about the ownership of data reported.

Kawamata, T. and Tomari, Y. (2010) 'Making RISC', *Trends in Biochemical Sciences*, 35(7), pp. 368–376. Available at: https://doi.org/10.1016/j.tibs.2010.03.009.

Kawanishi, Y. *et al.* (2014) 'Intra-articular injection of synthetic microRNA-210 accelerates avascular meniscal healing in rat medial meniscal injured model', *Arthritis Research & Therapy*, 16(6), p. 488. Available at: https://doi.org/10.1186/s13075-014-0488-y.

Keeton, M.R. *et al.* (1991) 'Identification of regulatory sequences in the type 1 plasminogen activator inhibitor gene responsive to transforming growth factor beta.', *Journal of Biological Chemistry*, 266(34), pp. 23048–23052. Available at: https://doi.org/10.1016/s0021-9258(18)54461-6.

Kellgren, J.H. and Lawrence, J.S. (1957) 'Radiological assessment of osteo-arthrosis', *Annals of the Rheumatic Diseases*, 16(4), pp. 494–502. Available at: https://doi.org/10.1136/ard.16.4.494.

Kelwick, R., Wagstaff, L., *et al.* (2015) 'Metalloproteinase-dependent and -independent processes contribute to inhibition of breast cancer cell migration, angiogenesis and liver metastasis by a disintegrin and metalloproteinase with thrombospondin motifs-15', *International Journal of Cancer*, 136(4), pp. E14–E26. Available at: https://doi.org/10.1002/ijc.29129.

Kelwick, R., Desanlis, I., *et al.* (2015) 'The ADAMTS (A Disintegrin and Metalloproteinase with Thrombospondin motifs) family', *Genome Biology*, 16(1), p. 113. Available at: https://doi.org/10.1186/s13059-015-0676-3.

Kevorkian, L. *et al.* (2004) 'Expression profiling of metalloproteinases and their inhibitors in cartilage', *Arthritis and Rheumatism*, 50(1), pp. 131–141. Available at: https://doi.org/10.1002/art.11433.

Khayal, L.A. *et al.* (2018) 'Transcriptional profiling of murine osteoblast differentiation based on RNA-seq expression analyses', *Bone*, 113, pp. 29–40. Available at: https://doi.org/https://doi.org/10.1016/j.bone.2018.04.006.

Khetarpal, U. *et al.* (1994) 'Expression and localization of COL2A1 mRNA and type II collagen in human fetal cochlea.', *Hearing Research*, 79(1–2), pp. 59–73. Available at: https://doi.org/10.1016/0378-5955(94)90127-9.

Khvorova, A., Reynolds, A. and Jayasena, S.D. (2003) 'Functional siRNAs and miRNAs exhibit strand bias', *Cell*, 115(2), pp. 209–216. Available at: https://doi.org/10.1016/s0092-8674(03)00801-8.

Kiani, C. *et al.* (2002) 'Structure and function of aggrecan', *Cell Research*, 12(1), pp. 19–32. Available at: https://doi.org/10.1038/sj.cr.7290106.

Kim, D. *et al.* (2019) 'Graph-based genome alignment and genotyping with HISAT2 and HISAT-genotype', *Nature Biotechnology*, 37(8), pp. 907–915. Available at: https://doi.org/10.1038/s41587-019-0201-4.

Kim, J. *et al.* (2004) 'Identification of many microRNAs that copurify with polyribosomes in mammalian neurons', *Proceedings of the National Academy of Sciences*, 101(1), pp. 360–365. Available at: https://doi.org/10.1073/pnas.2333854100.

Kim, K.-I., Park, Y.-S. and Im, G.-I. (2013) 'Changes in the epigenetic status of the SOX-9 promoter in human osteoarthritic cartilage', *Journal of Bone and Mineral Research*, 28(5), pp. 1050–1060. Available at: https://doi.org/https://doi.org/10.1002/jbmr.1843.

Klinger, P. *et al.* (2013) 'The transient chondrocyte phenotype in human osteophytic cartilage: a role of pigment epithelium-derived factor?', *Cartilage*, 4(3), pp. 249–255. Available at: https://doi.org/10.1177/1947603513480809.

Kloppenburg, M. *et al.* (2018) 'Etanercept in patients with inflammatory hand osteoarthritis (EHOA): a multicentre, randomised, double-blind, placebo-controlled trial', *Annals of the Rheumatic Diseases*, 77(12), pp. 1757–1764. Available at: https://doi.org/10.1136/annrheumdis-2018-213202.

Kloppenburg, M. *et al.* (2019) 'Phase IIa, placebo-controlled, randomised study of lutikizumab, an anti-interleukin-1α and anti-interleukin-1β dual variable domain immunoglobulin, in patients with erosive hand osteoarthritis', *Annals of the Rheumatic Diseases*, 78(3), pp. 413–420. Available at: https://doi.org/10.1136/annrheumdis-2018-213336.

Knight, S.W. and Bass, B.L. (2001) 'A role for the RNase III enzyme DCR-1 in RNA interference and germ line development in Caenorhabditis elegans', *Science*, 293(5538), pp. 2269–2271. Available at: http://science.sciencemag.org/content/293/5538/2269.abstract.

Ko, J.-Y. *et al.* (2017) 'MicroRNA-29a counteracts synovitis in knee osteoarthritis pathogenesis by targeting VEGF', *Scientific Reports*, 7(1), pp. 1–14. Available at: https://doi.org/10.1038/s41598-017-03616-w.

Ko, J.-Y.Y. *et al.* (2019) 'MicroRNA-29a mitigates subacromial bursa fibrosis in rotator cuff lesion with shoulder stiffness', *International Journal of Molecular Sciences*, 20(22), p. 5742. Available at: https://doi.org/10.3390/ijms20225742.

Kobayashi, H. *et al.* (2016) 'Biphasic regulation of chondrocytes by Rela through induction of anti-apoptotic and catabolic target genes', *Nature Communications*, 7, p. 13336. Available at: https://doi.org/10.1038/ncomms13336.

Kobayashi, T. *et al.* (2008) 'Dicer-dependent pathways regulate chondrocyte proliferation and differentiation', *Proceedings of the National Academy of Sciences*, 105(6), pp. 1949–1954. Available at: https://doi.org/10.1073/pnas.0707900105.

Kobayashi, T. *et al.* (2015) 'Early postnatal ablation of the microRNA-processing enzyme, Drosha, causes chondrocyte death and impairs the structural integrity of the articular cartilage', *Osteoarthritis and Cartilage*, 23(7), pp. 1214–1220. Available at: https://doi.org/10.1016/j.joca.2015.02.015.

Kolhe, R. *et al.* (2017) 'Gender-specific differential expression of exosomal miRNA in synovial fluid of patients with osteoarthritis', *Scientific Reports*, 7(1), pp. 1–14. Available at: https://doi.org/10.1038/s41598-017-01905-y.

Kong, L. *et al.* (2017) 'Association between smoking and risk of knee osteoarthritis: a systematic review and meta-analysis', *Osteoarthritis and Cartilage*, 25(6), pp. 809–816. Available at: https://doi.org/https://doi.org/10.1016/j.joca.2016.12.020.

Kopańska, M. *et al.* (2017) 'MiRNA expression in the cartilage of patients with osteoarthritis', *Journal of Orthopaedic Surgery and Research*, 12(1), pp. 1–7. Available at: https://doi.org/10.1186/s13018-017-0542-y.

Kosaka, N. *et al.* (2010) 'Secretory mechanisms and intercellular transfer of microRNAs in living cells', *Journal of Biological Chemistry*, 285(23), pp. 17442–17452. Available at: https://doi.org/10.1074/jbc.M110.107821.

Kostopoulou, F. *et al.* (2015) 'MicroRNA-33a regulates cholesterol synthesis and cholesterol efflux-related genes in osteoarthritic chondrocytes', *Arthritis Research & Therapy*, 17(1), p. 42. Available at: https://doi.org/10.1186/s13075-015-0556-y.

Kozomara, A., Birgaoanu, M. and Griffiths-Jones, S. (2019) 'miRBase: from microRNA sequences to function', *Nucleic Acids Research*, 47(D1), pp. D155–D162. Available at: https://doi.org/10.1093/nar/gky1141.

Kozomara, A. and Griffiths-Jones, S. (2014) 'miRBase: annotating high confidence microRNAs using deep sequencing data', *Nucleic Acids Research*, 42(D1), pp. D68–D73. Available at: https://doi.org/10.1093/nar/gkt1181.

Kraus, V.B. *et al.* (2012) 'Effects of intraarticular IL1-Ra for acute anterior cruciate ligament knee injury: a randomized controlled pilot trial (NCT00332254)', *Osteoarthritis and*

Cartilage, 20(4), pp. 271–278. Available at: https://doi.org/10.1016/j.joca.2011.12.009.

Kremer, E.A. *et al.* (2018) 'Interplay between TETs and microRNAs in the adult brain for memory formation', *Scientific Reports*, 8(1), p. 1678. Available at: https://doi.org/10.1038/s41598-018-19806-z.

Kremer Hovinga, J.A. *et al.* (2017) 'Thrombotic thrombocytopenic purpura', *Nature Reviews Disease Primers*, 3(1), pp. 1–17. Available at: https://doi.org/10.1038/nrdp.2017.20.

Ku, J.H. *et al.* (2009) 'Correlation of synovial fluid leptin concentrations with the severity of osteoarthritis', *Clinical Rheumatology*, 28(12), pp. 1431–1435. Available at: https://doi.org/10.1007/s10067-009-1242-8.

Kunisch, E. *et al.* (2016) 'Pro-inflammatory IL-1beta and/or TNF-alpha up-regulate matrix metalloproteases-1 and -3 mRNA in chondrocyte subpopulations potentially pathogenic in osteoarthritis: in situ hybridization studies on a single cell level', *International Journal of Rheumatic Diseases*, 19(6), pp. 557–566. Available at: https://doi.org/10.1111/1756-185x.12431.

Kusano, K. *et al.* (1998) 'Regulation of matrix metalloproteinases (MMP-2, -3, -9, and -13) by interleukin-1 and interleukin-6 in mouse calvaria: assoiation of MMP induciton with bone resporption', *Endocrinology*, 139(3), pp. 1338–1345. Available at: https://doi.org/10.1210/endo.139.3.5818.

Kutz, W.E. *et al.* (2011) 'ADAMTS10 protein interacts with fibrillin-1 and promotes its deposition in extracellular matrix of cultured fibroblasts.', *The Journal of Biological Chemistry*, 286(19), pp. 17156–17167. Available at: https://doi.org/10.1074/jbc.M111.231571.

Kwon, H.M. *et al.* (2020) 'Cigarette smoking and knee osteoarthritis in the elderly: data from the Korean National Health and Nutritional Examination Survey', *Experimental Gerontology*, 133(Nov), p. 110873. Available at: https://doi.org/10.1016/j.exger.2020.110873.

Kwon, J.J. *et al.* (2016) 'Novel role of miR-29a in pancreatic cancer autophagy and its therapeutic potential', *Oncotarget*, 7(44), pp. 71635–71650. Available at: https://doi.org/10.18632/oncotarget.11928.

Kwon, J.J. *et al.* (2018) 'A systematic review of miR-29 in cancer', *Molecular Therapy Oncolytics*, 12(March), pp. 173–194. Available at: https://doi.org/10.1016/j.omto.2018.12.011.

Lai, Y. *et al.* (2014) 'ADAMTS-7 forms a positive feedback loop with TNF-α in the pathogenesis of osteoarthritis', *Annals of the Rheumatic Diseases*, 73(8), pp. 1575–1584. Available at: https://doi.org/10.1136/annrheumdis-2013-203561.

Le, L. *et al.* (2014) 'The microRNA-29 family in osteoarthritis', *Osteoarthritis and Cartilage*, 22(2014), pp. S41–S42. Available at: https://doi.org/10.1016/j.joca.2014.02.097.

Le, L.T.T. (2015) *The roles of the microrna 29 family in cartilage homeostasis and osteoarthritis*.

Le, L.T.T. *et al.* (2016) 'The microRNA-29 family in cartilage homeostasis and osteoarthritis', *Journal of Molecular Medicine*, 94(5), pp. 583–596. Available at: https://doi.org/10.1007/s00109-015-1374-z.

Lee, I. *et al.* (2009) 'New class of microRNA targets containing simultaneous 5'-UTR and 3'-UTR interaction sites', *Genome Research*, 19(7), pp. 1175–1183. Available at: https://doi.org/10.1101/gr.089367.108.

Lee, R.C., Feinbaum, R.L. and Ambros, V. (1993) 'The C. elegans heterochronic gene lin-4 encodes small RNAs with antisense complementarity to lin-14', *Cell*, 75(5), pp. 843–854. Available at: https://doi.org/10.1016/0092-8674(93)90529-Y.

Lee, Y. *et al.* (2002) 'MicroRNA maturation: stepwise processing and subcellular localization', *EMBO Journal*, 21(17), pp. 4663–4670. Available at: https://doi.org/10.1093/emboj/cdf476.

Lee, Y. *et al.* (2003) 'The nuclear RNase III Drosha initiates microRNA processing', *Nature*, 425(6956), pp. 415–419. Available at: https://doi.org/10.1038/nature01957.

Lefebvre, V., Li, P. and de Crombrugghe, B. (1998) 'A new long form of Sox5 (L-Sox5), Sox6 and Sox9 are coexpressed in chondrogenesis and cooperatively activate the type II collagen gene', *The EMBO Journal*, 17(19), pp. 5718–5733. Available at: https://doi.org/https://doi.org/10.1093/emboj/17.19.5718.

Leung, Y.Y. *et al.* (2014) 'Cigarette smoking and risk of total knee replacement for severe osteoarthritis among Chinese in Singapore - the Singapore Chinese health study', *Osteoarthritis and Cartilage*, 22(6), pp. 764–770. Available at: https://doi.org/10.1016/j.joca.2014.03.013.

Lev Maor, G., Yearim, A. and Ast, G. (2015) 'The alternative role of DNA methylation in splicing regulation', *Trends in Genetics*, 31(5), pp. 274–280. Available at: https://doi.org/10.1016/j.tig.2015.03.002.

Lewis, B.P. *et al.* (2003) 'Prediction of mammalian microRNA targets', *Cell*, 115(7), pp. 787–798. Available at: https://doi.org/10.1016/S0092-8674(03)01018-3.

Li, H. *et al.* (2009) 'The sequence alignment/map format and SAMtools', *Bioinformatics*, 25(16), pp. 2078–2079. Available at: https://doi.org/10.1093/bioinformatics/btp352.

Li, J. *et al.* (2012) 'miR-146a, an IL-1β responsive miRNA, induces vascular endothelial growth factor and chondrocyte apoptosis by targeting Smad4', *Arthritis Research & Therapy*, 14(2), p. R75. Available at: https://doi.org/10.1186/ar3798.

Li, L. *et al.* (2017) 'Superficial cells are self-renewing chondrocyte progenitors, which form the articular cartilage in juvenile mice', *FASEB Journal*, 31(3), pp. 1067–1084. Available at: https://doi.org/10.1096/fj.201600918R.

Li, S. and Darwin, J.P. (1995) 'Transgenic mice with targeted for collagen II develop a skeleton with membranous and periosteal bone but no endochondral bone', pp. 2821–2830.

Li, S.W. *et al.* (2001) 'Transgenic mice with inactive alleles for procollagen N-proteinase (ADAMTS-2) develop fragile skin and male sterility', *Biochemical Journal*, 355(2), pp. 271–278. Available at: https://doi.org/10.1042/bj3550271.

Li, X. *et al.* (2016) 'MiR-29a and miR-140 protect chondrocytes against the anti-proliferation and cell matrix signaling changes by IL-1β', *Molecules and Cells*, 39(2), pp. 103–110. Available at: https://doi.org/10.14348/molcells.2016.2179.

Li, Y.H. *et al.* (2016) 'Identification of synovial fluid microRNA signature in knee osteoarthritis: differentiating early- and late-stage knee osteoarthritis', *Osteoarthritis and Cartilage*, 24(9), pp. 1577–1586. Available at: https://doi.org/10.1016/j.joca.2016.04.019.

Li, Z. *et al.* (2018) 'Analysis of gene expression and methylation datasets identified ADAMTS9, FKBP5, and PFKBF3 as biomarkers for osteoarthritis', *Journal of Cellular Physiology*, 234(6), pp. 8908–8917. Available at: https://doi.org/10.1002/jcp.27557.

Lian, W.-S. *et al.* (2018) 'MicroRNA-128a represses chondrocyte autophagy and exacerbates knee osteoarthritis by disrupting Atg12', *Cell Death & Disease*, 9(9), p. 919. Available at: https://doi.org/10.1038/s41419-018-0994-y.

Liang, Z.J. *et al.* (2012) 'MiRNA-140 is a negative feedback regulator of MMP-13 in IL-1β-stimulated human articular chondrocyte C28/I2 cells', *Inflammation Research*, 61(5), pp. 503–509. Available at: https://doi.org/10.1007/s00011-012-0438-6.

Lin, C.-C.C.-C. *et al.* (2011) 'A KLF4-miRNA-206 autoregulatory feedback loop can promote

or inhibit protein translation depending upon cell context', *Molecular and Cellular Biology*, 31(12), pp. 2513–2527. Available at: https://doi.org/10.1128/MCB.01189-10.

Little, C.B. *et al.* (2009) 'Matrix metalloproteinase 13-deficient mice are resistant to osteoarthritic cartilage erosion but not chondrocyte hypertrophy or osteophyte development', *Arthritis and Rheumatism*, 60(12), pp. 3723–3733. Available at: https://doi.org/10.1002/art.25002.

Liu, B. *et al.* (2018) 'Interplay between miRNAs and host genes and their role in cancer', *Briefings in Functional Genomics*, 18(4), pp. 255–266. Available at: https://doi.org/10.1093/bfgp/elz002.

Liu, C.-J. (2009) 'The role of ADAMTS-7 and ADAMTS-12 in the pathogenesis of arthritis', *Nature Clinical Practice Rheumatology*, 5(1), pp. 38–45. Available at: https://doi.org/10.1038/ncprheum0961.

Liu, C. *et al.* (2006) 'ADAMTS-12 associates with and degrades cartilage oligomeric matrix protein.', *The Journal of Biological Chemistry*, 281(23), pp. 15800–15808. Available at: https://doi.org/10.1074/jbc.M513433200.

Liu, H. *et al.* (2017) 'Evaluation of decalcification techniques for rat femurs using HE and immunohistochemical staining', *BioMed Research International*, 2017, p. 9050754. Available at: https://doi.org/10.1155/2017/9050754.

Liu, S.-S.S., Zhou, P. and Zhang, Y. (2016) 'Abnormal expression of key genes and proteins in the canonical Wnt/β-catenin pathway of articular cartilage in a rat model of exercise-induced osteoarthritis', *Molecular Medicine Reports*, 13(3), pp. 1999–2006. Available at: https://doi.org/10.3892/mmr.2016.4798.

Liu, S. *et al.* (2010) 'Sp1/NFκB/HDAC/miR-29b regulatory network in KIT-driven myeloid leukemia', *Cancer Cell*, 17(4), pp. 333–347. Available at: https://doi.org/10.1016/j.ccr.2010.03.008.

Liu, T. *et al.* (2017) 'NF-κB signaling in inflammation', *Signal Transduction and Targeted Therapy*, 2, p. 17023. Available at: https://doi.org/10.1038/sigtrans.2017.23.

Liu, Y. *et al.* (2015) 'Correlation of IL-17 level in synovia and severity of knee osteoarthritis', *Medical Science Monitor*, 21, pp. 1732–1736. Available at: https://doi.org/10.12659/msm.893771.

Livak, K.J. and Schmittgen, T.D. (2001) 'Analysis of relative gene expression data using real-time quantitative PCR and the 2(-Delta Delta C(T)) Method', *Methods*, 25(4), pp. 402–408. Available at: https://doi.org/10.1006/meth.2001.1262.

Lodewyckx, L. and Lories, R.J.U. (2009) 'WNT signaling in osteoarthritis and osteoporosis: What is the biological significance for the clinician?', *Current Rheumatology Reports*, 11(1), pp. 23–30. Available at: https://doi.org/10.1007/s11926-009-0004-6.

Loeser, R.F. (2010) 'Age-related changes in the musculoskeletal system and the development of osteoarthritis', *Clinics in Geriatric Medicine*, 26(3), pp. 371–386. Available at: https://doi.org/10.1016/j.cger.2010.03.002.

Loeser, R.F. *et al.* (2012) 'Osteoarthritis: a disease of the joint as an organ', *Arthritis and Rheumatism*, 64(6), pp. 1697–1707. Available at: https://doi.org/10.1002/art.34453.

Loeser, R.F. *et al.* (2013) 'Disease progression and phasic changes in gene expression in a mouse model of osteoarthritis', *PLOS ONE*, 8(1), pp. e54633–e54633. Available at: https://doi.org/10.1371/journal.pone.0054633.

Loeser, R.F., Collins, J.A. and Diekman, B.O. (2016) 'Ageing and the pathogenesis of osteoarthritis', *Nature Reviews Rheumatology*, 12(7), pp. 412–420. Available at: https://doi.org/10.1038/nrrheum.2016.65.

Long, F. *et al.* (2001) 'Genetic manipulation of hedgehog signaling in the endochondral skeleton reveals a direct role in the regulation of chondrocyte proliferation', *Development*, 128(24), pp. 5099–5108. Available at: https://doi.org/10.1242/dev.128.24.5099.

Lotz, M.K. *et al.* (2010) 'Cartilage cell clusters', *Arthritis and Rheumatism*, pp. 2206–2218. Available at: https://doi.org/10.1002/art.27528.

Louati, K. *et al.* (2015) 'Association between diabetes mellitus and osteoarthritis: systematic literature review and meta-analysis', *RMD Open*, 1(1), p. e000077. Available at: https://doi.org/10.1136/rmdopen-2015-000077.

Love, M.I., Huber, W. and Anders, S. (2014) 'Moderated estimation of fold change and dispersion for RNA-seq data with DESeq2', *Genome Biology*, 15(12), p. 550. Available at: https://doi.org/10.1186/s13059-014-0550-8.

Lu, J. *et al.* (2017) 'MicroRNA-218-5p as a potential target for the treatment of human osteoarthritis', *Molecular Therapy*, 25(12), pp. 2676–2688. Available at: https://doi.org/https://doi.org/10.1016/j.ymthe.2017.08.009.

Luan, Y. *et al.* (2008) 'Inhibition of ADAMTS-7 and ADAMTS-12 degradation of cartilage oligomeric matrix protein by alpha-2-macroglobulin', *Osteoarthritis and Cartilage*, 16(11), pp. 1413–1420. Available at: https://doi.org/10.1016/j.joca.2008.03.017.

Luna, C. *et al.* (2011) 'Cross-talk between miR-29 and transforming growth factor-betas in trabecular meshwork cells', *Investigative Ophthalmology & Visual Science*, 52(6), pp. 3567–3572. Available at: https://doi.org/10.1167/iovs.10-6448.

Lund, E. *et al.* (2004) 'Nuclear export of microRNA precursors', *Science*, 303(5654), pp. 95–98. Available at: http://science.sciencemag.org/content/303/5654/95.abstract.

Luo, Y. *et al.* (2017) 'The minor collagens in articular cartilage', *Protein and Cell*, 8(8), pp. 560–572. Available at: https://doi.org/10.1007/s13238-017-0377-7.

Lv, S. *et al.* (2020) 'MicroRNA-27b targets CBFB to inhibit differentiation of human bone marrow mesenchymal stem cells into hypertrophic chondrocytes', *Stem Cell Research & Therapy*, 11, p. 392. Available at: https://doi.org/10.1186/s13287-020-01909-y.

Lytle, J.R., Yario, T.A. and Steitz, J.A. (2007) 'Target mRNAs are repressed as efficiently by microRNA-binding sites in the 5' UTR as in the 3' UTR', *Proceedings of the National Academy of Sciences of the United States of America*, 104(23), pp. 9667–9672. Available at: https://doi.org/10.1073/pnas.0703820104.

Ma, S., Ouyang, C. and Ren, S. (2018) 'Relationship between ADAMTS14/rs4747096 gene polymorphism and knee osteoarthritis in Chinese population', *Bioscience Reports*, 38(5), p. BSR20181413. Available at: https://doi.org/10.1042/BSR20181413.

Maegdefessel, L. *et al.* (2012) 'Inhibition of microRNA-29b reduces murine abdominal aortic aneurysm development', *The Journal of Clinical Investigation*, 122(2), pp. 497–506. Available at: https://doi.org/10.1172/JCI61598.

Maes, C. *et al.* (2010) 'Osteoblast precursors, but not mature osteoblasts, move into developing and fractured bones along with invading blood vessels', *Developmental Cell*, 19(2), pp. 329–344. Available at: https://doi.org/10.1016/j.devcel.2010.07.010.

Maiese, K. (2016) 'Picking a bone with WISP1 (CCN4): new strategies against degenerative joint disease', *Journal of Translational Science*, 1(3), pp. 83–85. Available at: https://doi.org/10.15761/jts.1000120.

Majidinia, M. *et al.* (2018) 'The roles of Wnt/β-catenin pathway in tissue development and regenerative medicine', *Journal of Cellular Physiology*, 233(8), pp. 5598–5612. Available at: https://doi.org/10.1002/jcp.26265.

Majumdar, M.K. *et al.* (2007) 'Double-knockout of ADAMTS-4 and ADAMTS-5 in mice

results in physiologically normal animals and prevents the progression of osteoarthritis', *Arthritis and Rheumatism*, 56(11), pp. 3670–3674. Available at: https://doi.org/10.1002/art.23027.

Marcu, K.B. *et al.* (2010) 'NF-kappaB signaling: multiple angles to target OA', *Current Drug Targets*, 11(5), pp. 599–613. Available at: https://doi.org/10.2174/138945010791011938.

Maroudas, A., Palla, G. and Gilav, E. (1992) 'Racemization of aspartic acid in human articular cartilage', *Connective Tissue Research*, 28(3), pp. 161–169. Available at: https://doi.org/10.3109/03008209209015033.

Martel-Pelletier, J. *et al.* (2016) 'The levels of the adipokines adipsin and leptin are associated with knee osteoarthritis progression as assessed by MRI and incidence of total knee replacement in symptomatic osteoarthritis patients: A post hoc analysis', *Rheumatology*, 55(4), pp. 680–688. Available at: https://doi.org/10.1093/rheumatology/kev408.

Martinez-Sanchez, A., Dudek, K.A. and Murphy, C.L. (2012) 'Regulation of human chondrocyte function through direct inhibition of cartilage master regulator SOX9 by microRNA-145 (miRNA-145)', *Journal of Biological Chemistry*, 287(2), pp. 916–924. Available at: https://doi.org/10.1074/jbc.M111.302430.

Matsuo, K. and Irie, N. (2008) 'Osteoclast–osteoblast communication', *Archives of Biochemistry and Biophysics*, 473(2), pp. 201–209. Available at: https://doi.org/10.1016/j.abb.2008.03.027.

Maunakea, A.K. *et al.* (2010) 'Conserved role of intragenic DNA methylation in regulating alternative promoters', *Nature*, 466(7303), pp. 253–257. Available at: https://doi.org/10.1038/nature09165.

McDermott, B.T. *et al.* (2019) 'Translational regulation contributes to the secretory response of chondrocytic cells following exposure to interleukin-1β', *Journal of Biological Chemistry*, 294(35), pp. 13027–13039. Available at: https://doi.org/10.1074/jbc.RA118.006865.

Mead, T.J. *et al.* (2018) 'The metalloproteinase-proteoglycans ADAMTS7 and ADAMTS12 provide an innate, tendon-specific protective mechanism against heterotopic ossification', *JCI Insight*, 3(7), p. e92941. Available at: https://doi.org/10.1172/jci.insight.92941.

Meijer, H.A. *et al.* (2013) 'Translational repression and eIF4A2 activity are critical for microRNA-mediated gene regulation', *Science*, 340(6128), pp. 82–85. Available at: https://doi.org/10.1126/science.1231197.

Melchiorri, C. *et al.* (1998) 'Enhanced and coordinated in vivo expression of inflammatory cytokines and nitric oxide synthase by chondrocytes from patients with osteoarthritis', *Arthritis and Rheumatism*, 41(12), pp. 2165–2174. Available at: https://doi.org/10.1002/1529-0131(199812)41:12<2165::aid-art11>3.0.co;2-o.

Memari, F. *et al.* (2018) 'Epigenetics and epi-miRNAs: Potential markers/therapeutics in leukemia', *Biomedicine & Pharmacotherapy*, 106, pp. 1668–1677. Available at: https://doi.org/https://doi.org/10.1016/j.biopha.2018.07.133.

Mendler, M. *et al.* (1989) 'Cartilage contains mixed fibrils of collagen types II, IX, and XI.', *The Journal of Cell Biology*, 108(1), pp. 191–197. Available at: https://doi.org/10.1083/jcb.108.1.191.

Mengshol, J.A. *et al.* (2000) 'Interleukin-1 induction of collagenase 3 (matrix metalloproteinase 13) gene expression in chondrocytes requires p38, c-jun N-terminal kinase, and nuclear factor κB: Differential regulation of collagenase 1 and collagenase 3', *Arthritis and Rheumatism*, 43(4), pp. 801–811. Available at: https://doi.org/10.1002/1529-0131(200004)43:4<801::aid-anr10>3.0.co;2-4.

Mestdagh, P. *et al.* (2011) 'The microRNA body map: Dissecting microRNA function through

integrative genomics', *Nucleic Acids Research*, 39(20), pp. e136–e136. Available at: https://doi.org/10.1093/nar/gkr646.

Miao, G. *et al.* (2019) 'Bax targeted by miR-29a regulates chondrocyte apoptosis in osteoarthritis', *BioMed Research International*. Edited by M. Cucchiarini, 2019, p. 1434538. Available at: https://doi.org/10.1155/2019/1434538.

Millar, N.L. *et al.* (2015) 'MicroRNA29a regulates IL-33-mediated tissue remodelling in tendon disease', *Nature Communications*, 6(1), p. 6774. Available at: https://doi.org/10.1038/ncomms7774.

Miranda-Duarte, A. (2018) 'DNA methylation in osteoarthritis: current status and therapeutic implications', *The Open Rheumatology Journal*, 12, pp. 37–49. Available at: https://doi.org/10.2174/1874312901812010037.

Mitchell, P.G. *et al.* (1996) 'Cloning, expression, and type II collagenolytic activity of matrix metalloproteinase-13 from human osteoarthritic cartilage.', *The Journal of Clinical Investigation*, 97(3), pp. 761–768. Available at: https://doi.org/10.1172/JCI118475.

Mithieux, S.M. and Weiss, A.S. (2005) 'Elastin', in *Advances in Protein Chemistry*, pp. 437–461. Available at: https://doi.org/https://doi.org/10.1016/S0065-3233(05)70013-9.

Miyaki, S. *et al.* (2009) 'MicroRNA-140 is expressed in differentiated human articular chondrocytes and modulates interleukin-1 responses', *Arthritis and Rheumatism*, 60(9), pp. 2723–2730. Available at: https://doi.org/10.1002/art.24745.

Miyaki, S. *et al.* (2010) 'MicroRNA-140 plays dual roles in both cartilage development and homeostasis', *Genes and Development*, 24(11), pp. 1173–1185. Available at: https://doi.org/10.1101/gad.1915510.

Mnatzaganian, G. *et al.* (2013) 'Smoking and primary total hip or knee replacement due to osteoarthritis in 54,288 elderly men and women', *BMC Musculoskeletal Disorders*, 14(1), p. 262. Available at: https://doi.org/10.1186/1471-2474-14-262.

Moncada-Pazos, A. *et al.* (2012) 'ADAMTS-12 metalloprotease is necessary for normal inflammatory response', *Journal of Biological Chemistry*, 287(47), pp. 39554–39563. Available at: https://doi.org/10.1074/jbc.M112.408625.

Monemdjou, R., Fahmi, H. and Kapoor, M. (2010) 'Synovium in the pathophysiology of osteoarthritis', *Therapy*, 7(6), pp. 661–668. Available at: https://doi.org/10.2217/thy.10.72.

Monteys, A.M. *et al.* (2010) 'Structure and activity of putative intronic miRNA promoters', *RNA*, 16(3), pp. 495–505. Available at: https://doi.org/10.1261/rna.1731910.

Morita, S. *et al.* (2013) 'miR-29 represses the activities of DNA methyltransferases and DNA demethylases', *International Journal of Molecular Sciences*, 14(7), pp. 14647–14658. Available at: https://doi.org/10.3390/ijms140714647.

Mott, J.L. *et al.* (2010) 'Transcriptional suppression of mir-29b-1/mir-29a promoter by c-Myc, hedgehog, and NF-kappaB', *Journal of Cellular Biochemistry*, 110(5), pp. 1155–1164. Available at: https://doi.org/10.1002/jcb.22630.

Moulharat, N. *et al.* (2004) 'Effects of transforming growth factor-beta on aggrecanase production and proteoglycan degradation by human chondrocytes in vitro.', *Osteoarthritis and Cartilage*, 12(4), pp. 296–305. Available at: https://doi.org/10.1016/j.joca.2003.11.009.

Mularczyk, E.J. *et al.* (2018) 'ADAMTS10-mediated tissue disruption in Weill-Marchesani syndrome', *Human Molecular Genetics*, 27(21), pp. 3675–3687. Available at: https://doi.org/10.1093/hmg/ddy276.

Munjal, A. *et al.* (2019) 'Advances in molecular biomarker for early diagnosis of osteoarthritis', *Biomolecular Concepts*, 10(1), pp. 111–119. Available at: https://doi.org/10.1515/bmc-2019-0014.

Mustafa, Z. *et al.* (2000) 'Linkage analysis of candidate genes as susceptibility loci for osteoarthritis-suggestive linkage of COL9A1 to female hip osteoarthritis', *Rheumatology*, 39(3), pp. 299–306. Available at: https://doi.org/10.1093/rheumatology/39.3.299.

Musumeci, G. *et al.* (2014) 'Lubricin expression in human osteoarthritic knee meniscus and synovial fluid: A morphological, immunohistochemical and biochemical study', *Acta Histochemica*, 116(5), pp. 965–972. Available at: https://doi.org/10.1016/j.acthis.2014.03.011.

Muthuri, S.G. *et al.* (2011) 'History of knee injuries and knee osteoarthritis: A meta-analysis of observational studies', *Osteoarthritis and Cartilage*, 19(11), pp. 1286–1293. Available at: https://doi.org/10.1016/j.joca.2011.07.015.

Naito, S. *et al.* (2007) 'Expression of ADAMTS4 (aggrecanase-1) in human osteoarthritic cartilage', *Pathology International*, 57(11), pp. 703–711. Available at: https://doi.org/10.1111/j.1440-1827.2007.02167.x.

Nakamura, A. *et al.* (2016) 'Identification of microRNA-181a-5p and microRNA-4454 as mediators of facet cartilage degeneration', *JCI Insight*, 1(12), pp. e86820–e86820. Available at: https://doi.org/10.1172/jci.insight.86820.

Nakamura, Y. *et al.* (2011) 'Chondrocyte-specific microRNA-140 regulates endochondral bone development and targets Dnpep to modulate bone morphogenetic protein signaling', *Molecular and Cellular Biology*, 31(14), pp. 3019–3028. Available at: https://doi.org/10.1128/mcb.05178-11.

Nakamura, Y. *et al.* (2012) 'Sox9 is upstream of microRNA-140 in cartilage', *Applied Biochemistry and Biotechnology*, 166(1), pp. 64–71. Available at: https://doi.org/10.1007/s12010-011-9404-y.

Näkki, A. *et al.* (2010) 'Candidate gene association study of magnetic resonance imaging-based hip osteoarthritis (OA): Evidence for COL9A2 gene as a common predisposing factor for hip OA and lumbar disc degeneration', *The Journal of Rheumatology*, 38(4), pp. 747–752. Available at: https://doi.org/10.3899/jrheum.100080.

Nandadasa, S. *et al.* (2019) 'Secreted metalloproteases ADAMTS9 and ADAMTS20 have a non-canonical role in ciliary vesicle growth during ciliogenesis', *Nature Communications*, 10(1), p. 953. Available at: https://doi.org/10.1038/s41467-019-08520-7.

Neuhold, L.A. *et al.* (2001) 'Postnatal expression in hyaline cartilage of constitutively active human collagenase-3 (MMP-13) induces osteoarthritis in mice', *The Journal of Clinical Investigation*, 107(1), pp. 35–44. Available at: https://doi.org/10.1172/JCI10564.

Nguyen, L.T. *et al.* (2017) 'Review of prospects of biological fluid biomarkers in osteoarthritis', *International Journal of Molecular Sciences*, 18(3), p. 601. Available at: https://doi.org/10.3390/ijms18030601.

Nishimura, R. *et al.* (2020) 'Role of signal transduction pathways and transcription factors in cartilage and joint diseases', *International Journal of Molecular Sciences*, 21(4), p. 1340. Available at: https://doi.org/10.3390/ijms21041340.

Noyce, A.J. *et al.* (2012) 'Meta-analysis of early nonmotor features and risk factors for Parkinson disease', *Annals of Neurology*, 72(6), pp. 893–901. Available at: https://doi.org/https://doi.org/10.1002/ana.23687.

Ntoumou, E. *et al.* (2017) 'Serum microRNA array analysis identifies potential osteoarthritis biomarkers involved in metabolic processes', pp. 1–15. Available at: https://doi.org/10.1186/s13148-017-0428-1.

Nugent, A.E. *et al.* (2009) 'Advanced osteoarthritis in humans is associated with altered collagen VI expression and upregulation of ER-stress markers Grp78 and bag-1', *Journal of Histochemistry and Cytochemistry*, 57(10), pp. 923–931. Available at:

https://doi.org/10.1369/jhc.2009.953893.

O'Brien, J. *et al.* (2018) 'Overview of microRNA biogenesis, mechanisms of actions, and circulation', *Frontiers in Endocrinology*, 9(Aug), pp. 1–12. Available at: https://doi.org/10.3389/fendo.2018.00402.

O'Brien, M.S. and McDougall, J.J. (2019) 'Age and frailty as risk factors for the development of osteoarthritis', *Mechanisms of Ageing and Development*, 180(Jan), pp. 21–28. Available at: https://doi.org/10.1016/j.mad.2019.03.003.

Oettmeier, R., Abendroth, K. and Oettmeier, S. (1989) 'Analyses of the tidemark on human femoral heads. II. Tidemark changes in osteoarthrosis--a histological and histomorphometric study in non-decalcified preparations.', *Acta Morphologica Hungarica*, 37(3–4), pp. 169–180.

Oichi, T. *et al.* (2019) 'Adamts17 is involved in skeletogenesis through modulation of BMP-Smad1/5/8 pathway', *Cellular and Molecular Life Sciences*, 76(23), pp. 4795–4809. Available at: https://doi.org/10.1007/s00018-019-03188-0.

Okano, M. *et al.* (1999) 'DNA methyltransferases Dnmt3a and Dnmt3b are essential for de novo methylation and mammalian development', *Cell*, 99(3), pp. 247–257. Available at: https://doi.org/10.1016/s0092-8674(00)81656-6.

Oliviero, A. *et al.* (2019) 'MicroRNA in osteoarthritis: physiopathology, diagnosis and therapeutic challenge', *British Medical Bulletin*, 130(1), pp. 137–147. Available at: https://doi.org/10.1093/bmb/ldz015.

Olsen, P.H. and Ambros, V. (1999) 'The lin-4 regulatory RNA controls developmental timing in Caenorhabditis elegans by blocking LIN-14 protein synthesis after the initiation of translation', *Developmental Biology*, 216(2), pp. 671–680. Available at: https://doi.org/10.1006/dbio.1999.9523.

Ooi, S.K.T. *et al.* (2007) 'DNMT3L connects unmethylated lysine 4 of histone H3 to de novo methylation of DNA', *Nature*, 448(7154), pp. 714–717. Available at: https://doi.org/10.1038/nature05987.

Papadopoulou, A.S. *et al.* (2015) 'Deficiency of the miR-29a/b-1 cluster leads to ataxic features and cerebellar alterations in mice', *Neurobiology of Disease*, 73, pp. 275–288. Available at: https://doi.org/10.1016/j.nbd.2014.10.006.

Park, Su Jin *et al.* (2013) 'MicroRNA-127-5p regulates matrix metalloproteinase 13 expression and interleukin-1β–induced catabolic effects in human chondrocytes', *Arthritis & Rheumatism*, 65(12), pp. 3141–3152. Available at: https://doi.org/https://doi.org/10.1002/art.38188.

Park, S J, Cheon, E.J. and Kim, H.A. (2013) 'MicroRNA-558 regulates the expression of cyclooxygenase-2 and IL-1β-induced catabolic effects in human articular chondrocytes', *Osteoarthritis and Cartilage*, 21(7), pp. 981–989. Available at: https://doi.org/https://doi.org/10.1016/j.joca.2013.04.012.

Paul, P. *et al.* (2017) 'Interplay between miRNAs and human diseases', *Journal of Cellular Physiology*, 233(3), pp. 2007–2018. Available at: https://doi.org/10.1002/jcp.25854.

Paulissen, G. *et al.* (2012) 'Control of allergen-induced inflammation and hyperresponsiveness by the metalloproteinase ADAMTS-12', *The Journal of Immunology*, 189(8), pp. 4135–4143. Available at: https://doi.org/10.4049/jimmunol.1103739.

Pearle, A.D., Warren, R.F. and Rodeo, S.A. (2005) 'Basic science of articular cartilage and osteoarthritis', *Clinics in Sports Medicine*, 24(1), pp. 1–12. Available at: https://doi.org/10.1016/j.csm.2004.08.007.

Pereira, P.A. *et al.* (2016) 'Recombinant pre-miR-29b for Alzheimer´s disease therapeutics', *Scientific Reports*, 6(1), p. 19946. Available at: https://doi.org/10.1038/srep19946.

Pérez-García, S. *et al.* (2016) 'Healthy and osteoarthritic synovial fibroblasts produce a disintegrin and metalloproteinase with thrombospondin motifs 4, 5, 7, and 12', *The American Journal of Pathology*, 186(9), pp. 2449–2461. Available at: https://doi.org/10.1016/j.ajpath.2016.05.017.

Pfaff, M. *et al.* (1993) 'Integrin and Arg-Gly-Asp dependence of cell adhesion to the native and unfolded triple helix of collagen type VI', *Experimental Cell Research*, 206(1), pp. 167–176. Available at: https://doi.org/https://doi.org/10.1006/excr.1993.1134.

Pickarski, M. *et al.* (2011) 'Molecular changes in articular cartilage and subchondral bone in the rat anterior cruciate ligament transection and meniscectomized models of osteoarthritis', *BMC Musculoskeletal Disorders*, 12(1), p. 197. Available at: https://doi.org/10.1186/1471-2474-12-197.

Poonpet, T. *et al.* (2013) 'ADAMTS14 gene polymorphism associated with knee osteoarthritis in Thai women.', *Genetics and Molecular Research*, 12(4), pp. 5301–5309. Available at: https://doi.org/10.4238/2013.November.7.5.

Pöschl, E. *et al.* (2005) 'DNA methylation is not likely to be responsible for aggrecan down regulation in aged or osteoarthritic cartilage', *Annals of the Rheumatic Diseases*, 64(3), pp. 477–480. Available at: https://doi.org/10.1136/ard.2004.022509.

Poulet, B. *et al.* (2016) 'Connective tissue growth factor deficiency in adult articular cartilage promotes cartilage degeneration at early timepoints in mouse posttraumatic osteoarthritis', *Osteoarthritis and Cartilage*, 24, p. S392. Available at: https://doi.org/10.1016/j.joca.2016.01.705.

Poulsen, E. *et al.* (2019) 'Knee osteoarthritis risk is increased 4-6 fold after knee injury – a systematic review and meta-analysis', *British Journal of Sports Medicine*, 53(23), pp. 1454–1463. Available at: https://doi.org/10.1136/bjsports-2018-100022.

Pratta, Michael A. *et al.* (2003) 'Aggrecan protects cartilage collagen from proteolytic cleavage.', *Journal of Biological Chemistry*, 278(46), pp. 45539–45545. Available at: https://doi.org/10.1074/jbc.m303737200.

Pratta, Michael A *et al.* (2003) 'Induction of aggrecanase 1 (ADAM-TS4) by interleukin-1 occurs through activation of constitutively produced protein', *Arthritis and Rheumatism*, 48(1), pp. 119–133. Available at: https://doi.org/10.1002/art.10726.

Prein, C. and Beier, F. (2019) *ECM signaling in cartilage development and endochondral ossification*, *Vertebrate Skeletal Development*. Available at: https://doi.org/10.1016/bs.ctdb.2018.11.003.

Qin, W. *et al.* (2011) 'TGF-β/Smad3 signaling promotes renal fibrosis by inhibiting miR-29', *Journal of the American Society of Nephrology*, 22(8), pp. 1462–1474. Available at: https://doi.org/10.1681/ASN.2010121308.

Qiu, X. *et al.* (2016) 'Aberrant methylation of TRIM58 in hepatocellular carcinoma and its potential clinical implication.', *Oncology Reports*, 36(2), pp. 811–818. Available at: https://doi.org/10.3892/or.2016.4871.

Quillet, A. *et al.* (2020) 'Improving bioinformatics prediction of microRNA targets by ranks aggregation', *Frontiers in Genetics*, 10(Jan), pp. 1–14. Available at: https://doi.org/10.3389/fgene.2019.01330.

Radin, E.L., Paul, I.L. and Weisser, P.A. (1971) 'Joint lubrication with artificial lubricants', *Arthritis & Rheumatism*, 14(1), pp. 126–129. Available at: https://doi.org/https://doi.org/10.1002/art.1780140116.

Ramirez, F. and Rifkin, D.B. (2009) 'Extracellular microfibrils: contextual platforms for TGFβ and BMP signaling', *Current Opinion in Cell Biology*, 21(5), pp. 616–622. Available at: https://doi.org/https://doi.org/10.1016/j.ceb.2009.05.005.

Ramos, Y.F.M. *et al.* (2014) 'Genes involved in the osteoarthritis process identified through genome wide expression analysis in articular cartilage; the RAAK study', *PLOS ONE*, 9(7), p. e103056. Available at: https://doi.org/10.1371/journal.pone.0103056.

Rasheed, Z. *et al.* (2019) 'MicroRNA-125b-5p regulates IL-1β induced inflammatory genes via targeting TRAF6-mediated MAPKs and NF-κB signaling in human osteoarthritic chondrocytes', *Scientific Reports*, 9(1), p. 6882. Available at: https://doi.org/10.1038/s41598-019-42601-3.

Rauch, F. (2005) 'Bone growth in length and width: the Yin and Yang of bone stability.', *Journal of Musculoskeletal & Neuronal Interactions*, 5(3), pp. 194–201.

Raud, B. *et al.* (2020) 'Level of obesity is directly associated with the clinical and functional consequences of knee osteoarthritis', *Scientific Reports*, 10(1), pp. 1–7. Available at: https://doi.org/10.1038/s41598-020-60587-1.

Raudvere, U. *et al.* (2019) 'g:Profiler: a web server for functional enrichment analysis and conversions of gene lists (2019 update)', *Nucleic Acids Research*, 47(W1), pp. W191–W198. Available at: https://doi.org/10.1093/nar/gkz369.

Reboul, P. *et al.* (1996) 'The new collagenase, collagenase-3, is expressed and synthesized by human chondrocytes but not by synoviocytes. A role in osteoarthritis', *Journal of Clinical Investigation*, 97(9), pp. 2011–2019. Available at: https://doi.org/10.1172/JCI118636.

Reinhart, B.J. *et al.* (2000) 'The 21-nucleotide let-7 RNA regulates developmental timing in Caenorhabditis elegans', *Nature*, 403(6772), pp. 901–906. Available at: https://doi.org/10.1038/35002607.

Remst, D.F.G. *et al.* (2014) 'Gene expression analysis of murine and human osteoarthritis synovium reveals elevation of transforming growth factor β–responsive genes in osteoarthritis-related fibrosis', *Arthritis & Rheumatology*, 66(3), pp. 647–656. Available at: https://doi.org/https://doi.org/10.1002/art.38266.

van der Rest, M. and Mayne, R. (1988) 'Type IX collagen proteoglycan from cartilage is covalently cross-linked to type II collagen.', *Journal of Biological Chemistry*, 263(4), pp. 1615–1618. Available at: https://doi.org/10.1016/s0021-9258(19)77922-8.

Reynard, L.N. (2017) 'Analysis of genetics and DNA methylation in osteoarthritis: What have we learnt about the disease?', *Seminars in Cell & Developmental Biology*, 62, pp. 57–66. Available at: https://doi.org/https://doi.org/10.1016/j.semcdb.2016.04.017.

Riccio, A. *et al.* (1992) 'Transforming growth factor beta 1-responsive element: closely associated binding sites for USF and CCAAT-binding transcription factor-nuclear factor I in the type 1 plasminogen activator inhibitor gene', *Molecular and Cellular Biology*, 12(4), pp. 1846–1855. Available at: https://doi.org/10.1128/mcb.12.4.1846-1855.1992.

Rim, Y.A. and Ju, J.H. (2020) 'The role of fibrosis in osteoarthritis progression.', *Life*, 11(3), p. 1. Available at: https://doi.org/10.3390/life11010003.

Rima, M. *et al.* (2016) 'Protein partners of the calcium channel β subunit highlight new cellular functions', *Biochemical Journal*, 473(13), pp. 1831–1844. Available at: https://doi.org/10.1042/BCJ20160125.

Roach, H.I. *et al.* (2005) 'Association between the abnormal expression of matrix-degrading enzymes by human osteoarthritic chondrocytes and demethylation of specific CpG sites in the promoter regions', *Arthritis and Rheumatism*, 52(10), pp. 3110–3124. Available at: https://doi.org/10.1002/art.21300.

Robertson, I.B. *et al.* (2015) 'Latent TGF-β-binding proteins.', *Matrix Biology : Journal of the International Society for Matrix Biology*, 47, pp. 44–53. Available at: https://doi.org/10.1016/j.matbio.2015.05.005.

Rodriguez-Lopez, J. *et al.* (2009) 'Association of a nsSNP in ADAMTS14 to some

osteoarthritis phenotypes', *Osteoarthritis and Cartilage*, 17(3), pp. 321–327. Available at: https://doi.org/https://doi.org/10.1016/j.joca.2008.07.012.

Rogerson, F.M. *et al.* (2019) 'ADAMTS-9 in mouse cartilage has aggrecanase activity that is distinct from ADAMTS-4 and ADAMTS-5', *International Journal of Molecular Sciences*, 20(3), pp. 1–12. Available at: https://doi.org/10.3390/ijms20030573.

van Rooij, E. *et al.* (2008) 'Dysregulation of microRNAs after myocardial infarction reveals a role of miR-29 in cardiac fibrosis', *Proceedings of the National Academy of Sciences*, 105(35), pp. 13027–13032. Available at: https://doi.org/10.1073/pnas.0805038105.

Rousseau, J.-C.C. *et al.* (2020) 'Association of circulating microRNAs with prevalent and incident knee osteoarthritis in women: The OFELY study', *Arthritis Research and Therapy*, 22(1), p. 2. Available at: https://doi.org/10.1186/s13075-019-2086-5.

Rowan, A.D. (2001) 'Cartilage catabolism in arthritis: factors that influence homeostasis', *Expert Reviews in Molecular Medicine*, 3(17), pp. 1–20. Available at: https://doi.org/10.1017/s1462399401003209.

Ruby, J.G., Jan, C.H. and Bartel, D.P. (2007) 'Intronic microRNA precursors that bypass Drosha processing', *Nature*, 448(7149), pp. 83–86. Available at: https://doi.org/10.1038/nature05983.

Rushton, M.D. *et al.* (2014) 'Characterization of the cartilage DNA methylome in knee and hip osteoarthritis', *Arthritis & Rheumatology*, 66(9), pp. 2450–2460. Available at: https://doi.org/https://doi.org/10.1002/art.38713.

Rutledge, E.A. *et al.* (2019) 'Morphogenesis of the kidney and lung requires branch-tip directed activity of the Adamts18 metalloprotease', *Developmental Biology*, 454(2), pp. 156–169. Available at: https://doi.org/10.1016/j.ydbio.2019.06.012.

Saito, T. and Tanaka, S. (2017) 'Molecular mechanisms underlying osteoarthritis development: Notch and NF-κB', *Arthritis Research & Therapy*, 19(1), p. 94. Available at: https://doi.org/10.1186/s13075-017-1296-y.

Sakai, K. *et al.* (2001) 'Stage-and tissue-specific expression of a Col2a1-Cre fusion gene in transgenic mice', *Matrix Biology*, 19(8), pp. 761–767. Available at: https://doi.org/10.1016/s0945-053x(00)00122-0.

Saklatvala, J. (1986) 'Tumour necrosis factor alpha stimulates resorption and inhibits synthesis of proteoglycan in cartilage', *Nature*, 322(6079), pp. 547–549. Available at: https://doi.org/10.1038/322547a0.

Salis, Z. *et al.* (2022) 'Weight loss is associated with reduced risk of knee and hip replacement: a survival analysis using Osteoarthritis Initiative data', *International Journal of Obesity*, 46(4), pp. 874–884. Available at: https://doi.org/10.1038/s41366-021-01046-3.

Samvelyan, H.J. *et al.* (2020) 'Models of osteoarthritis: relevance and new insights', *Calcified Tissue International*, 109(3), pp. 243–256. Available at: https://doi.org/10.1007/s00223-020-00670-x.

Sandell, L.J. (2009) 'Obesity and osteoarthritis: Is leptin the link?', *Arthritis and Rheumatism*, 60(10), pp. 2858–2860. Available at: https://doi.org/10.1002/art.24862.

Sandmark, H. *et al.* (1999) 'Osteoarthrosis of the knee in men and women in association with overweight, smoking, and hormone therapy', *Annals of the Rheumatic Diseases*, 58(3), pp. 151–155. Available at: https://doi.org/10.1136/ard.58.3.151.

Sandy, J.D. *et al.* (1991) 'Catabolism of aggrecan in cartilage explants. Identification of a major cleavage site within the interglobular domain.', *Journal of Biological Chemistry* , 266(14), pp. 8683–8685. Available at: http://www.jbc.org/content/266/14/8683.abstract.

Sandy, J.D. *et al.* (1992) 'The structure of aggrecan fragments in human synovial fluid.

Evidence for the involvement in osteoarthritis of a novel proteinase which cleaves the Glu 373-Ala 374 bond of the interglobular domain.', *The Journal of Clinical Investigation*, 89(5), pp. 1512–1516. Available at: https://doi.org/10.1172/JCI115742.

Santini, P. *et al.* (2014) 'The inflammatory circuitry of miR-149 as a pathological mechanism in osteoarthritis', *Rheumatology International*, 34(5), pp. 711–716. Available at: https://doi.org/10.1007/s00296-013-2754-8.

Sasser, T.A., Chapman, S.E. and Leevy, W.M. (2012) 'Albira CT wystem/PMOD software protocol for obtaining bone mineral density units using a hydroxyapatite phantom', *Scientific Insights* [Preprint].

Sassi, Y. *et al.* (2017) 'Cardiac myocyte miR-29 promotes pathological remodeling of the heart by activating Wnt signaling', *Nature Communications*, 8(1), p. 1614. Available at: https://doi.org/10.1038/s41467-017-01737-4.

Sato, T. *et al.* (2006) 'Comparative analysis of gene expression profiles in intact and damaged regions of human osteoarthritic cartilage', *Arthritis & Rheumatism*, 54(3), pp. 808–817. Available at: https://doi.org/https://doi.org/10.1002/art.21638.

Scharstuhl, A. *et al.* (2003) 'Reduction of osteophyte formation and synovial thickening by adenoviral overexpression of transforming growth factor β/bone morphogenetic protein inhibitors during experimental osteoarthritis', *Arthritis & Rheumatism*, 48(12), pp. 3442–3451. Available at: https://doi.org/https://doi.org/10.1002/art.11328.

Schett, G. *et al.* (2013) 'Diabetes is an independent predictor for severe osteoarthritis: results from a longitudinal cohort study', *Diabetes Care*, 36(2), pp. 403–409. Available at: https://doi.org/10.2337/dc12-0924.

Schett, G., Dayer, J. and Manger, B. (2016) 'Interleukin-1 function and role in rheumatic disease', *Nature Reviews Rheumatology*, 12(1), pp. 14–24. Available at: https://doi.org/10.1038/nrrheum.2016.166.

Schipani, E. *et al.* (2001) 'Hypoxia in cartilage: HIF-1α is essential for chondrocyte growth arrest and survival', *Genes and Development*, 15(21), pp. 2865–2876. Available at: https://doi.org/10.1101/gad.934301.

Schwarz, D.S. *et al.* (2003) 'Asymmetry in the assembly of the RNAi enzyme complex', *Cell*, 115(2), pp. 199–208. Available at: https://doi.org/10.1016/s0092-8674(03)00759-1.

Scott, J.L. *et al.* (2010) 'Superoxide dismutase downregulation in osteoarthritis progression and end-stage disease', *Annals of the Rheumatic Diseases*, 69(8), pp. 1502–1510. Available at: https://doi.org/10.1136/ard.2009.119966.

Seggerson, K., Tang, L. and Moss, E.G. (2002) 'Two genetic circuits repress the caenorhabditis elegans heterochronic gene lin-28 after translation initiation', *Developmental Biology*, 243(2), pp. 215–225. Available at: https://doi.org/10.1006/dbio.2001.0563.

Séguin, C.A. and Bernier, S.M. (2003) 'TNFα suppresses link protein and type II collagen expression in chondrocytes: Role of MEK1/2 and NF-κB signaling pathways', *Journal of Cellular Physiology*, 197(3), pp. 356–369. Available at: https://doi.org/10.1002/jcp.10371.

Sekiya, I. *et al.* (2000) 'SOX9 enhances aggrecan gene promoter/enhancer activity and is up-regulated by retinoic acid in a cartilage-derived cell line, TC6.', *The Journal of Bological Chemistry*, 275(15), pp. 10738–10744. Available at: https://doi.org/10.1074/jbc.275.15.10738.

Serra, R. *et al.* (1997) 'Expression of a truncated, kinase-defective TGF-beta type II receptor in mouse skeletal tissue promotes terminal chondrocyte differentiation and osteoarthritis', *The Journal of Cell Biology*, 139(2), pp. 541–552. Available at: https://doi.org/10.1083/jcb.139.2.541.

Sesselmann, S. *et al.* (2009) 'DNA methylation is not responsible for p21WAF1/CIP1 down-

regulation in osteoarthritic chondrocytes', *Osteoarthritis and Cartilage*, 17(4), pp. 507–512. Available at: https://doi.org/10.1016/j.joca.2008.09.006.

Shan, Y. *et al.* (2017) 'Increased frequency of peripheral blood follicular helper T cells and elevated serum IL-21 levels in patients with knee osteoarthritis', *Molecular Medicine Reports*, 15(3), pp. 1095–1102. Available at: https://doi.org/10.3892/mmr.2017.6132.

Shen, J. *et al.* (2013) 'Deletion of the transforming growth factor β receptor type II gene in articular chondrocytes leads to a progressive osteoarthritis-like phenotype in mice', *Arthritis and Rheumatism*, 65(12), pp. 3107–3119. Available at: https://doi.org/10.1002/art.38122.

Shen, J. *et al.* (2017) 'DNA methyltransferase 3b regulates articular cartilage homeostasis by altering metabolism', *JCI Insight*, 2(12), p. e93612. Available at: https://doi.org/10.1172/jci.insight.93612.

Shen, J., Li, S. and Chen, D. (2014) 'TGF-β signaling and the development of osteoarthritis', *Bone Research*, 2(1), p. 14002. Available at: https://doi.org/10.1038/boneres.2014.2.

Shetty, A.A. *et al.* (2014) *Articular cartilage: histology and physiology*, *Techniques in Cartilage Repair Surgery*. Available at: https://doi.org/10.1007/978-3-642-41921-8.

Shi, J. *et al.* (2018) 'miR-486-5p is upregulated in osteoarthritis and inhibits chondrocyte proliferation and migration by suppressing SMAD2', *Mol Med Rep*, 18(1), pp. 502–508. Available at: https://doi.org/10.3892/mmr.2018.8931.

Shlopov, B. V. *et al.* (1999) 'Differential patterns of response to doxycycline and transforming growth factor β1 in the down-regulation of collagenases in osteoarthritic and normal human chondrocytes', *Arthritis and Rheumatism*, 42(4), pp. 719–727. Available at: https://doi.org/10.1002/1529-0131(199904)42:4<719::aid-anr15>3.0.co;2-t.

Shoulders, M.D. and Raines, R.T. (2009) 'Collagen structure and stability', *Annual Review of Biochemistry*, 78(1), pp. 929–958. Available at: https://doi.org/10.1146/annurev.biochem.77.032207.120833.

Si, H. *et al.* (2016) 'Expression of miRNA-140 in chondrocytes and synovial fluid of knee joints in patients with osteoarthritis.', *Chinese Medical Sciences Journal*, 31(4), pp. 207–212. Available at: https://doi.org/10.1016/s1001-9294(17)30002-0.

Si, H. -b. B. *et al.* (2017) 'Intra-articular injection of microRNA-140 (miRNA-140) alleviates osteoarthritis (OA) progression by modulating extracellular matrix (ECM) homeostasis in rats', *Osteoarthritis and Cartilage*, 25(10), pp. 1698–1707. Available at: https://doi.org/10.1016/j.joca.2017.06.002.

Sif, S. and Gilmore, T.D. (1994) 'Interaction of the v-Rel oncoprotein with cellular transcription factor Sp1', *Journal of Virology*, 68(11), pp. 7131–7138. Available at: http://jvi.asm.org/content/68/11/7131.abstract.

Silvestri, T. *et al.* (2006) 'Elevated serum levels of soluble interleukin-4 receptor in osteoarthritis', *Osteoarthritis and Cartilage*, 14(7), pp. 717–719. Available at: https://doi.org/10.1016/j.joca.2006.02.015.

Smeriglio, P. *et al.* (2020) 'Inhibition of TET1 prevents the development of osteoarthritis and reveals the 5hmC landscape that orchestrates pathogenesis', *Science Translational Medicine*, 12(539), p. eaax2332. Available at: https://doi.org/10.1126/scitranslmed.aax2332.

Smith, K.M. *et al.* (2012) 'miR-29ab1 deficiency identifies a negative feedback loop controlling Th1 bias that is dysregulated in multiple sclerosis', *The Journal of Immunology*, 189(4), pp. 1567–1576. Available at: https://doi.org/10.4049/jimmunol.1103171.

Smith, M.D. (2011) 'The normal synovium', *The Open Rheumatology Journal*, 5, pp. 100–106. Available at: https://doi.org/10.2174/1874312901105010100.

Snelling, S. *et al.* (2014) 'A gene expression study of normal and damaged cartilage in anteromedial gonarthrosis, a phenotype of osteoarthritis', *Osteoarthritis and Cartilage*, 22(2), pp. 334–343. Available at: https://doi.org/10.1016/j.joca.2013.12.009.

Song, H. and Park, K.-H. (2020) 'Regulation and function of SOX9 during cartilage development and regeneration', *Seminars in Cancer Biology*, 67(Apr), pp. 12–23. Available at: https://doi.org/10.1016/j.semcancer.2020.04.008.

Song, J., Lee, M., *et al.* (2013) 'MicroRNA-181b regulates articular chondrocytes differentiation and cartilage integrity', *Biochemical and Biophysical Research Communications*, 431(2), pp. 210–214. Available at: https://doi.org/https://doi.org/10.1016/j.bbrc.2012.12.133.

Song, J., Kim, D., *et al.* (2013) 'MicroRNA-488 regulates zinc transporter SLC39A8/ZIP8 during pathogenesis of osteoarthritis', *Journal of Biomedical Science*, 20(1), p. 31. Available at: https://doi.org/10.1186/1423-0127-20-31.

Song, R.H. *et al.* (2007) 'Aggrecan degradation in human articular cartilage explants is mediated by both ADAMTS-4 and ADAMTS-5', *Arthritis and Rheumatism*, 56(2), pp. 575–585. Available at: https://doi.org/10.1002/art.22334.

Sophia Fox, A.J., Bedi, A. and Rodeo, S.A. (2009) 'The basic science of articular cartilage: structure, composition, and function', *Sports Health*, 1(6), pp. 461–468. Available at: https://doi.org/10.1177/1941738109350438.

Soul, J. *et al.* (2019) 'SkeletalVis: an exploration and meta-analysis data portal of cross-species skeletal transcriptomics data', *Bioinformatics*, 35(13), pp. 2283–2290. Available at: https://doi.org/10.1093/bioinformatics/bty947.

Später, D. *et al.* (2006) 'Wnt9a signaling is required for joint integrity and regulation of Ihh during chondrogenesis', *Development*, 133(15), pp. 3039–3049. Available at: https://doi.org/10.1242/DEV.02471.

Staal, B. *et al.* (2014) 'Cartilage-specific deletion of Mig-6 results in osteoarthritis-like disorder with excessive articular chondrocyte proliferation', *Proceedings of the National Academy of Sciences of the United States of America*, 111(7), pp. 2590–2595. Available at: https://doi.org/10.1073/pnas.1400744111.

Stannus, O.P. *et al.* (2013) 'Cross-sectional and longitudinal associations between circulating leptin and knee cartilage thickness in older adults', *Annals of the Rheumatic Diseases*, 74(1), pp. 82–88. Available at: https://doi.org/10.1136/annrheumdis-2013-203308.

Stockwell, R.. A. (1967) 'The cell density of human articular and costal cartilage.', *Journal of Anatomy*, 101(Pt 4), pp. 753–763. Available at: https://doi.org/10.1111/(ISSN)1469-7580.

Sun, D. *et al.* (2018) 'MiR-29c reduces the cisplatin resistance of non-small cell lung cancer cells by negatively regulating the PI3K/Akt pathway', *Scientific Reports*, 8(1), p. 8007. Available at: https://doi.org/10.1038/s41598-018-26381-w.

Sun, J.L. *et al.* (2020) 'MicroRNA-29b promotes subchondral bone loss in TMJ osteoarthritis', *Journal of Dental Research*, 99(13), pp. 1469–1477. Available at: https://doi.org/10.1177/0022034520937617.

Swahari, V. *et al.* (2021) 'MicroRNA-29 is an essential regulator of brain maturation through regulation of CH methylation', *Cell Reports*, 35(1), p. 108946. Available at: https://doi.org/10.1016/j.celrep.2021.108946.

Swann, D.A. *et al.* (1985) 'The molecular structure and lubricating activity of lubricin isolated from bovine and human synovial fluids', *Biochemical Journal*, 225(1), pp. 195–201. Available at: https://doi.org/10.1042/bj2250195.

Swingler, T.E. *et al.* (2009) 'Degradome expression profiling in human articular cartilage',

Arthritis Research & Therapy, 11(3), p. R96. Available at: https://doi.org/10.1186/ar2741.

Swingler, T.E. *et al.* (2012) 'The expression and function of microRNAs in chondrogenesis and osteoarthritis', *Arthritis and Rheumatism*, 64(6), pp. 1909–1919. Available at: https://doi.org/10.1002/art.34314.

Swingler, T.E. *et al.* (2019) 'The function of microRNAs in cartilage and osteoarthritis', *Clinical and Experimental Rheumatology*, 37(5), pp. 40–47.

Tabara, H. *et al.* (1999) 'The rde-1 gene, RNA interference, and transposon silencing in C. elegans', *Cell*, 99(2), pp. 123–132. Available at: https://doi.org/10.1016/s0092-8674(00)81644-x.

Tachmazidou, I. *et al.* (2019) 'Identification of new therapeutic targets for osteoarthritis through genome-wide analyses of UK Biobank data', *Nature Genetics*, 51(2), pp. 230–236. Available at: https://doi.org/10.1038/s41588-018-0327-1.

Takayama, K. *et al.* (2015) 'TET2 repression by androgen hormone regulates global hydroxymethylation status and prostate cancer progression', *Nature Communications*, 6(1), p. 8219. Available at: https://doi.org/10.1038/ncomms9219.

Takiguchi, R. *et al.* (2019) 'Modifiable factors associated with symptomatic knee osteoarthritis: The Murakami cohort study', *Maturitas*, 128(Jun), pp. 53–59. Available at: https://doi.org/10.1016/j.maturitas.2019.06.013.

Tan, M., Wu, J. and Cai, Y. (2013) 'Suppression of Wnt signaling by the miR-29 family is mediated by demethylation of WIF-1 in non-small-cell lung cancer', *Biochemical and Biophysical Research Communications*, 438(4), pp. 673–679. Available at: https://doi.org/10.1016/j.bbrc.2013.07.123.

Tardif, G. *et al.* (2009) 'Regulation of the IGFBP-5 and MMP-13 genes by the microRNAs miR-140 and miR-27a in human osteoarthritic chondrocytes', *BMC Musculoskeletal Disorders*, 10(1), p. 148. Available at: https://doi.org/10.1186/1471-2474-10-148.

Taylor, S.E.B. *et al.* (2014) 'A global increase in 5-hydroxymethylcytosine levels marks osteoarthritic chondrocytes', *Arthritis & Rheumatology*, 66(1), pp. 90–100. Available at: https://doi.org/10.1002/art.38200.

Teng, P. *et al.* (2019) 'Nicotine attenuates osteoarthritis pain and matrix metalloproteinase-9 expression via the α7 nicotinic acetylcholine receptor', *The Journal of Immunology*, 203(2), pp. 485–492. Available at: https://doi.org/10.4049/jimmunol.1801513.

Toivanen, A.T. *et al.* (2010) 'Obesity, physically demanding work and traumatic knee injury are major risk factors for knee osteoarthritis-a population-based study with a follow-up of 22 years', *Rheumatology*, 49(2), pp. 308–314. Available at: https://doi.org/10.1093/rheumatology/kep388.

Tortora, G.J. and Derrickson, B. (2017) 'Joints', in *Principles of Anatomy & Physiology*, pp. 225–250. Available at: http://search.ebscohost.com/login.aspx?direct=true&db=cat01883a&AN=uea.003889505&authtype=sso&custid=s8993828&site=eds-live&scope=site.

Tortorella, M.D. *et al.* (1999) 'Purification and cloning of aggrecanase-1: A member of the ADAMTS family of proteins', *Science*, 284(5420), pp. 1664–1666. Available at: https://doi.org/10.1126/science.284.5420.1664.

Troeberg, L. and Nagase, H. (2012) 'Proteases involved in cartilage matrix degradation in osteoarthritis', *Biochimica et Biophysica Acta - Proteins and Proteomics*, 1824(1), pp. 133–145. Available at: https://doi.org/10.1016/j.bbapap.2011.06.020.

Tseng, S., Reddi, A.H. and Di Cesare, P.E. (2009) 'Cartilage oligomeric matrix protein (COMP): A biomarker of arthritis', *Biomarker Insights*, 4(4), pp. 33–44. Available at: https://doi.org/10.4137/bmi.s645.

Tuddenham, L. *et al.* (2006) 'The cartilage specific microRNA-140 targets histone deacetylase 4 in mouse cells', *FEBS Letters*, 580(17), pp. 4214–4217. Available at: https://doi.org/10.1016/j.febslet.2006.06.080.

Turchinovich, A. *et al.* (2011) 'Characterization of extracellular circulating microRNA', *Nucleic Acids Research*, 39(16), pp. 7223–7233. Available at: https://doi.org/10.1093/nar/gkr254.

Tyler, J.A. (1985) 'Articular cartilage cultured with catabolin (pig interleukin 1) synthesizes a decreased number of normal proteoglycan molecules', *The Biochemical Journal*, 227(3), pp. 869–878. Available at: https://doi.org/10.1042/bj2270869.

Tzavlaki, K. and Moustakas, A. (2020) 'TGF-β signaling', *Biomolecules*, 10(3), pp. 1–38. Available at: https://doi.org/10.3390/biom10030487.

Umlauf, D. *et al.* (2010) 'Cartilage biology, pathology, and repair', *Cellular and Molecular Life Sciences*, 67(24), pp. 4197–4211. Available at: https://doi.org/10.1007/s00018-010-0498-0.

Vadon-Le Goff, S., Hulmes, D.J.S.S. and Moali, C. (2015) 'BMP-1/tolloid-like proteinases synchronize matrix assembly with growth factor activation to promote morphogenesis and tissue remodeling', *Matrix Biology*, 44–46, pp. 14–23. Available at: https://doi.org/10.1016/j.matbio.2015.02.006.

Valinezhad Orang, A., Safaralizadeh, R. and Kazemzadeh-Bavili, M. (2014) 'Mechanisms of miRNA-mediated gene regulation from common downregulation to mRNA-specific upregulation', *International Journal of Genomics*, 2014, pp. 1–15. Available at: https://doi.org/10.1155/2014/970607.

Valverde-Franco, G. *et al.* (2016) 'Cartilage-specific deletion of ephrin-B2 in mice results in early developmental defects and an osteoarthritis-like phenotype during aging in vivo', *Arthritis Research & Therapy*, 18(1), p. 65. Available at: https://doi.org/10.1186/s13075-016-0965-6.

Venn, M. and Maroudas, A. (1977) 'Chemical composition and swelling of normal and osteoarthrotic femoral head cartilage.', *Annals of the Rheumatic Diseases*, 36(2), pp. 121–129. Available at: https://doi.org/10.1136/ard.36.2.121.

Verbruggen, G. *et al.* (2012) 'Tumour necrosis factor blockade for the treatment of erosive osteoarthritis of the interphalangeal finger joints: a double blind, randomised trial on structure modification', *Annals of the Rheumatic Diseases*, 71(6), pp. 891–898. Available at: https://doi.org/10.1136/ard.2011.149849.

Verdier, M.P. *et al.* (2005) 'Immunohistochemical analysis of transforming growth factor beta isoforms and their receptors in human cartilage from normal and osteoarthritic femoral heads', *Rheumatology International*, 25(2), pp. 118–124. Available at: https://doi.org/10.1007/s00296-003-0409-x.

Verma, P. and Dalal, K. (2013) 'Serum cartilage oligomeric matrix protein (COMP) in knee osteoarthritis: A novel diagnostic and prognostic biomarker', *Journal of Orthopaedic Research*, 31(7), pp. 999–1006. Available at: https://doi.org/10.1002/jor.22324.

Versus Arthritis (2021) *The state of musculoskeletal health 2021*. Available at: https://www.versusarthritis.org/about-arthritis/data-and-statistics/the-state-of-musculoskeletal-health/.

Viguet-Carrin, S., Garnero, P. and Delmas, P.D. (2006) 'The role of collagen in bone strength', *Osteoporosis International*, 17(3), pp. 319–336. Available at: https://doi.org/10.1007/s00198-005-2035-9.

Vincent, T.L. and Watt, F.E. (2022) 'Osteoarthritis', *Medicine*, 50(2), pp. 116–124. Available at: https://doi.org/10.1016/j.mpmed.2021.11.009.

Vizard, D.L. *et al.* (2010) 'Analytical radiography for planar radiographic images implemented with a multi-modal system', *Computer Methods and Programs in Biomedicine*, 99(1), pp. 88–97. Available at: https://doi.org/10.1016/j.cmpb.2010.01.003.

Voinnet, O. (2009) 'Origin, biogenesis, and activity of plant microRNAs', *Cell*, 136(4), pp. 669–687. Available at: https://doi.org/10.1016/j.cell.2009.01.046.

Vonk, L.A. *et al.* (2014) 'Overexpression of hsa-miR-148a promotes cartilage production and inhibits cartilage degradation by osteoarthritic chondrocytes', *Osteoarthritis and Cartilage*, 22(1), pp. 145–153. Available at: https://doi.org/https://doi.org/10.1016/j.joca.2013.11.006.

Wan, L. *et al.* (2018) 'Plasma miR-136 can be used to screen patients with knee osteoarthritis from healthy controls by targeting IL-17', *Experimental and Therapeutic Medicine*, 16(4), pp. 3419–3424. Available at: https://doi.org/10.3892/etm.2018.6625.

Wang, B. *et al.* (2012) 'Suppression of microRNA-29 expression by TGF-β1 promotes collagen expression and renal fibrosis', *Journal of the American Society of Nephrology*, 23(2), pp. 252–265. Available at: https://doi.org/10.1681/ASN.2011010055.

Wang, H. *et al.* (2008) 'NF-κB-YY1-miR-29 regulatory circuitry in skeletal myogenesis and rhabdomyosarcoma', *Cancer Cell*, 14(5), pp. 369–381. Available at: https://doi.org/10.1016/j.ccr.2008.10.006.

Wang, Haidong *et al.* (2019) 'Exosome-mediated miR-29 transfer reduces muscle atrophy and kidney fibrosis in mice', *Molecular Therapy*, 27(3), pp. 571–583. Available at: https://doi.org/https://doi.org/10.1016/j.ymthe.2019.01.008.

Wang, Haiming *et al.* (2019) 'Prediction of microRNA and gene target in synovium-associated pain of knee osteoarthritis based on canonical correlation analysis', *BioMed Research International*, 2019, p. 4506876. Available at: https://doi.org/10.1155/2019/4506876.

Wang, J.H. *et al.* (2013) 'Histone deacetylase inhibitors increase microRNA-146a expression and enhance negative regulation of interleukin-1β signaling in osteoarthritis fibroblast-like synoviocytes', *Osteoarthritis and Cartilage*, 21(12), pp. 1987–1996. Available at: https://doi.org/https://doi.org/10.1016/j.joca.2013.09.008.

Wang, X. *et al.* (2018) 'Integrated bioinformatics analysis of the osteoarthritis-associated microRNA expression signature', *Molecular Medicine Reports*, 17(1), pp. 1833–1838. Available at: https://doi.org/10.3892/mmr.2017.8057.

Wang, X.B. *et al.* (2019) 'MicroRNA-21-5p as a novel therapeutic target for osteoarthritis', *Rheumatology*, 58(8), pp. 1485–1497. Available at: https://doi.org/10.1093/rheumatology/kez102.

Wang, Y. *et al.* (2019) 'Wnt signaling: a promising target for osteoarthritis therapy', *Cell Communication and Signaling*, 17(1), pp. 1–14. Available at: https://doi.org/10.1186/s12964-019-0411-x.

Watanabe, H., Yamada, Y. and Kimata, K. (1998) 'Roles of aggrecan, a large chondroitin sulfate proteoglycan, in cartilage structure and function', *Journal of Biochemistry*, 124(4), pp. 687–693. Available at: https://doi.org/10.1093/oxfordjournals.jbchem.a022166.

Watts, A.E. *et al.* (2017) 'MicroRNA29a treatment improves early tendon injury', *Molecular Therapy*, 25(10), pp. 2415–2426. Available at: https://doi.org/10.1016/j.ymthe.2017.07.015.

Wei, C. *et al.* (2021) 'LncRNA NONMMUT055714 acts as the sponge of microRNA-7684-5p to protect against postoperative cognitive dysfunction', *Aging*, 13(9), pp. 12552–12564. Available at: https://doi.org/10.18632/aging.202932.

Wei, J.-L. *et al.* (2018) 'Role of ADAMTS-12 in protecting against inflammatory arthritis in mice by interacting with and inactivating proinflammatory connective tissue growth factor',

Arthritis & Rheumatology, 70(11), pp. 1745–1756. Available at: https://doi.org/10.1002/art.40552.

Westerhausen, D.R., Hopkins, W.E. and Billadello, J.J. (1991) 'Multiple transforming growth factor-beta-inducible elements regulate expression of the plasminogen activator inhibitor type-1 gene in Hep G2 cells', *Journal of Biological Chemistry*, 266(2), pp. 1092–1100. Available at: https://doi.org/10.1016/s0021-9258(17)35287-0.

Westling, J. *et al.* (2002) 'ADAMTS4 cleaves at the aggrecanase site (Glu373-Ala374) and secondarily at the matrix metalloproteinase site (Asn341-Phe342) in the aggrecan interglobular domain', *Journal of Biological Chemistry*, 277(18), pp. 16059–16066. Available at: https://doi.org/10.1074/jbc.m108607200.

WHO (2016) *Chronic rheumatic conditions*, *WHO*. Available at: http://www.who.int/chp/topics/rheumatic/en/ (Accessed: 18 January 2018).

Wilder, F.V. V, Hall, B.J.J. and Barrett, J.P.P. (2003) 'Smoking and osteoarthritis: Is there an association? The Clearwater Osteoarthritis Study', *Osteoarthritis and Cartilage*, 11(1), pp. 29–35. Available at: https://doi.org/10.1053/joca.2002.0857.

Wojdasiewicz, P., Poniatowski, Ł.A. and Szukiewicz, D. (2014) 'The role of inflammatory and anti-inflammatory cytokines in the pathogenesis of osteoarthritis.', *Mediators of Inflammation*, 2014, p. 561459. Available at: https://doi.org/10.1155/2014/561459.

Wu, J. *et al.* (2017) 'Effect of the interaction between MiR-200b-3p and DNMT3A on cartilage cells of osteoarthritis patients.', *Journal of Cellular and Molecular Medicine*, 21(10), pp. 2308–2316. Available at: https://doi.org/10.1111/jcmm.13152.

Wu, Z. *et al.* (2020) 'The methylation pattern for knee and hip osteoarthritis', *Frontiers in Cell and Developmental Biology*, p. 602024. Available at: https://www.frontiersin.org/article/10.3389/fcell.2020.602024.

Wünnemann, F. *et al.* (2020) 'Loss of ADAMTS19 causes progressive non-syndromic heart valve disease', *Nature Genetics*, 52(1), pp. 40–47. Available at: https://doi.org/10.1038/s41588-019-0536-2.

Xia, S., Yan, K. and Wang, Y. (2016) 'Increased miR-381a-3p contributes to osteoarthritis by targeting IkBα', *Annals of Clinical & Laboratory Science*, 46(3), pp. 247–253. Available at: http://www.annclinlabsci.org/content/46/3/247.abstract.

Xiao, J. *et al.* (2012) 'miR-29 inhibits bleomycin-induced pulmonary fibrosis in mice', *Molecular Therapy*, 20(6), pp. 1251–1260. Available at: https://doi.org/https://doi.org/10.1038/mt.2012.36.

Xie, W. *et al.* (2019) 'Synovial fluid microRNA-210 as a potential biomarker for early prediction of osteoarthritis.', *BioMed Research International*, 2019, p. 7165406. Available at: https://doi.org/10.1155/2019/7165406.

Xu, B. *et al.* (2016) 'Roles of microRNA and signaling pathway in osteoarthritis pathogenesis', *Journal of Zhejiang University. Science. B*, 17(3), pp. 200–208. Available at: https://doi.org/10.1631/jzus.B1500267.

Xu, L. *et al.* (2009) 'Early-onset osteoarthritis of mouse temporomandibular joint induced by partial discectomy', *Osteoarthritis and Cartilage*, 17(7), pp. 917–922. Available at: https://doi.org/10.1016/j.joca.2009.01.002.

Xu, W. *et al.* (2014) 'Identifying microRNA targets in different gene regions', *BMC Bioinformatics*, 15(Suppl 7), pp. 6–8. Available at: https://doi.org/10.1186/1471-2105-15-S7-S4.

Xue, J. *et al.* (2013) 'Tumor necrosis factor-α induces ADAMTS-4 expression in human osteoarthritis chondrocytes', *Molecular Medicine Reports*, 8(6), pp. 1755–1760. Available at: https://doi.org/10.3892/mmr.2013.1729.

Xue, M. *et al.* (2016) 'The treatment of fibrosis of joint synovium and frozen shoulder by Smad4 gene silencing in rats', *PLOS ONE*, 11(6), p. e0158093. Available at: https://doi.org/10.1371/journal.pone.0158093.

Yamamoto, K. *et al.* (2013) 'LRP-1-mediated endocytosis regulates extracellular activity of ADAMTS-5 in articular cartilage', *FASEB Journal*, 27(2), pp. 511–521. Available at: https://doi.org/10.1096/fj.12-216671.

Yamamoto, K. *et al.* (2014) 'Low density lipoprotein receptor-related protein 1 (LRP1)-mediated endocytic clearance of a disintegrin and metalloproteinase with thrombospondin motifs-4 (ADAMTS-4): functional differences of non-catalytic domains of ADAMTS-4 and ADAMTS-5 in LRP1 binding', *Journal of Biological Chemistry*, 289(10), pp. 6462–6474. Available at: https://doi.org/10.1074/jbc.M113.545376.

Yamamoto, K. *et al.* (2016) 'MMP-13 is constitutively produced in human chondrocytes and co-endocytosed with ADAMTS-5 and TIMP-3 by the endocytic receptor LRP1', *Matrix Biology*, 56, pp. 57–73. Available at: https://doi.org/https://doi.org/10.1016/j.matbio.2016.03.007.

Yamamoto, K. *et al.* (2017) 'Inhibition of shedding of low-density lipoprotein receptor-related protein 1 reverses cartilage matrix degradation in osteoarthritis', *Arthritis and Rheumatology*, 69(6), pp. 1246–1256. Available at: https://doi.org/10.1002/art.40080.

Yamamoto, K., Wilkinson, D. and Bou-Gharios, G. (2021) 'Targeting dysregulation of metalloproteinase activity in osteoarthritis', *Calcified Tissue International*, 109(3), pp. 277–290. Available at: https://doi.org/10.1007/s00223-020-00739-7.

Yamanishi, Y. *et al.* (2002) 'Expression and regulation of aggrecanase in arthritis: the role of TGF-β', *The Journal of Immunology*, 168(3), pp. 1405–1412. Available at: https://doi.org/10.4049/jimmunol.168.3.1405.

Yan, C. *et al.* (2011) 'MicroRNA regulation associated chondrogenesis of mouse MSCs grown on polyhydroxyalkanoates', *Biomaterials*, 32(27), pp. 6435–6444. Available at: https://doi.org/10.1016/j.biomaterials.2011.05.031.

Yan, X., Xiong, X. and Chen, Y.-G. (2017) 'Feedback regulation of TGF-β signaling', *Acta Biochimica et Biophysica Sinica*, 50(1), pp. 37–50. Available at: https://doi.org/10.1093/abbs/gmx129.

Yang, B. *et al.* (2011) 'MicroRNA-145 regulates chondrogenic differentiation of mesenchymal stem cells by targeting SOX9', *PLOS ONE*. Edited by R. Linden, 6(7), p. e21679. Available at: https://doi.org/10.1371/journal.pone.0021679.

Yang, C.Y.-Y., Chanalaris, A. and Troeberg, L. (2017) 'ADAMTS and ADAM metalloproteinases in osteoarthritis – looking beyond the "usual suspects"', *Osteoarthritis and Cartilage*, 25(7), pp. 1000–1009. Available at: https://doi.org/10.1016/j.joca.2017.02.791.

Yang, J. *et al.* (2011) 'MiR-140 is co-expressed with Wwp2-C transcript and activated by Sox9 to target Sp1 in maintaining the chondrocyte proliferation', *FEBS Letters*, 585(19), pp. 2992–2997. Available at: https://doi.org/10.1016/j.febslet.2011.08.013.

Yang, S. *et al.* (2010) 'Conserved vertebrate mir-451 provides a platform for Dicer-independent, Ago2-mediated microRNA biogenesis', *Proceedings of the National Academy of Sciences of the United States of America*, 107(34), pp. 15163–15168. Available at: https://doi.org/10.1073/pnas.1006432107.

Yang, X. *et al.* (2001) 'TGF-β/SMAD3 signals repress chondrocyte hypertrophic differentiation and are required for maintaining articular cartilage', *The Journal of Cell Biology*, 153(1), pp. 35–46. Available at: http://jcb.rupress.org/content/153/1/35.abstract.

Yang, X. *et al.* (2016) 'Mechanical and IL-1β responsive miR-365 contributes to

osteoarthritis development by targeting histone deacetylase 4', *International Journal of Molecular Sciences*, p. 436. Available at: https://doi.org/10.3390/ijms17040436.

Yang, X. *et al.* (2017) 'Effect of nicotine on the proliferation and chondrogenic differentiation of the human Wharton's jelly mesenchymal stem cells', *Bio-Medical Materials and Engineering*, 28(s1), pp. S217–S228. Available at: https://doi.org/10.3233/bme-171644.

Yasuda, E. *et al.* (2018) 'Association between the severity of symptomatic knee osteoarthritis and cumulative metabolic factors', *Aging Clinical and Experimental Research*, 30(5), pp. 481–488. Available at: https://doi.org/10.1007/s40520-017-0808-6.

Yates, A.D. *et al.* (2020) 'Ensembl 2020', *Nucleic Acids Research*, 48(D1), pp. D682–D688. Available at: https://doi.org/10.1093/nar/gkz966.

Yaykasli, K.O. *et al.* (2014) 'Leptin induces ADAMTS-4, ADAMTS-5, and ADAMTS-9 genes expression by mitogen-activated protein kinases and NF-κB signaling pathways in human chondrocytes', *Cell Biology International*, 39(1), pp. 104–112. Available at: https://doi.org/10.1002/cbin.10336.

Yin, X., Wang, J. and Yan, S. (2017) 'Reduced miR-26a and miR-26b expression contributes to the pathogenesis of osteoarthritis via the promotion of p65 translocation', *Mol Med Rep*, 15(2), pp. 551–558. Available at: https://doi.org/10.3892/mmr.2016.6035.

Ying, X. *et al.* (2012) 'Nicotine promotes proliferation and collagen synthesis of chondrocytes isolated from normal human and osteoarthritis patients', *Molecular and Cellular Biochemistry*, 359(1–2), pp. 263–269. Available at: https://doi.org/10.1007/s11010-011-1020-1.

Yoon, S.W. *et al.* (2008) 'α-MSH inhibits TNF-α-induced matrix metalloproteinase-13 expression by modulating p38 kinase and nuclear factor κB signaling in human chondrosarcoma HTB-94 cells', *Osteoarthritis and Cartilage*, 16(1), pp. 115–124. Available at: https://doi.org/10.1016/j.joca.2007.05.026.

Yu, Q. and Stamenkovic, I. (2000) 'Cell surface-localized matrix metalloproteinase-9 proteolytically activates TGF-β and promotes tumor invasion and angiogenesis', *Genes & Development* , 14(2), pp. 163–176. Available at: http://genesdev.cshlp.org/content/14/2/163.abstract.

Yuasa, T. *et al.* (2008) 'Wnt/β-catenin signaling stimulates matrix catabolic genes and activity in articular chondrocytes: its possible role in joint degeneration', *Laboratory Investigation*, 88(3), pp. 264–274. Available at: https://doi.org/10.1038/labinvest.3700747.

Zeng, G.Q. *et al.* (2015) 'High MMP-1, MMP-2, and MMP-9 protein levels in osteoarthritis.', *Genetics and Molecular Research*, 14(4), pp. 14811–14822. Available at: https://doi.org/10.4238/2015.November.18.46.

Zeng, W. *et al.* (2006) 'Glycosaminoglycan-binding properties and aggrecanase activities of truncated ADAMTSs: Comparative analyses with ADAMTS-5, -9, -16 and -18', *Biochimica et Biophysica Acta - General Subjects*, 1760(3), pp. 517–524. Available at: https://doi.org/10.1016/j.bbagen.2006.01.013.

Zhai, G., Doré, J. and Rahman, P. (2015) 'TGF-β signal transduction pathways and osteoarthritis', *Rheumatology International*, 35(8), pp. 1283–1292. Available at: https://doi.org/10.1007/s00296-015-3251-z.

Zhang, D. *et al.* (2015) 'MiR-210 inhibits NF-κB signaling pathway by targeting DR6 in osteoarthritis', *Scientific Reports*, 5(1), p. 12775. Available at: https://doi.org/10.1038/srep12775.

Zhang, G. *et al.* (2020) 'Inhibition of microRNA-27b-3p relieves osteoarthritis pain via regulation of KDM4B-dependent DLX5.', *BioFactors*, 46(5), pp. 788–802. Available at: https://doi.org/10.1002/biof.1670.

Zhang, J. *et al.* (2018) 'Oncogenic role of microRNA-532-5p in human colorectal cancer via targeting of the 5'UTR of RUNX3', *Oncology Letters*, 15(5), pp. 7215–7220. Available at: https://doi.org/10.3892/ol.2018.8217.

Zhang, L. *et al.* (2021) 'Knockdown of hsa_circ_0134111 alleviates the symptom of osteoarthritis via sponging microRNA-224-5p', *Cell Cycle*, 20(11), pp. 1052–1066. Available at: https://doi.org/10.1080/15384101.2021.1919838.

Zhang, Y. *et al.* (1994) 'Positional cloning of the mouse obese gene and its human homologue', *Nature*, 372(6505), pp. 425–432. Available at: https://doi.org/10.1038/372425a0.

Zhang, Y. *et al.* (2014) 'MicroRNA-21 controls the development of osteoarthritis by targeting GDF-5 in chondrocytes', *Experimental & Molecular Medicine*, 46(2), pp. e79–e79. Available at: https://doi.org/10.1038/emm.2013.152.

Zhang, Z. *et al.* (2011) 'Uracils at nucleotide position 9-11 are required for the rapid turnover of miR-29 family', *Nucleic Acids Research*, 39(10), pp. 4387–4395. Available at: https://doi.org/10.1093/nar/gkr020.

Zhang, Z. *et al.* (2015) 'MiR-455-3p regulates early chondrogenic differentiation via inhibiting Runx2', *FEBS Letters*, 589(23), pp. 3671–3678. Available at: https://doi.org/10.1016/j.febslet.2015.09.032.

Zhao, C. *et al.* (2019) 'MicroRNA-29b regulates hypertrophy of murine mesenchymal stem cells induced toward chondrogenesis', *Journal of Cellular Biochemistry*, 120(5), pp. 8742–8753. Available at: https://doi.org/10.1002/jcb.28161.

Zhao, Q. *et al.* (1997) 'Parallel expression of Sox9 and Col2a1 in cells undergoing chondrogenesis', *Developmental Dynamics*, 209(4), pp. 377–386. Available at: https://doi.org/10.1002/(SICI)1097-0177(199708)209:4<377::AID-AJA5>3.0.CO;2-F.

Zhao, Z. *et al.* (2019) 'MicroRNA-26a reduces synovial inflammation and cartilage injury in osteoarthritis of knee joints through impairing the NF-κB signaling pathway', *Bioscience Reports*, 39(4), p. BSR20182025. Available at: https://doi.org/10.1042/BSR20182025.

Zhen, G. *et al.* (2013) 'Inhibition of TGF-β signaling in mesenchymal stem cells of subchondral bone attenuates osteoarthritis', *Nature Medicine*, 19(6), pp. 704–712. Available at: https://doi.org/10.1038/nm.3143.

Zheng, J., Luo, W. and Tanzer, M.L. (1998) 'Aggrecan synthesis and secretion. A paradigm for molecular and cellular coordination of multiglobular protein folding and intracellular trafficking', *Journal of Biological Chemistry*, 273(21), pp. 12999–13006. Available at: https://doi.org/10.1074/jbc.273.21.12999.

Zheng, W.D. *et al.* (2018) 'Investigation for the role of CTX-III and microRNA-98 in diagnosis and treatment of osteoarthritis', *European Review for Medical and Pharmacological Sciences*, 22(17), pp. 5424–5428. Available at: https://doi.org/10.26355/eurrev_201809_15801.

Zheng, X. *et al.* (2017) 'Downregulation of miR-221-3p contributes to IL-1β-induced cartilage degradation by directly targeting the SDF1/CXCR4 signaling pathway', *Journal of Molecular Medicine*, 95(6), pp. 615–627. Available at: https://doi.org/10.1007/s00109-017-1516-6.

Zhou, J. and Rossi, J. (2017) 'Aptamers as targeted therapeutics: current potential and challenges', *Nature Reviews Drug Discovery*, 16(3), pp. 181–202. Available at: https://doi.org/10.1038/nrd.2016.199.

Zhou, N. *et al.* (2015) 'HIF-1α as a regulator of BMP2-induced chondrogenic differentiation, osteogenic differentiation, and endochondral ossification in stem cells', *Cellular Physiology and Biochemistry*, 36(1), pp. 44–60. Available at: https://doi.org/10.1159/000374052.

Zhou, Y. *et al.* (2017) 'Wnt/β-catenin signaling in osteoarthritis and in other forms of arthritis', *Current Rheumatology Reports*, 19(9), p. 53. Available at: https://doi.org/10.1007/s11926-017-0679-z.

Zhou, Y. *et al.* (2020) 'Identification of differentially expressed miRNAs and mRNAs in synovial of osteoarthritis via RNA-sequencing', *BMC Medical Genetics*, 21(1), p. 46. Available at: https://doi.org/10.1186/s12881-020-0978-5.

Zhu, M. *et al.* (2008) 'Inhibition of β-catenin signaling in articular chondrocytes results in articular cartilage destruction', *Arthritis and Rheumatism*, 58(7), pp. 2053–2064. Available at: https://doi.org/10.1002/art.23614.

Zhu, M. *et al.* (2009) 'Activation of β-catenin signaling in articular chondrocytes leads to osteoarthritis-like phenotype in adult β-catenin conditional activation mice', *Journal of Bone and Mineral Research*, pp. 12–21. Available at: https://doi.org/10.1359/jbmr.080901.

Zhu, Y. *et al.* (2015) 'Transforming growth factor-β1 induces type II collagen and aggrecan expression via activation of extracellular signal-regulated kinase 1/2 and Smad2/3 signaling pathways', *Molecular Medicine Reports*, 12(4), pp. 5573–5579. Available at: https://doi.org/10.3892/mmr.2015.4068.

Ziller, M.J. *et al.* (2011) 'Genomic distribution and inter-sample variation of non-CpG methylation across human cell types', *PLOS Genetics*, 7(12), p. e1002389. Available at: https://doi.org/10.1371/journal.pgen.1002389.

Appendix

Appendix table 1. ADAMTS 3'-UTR cloning and mutagenesis primers.

Gene	Primer	Sequence (5' - 3')
ADAMTS2	2.1 Forward	GCTCGCTAGCCTCGAAGAACTAAAGGCCTTCTGACC
	2.1 Reverse	CGACTCTAGACTCGACATGTGCAGCCTCAGACAAA
	2.1 Mutant site 1	AGACATTCAGATGCCGTACAGCATGGAATTCAAGAAGGTCA GAAGGCCTTTAGTTC
	2.1 Mutant site 2	ACAGGGGAGAGGCCTGGGAGGAATTCCCACTGTTTTCTTGG CATGG
	2.1 Mutant site 3	CTATTTCTCTCTTACTCGCATGTTGCTCACAAGAATTCATTCT CTGGAAAATAGGAGCTATTAAAGTTTTC
	2.1 Mutant site 4	ATGTGCAGCCTCAGACAAACATACTTATTGAATTCTCAAAACT CAGTAGAAGGTAGCCACTATG
	2.2 Forward	GCTCGCTAGCCTCGAACTGGAGAAAACCTTTCTGAGT
	2.2 Reverse	CGACTCTAGACTCGAAGCCAGAATTTTGTGATTTGAGT
	2.2 Mutant site 1	GCCCAGTTCTTCAGCCTGTGAATGAATTCAGCTGTCCTGGGT TCAACCAACA
	2.2 Mutant site 2	TCATAAACTGCTTCATCTGCTAAGATGTTGCTATTGGAATTCA TGTATATACTCAAAACAAACAGAAAAACCTTAAAAT
	2.2 Mutant site 3	CTCGAAGCCAGAATTTTGTGATTTGAGTTCGAATTCTTGATTC AGTATAGTGGCTACCTGTCATAC
ADAMTS5	Forward	GCTCGCTAGCCTCGAGTGGCTTCAACTAACTGGACC
	Reverse	CGACTCTAGACTCGATGCTGAGGACTTAGTGAATGC
	Mutant site 1	GACAGTCGGTCACGAAAGATGTTGTCGACTCAATAAAAATTA GAATTGTTCATTGGGTGTG
ADAMTS7	Forward	GCTCGCTAGCCTCGACGACCGACAGACCTCAGTG
	Reverse	CGACTCTAGACTCGAGCTTTGGAATGGTAGATGCTCA
	Mutant site 1	TGAGAGGGGGTTGTCGACATTAGGGCGCAGGGGGCGGG
ADAMTS9	Forward	GCTCGCTAGCCTCGACTAAGGTGCTTTGAAGAGGA
	Reverse	CGACTCTAGACTCGAGGTAAAGAGCTGGTCTTATTTC
	Mutant site 1	CATCCATAATGGCTTCCTCTTCAAGAATTCTTAGTCGAGGCT AGCGAGCTCGTTT
	Mutant site 2	CTTGCCTAGAAATGCCAAAAATATCTTTTATACAACTCTTATG AATTCTTGATGATGGCTAGATTGTTTTAAAAAAATTCATTTTAA AAA
	Mutant site 3	GAGTCGGATGATCATTTAAATACATACAATATTGAATTCAAGG CAGCATATTTTTTTCCCAGAGATCACATG
ADAMTS12	12.1 Forward	GCTCGCTAGCCTCGACGTCTCCCTTTACCTATCCGT
	12.1 Reverse	CGACTCTAGACTCGAGGAGCCAATGTTCTGCCTTT
	12.1 Mutant site 1	ACCATCTAGATATTAGCACCATTTTTTTAATGAATTCATTCTG CTGAACGGATAGGTAAAGGGAGACG
	12.1 Mutant site 2	TCTGCCACCATCTAGATATTGTCGACATTTTTTTAATAGCACC ATTCTGCTGAACGGATAG
	12.1 Mutant site 3	AACTGGAAAAAGACCTAGAATGGGAATTCTGGCCAAACTCTC TCCACATGTCTACC
	12.2 Forward	GCTCGCTAGCCTCGAGGGGACTCAGATCAACAGGA
	12.2 Reverse	CGACTCTAGACTCGATCATGTCATGTGGCCTCTCC
	12.2 Mutant site 1	GATAAAGTAAATCAACAACTCTGCTTCATATCGAATTCCAAGT ATCAAAGATGTAAGATACCATGCAGGT
	12.2 Mutant site 2	GTGAATCACTGTGGACCAGAATTCAGAAACATCGTCCCAAAG ATTCATCTTGAAGTCAG
ADAMTS15	15.1 Forward	GCTCGCTAGCCTCGAAGAGGCTTTGAGGTGCAGG
	15.1 Reverse	CGACTCTAGACTCGAGCAGCTTCCTCCTCCCTATC
	15.1 Mutant site 1	CTTGGAAACTGGGCCTCGAATTCTTCTGCCCTGCACCTCAAA GCCTCTTC
	15.1 Mutant site 2	CAGTTCAAAATGGAAAGTGGGCTAAAGAATTCGTGAAAACCC TGCCTCGTTCAGACAC
	15.1 Mutant site 3	AAGCCAGGCCCAGAGCTCGAATTCAACCCCAGTCCAGTGAC AGC
	15.2 Forward	GCTCGCTAGCCTCGATCTCTGGCTCCTGACACAAG
	15.2 Reverse	CGACTCTAGACTCGAACAGTATACACAGCCCAGCC

	15.2 Mutant site 1	AGAAAAACCACCACAACAGATAAAGAATTCGAGGCCTGGCTTGTGTCAGGAGCC
	15.2 Mutant site 2	GAACAGTATACACAGCCCAGCCGAATTCCAGGTCCTTCCATCCTTCTGCA
ADAMTS16	Forward	GCTCGCTAGCCTCGAGGACTGCATTCTGGTTTGGG
	Reverse	CGACTCTAGACTCGACCCTTTGGAATGGAGCCA
	Mutant site 1	CCTTCAATGCATGAATCTGAAAGAGATAGAGAATTCTTAGCAGGAATTTCATTTTTCCCATTTCCATAGG
	Mutant site 2	ACCCTTTGGAATGGAGCCACGAATTCGGACAGGAGAACAGCAGCCG
ADAMTS18	Forward	GCTCGCTAGCCTCGAAGGGTTCAAGGGCAAAGACA
	Reverse	CGACTCTAGACTCGAGTAGCATTCCCAAAGAGCGG
	Mutant site 1	GCAGCAAGCACAATTGCGGAATTCATTTGGCTTCTCATAGAACTCCTGGCTTGGGT
	Mutant site 2	TTCATGGACTGATTCAGCAGAATTCAAAAGTTACGAGGTTGATAACATGTGAAGGGCATCCA
ADAMTS20	Forward	GCTCGCTAGCCTCGAACATTTAGAAGGGGGAAGTATG
	Reverse	CGACTCTAGACTCGAAGGTATAAAATAAGTGTGGTCC
	Mutant site 1	GAAATCTCGGGAAGGGAGATATAAAGAAATGTCTAGAAGTTATTTGAATATTCCAGAGAATATCCCCT
	Mutant site 2	CCAATATGTCTCTGCCTTTTTTTCAGGTCGACCATCAGGGATTCAAATCACTGCTTAA
Colony PCR pmirGLO	Forward	GCAACACCCCAACATCTTCG
	Reverse	TGTTGTTAACTTGTTTATTGCAGCT

Appendix table 2. Stability of housekeeping genes in qRT-PCR experiments

Experiment	Mean CT difference	p-value	95% CI	
			Lower	Upper
SW1353 TGF-β treatment 0 - 8 hours* / 0 - 24 hours 18S rRNA*	0.181 / 0.080	0.905 / 0.980	-1.108 / -1.209	1.469 / 1.369
HAC TGF-β treatment 18S rRNA**	0.046	0.484	-0.119	0.211
SW1353 miR-29b transfection 18S rRNA**	-0.042	0.890	-0.828	0.745
HAC miR-29b transfection 18S rRNA**	0.303	0.509	-0.856	1.462
SW1353 miR-29b transfection (methylation array)** 18S rRNA	0.356	0.158	-0.184	0.895
AB1-KO 18S rRNA**	0.255	0.126	-0.083	0.592
B2C-KO 18S rRNA**	0.055	0.897	-0.849	0.959
DKO 18S rRNA**	-0.195	0.518	-0.814	0.423
AB1-KO U6 snRNA**	-0.050	0.685	-0.312	0.212

** One-way ANOVA, ** Student's t-test*

Appendix table 3. qRT-PCR primers and probes

Gene	Primer	Sequence (5' - 3')
18S rRNA	Forward	GCCGCTAGAGGTGAAATTCTTG
	Reverse	CATTCTTGGCAAATGCTTTCG
	Probe	ACCGGCGCAAGACGGA
ADAMTS1	Forward	GGACAGGTGCAAGCTCATCTG
	Reverse	TCTACAACCTTGGGCTGCAAA
	Probe	FAM-CAAGCCAAAGGCATTGGCTACTTCTTCG-TAMRA
ADAMTS2	Forward	CTGGCAAGCATTGTTTTAAAGGA
	Reverse	GGAGCCAAACGGACTCCAA
	Probe	FAM-ATCTGGCTGACACCTGACATCCTCAAACG-TAMRA
		N.B. will not detect shortest splice variant
ADAMTS3	Forward	GCAGCATTCCATCGTTACCA
	Reverse	CCATAGAATAATTGATTCCAGGAAGTT
	Probe	FAM-CCATTCCTATGACTGTCTCCTTGATGACCC-TAMRA
ADAMTS4	Forward	CAAGGTCCCATGTGCAACGT
	Reverse	CATCTGCCACCACCAGTGTCT
	Probe	FAM-CCGAAGAGCCAAGCGCTTTGCTTC-TAMRA
ADAMTS5	Forward	TGTCCTGCCAGCGGATGT
	Reverse	ACGGAATTACTGTACGGCCTACA
	Probe	FAM-TTCTCCAAAGGTGACCGATGGCACTG-TAMRA
ADAMTS6	Forward	GGCTGAATGACACATCCACTGTT
	Reverse	CAAACCGTTCAATGCTCACTGA
	Probe	FAM-CACTACCAATTAACAACACACATATCCACCACAGACAG-TAMRA
ADAMTS7	Forward	CAGCCTACGCCCAAATACAAA
	Reverse	CCCTTGTAGAGCATAGCGTCAAA
	Probe	FAM-AAGCGCTTCCGCCTCTGCAACC-TAMRA
ADAMTS8	Forward	CCGCCACCCAGAGCACTA
	Reverse	TCGATCACGGAGCAGCTTTT
	Probe	FAM-CCATCCTGCTCACCAGACAGAACTTCTGTG-TAMRA
ADAMTS9	Forward	TTAGTGAAGATAGTGGATTGAGTACAGCTT
	Reverse	TGTTGGAGCCATGACATGCT
	Probe	FAM-ATCGCCCATGAGCTGGGCCA-TAMRA
ADAMTS10	Forward	AGAGAACGGTGTGGCTAACCA
	Reverse	TCTCTCGCGCTCACACATTC
	Probe	FAM-CAGTGCTCATCACACGCTATGACATCTGC-TAMRA
ADAMTS12	Forward	CACGACGTGGCTGTCCTTCT
	Reverse	CCGAATCTTCATTGATGTTACAACTG
	Probe	FAM-AGGACATCTGTGCTGGTTTCAATCGCC-TAMRA
ADAMTS13	Forward	CAGAGCGAGAGAATATGTCACATTTC
	Reverse	ACCGCCAAGTGTGTGAAGAGA
	Probe	FAM-CCAACCTGACCAGTGTCTACATTGCCAAC-TAMRA
ADAMTS14	Forward	CGCTGGATGGGACTGAGTGT
	Reverse	CGCGAACATGACCCAAACTT
	Probe	FAM-CCCGGCAAGTGGTGCTTCAAAGGT-TAMRA

ADAMTS15	Forward	ATGTGCTGGCACCCAAGGT
	Reverse	CAGCCAGCCTTGATGCACTT
	Probe	FAM-CCTGACTCCACCTCCGTCTGTGTCCA-TAMRA
ADAMTS16	Forward	GCCCATGAGTCTGGACACAA
	Reverse	GCAGGGTGACCAGGAGAAGA
	Probe	FAM-TGCAAAAAGTCCGAGGGCAACATCAT-TAMRA
ADAMTS17	Forward	GGTCTCAATTTGGCCTTTACCAT
	Reverse	GACCTGCCAGCGCAAGAT
	Probe	FAM-CCACAACTTGGGCATGAACCACGA-TAMRA
ADAMTS18	Forward	CTCATTGGAAAGAATGGCAAGAG
	Reverse	GGTACAACTTCGGTACTTAGAGCACAT
	Probe	FAM-TGTGACACTCTAGGGTTTGCCCCCAC-TAMRA
ADAMTS19	Forward	GGTGTAAGGCTGGAGAATGTACCA
	Reverse	TGCGCTCTCGACTGCTGAT
	Probe	FAM-CCTCAGCACCTGAACATCTGGCCG-TAMRA
ADAMTS20	Forward	ACTGTCCCGAGTGACGAGAGA
	Reverse	AACAAGGCACTCGCTCCATT
	Probe	FAM-AATTTTCCTGTCCCAGTTGGGCTGCTA-TAMRA
PAI-1	Forward	CAGAGGTGGAGAGAGCCAGATT
	Reverse	CTGGTCCACGGCTCCTTTC
	Probe	FAM-GTGAAGACACACACAAAAGGTATGATCAGCAACTT-TAMRA
MiR-29a	Forward	AGCACCATCTGAAATCGGTTA
	Reverse	TCCAACGTCAGCAATAACGTA
	Probe	UPL #60
MiR-29b1	Forward	GTGATTGTCTAGCACCATTTGAA
	Reverse	TTCAGGGCTGTACACTCATTTC
	Probe	UPL #22
MiR-29b2	Forward	AAGAATTGCAGCACAGCAGA
	Reverse	TCCCTTGATTTCTCGAAGGAG
	Probe	UPL #6
MiR-29c	Forward	TCGGTCCATCTCTTACACAGG
	Reverse	TCAAATGGTGCTAGACAAAAACA
	Probe	UPL #2
DNMT1	Forward	GTCTGGCTGAGATGAGGCAA
	Reverse	TGAGTAGTAGAGGACCCGGC
	Probe	UPL #7
DNMT3A	Forward	GAGGACATCTTATGGTGCACTG
	Reverse	GCTCATGTTGGAGACGTCAG
	Probe	UPL #48
DNMT3B	Forward	CGGTGTTTCTGTGTGGAGTG
	Reverse	CGCACGTTCCAGTCCTTC
	Probe	UPL #1
TET1	Forward	CAGCCATCAGATCTGTAAGAAAAG
	Reverse	GGCCTCTTGTTTTCCTTTATAACC
	Probe	UPL #17

TET2	Forward	ACGCTTGGAAGCAGGAGAT
	Reverse	AAGGCTGCCCTCTAGTTGAA
	Probe	UPL #2
TET3	Forward	CGCCTCTATCCGGGAACT
	Reverse	CTTCCCCGTGTAGATGACCT
	Probe	UPL #25
TDG	Forward	GCAGTTGTGAATGAACAGCAA
	Reverse	TTTCTTCCTTTTGGAGCCTCT
	Probe	UPL #15
ACAN	Forward	TGAAGCAGAAGGTCTGGACA
	Reverse	CCAGAAGGAATCCCACTAACA
	Probe	UPL #34
COL2A1	Forward	AGCTCCTGGGAAGGATGG
	Reverse	CAGGAGGTCCGACTTCTCC
	Probe	UPL #3
TRAP	Forward	GGTCAGCAGCTCCCTAGAAG
	Reverse	GGAGTGGGAGCCATATGATTT
	Probe	UPL #3
GM27019	Forward	GCACCGTGAATGTGTAAGCC
	Reverse	TCCCTCCAAATGGTAACTGAGC
	Probe	UPL #108

Appendix table 4. Differentially expressed genes (q ≤ 0.05) in DKO hip cartilage mRNA-seq data with outliers included.

Upregulated gene	Log_2 fold change	Adjusted p-value
2610300M13Rik	-6.657	3.87E-03
Ak5	-1.990	9.60E-03
Ankrd6	-4.189	4.77E-02
Ano3	-5.852	2.67E-02
Car3	-3.595	3.06E-02
Ccdc194	-5.013	3.40E-03
Cd52	-3.533	2.02E-02
Chn1	-3.247	1.64E-02
Dmp1	-4.438	4.80E-02
Dntt	-8.861	6.45E-03
Ear6	-8.448	2.36E-02
Fam78b	-3.746	4.80E-02
Ffar4	-5.113	2.14E-02
Gm19299	-8.791	4.07E-03
Gm27019	-6.571	1.78E-08
Gm30948	-8.494	2.02E-02
Gm36161	-7.582	3.26E-03
Ifi209	-6.082	3.79E-02
Ighm	-3.008	4.77E-02
Insc	-4.194	3.95E-02
Lpar3	-4.391	9.31E-03
Lurap1l	-4.904	3.26E-03
Mucl3	-4.625	2.72E-02
Oas3	-8.112	2.57E-02
Pklr	-24.370	5.62E-09
Ppm1e	-3.451	3.13E-02
Prss34	-7.332	2.04E-02
Serpina12	-5.437	2.57E-02
Shc2	-3.260	1.39E-02
Siglec15	-8.374	3.28E-03
Snx10	-3.150	2.00E-02
Spn	-4.887	3.52E-03
Spo11	-5.232	4.62E-02
Tm4sf19	-6.904	4.77E-02

Downregulated gene	Log_2 fold change	Adjusted p-value
4931422A03Rik	5.666	3.79E-02
Alb	7.723	3.02E-02
Ambp	3.470	4.80E-02
Apoa2	11.965	9.04E-04
Apoa5	8.057	4.80E-02
Apob	23.681	9.78E-09
Apoc3	23.933	9.56E-09
Ces1c	23.520	1.09E-08
Cps1	9.938	2.74E-02
Cyp2f2	6.418	3.37E-02
D930030I03Rik	7.672	3.04E-03
Disp3	6.531	4.20E-02
Fabp1	23.472	1.09E-08
Fgb	23.275	1.43E-08
Gm8210	8.138	8.68E-05
Lgr5	2.516	3.95E-02
Lrfn1	1.640	4.62E-02
Lrrc4b	7.280	3.22E-02
Mat1a	23.722	9.78E-09
Nppc	8.982	4.07E-03
Nudt10	2.705	2.67E-02
Otof	7.211	2.14E-02
Prss23	3.649	2.04E-02
Serpina3k	24.630	5.62E-09
Shisal1	8.245	9.60E-03
Tat	8.202	3.47E-02

Appendix table 5. Differentially expressed genes (q ≤ 0.05) in DKO hip cartilage mRNA-seq data with outliers removed.

Upregulated gene	Log_2 fold change	Adjusted p-value	Downregulated gene	Log_2 fold change	Adjusted p-value
1700066M21Rik	-2.367	1.76E-03	1700007J10Rik	2.948	4.10E-02
2610300M13Rik	-7.423	6.14E-04	1700039M10Rik	6.316	1.33E-02
2810025M15Rik	-1.698	2.10E-02	1700047M11Rik	1.718	2.05E-02
4833422C13Rik	-3.946	6.45E-03	1700102P08Rik	2.240	3.07E-02
8030451A03Rik	-5.075	1.58E-02	1700126G02Rik	6.695	2.62E-02
Abcb4	-4.017	2.22E-05	2600014E21Rik	2.129	8.72E-03
Abcg1	-1.941	2.44E-02	2610035D17Rik	1.257	2.39E-02
Abracl	-1.547	4.63E-02	2810039B14Rik	2.464	7.42E-04
Acp5	-4.594	7.50E-10	2810433D01Rik	3.853	1.03E-03
Acsl5	-1.195	1.95E-02	4833413G10Rik	2.419	4.20E-02
Acss1	-1.920	4.93E-02	4930426I24Rik	7.584	4.34E-02
Actb	-1.141	5.63E-03	4930447C04Rik	2.722	1.47E-04
Actg1	-0.998	2.10E-03	4930474M22Rik	3.295	1.06E-02
Actr2	-1.060	2.49E-02	4930556I23Rik	7.353	5.57E-03
Actr3	-1.088	9.34E-03	4930581F22Rik	1.078	8.11E-03
Adam10	-1.437	3.33E-03	4931422A03Rik	6.454	2.56E-02
Adam12	-3.535	7.76E-06	4933431E20Rik	1.198	2.63E-02
Adamts2	-2.421	2.02E-02	4933432I09Rik	3.488	2.02E-02
Adamts4	-2.797	5.57E-03	9030622O22Rik	3.740	9.75E-04
Adarb2	-5.575	3.35E-02	9330151L19Rik	1.083	4.47E-02
Adgrd1	-5.446	1.94E-02	9330188P03Rik	1.760	2.74E-03
Adgre5	-1.960	3.86E-03	A230057D06Rik	2.445	2.06E-03
Adssl1	-2.727	2.04E-02	A430110L20Rik	1.944	2.97E-02
Agap1	-1.508	2.42E-05	A530064N14Rik	2.346	2.36E-05
Ahsa1	-0.807	2.44E-02	A730011C13Rik	1.916	3.63E-02
AI662270	-4.681	3.07E-02	A730017L22Rik	1.570	4.74E-02
Ak5	-2.152	1.50E-02	Abca8b	1.754	5.89E-03
Akr1b3	-1.276	1.80E-02	Abhd18	1.168	2.78E-02
Alcam	-3.430	3.46E-02	Ablim3	4.176	3.86E-02
Ammecr1	-1.790	4.46E-03	Acot11	1.188	2.79E-02
Amph	-8.179	5.25E-03	Acvr1b	1.102	4.54E-03
Angpt2	-3.411	2.33E-02	Adam1a	1.899	2.05E-03
Angpt4	-5.297	3.56E-02	Adamts10	1.275	2.13E-02
Ankrd33b	-3.398	2.99E-02	Adamts3	1.675	7.00E-03
Ankrd6	-4.993	1.71E-05	Adamts6	1.746	6.84E-03
Ano1	-1.386	2.36E-02	Adamtsl1	3.357	2.73E-03
Ano6	-1.406	4.78E-02	Adgrb2	1.857	8.26E-05
Anp32a	-0.944	1.96E-02	Adgrg2	1.358	4.87E-02
Anp32e	-1.025	2.60E-02	Adhfe1	1.770	1.66E-02
Antxr2	-2.070	2.44E-02	Ahsg	25.175	1.01E-06
Apbb1ip	-3.911	7.40E-07	AI182371	2.227	3.16E-02
Apobr	-3.527	2.79E-02	AI838599	1.320	1.53E-03
Arhgap27	-2.680	1.74E-03	Airn	1.229	2.96E-02

Arhgap27os3	-5.517	2.44E-02	Alb	7.480	4.82E-02
Arhgap30	-3.673	1.71E-02	Alkbh1	0.903	2.96E-02
Arhgap31	-1.197	1.61E-02	Aloxe3	7.783	1.42E-02
Arhgdib	-1.617	4.89E-03	Ambp	3.737	2.28E-02
Arl4d	-2.073	2.94E-02	Amhr2	1.644	3.46E-02
Arl6ip1	-1.454	3.26E-02	Ankrd16	0.904	2.13E-02
Arl8b	-0.916	1.79E-02	Ankrd28	0.880	2.03E-02
Arnt2	-1.711	3.86E-02	Ankrd35	1.398	1.20E-02
Arpc2	-0.740	2.72E-02	Ankzf1	0.975	1.31E-02
Arpc3	-1.217	8.06E-03	Aopep	1.288	3.07E-03
Arpc4	-1.305	1.85E-02	Ap1m2	7.440	9.79E-03
Arpp21	-5.746	3.09E-02	Apc2	2.535	2.48E-02
Arrdc4	-1.903	2.28E-02	Apoa2	11.914	2.08E-03
Arsb	-2.544	1.67E-02	Apoa5	8.004	2.39E-02
Atf6	-1.502	2.10E-02	Apob	21.689	4.48E-05
Atp5j2	-0.968	3.25E-02	Apoc3	21.812	4.03E-05
Atp5mpl	-0.965	2.33E-02	Apoh	9.343	4.47E-04
Atp5pb	-1.110	3.16E-02	Apom	4.698	3.49E-02
Atp6v0c	-1.397	2.41E-02	Appl2	0.910	1.08E-02
Atp6v1a	-1.243	5.73E-03	Arfgap1	0.979	4.82E-02
Atp6v1b2	-2.120	2.03E-05	Arhgap33	1.260	4.25E-02
Atp6v1c1	-1.296	2.37E-02	Arhgef1	1.165	8.48E-03
Atp6v1d	-1.166	2.15E-02	Arhgef17	1.093	4.93E-02
Atp6v1e1	-1.350	2.04E-03	Arhgef25	1.125	3.69E-02
Atp6v1f	-1.280	2.44E-02	Arhgef28	1.442	5.88E-03
Atp6v1g1	-1.246	1.49E-03	Arhgef37	1.589	2.31E-02
Atp6v1h	-1.037	4.82E-02	Asap2	1.082	4.86E-03
Atpif1	-0.870	3.03E-02	Asap3	1.542	2.79E-02
Atrnl1	-1.738	5.25E-03	Asgr1	8.272	1.20E-04
B2m	-2.045	6.31E-03	Atg16l2	1.162	1.55E-02
B3gnt3	-2.870	1.36E-04	Atl1	1.000	4.40E-02
Bbln	-1.878	2.85E-02	Avil	2.512	5.79E-05
BC035044	-7.093	5.68E-03	Axdnd1	7.943	2.07E-03
BC055402	-5.743	1.23E-02	Azgp1	3.207	1.91E-02
Bcar3	-2.774	5.39E-04	B930095G15Rik	1.467	1.76E-02
Bcl2a1b	-7.179	1.31E-02	Bbox1	2.490	1.27E-03
Bex4	-8.608	5.73E-03	BC006965	2.341	6.03E-05
Bglap	-4.174	3.97E-23	Bckdhb	1.555	2.18E-02
Bglap2	-4.158	4.48E-05	Bcl6	1.224	3.98E-02
Bin2	-3.636	1.95E-02	Bcl9l	1.050	9.20E-03
Bmp3	-2.175	1.01E-02	Bhmt	23.313	7.76E-06
Bok	-1.643	4.20E-02	Bicral	1.208	5.47E-03
Bst2	-2.724	4.00E-05	Btf3-ps18	7.544	4.77E-03
Btk	-4.082	2.31E-02	C2cd5	0.984	4.07E-03
Btla	-3.002	2.76E-03	C430049B03Rik	1.367	9.11E-05
Btnl10	-5.341	2.04E-02	C4b	1.837	1.78E-02

C1galt1	-1.434	2.31E-02	Cacna1d	2.247	3.93E-03
C6	-10.995	1.54E-12	Cacna1h	2.367	7.19E-03
Cadm1	-3.809	3.26E-10	Cacng7	1.420	2.09E-02
Cald1	-1.584	1.21E-03	Calb2	7.353	4.32E-02
Calm1	-1.000	2.04E-03	Caprin2	1.855	4.86E-03
Calm2	-0.854	1.47E-02	Car11	1.343	2.80E-02
Car2	-4.200	4.43E-02	Casc1	2.097	4.91E-02
Car3	-4.514	1.02E-11	Catsperg1	2.020	3.61E-02
Card6	-2.136	8.47E-03	Cblc	7.171	4.27E-02
Carhsp1	-1.101	3.07E-02	Ccdc113	7.710	1.31E-02
Cbfa2t3	-3.327	3.98E-02	Ccdc136	1.481	1.61E-02
Cblb	-1.378	2.28E-02	Ccdc157	1.372	1.00E-04
Cbr3	-1.563	2.72E-02	Ccdc159	1.528	4.21E-02
Ccbe1	-4.882	2.94E-02	Ccdc62	1.435	5.57E-03
Ccdc12	-1.057	2.67E-02	Ccdc88c	1.136	1.79E-02
Ccdc194	-5.870	1.11E-07	Ccnl2	0.777	4.01E-02
Ccl9	-3.178	2.95E-04	Ccnt2	0.927	4.54E-03
Ccm2l	-2.065	3.53E-02	Cdc14a	1.334	4.86E-03
Ccn4	-2.601	3.15E-06	Cdkl5	1.512	1.49E-03
Ccn5	-2.103	1.45E-04	Cds1	2.328	2.18E-06
Ccr1	-4.871	2.83E-04	Cep170b	0.819	4.25E-02
Cct5	-0.834	4.78E-02	Cep85l	1.245	2.41E-03
Cd19	-4.116	5.89E-03	Cercam	1.319	2.97E-02
Cd244a	-6.842	5.01E-03	Cerox1	1.749	2.53E-02
Cd28	-3.243	1.32E-02	Ces1c	22.536	1.84E-05
Cd34	-1.999	1.20E-02	Cfap69	2.054	1.25E-03
Cd37	-3.115	4.27E-03	Cfap74	1.349	3.58E-02
Cd40	-4.086	1.01E-02	Chd2	0.869	4.27E-02
Cd44	-2.352	2.05E-02	Chd6	0.729	2.77E-02
Cd48	-3.550	4.68E-02	Chka	1.458	1.27E-03
Cd52	-4.309	3.30E-07	Chrdl2	1.368	3.74E-03
Cd59a	-2.452	3.51E-04	Cidea	5.567	3.35E-04
Cd68	-2.813	1.11E-04	Clasrp	1.146	2.51E-02
Cd69	-8.195	1.16E-02	Clcn1	7.239	1.23E-02
Cd72	-2.980	1.60E-02	Clk1	1.052	7.36E-03
Cd74	-2.988	7.61E-04	Clk4	0.726	2.42E-02
Cd84	-4.470	5.17E-03	Col20a1	1.683	5.98E-04
Cdc42	-0.900	2.69E-02	Col27a1	1.184	1.05E-02
Cdc42ep1	-1.365	7.66E-03	Col4a3	3.949	1.85E-04
Cdh2	-5.743	1.79E-02	Col4a5	1.371	3.07E-02
Cdh5	-2.486	1.80E-03	Col4a6	2.436	1.58E-07
Cdk5r1	-1.656	4.59E-02	Col7a1	2.280	1.40E-02
Cdkn1a	-1.216	2.31E-03	Cox4i2	1.165	3.91E-02
Cdo1	-2.819	5.96E-06	Cplane1	1.043	2.97E-02
Ces2g	-4.141	2.94E-02	Cpne8	1.076	5.30E-03
Cfh	-4.757	1.40E-08	Cps1	9.887	2.00E-02

Cfl1	-1.561	3.28E-04	Cracd	1.309	1.04E-02
Cgref1	-1.694	4.73E-03	Crispld1	1.352	1.70E-02
Chchd2	-0.904	2.94E-02	Crlf3	1.137	1.25E-02
Chchd3	-1.141	4.43E-02	Crtc1	1.024	2.95E-02
Chmp1b	-1.752	7.70E-03	Crtc3	1.087	5.89E-03
Chn1	-4.004	1.75E-07	Cspg4b	2.337	7.16E-06
Ckb	-1.583	1.25E-02	Ctcfl	1.614	2.58E-04
Cldn1	-3.599	4.91E-02	Ctcflos	1.670	1.60E-05
Cldn13	-5.380	5.04E-03	Ctdspl	1.077	4.82E-03
Cldn5	-2.258	2.06E-03	Cul7	1.076	2.02E-02
Clec4a2	-2.849	2.46E-03	Cyp26b1	1.383	1.72E-02
Clta	-0.855	8.02E-03	Cyp2f2	5.378	2.94E-02
Cnn2	-2.313	1.21E-05	Cyp3a13	1.477	1.11E-02
Coa5	-1.598	2.66E-04	Cyp4f17	1.640	1.91E-03
Col1a1	-2.847	2.39E-05	D2hgdh	1.311	2.84E-02
Col1a2	-2.664	9.75E-05	D630003M21Rik	1.536	2.31E-02
Col8a1	-2.430	1.95E-02	D930007P13Rik	2.656	2.10E-04
Coro1c	-1.415	2.11E-04	D930030I03Rik	7.621	6.03E-03
Cotl1	-1.747	1.47E-02	Dact3	1.215	1.16E-02
Cox5a	-1.420	4.36E-02	Ddb2	1.014	2.28E-02
Cox5b	-0.855	1.74E-02	Ddhd2	1.003	2.85E-02
Cox6b1	-1.017	2.72E-02	Dele1	0.718	4.84E-02
Cox6c	-0.735	4.07E-02	Dennd2c	1.271	2.99E-02
Cox7b	-0.944	4.24E-02	Dhtkd1	1.335	4.47E-02
Cox8a	-0.903	2.44E-02	Dhx57	0.886	2.70E-02
Cp	-2.143	7.98E-04	Disp1	1.352	5.03E-03
Cplx2	-1.324	1.15E-02	Disp3	7.202	2.19E-02
Cpz	-2.696	4.46E-02	Dixdc1	1.148	3.25E-03
Crnkl1	-1.467	3.09E-02	Dlg4	1.203	3.42E-03
Cs	-1.044	4.29E-02	Dnah1	1.441	8.06E-03
Csf1	-1.349	5.90E-03	Dnah7b	2.774	4.98E-03
Csf1r	-3.257	2.64E-03	Dnhd1	1.457	8.88E-03
Csf2rb	-3.330	4.20E-02	Dnm1	1.162	1.68E-03
Cstb	-1.619	4.03E-05	Dnm3os	0.996	1.03E-02
Cthrc1	-2.084	4.98E-02	Dop1b	1.199	2.25E-02
Ctnnb1	-1.113	3.61E-02	Drp2	1.668	1.25E-02
Ctsc	-3.358	4.02E-05	Dtx3	0.998	2.00E-02
Ctsh	-2.014	1.50E-03	Dusp15	2.929	4.33E-06
Ctsk	-3.563	2.09E-07	Duxbl1	1.893	8.50E-04
Ctsw	-2.793	2.32E-02	Dzip3	0.920	3.18E-02
Cux1	-1.120	1.95E-02	Efcab8	3.222	1.81E-02
Cx3cr1	-3.487	3.13E-02	Efemp1	1.714	1.37E-02
Cxcl12	-3.935	1.42E-06	Efr3b	0.960	2.35E-02
Cxcr4	-3.402	4.49E-02	Efs	0.878	2.44E-02
Cycs	-1.224	8.36E-03	Elapor1	7.425	2.32E-02
Cyfip1	-1.091	1.22E-02	Eno2	1.569	2.28E-02

D16Ertd472e	-1.802	3.11E-04	Epb41l1	1.116	2.44E-02
Dapk2	-2.830	4.62E-04	Eps8l2	1.186	1.55E-02
Dazap2	-1.286	5.70E-04	Ercc2	1.086	1.96E-02
Dbf4	-1.343	4.30E-02	Erich6	2.567	5.15E-03
Dck	-1.650	3.26E-02	Etnk1	1.317	1.57E-05
Dcn	-2.231	4.78E-02	Etnk2	2.711	1.27E-03
Dcstamp	-4.551	1.93E-02	Extl1	1.283	1.15E-02
Denn2b	-1.498	1.59E-02	Ezh1	1.069	2.05E-02
Dlx3	-2.798	7.89E-03	F12	7.948	2.95E-02
Dlx6	-2.488	2.64E-03	Fabp1	22.485	1.95E-05
Dmp1	-5.378	2.72E-10	Fam131a	1.022	1.56E-02
Dntt	-9.732	5.04E-03	Fam131b	5.425	2.51E-02
Dok3	-1.849	2.97E-02	Fam161a	1.375	1.63E-02
Dpep1	-3.936	3.91E-02	Fam189a1	1.726	3.43E-02
Drc7	-8.594	3.00E-03	Fam221a	1.380	2.79E-02
Dstn	-1.468	5.28E-05	Farp1	0.927	4.00E-02
Dtna	-2.009	2.23E-02	Fasn	0.816	3.19E-02
Dtx4	-2.949	7.55E-07	Fbxl2	1.708	5.47E-04
Dusp2	-4.969	3.43E-02	Fbxo17	1.042	4.75E-02
Dusp3	-1.399	1.95E-02	Fbxo44	1.380	1.93E-02
Dusp6	-2.270	1.63E-07	Fbxw10	2.148	3.21E-03
E2f2	-2.085	9.66E-03	Fgb	22.620	1.69E-05
Ear6	-8.563	4.61E-02	Fgfr1	0.736	4.07E-02
Efnb1	-1.938	1.11E-02	Fgfr3	1.156	2.32E-02
Ehd1	-1.076	2.82E-02	Fggy	1.925	3.31E-04
Ehd4	-1.240	3.75E-02	Firre	1.008	1.15E-02
Eif3e	-0.968	8.43E-03	Fnip1	0.758	4.99E-02
Elmo1	-2.234	1.65E-02	Focad	1.225	7.36E-03
Emcn	-3.074	1.82E-03	Foxa2	1.631	3.58E-02
Emid1	-1.979	1.89E-02	Foxo6	2.180	4.34E-02
Enpp6	-5.645	1.60E-02	Foxp2	1.428	4.34E-02
Entpd3	-6.209	4.87E-03	Frzb	1.889	3.00E-03
Epb41l2	-1.219	2.66E-04	Fuz	0.915	3.95E-02
Epb41l3	-1.587	2.12E-02	Fxyd3	1.758	1.47E-02
Epor	-4.159	9.66E-03	G0s2	2.085	2.38E-02
Esd	-0.935	1.10E-02	Gabre	1.740	1.84E-02
Etl4	-1.706	4.51E-03	Ghr	1.460	4.48E-05
Fabp5	-1.763	1.37E-02	Gigyf1	0.967	3.37E-02
Fahd1	-1.534	1.13E-02	Gjc3	1.340	1.98E-02
Fam111a	-1.614	2.04E-02	Glis1	2.315	4.57E-03
Fam167a	-2.122	9.42E-03	Glp1r	1.692	1.25E-02
Fam210b	-2.110	3.51E-04	Gls	0.942	1.77E-02
Fam78b	-4.689	9.12E-10	Gm10000	1.912	3.21E-03
Fat3	-4.476	1.02E-03	Gm10605	7.467	1.94E-02
Fbln2	-1.809	9.18E-03	Gm11615	3.227	1.87E-02
Fcho1	-4.224	2.00E-02	Gm11739	1.875	4.95E-03

Fcmr	-7.636	3.34E-02	Gm12940	0.975	9.66E-03
Fermt3	-1.777	4.15E-02	Gm14168	2.724	2.72E-02
Ffar4	-5.376	2.05E-02	Gm14439	6.950	4.20E-02
Fhl2	-1.910	1.76E-02	Gm15445	3.078	7.09E-03
Filip1l	-2.879	2.07E-04	Gm15567	2.082	2.86E-02
Fmnl1	-2.668	7.06E-03	Gm16070	2.208	1.44E-06
Fmnl2	-1.752	7.13E-03	Gm16206	7.778	4.48E-03
Foxs1	-1.897	2.84E-02	Gm16574	1.350	2.60E-02
Frrs1	-2.275	1.36E-02	Gm17160	3.919	4.72E-02
Fyb	-3.919	1.05E-02	Gm17200	7.554	3.75E-03
Fyn	-1.998	8.63E-04	Gm17529	2.926	4.10E-02
Fzd5	-2.374	6.99E-03	Gm18284	3.713	1.93E-02
Gab2	-1.638	1.15E-02	Gm18494	4.568	2.82E-02
Gabrb3	-8.245	6.03E-03	Gm19325	7.264	2.03E-02
Gal	-9.508	1.27E-06	Gm20257	1.217	1.10E-02
Galnt3	-2.818	1.22E-05	Gm20342	1.193	1.86E-02
Gbp3	-4.062	1.90E-02	Gm20493	8.051	4.55E-03
Gbp7	-2.004	2.31E-02	Gm20522	6.970	2.04E-02
Gda	-1.750	8.47E-03	Gm20548	3.881	4.77E-03
Gfi1b	-4.825	3.83E-02	Gm21811	0.978	3.82E-02
Ggt5	-3.356	3.12E-04	Gm21955	7.434	3.25E-02
Ggta1	-1.791	6.43E-04	Gm23645	6.676	4.58E-02
Gimap6	-2.223	8.47E-03	Gm26511	6.971	2.63E-02
Gimap8	-3.315	4.91E-02	Gm26660	1.629	2.28E-02
Gja1	-3.186	2.95E-04	Gm27209	3.445	2.18E-02
Gja4	-2.025	4.60E-02	Gm29183	7.911	2.07E-03
Glb1	-2.325	5.51E-03	Gm35455	7.512	1.70E-02
Glipr1	-5.084	1.46E-02	Gm36033	9.253	2.42E-04
Glrx5	-1.412	3.03E-03	Gm37090	1.349	9.45E-04
Glul	-1.365	2.08E-02	Gm37200	7.588	9.35E-03
Gm11243	-8.777	5.70E-04	Gm37607	1.461	4.36E-02
Gm12250	-8.337	1.18E-02	Gm37694	1.616	2.95E-02
Gm16118	-7.280	3.83E-04	Gm37969	3.961	2.11E-02
Gm17322	-6.393	1.31E-02	Gm38021	3.103	1.94E-02
Gm19299	-9.340	6.37E-06	Gm38150	7.061	1.54E-02
Gm21188	-6.920	4.26E-02	Gm38218	6.933	1.82E-02
Gm266	-2.192	2.84E-02	Gm38563	2.370	4.03E-02
Gm27019	-5.770	1.53E-03	Gm42560	7.498	3.93E-03
Gm27048	-7.599	3.85E-02	Gm43272	3.569	9.54E-04
Gm2a	-1.820	1.86E-02	Gm43292	7.241	1.14E-02
Gm30948	-9.070	1.65E-02	Gm43481	1.360	3.61E-03
Gm32098	-7.634	5.27E-03	Gm43672	1.615	2.32E-02
Gm34680	-6.138	7.34E-03	Gm44014	7.818	4.05E-03
Gm36161	-7.991	1.42E-02	Gm44667	1.701	2.82E-02
Gm5518	-1.544	1.14E-02	Gm45237	3.007	3.43E-02
Gnai1	-2.762	1.33E-03	Gm45238	7.645	1.59E-02

Gng11	-1.554	6.69E-03	Gm45601	7.283	1.74E-02
Gpc1	-1.701	1.39E-02	Gm47071	1.814	4.29E-02
Gpr137b	-2.217	6.98E-03	Gm47232	2.414	1.30E-02
Gpr137b-ps	-2.901	2.24E-09	Gm47391	3.431	3.76E-02
Gpr68	-3.738	3.37E-02	Gm47550	2.672	3.01E-02
Gpx1	-1.077	7.34E-03	Gm47980	4.401	2.31E-02
Grap2	-5.745	1.90E-02	Gm48427	3.474	2.94E-02
Gsr	-2.048	2.34E-04	Gm48717	3.313	4.57E-02
Gstm2	-3.480	2.49E-02	Gm49308	7.508	5.69E-03
Gucy1b1	-2.014	3.38E-02	Gm49601	1.422	6.22E-03
Gvin3	-9.141	7.61E-04	Gm49694	7.038	3.95E-02
H2-D1	-1.798	1.24E-03	Gm49759	1.443	2.04E-02
H2-Eb1	-2.212	2.87E-02	Gm50107	1.613	4.98E-03
H2-K1	-1.864	1.00E-03	Gm50243	7.174	4.82E-02
H2-Ob	-4.990	4.43E-02	Gm53058	2.642	1.43E-03
H2-Q4	-2.079	1.46E-03	Gm5860	3.154	1.30E-02
H2-Q5	-5.690	8.64E-03	Gm6260	7.039	2.49E-02
H2-T23	-2.538	7.48E-04	Gm6723	7.692	4.07E-03
H3f3a	-0.980	2.01E-02	Gm7972	2.214	9.66E-03
Hck	-3.843	8.67E-03	Gm8210	7.056	7.79E-04
Helz2	-1.122	2.71E-02	Gm831	8.385	1.72E-03
Heph	-4.037	4.51E-03	Gm8428	7.255	2.46E-02
Hexb	-2.360	9.86E-03	Gm973	2.063	8.98E-03
Hey2	-3.750	2.86E-02	Gm9918	8.730	6.47E-05
Heyl	-2.762	6.34E-04	Golgb1	0.942	4.32E-02
Hmgb2	-1.499	1.87E-02	Gpatch8	0.841	5.00E-02
Hmgb3	-2.073	2.53E-02	Gpld1	1.974	4.48E-02
Hmox1	-1.809	2.02E-02	Gpr162	0.975	1.05E-02
Hoxb4	-2.246	2.93E-03	Gprasp1	1.024	4.81E-02
Hpcal1	-1.993	5.49E-05	Gprasp2	1.659	1.90E-02
Hpgd	-2.348	1.53E-03	Gpsm1	1.081	1.07E-02
Hsp90ab1	-0.819	1.10E-02	Gramd1c	1.715	4.78E-04
Hspa8	-0.980	2.77E-02	Gramd2	1.548	4.22E-06
Hvcn1	-2.474	2.84E-02	Grid2ip	2.215	4.85E-02
Icosl	-3.793	2.38E-02	Grin2d	1.324	2.20E-02
Id3	-1.600	8.31E-03	Gys1	1.438	5.17E-03
Ifi204	-2.244	2.22E-02	H3f3aos	7.475	3.62E-02
Ifi209	-6.986	1.29E-03	Hdhd5	1.271	2.03E-02
Ifi47	-4.290	4.67E-03	Hectd2	1.544	3.21E-02
Ifih1	-2.577	1.12E-02	Hemk1	1.380	2.06E-02
Ifitm3	-2.592	3.18E-03	Hgd	7.744	4.07E-03
Ifitm5	-3.508	3.28E-04	Hhipl1	1.228	1.20E-02
Ighm	-3.761	5.96E-06	Hip1r	1.131	1.93E-02
Igkc	-3.588	4.47E-02	Hmcn1	1.403	3.78E-02
Il12a	-5.625	4.85E-02	Hoxa2	1.394	2.72E-02
Il12rb1	-4.895	1.84E-02	Hoxa3	1.265	2.08E-03

Il13ra1	-1.431	2.84E-02	Hoxa5	1.659	1.64E-03
Il13ra2	-8.709	2.46E-03	Hoxa9	1.027	3.02E-03
Il1rl2	-3.732	2.04E-02	Hoxc8	1.342	1.35E-02
Il33	-5.352	1.29E-02	Hpx	3.740	4.65E-03
Inpp5d	-2.865	1.24E-02	Hr	1.454	1.52E-02
Insc	-5.076	2.60E-05	Hspd1-ps4	7.400	1.01E-02
Insig2	-1.339	1.47E-03	Id4	1.260	2.19E-02
Irf2bp2	-1.336	2.59E-02	Ifitm10	1.583	1.96E-05
Irf8	-3.609	2.86E-02	Igdcc4	1.096	8.04E-03
Irgm2	-1.656	1.11E-02	Iglon5	7.906	1.61E-02
Itga2	-3.257	1.63E-08	Il11ra1	1.533	6.14E-03
Itgal	-4.229	3.12E-03	Il25	4.592	4.11E-02
Itgax	-4.248	1.33E-02	Inppl1	0.922	3.83E-02
Itgb2	-4.001	8.90E-03	Irs3	4.094	1.40E-03
Itgb2l	-7.881	1.59E-02	Ism1	1.619	5.25E-03
Itgb3	-3.790	1.24E-04	Itga10	1.444	8.31E-03
Itgb7	-2.453	2.44E-02	Itga7	1.371	2.67E-02
Jdp2	-1.159	3.54E-02	Itih5l-ps	1.567	7.10E-03
Jup	-1.695	4.92E-05	Itpr3	1.148	1.20E-02
Kalrn	-1.975	8.53E-04	Ivd	1.273	1.71E-02
Kazn	-2.304	1.75E-07	Ivns1abp	1.094	2.35E-02
Kbtbd11	-1.928	4.94E-02	Jph2	1.610	4.35E-02
Kctd12b	-2.323	6.03E-03	Katnal2	3.830	8.70E-04
Kif21b	-2.711	1.32E-02	Kcnq1ot1	1.320	2.42E-04
Kitl	-2.296	9.43E-03	Kctd15	1.066	2.14E-02
Klhl6	-2.302	3.09E-02	Kif21a	1.163	5.57E-03
Knl1	-1.940	3.18E-02	Kif5a	2.533	5.21E-05
Kpna2	-1.487	2.41E-02	Klf8	1.354	4.25E-02
Laptm5	-2.849	1.57E-04	Klhdc8b	1.396	4.82E-02
Lasp1	-1.017	2.62E-02	Klhl29	1.448	2.04E-02
Lcp1	-3.353	4.48E-05	Klhl35	5.273	2.42E-04
Lcp2	-3.695	1.45E-04	Krba1	1.134	2.75E-03
Lepr	-3.809	4.78E-08	Krt75	3.320	2.20E-02
Lgals9	-1.936	1.23E-02	Lcat	1.232	5.56E-03
Lgmn	-1.856	3.42E-03	Ldlrad3	1.095	1.04E-03
Lif	-5.317	9.31E-03	Lgr5	2.825	1.41E-02
Lifr	-2.186	3.35E-04	Lgr6	1.352	8.88E-03
Limch1	-2.903	1.75E-07	Lhcgr	7.713	2.99E-02
Lingo3	-6.229	7.83E-03	Lmtk3	1.573	3.39E-02
Lmnb1	-1.641	4.05E-03	Lmx1b	2.412	9.67E-04
Lmo2	-3.415	1.59E-06	Lncppara	1.549	2.42E-04
Lox	-1.547	2.23E-02	Lonrf1	1.615	4.72E-03
Lpar3	-5.340	5.08E-09	Lrfn1	1.853	1.04E-02
Lpar6	-3.803	3.20E-02	Lrrc4b	7.958	1.51E-02
Lrg1	-2.008	3.09E-02	Lsp1	1.036	2.46E-03
Lrmp	-2.324	4.15E-02	Lss	1.271	5.51E-03

Lrp4	-2.717	2.20E-06	Luc7l2	0.774	2.04E-02
Lrrc8b	-2.012	3.21E-03	Lzts3	1.171	2.57E-02
Lurap1l	-5.675	2.09E-07	Map2	1.538	2.73E-04
Ly6c1	-2.033	8.93E-03	Map3k21	1.158	2.09E-02
Ly9	-5.595	1.10E-02	Map7d2	2.957	3.82E-02
Lyn	-2.897	9.54E-04	Map7d3	1.423	5.98E-04
Lyzl4	-6.944	2.69E-02	Mapk8ip2	4.024	1.94E-02
Mamdc2	-2.347	2.59E-02	Mapk8ip3	1.207	5.47E-03
Map4k4	-0.991	1.68E-02	Mas1	2.188	2.08E-02
Marcks	-2.003	1.88E-02	Mat1a	23.471	6.55E-06
Marcksl1	-2.290	1.47E-04	Matn1	2.041	1.76E-06
Matk	-2.139	2.44E-02	Mdm4	0.891	2.79E-02
Mbd2	-1.037	4.78E-02	Meg3	1.616	5.49E-05
Mcam	-2.331	1.64E-03	Mertk	0.938	2.02E-02
Mdh2	-0.904	3.27E-02	Mfsd4b4	1.623	4.25E-04
Me2	-2.135	1.66E-03	Mgat4a	1.131	8.47E-03
Metrnl	-2.188	1.76E-04	Mical1	0.910	1.93E-02
Mirt1	-7.919	4.29E-04	Micu3	0.983	4.00E-02
Mki67	-1.681	3.56E-02	Miga1	1.086	1.97E-02
Mknk2	-0.841	3.42E-02	Mir100hg	1.340	7.46E-03
Mlip	-3.461	2.96E-02	Mir351	1.860	1.87E-02
Mmp13	-3.752	4.98E-08	Mir99a	2.463	1.42E-02
Mmp15	-1.866	2.79E-02	Mirg	1.556	4.25E-04
Mmp16	-1.692	3.37E-02	Mmaa	1.421	3.98E-02
Mmp9	-4.251	4.20E-07	Mok	2.402	1.09E-02
Mob1a	-1.259	4.35E-02	Mroh7	4.810	6.43E-04
Mob3b	-4.183	3.39E-02	Mtf2	1.006	1.91E-02
Mrpl34	-1.338	2.47E-02	Mthfr	0.950	3.12E-02
Msln	-5.305	3.56E-02	Mtmr1	0.858	1.95E-02
Msn	-0.973	2.69E-03	Mtmr10	1.227	6.03E-04
Mt1	-1.719	2.97E-02	Mttp	2.039	7.83E-03
Mt3	-3.177	2.27E-03	Muc2	2.033	1.05E-04
Mtpn	-1.216	2.48E-03	Mycbpap	2.046	1.65E-02
Mtss1	-3.189	1.41E-06	Myh14	1.379	3.03E-02
Mx1	-7.967	1.64E-02	Mylk2	3.897	1.15E-03
Myb	-4.650	7.62E-03	Myo15b	3.290	1.74E-02
Mycn	-5.070	2.54E-02	Myo5a	1.014	5.90E-03
Myh9	-1.486	2.28E-04	Myo9b	1.106	1.86E-02
Myo10	-1.429	2.03E-03	Myom1	1.669	2.74E-02
Myo18a	-0.989	2.35E-02	Mysm1	0.969	3.27E-02
Myo1b	-3.756	1.57E-05	Mzf1	1.114	4.53E-02
N4bp3	-2.560	2.53E-04	Napb	1.578	4.03E-03
Nav1	-1.011	7.75E-03	Ncs1	1.157	3.62E-02
Ncald	-3.454	7.36E-05	Neat1	1.167	1.40E-03
Ncf1	-2.010	3.61E-02	Necab3	1.853	2.58E-02
Ncf2	-2.126	1.43E-02	Nexn	1.640	2.15E-02

Ncf4	-3.708	2.63E-02	Nfasc	1.649	3.90E-03
Nckap1l	-3.964	1.76E-08	Nfat5	0.967	3.76E-02
Ndufa3	-1.269	1.23E-02	Nipal2	1.783	7.36E-03
Ndufa4	-1.169	4.91E-02	Nkapl	7.375	1.04E-02
Ndufb1	-1.453	6.55E-03	Nod1	1.273	9.66E-03
Ndufb6	-1.559	1.83E-02	Npas3	1.367	3.83E-02
Ndufs5	-1.271	4.24E-02	Nphp3	1.044	7.47E-03
Ndufs6	-1.263	1.09E-02	Nppc	8.936	4.46E-03
Nectin3	-1.583	1.60E-02	Npr2	1.313	1.14E-02
Nek2	-1.740	4.27E-02	Nr4a1	2.120	2.56E-02
Nes	-1.957	2.95E-04	Nrbp2	1.246	1.13E-02
Neurl3	-2.526	3.01E-02	Ntrk2	2.340	1.13E-02
Nfam1	-3.791	1.40E-02	Nudt10	3.071	2.33E-02
Nhsl1	-2.472	1.12E-03	Numbl	1.049	5.30E-03
Nkg7	-7.964	2.35E-02	Nyap1	1.603	9.60E-03
Npc2	-1.361	1.23E-02	Obsl1	1.060	6.97E-04
Npl	-2.870	4.95E-02	Ocrl	0.913	2.97E-02
Nts	-8.707	3.29E-02	Odf2l	0.930	1.34E-02
Nudt4	-1.288	1.64E-03	Oplah	1.252	4.38E-02
Nup210	-2.354	2.28E-02	Osbpl5	0.931	2.79E-02
Nyap2	-6.712	1.56E-06	Otoa	2.400	3.20E-02
Oas3	-8.484	1.33E-03	Otof	7.161	2.00E-02
Ocstamp	-4.411	5.35E-06	Pacsin3	1.461	2.00E-02
Olfml2b	-1.860	4.87E-02	Pank1	1.055	4.36E-02
Olfr289-ps1	-8.178	6.68E-03	Panx2	1.562	4.18E-02
Oscar	-3.215	2.96E-02	Pcgf2	1.059	2.86E-02
Ostm1	-1.898	3.78E-02	Pcx	1.669	2.73E-02
Palld	-1.183	1.08E-02	Pdk1	0.954	2.56E-02
Pappa	-1.832	1.88E-03	Pdzrn4	2.176	1.37E-03
Paqr7	-2.019	4.74E-02	Peg3	1.623	2.10E-04
Pard6g	-2.767	2.80E-09	Penk	2.378	2.66E-04
Parp14	-2.302	1.74E-02	Pfkm	1.015	1.74E-02
Parvb	-1.514	1.24E-02	Phf1	1.310	3.93E-02
Pcdh20	-7.143	2.69E-02	Phka1	1.309	5.73E-03
Pcdh7	-5.831	5.76E-07	Phka2	1.263	3.68E-02
Pcna	-1.458	6.68E-03	Phldb1	1.155	1.64E-02
Pde5a	-2.160	1.99E-03	Phtf2	1.103	1.31E-02
Pde9a	-3.086	1.09E-02	Pitpnc1	0.945	6.42E-03
Pdgfa	-1.611	1.64E-03	Pitpnm3	1.287	1.12E-02
Pdgfb	-2.714	1.27E-02	Pitx1	1.659	1.17E-02
Pdgfc	-2.141	3.17E-04	Pla2g2a	3.080	1.85E-02
Pdlim1	-2.673	6.68E-04	Pla2g2c	7.206	1.89E-02
Peg13	-1.783	1.34E-02	Plagl1	1.098	4.49E-02
Pfn1	-0.848	1.21E-02	Plekha4	1.672	1.44E-03
Pgbd5	-4.071	2.69E-02	Plekha5	1.737	5.96E-06
Pgf	-3.046	1.53E-03	Plekhg3	1.045	4.20E-02

Pgpep1	-1.346	4.46E-02	Plekhh2	1.271	2.09E-02
Phex	-3.852	5.34E-05	Plppr2	1.643	1.91E-03
Phldb3	-5.846	3.97E-03	Plxnb1	1.381	2.71E-03
Pik3ap1	-3.874	2.00E-02	Pnpla3	3.272	1.69E-13
Pip5k1b	-5.630	3.45E-02	Pnpla5	4.010	1.17E-03
Pklr	-10.952	6.22E-03	Pogz	1.009	9.34E-03
Pkp4	-1.120	9.23E-03	Pou3f3	1.729	2.41E-04
Pla2g12a	-1.508	6.98E-03	Ppm1m	1.052	2.77E-02
Pla2g7	-2.262	8.43E-03	Ppp1r3b	1.684	1.40E-04
Plac8	-4.273	9.76E-03	Ppp1r3c	1.504	2.74E-03
Plcb2	-5.088	5.35E-04	Ppp4r1l-ps	1.254	6.11E-03
Pld4	-2.318	2.99E-02	Prdm5	1.051	1.78E-02
Plekha2	-2.159	1.97E-02	Prdm9	1.237	3.14E-02
Pls3	-1.228	1.43E-03	Prkag2os1	5.360	5.98E-03
Pltp	-2.053	2.44E-02	Prkcz	1.094	4.59E-02
Plxnd1	-2.154	2.63E-04	Prpf39	0.948	6.31E-03
Pmaip1	-6.047	2.33E-04	Prpf40b	1.230	2.80E-02
Pomp	-0.974	3.09E-02	Prr33	1.559	3.36E-02
Ppfia2	-4.479	1.97E-03	Prss23	3.047	3.16E-02
Ppm1e	-4.368	2.10E-11	Ptbp2	0.801	2.17E-02
Ppp1cb	-1.083	4.69E-03	Ptger1	2.479	4.85E-02
Ppp2cb	-1.163	2.27E-02	Ptp4a1	2.994	1.34E-05
Prcp	-2.418	2.03E-02	Ptpn23	1.177	1.45E-02
Prdm1	-3.500	4.64E-02	Ptpn3	1.497	3.54E-03
Prdx2	-1.321	2.66E-04	Ptpru	1.330	1.95E-02
Prdx3	-1.350	1.14E-02	Pwwp3b	1.483	5.08E-03
Prep	-1.015	1.46E-02	Rab11fip4	0.972	1.08E-02
Prex1	-1.504	1.22E-02	Rab36	1.835	1.78E-03
Prkch	-1.467	4.64E-02	Rarg	0.895	4.78E-02
Prr15	-7.838	2.03E-02	Rasgef1a	1.955	2.99E-02
Prss46	-7.651	3.25E-02	Raver2	1.662	4.21E-02
Psat1	-2.522	2.85E-03	Rbak	0.863	3.80E-02
Psma2	-1.015	2.05E-02	Rbm20	1.698	7.60E-03
Psmb5	-1.094	1.10E-02	Rbm5	1.144	5.56E-03
Psmb7	-1.145	1.96E-02	Rdh12	1.539	3.16E-02
Psmb8	-2.835	2.71E-04	Rflna	1.279	9.66E-03
Psme1	-1.067	4.26E-02	Rfxank	1.318	3.07E-02
Psme2	-1.098	2.12E-02	Rgs11	1.792	3.87E-03
Ptbp3	-1.108	4.65E-02	Rhpn1	1.829	1.25E-02
Ptk2b	-4.028	1.36E-02	Rian	1.446	4.25E-04
Ptma	-1.084	1.40E-04	Rlf	0.929	5.73E-03
Ptpn1	-0.969	3.80E-02	Rnf208	2.665	2.94E-02
Ptpn6	-2.772	6.69E-03	Rnf32	2.034	3.25E-02
Ptprc	-3.843	1.15E-02	Rnf39	1.481	6.50E-03
Ptprk	-2.388	1.09E-04	Rnft2	1.124	4.93E-02
Ptprz1	-4.612	6.68E-04	Rorc	1.944	7.57E-05

Rab38	-5.192	1.54E-06	Rrnad1	1.080	1.72E-02
Rab5c	-0.720	4.91E-02	Rtl1	1.937	5.79E-05
Rab7	-0.866	7.19E-03	Rtl3	1.443	3.46E-02
Rac1	-0.787	2.94E-02	Rxrg	7.315	4.20E-02
Rac2	-3.865	1.44E-06	S100pbp	0.736	3.74E-02
Rad54l	-1.607	3.47E-02	Scml2	1.531	2.58E-02
Rag1	-5.956	1.50E-03	Scube1	1.594	1.05E-04
Ralgps2	-2.820	5.43E-04	Scube3	1.722	2.04E-03
Rap1b	-1.234	1.89E-02	Sec14l2	1.076	2.73E-02
Rap2a	-1.487	1.00E-03	Sec16a	0.793	3.16E-02
Rap2b	-1.294	2.65E-02	Sec31b	2.310	7.19E-03
Rasa3	-0.891	4.47E-02	Sec61a2	1.099	2.79E-02
Rasal3	-5.024	1.17E-02	Sema6c	1.781	5.73E-03
Rassf3	-1.187	2.63E-02	Septin5	0.989	4.36E-02
Rassf4	-2.967	2.37E-06	Serpina1a	2.575	3.76E-02
Rbm15b	-1.093	3.61E-02	Serpina1d	4.390	3.42E-03
Rbm38	-2.412	1.41E-02	Serpina3k	24.287	2.53E-06
Rec8	-4.944	4.25E-02	Serpina3n	1.916	5.21E-03
Redrum	-8.139	7.36E-03	Serpinf2	7.539	2.10E-02
Rerg	-2.038	1.67E-02	Setd5	0.714	4.57E-02
Rftn1	-3.023	2.10E-05	Sfi1	0.876	2.55E-02
Rgs10	-1.081	4.05E-02	Sfrp5	2.031	6.90E-03
Rgs3	-0.993	2.03E-02	Sfxn2	1.147	5.70E-03
Rhob	-1.088	1.56E-02	Sfxn4	1.438	4.35E-02
Rhov	-7.053	1.85E-02	Sgsm2	1.317	2.38E-02
Rnd3	-1.269	4.91E-02	Sh3d21	1.379	4.49E-02
Robo2	-2.161	2.42E-02	Sh3rf2	2.029	1.51E-02
Rp2	-1.788	4.53E-02	Shisal1	8.203	7.75E-03
Rpe	-1.125	4.82E-02	Shroom1	1.368	1.18E-02
Rps27l	-1.151	1.06E-02	Sim2	1.735	9.15E-03
Rsad2	-4.546	2.27E-03	Sipa1l1	1.148	2.44E-02
Rsrc1	-1.261	3.23E-02	Slc19a3	2.238	4.31E-02
Runx1	-2.005	5.99E-04	Slc22a17	0.949	1.45E-02
S100a11	-1.041	1.40E-03	Slc23a3	3.825	3.44E-03
S1pr1	-2.085	2.25E-02	Slc25a36	1.491	8.59E-06
S1pr3	-4.405	3.26E-10	Slc25a47	1.554	6.70E-03
Samd9l	-1.715	1.31E-02	Slc38a2	1.246	1.40E-04
Samsn1	-5.832	2.73E-02	Slc38a3	1.539	7.77E-05
Sash3	-4.473	4.95E-02	Slc4a3	1.350	3.08E-02
Satb2	-5.606	3.63E-02	Slc6a1	1.938	8.71E-09
Scn4b	-9.034	8.02E-04	Slc6a17	2.001	3.30E-02
Sdc1	-1.161	3.83E-02	Slc9a8	1.003	1.34E-02
Sdc2	-1.909	2.59E-02	Sned1	1.321	1.01E-02
Sdhc	-0.939	2.72E-02	Snhg14	1.800	3.54E-02
Sdhd	-0.942	3.70E-02	Snhg17	1.144	5.57E-03
Sem1	-0.893	4.08E-02	Snord94	6.773	2.99E-02

Sema6d	-2.569	4.30E-05	Snph	1.388	1.27E-03
Sema7a	-2.619	5.87E-04	Snrnp48	0.717	4.84E-02
Septin11	-1.478	3.48E-02	Sorbs1	1.322	8.46E-04
Septin4	-1.647	3.03E-03	Spag4	1.523	1.30E-02
Serbp1	-0.920	4.10E-02	Spata1	1.823	1.03E-05
Serpina12	-5.877	2.41E-02	Spon1	1.422	2.66E-04
Serpina3f	-4.424	2.69E-02	Srrm1	0.929	4.12E-03
Serpine2	-2.059	8.23E-04	Srsf11	0.773	2.84E-02
Sgms2	-2.051	9.58E-05	Sstr3	4.520	6.98E-03
Sh3bgrl	-1.311	2.13E-03	Stac2	1.460	1.74E-02
Sh3bgrl2	-1.929	2.28E-02	Stk26	1.350	3.31E-03
Sh3bgrl3	-1.357	1.50E-03	Stk32b	1.388	2.77E-02
Sh3bp4	-1.319	3.03E-02	Stxbp1	1.093	2.12E-02
Sh3bp5	-1.859	2.63E-02	Stxbp5	0.798	4.14E-02
Sh3pxd2b	-2.398	2.99E-06	Sult4a1	8.808	2.52E-03
Shb	-1.690	3.11E-02	Sybu	1.141	7.19E-03
Shc2	-4.083	5.30E-14	Syn3	2.613	1.68E-02
Shtn1	-4.031	1.05E-02	Syngap1	0.804	4.41E-02
Siglec15	-9.261	4.77E-05	Syt7	1.850	3.84E-02
Siglech	-5.773	6.30E-03	Taf1a	0.943	2.12E-02
Sinhcaf	-3.727	2.05E-02	Tat	8.150	1.87E-02
Skap2	-1.951	1.59E-03	Tcea2	1.334	2.22E-03
Sla	-3.793	2.95E-02	Tcea3	1.479	4.22E-02
Slamf6	-5.453	2.07E-02	Tdo2	8.601	1.15E-02
Slc13a3	-6.250	7.83E-03	Tectb	7.649	8.64E-03
Slc16a10	-1.654	1.89E-02	Tenm3	2.266	4.15E-02
Slc25a39	-0.853	1.53E-02	Tgm3	7.962	2.86E-02
Slc25a5	-1.946	1.66E-03	Tincr	2.281	1.22E-02
Slc36a2	-6.089	6.07E-03	Tlcd1	1.021	3.18E-02
Slco3a1	-2.103	8.93E-03	Tm7sf2	1.357	1.60E-02
Slco4a1	-5.977	3.72E-03	Tmc4	1.312	1.10E-02
Slfn1	-6.875	4.03E-02	Tmem25	7.855	1.40E-03
Slfn10-ps	-7.668	2.94E-02	Tmem63a	1.272	2.82E-02
Slfn5	-2.664	9.66E-03	Tnfrsf10b	1.335	3.83E-02
Slitrk6	-2.817	1.29E-03	Tnfrsf25	1.737	9.71E-03
Smagp	-2.487	1.60E-02	Tns2	1.063	2.94E-02
Snn	-2.368	7.98E-04	Tom1l2	1.312	1.09E-02
Snu13	-0.928	4.97E-02	Tpra1	0.890	3.29E-02
Snx10	-3.951	1.34E-06	Tra2a	0.734	3.31E-02
Snx20	-4.998	2.40E-02	Trim39	1.204	2.26E-04
Sord	-1.352	4.31E-02	Trim68	1.112	3.72E-03
Sost	-2.509	1.91E-02	Trmu	0.999	2.84E-02
Sp100	-3.379	4.38E-02	Tro	1.649	4.68E-05
Sp7	-1.289	3.95E-02	Trpm3	2.564	4.03E-05
Specc1	-1.673	4.95E-03	Trpv4	1.304	6.62E-03
Spib	-4.140	2.66E-02	Trrap	0.775	2.27E-02

Spn	-5.604	9.58E-05	Trub1	1.231	5.27E-03
Spp1	-1.790	8.94E-03	Tsga13	7.618	2.46E-02
Spta1	-4.055	1.86E-02	Tspan32os	3.121	3.48E-02
Sptb	-2.335	2.30E-03	Tspyl2	1.089	3.23E-02
Sstr2	-3.289	8.63E-04	Ttc14	0.787	3.70E-02
St18	-7.608	4.07E-03	Ttc22	2.735	2.44E-02
St3gal1	-2.193	6.48E-04	Ttll10	2.864	9.34E-03
St6galnac4	-1.159	3.17E-02	Tubb2b	1.469	2.94E-02
St8sia4	-4.151	1.42E-02	Ulk3	1.114	1.95E-04
Stab1	-2.132	3.64E-02	Usp29	1.842	7.79E-04
Steap4	-2.404	4.62E-04	Usp48	0.907	2.28E-02
Stk17b	-2.315	5.32E-03	Usp53	1.473	9.56E-04
Stx7	-1.082	1.71E-02	Uvssa	1.084	1.36E-02
Svbp	-1.467	6.98E-03	Vav3	1.038	4.66E-02
Syk	-3.681	1.21E-06	Vegfa	0.991	1.36E-02
Tbx2	-2.384	5.56E-03	Vill	1.917	1.78E-03
Tcf7	-2.189	7.93E-04	Vipr2	2.395	2.87E-04
Tcn2	-2.044	1.02E-03	Vmn2r57	5.060	3.29E-02
Tead2	-1.944	7.09E-03	Wfikkn1	2.146	4.76E-02
Tecrl	-8.415	4.50E-03	Wnk4	1.742	2.36E-03
Tes	-2.548	1.82E-02	Wsb1	1.468	1.68E-06
Tfpi	-3.878	2.80E-02	Wwp2	1.541	2.39E-03
Tgfbr1	-1.233	1.31E-02	Zbtb48	1.370	3.42E-02
Tgtp2	-5.274	9.34E-03	Zdhhc23	2.059	1.82E-03
Tie1	-2.538	1.63E-02	Zfp101	1.025	1.42E-02
Tifa	-3.021	1.00E-03	Zfp184	2.357	4.35E-02
Timp1	-1.606	8.54E-05	Zfp286	1.147	4.95E-02
Tlnrd1	-1.295	9.43E-03	Zfp385b	1.168	1.68E-03
Tm4sf19	-7.791	3.01E-04	Zfp385c	1.511	1.55E-02
Tmem123	-1.896	5.05E-03	Zfp395	1.184	1.33E-02
Tmem14c	-1.330	3.45E-03	Zfp408	0.973	2.44E-02
Tmem176a	-2.028	9.49E-03	Zfp420	1.313	2.61E-03
Tmem176b	-2.312	2.05E-03	Zfp459	6.065	4.40E-02
Tmem178	-4.185	2.72E-02	Zfp512b	0.816	1.86E-02
Tmem200a	-8.511	1.91E-03	Zfp566	1.551	3.83E-02
Tmem204	-2.007	2.02E-02	Zfp612	2.208	1.71E-03
Tmem229b	-2.407	9.84E-03	Zfp660	1.735	2.77E-02
Tmem59	-1.266	3.95E-02	Zfp783	0.773	4.93E-02
Tmsb10	-1.191	9.75E-05	Zfp950	1.273	2.88E-04
Tmsb4x	-2.189	4.20E-07	Zfpl1	0.904	4.20E-02
Tmtc2	-2.780	1.05E-05	Zfr2	1.184	2.46E-03
Tnc	-3.780	1.13E-09	Zim1	1.915	6.47E-06
Tnfaip2	-2.124	3.83E-04	Zkscan7	1.218	2.99E-02
Tnfrsf11a	-4.930	1.64E-03	Zmiz1os1	5.280	1.52E-04
Tnfrsf19	-1.647	2.00E-02	Zmym3	1.005	1.90E-02
Tomm22	-0.948	1.52E-02	Zmym5	0.980	1.92E-02

Tpm1	-1.703	7.80E-04
Tpm4	-0.904	3.26E-02
Traf3ip3	-6.279	2.08E-02
Trak2	-0.863	1.89E-02
Trim12c	-1.360	1.36E-02
Trp53i11	-1.891	6.29E-03
Tspan10	-7.825	2.05E-02
Tspan14	-2.003	1.20E-02
Tspan17	-1.366	2.14E-02
Tuba1b	-1.006	3.74E-02
Tuba8	-7.560	4.00E-02
Tubb6	-1.760	9.03E-03
Tyrobp	-3.587	1.12E-05
Uba7	-1.572	2.25E-02
Ubb	-0.951	4.13E-02
Ube2a	-1.252	1.46E-02
Uchl1	-2.592	4.48E-05
Uchl5	-1.139	3.42E-02
Ucp2	-2.424	3.14E-07
Unc5b	-2.323	2.69E-03
Uqcrfs1	-1.610	3.01E-04
Uqcrh	-0.748	4.63E-02
Uqcrq	-1.032	1.15E-02
Ushbp1	-2.474	1.44E-02
Vav1	-4.089	7.19E-03
Vcan	-2.199	2.31E-03
Vdr	-1.907	9.49E-04
Vldlr	-1.384	4.51E-02
Vstm4	-2.321	4.22E-02
Wdfy4	-4.273	6.14E-03
Wdr86	-4.663	5.20E-04
Wnt4	-2.219	2.64E-02
Xpr1	-1.347	4.95E-02
Ywhab	-0.922	2.57E-02
Ywhag	-1.023	1.37E-02
Ywhaz	-0.961	4.38E-02
Zdhhc14	-3.873	5.98E-03
Zeb2	-2.580	5.76E-07
Zfp36l1	-1.487	4.27E-03
Zfp706	-0.882	2.75E-02
Zfpm1	-1.661	3.32E-02
Zswim5	-6.945	1.40E-03